UNIVERSITÀ POLITECNICA DELLE MARCHE

FACOLTÀ DI SCIENZE

Doctoral Program in Life and Environmental Sciences
XIV cycle

Civil and Environmental Protection

INTEGRATED APPROACHES FOR THE MONITORING AND ASSESSMENT OF ENVIRONMENTAL STATUS OF THE ADRIATIC SEA IN THE FRAMEWORK OF THE EUROPEAN MARINE STRATEGY DIRECTIVE

PhD candidate
Claudia Busca

Tutor
Prof. Antonio Dell'Anno

Co-tutors
Prof. Aniello Russo
Dott. Antonio Novellino

Abstract

There are growing evidence that human activities together with climate change are driving profound changes of marine ecosystems with important repercussions on the goods and services they provide for human wellbeing. The Marine Strategy Framework Directive (MSFD, 2008/56/EU), approved in 2008 by the European Parliament and transposed at Italian level in 2010 (Legislative Decree 190/2010), requires Member States to provide information on marine environmental status and to take the necessary measures to achieve or maintain Good Environmental Status (GES) of the marine environment by the year 2020. The main objective of this PhD thesis is to improve knowledge on the trophic and thermohaline conditions of the Adriatic Sea related to descriptors 5 (eutrophication) and 7 (hydrographic alterations) which are included in the MSFD and used along with other 9 descriptors for the assessment of GES, through the use and integration of outputs of predictive models, physical and biological data measured *in situ* and satellite data analyzed at different spatial and temporal scales. In order to better clarify dynamics occurring at local scale, data on thermohaline and biogeochemical characteristics of coastal waters of Marche Region have been acquired along with information on the river outflows and nutrient load. Results of this study highlight that during the investigated period temporal patterns occurring at the basin scale are different than those observed at local scale. In particular, while at the basin an increase of water temperature and salinity together with an increase of the phytoplankton biomass have been observed in the last 10-15 years, at a local scale patterns of thermohaline and biogeochemical characteristics on a decade are generally opposite and influenced by the river dynamics. Overall results of this study on the one hand highlight the importance of using integrated tools and approaches for the study of the thermohaline and biogeochemical characteristics at different spatial scales (Adriatic basin *vs.* local scale), and on the other represent an important benchmark for a better understanding of the functioning of the Adriatic Sea and the potential changes that could affect the achievement of GES and its maintenance over time.

Table of contents

Introduction

The marine strategy: a framework for community action in the field of marine environmental policy

The Marine Strategy Framework Directive (MSFD, 2008/56/EU) requires European Countries to provide information about marine environmental status and related strategies for improving ecosystem quality, where necessary, in order to ensure resources exploitation for the next generations.

The Marine Strategy Framework Directive (MSFD, 2008/56/EC) was approved in 2008, by the European Parliament and the European Council, for "*establishing a framework for community action in the field of marine environmental policy*" (European Commission, 2008).By now at the second implementation, it is the environmental pillar of the Integrated Maritime Policy. It requires Member States to '*take the necessary measures to achieve or maintain Good Environmental Status (GES) in the marine environment by the year 2020 at the latest'* (OJ L 164/9, Chapter I, Article 1.1; 2008). The Directive defines the Good Environmental Status (GES) as "the environmental status of marine waters where these provide ecologically diverse and dynamic oceans and seas which are clear, healthy and productive". GES means that the different uses made of the marine resources are conducted at a sustainable level, ensuring their continuity for future generations. In order to achieve GES by 2020, each Member State is required to develop a strategy for its marine waters (or Marine Strategy). In addition, because the Directive follows an adaptive management approach, the Marine Strategies must be kept up-to-date and reviewed every 6 years. Figure 1 from Claussen *et al.* (2011) shows the management cycle of the MSFD.

Several discussions arise for the definition of GES under Article 3(5), because of its vagueness and lack of legal precision, leading to over 20 different GES determinants across the Member States with Article 10 not clearly defining or exactly prescribing the difference between GES and targets or how they relate to each other. Moreover, on the achievement and maintenance of GES, the MSFD considers only direct pressures due to anthropogenic activities while also climate change should be strongly kept into account, especially because of its unmanaged nature. All regional seas, their catchments and the adjacent areas will be affected by climate change, one of many stressors in a wider typology of marine hazards and risks (Elliott *et al*, 2016).

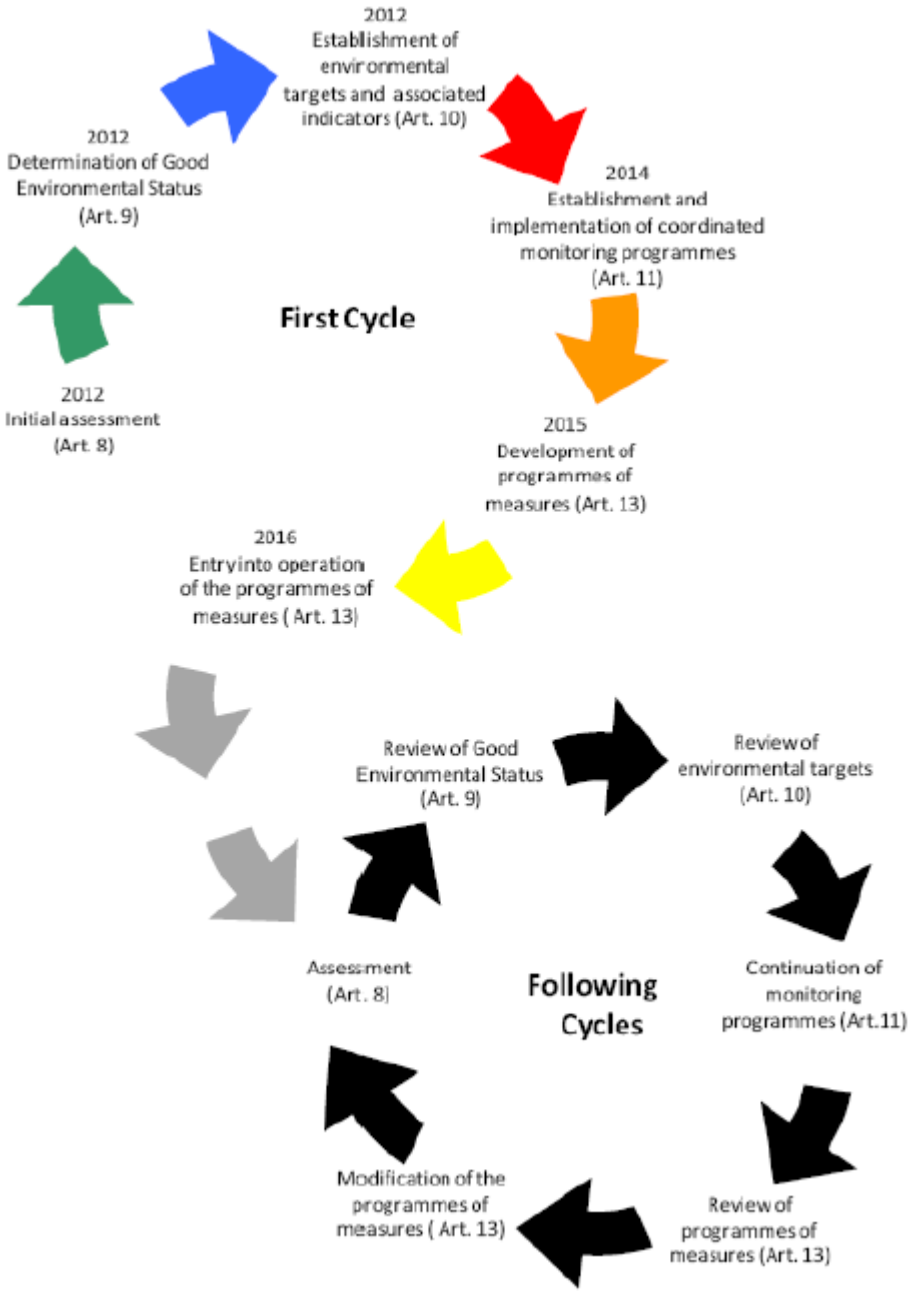

Figure 1- MSFD management cycle (summarized by Claussen et al., 2011).

The MSFD includes a set of 11 descriptors on the basis of which GES should be determined. The eleven descriptors are listed below:

Descriptor 1. Biodiversity is maintained.

Descriptor 2. Non-indigenous species do not adversely alter the ecosystem.

Descriptor 3. The population of commercial fish species is healthy.

Descriptor 4. Elements of food webs ensure long-term abundance and reproduction.

Descriptor 5. Eutrophication is minimised.

Descriptor 6. The sea-floor integrity ensures functioning of the ecosystem.

Descriptor 7. Permanent alteration of hydrographical conditions does not adversely affect the ecosystem.

Descriptor 8. Concentrations of contaminants give no effects.

Descriptor 9. Contaminants in seafood are below safe levels.

Descriptor 10. Marine litter does not cause harm.

Descriptor 11. Introduction of energy (including underwater noise) does not adversely affect the ecosystem.

Moreover, commission decision 2010/477/EU includes 29 agreed criteria and 56 indicators on which GES could be defined (Table 1).

Table 1- Descriptors, criteria and indicators for ecosystems monitoring

Descriptor	Criteria	Indicator
Descriptor 1. Biodiversity is maintained	1.1. Species distribution	- Distributional range (1.1.1) - Distributional pattern within the latter, where appropriate (1.1.2) - Area covered by the species (for sessile/benthic species) (1.1.3)
	1.2. Population size	- Population abundance and/or biomass, as appropriate (1.2.1)
	1.3. Population condition	- Population demographic characteristics (e.g. body size or age class structure, sex ratio, fecundity rates, survival/mortality rates) (1.3.1) - Population genetic structure, where appropriate (1.3.2)
	1.4. Habitat distribution	- Distributional range (1.4.1) - Distributional pattern (1.4.2)
	1.5. Habitat extent	- Habitat area (1.5.1) - Habitat volume, where relevant (1.5.2)
	1.6. Habitat condition	- Condition of the typical species and communities (1.6.1) - Relative abundance and/or biomass, as appropriate (1.6.2) - Physical, hydrological and chemical conditions (1.6.3)
	1.7. Ecosystem structure	- Composition and relative proportions of ecosystem components (habitats and species) (1.7.1)
Descriptor 2. Non-	2.1. Abundance and	- Trends in abundance, temporal

indigenous species do not adversely alter the ecosystem	state characterisation of non-indigenous species, in particular invasive species	occurrence and spatial distribution in the wild of non-indigenous species, particularly invasive non-indigenous species, notably in risk areas, in relation to the main vectors and pathways of spreading of such species (2.1.1)
	2.2. Environmental impact of invasive non-indigenous species	- Ratio between invasive non-indigenous species and native species in some well-studied taxonomic groups (e.g. fish, macroalgae, molluscs) that may provide a measure of change in species composition (e.g. further to the displacement of native species) (2.2.1) - Impacts of non-indigenous invasive species at the level of species, habitats and ecosystem, where feasible (2.2.2)
Descriptor 3. The population of commercial fish species is healthy	3.1. Level of pressure of the fishing activity	- Fishing mortality (F) (3.1.1). *(primary indicator*) - Ratio between catch and biomass index (hereinafter 'catch/biomass ratio') (3.1.2). (*secondary indicator)*
	3.2. Reproductive capacity of the stock	- Spawning Stock Biomass (SSB) (3.2.1). *(primary indicator)* - Biomass indices (3.2.2) *(secondary indicator)*
	3.3. Population age and size distribution	- Proportion of fish larger than the mean size of first sexual maturation (3.3.1) (*primary indicator*) - Mean maximum length across all species found in research vessel surveys (3.3.2) *(primary indicator*) - 95 % percentile of the fish length distribution observed in research vessel surveys (3.3.3) *(primary indicator)* - Size at first sexual maturation, which may reflect the extent of undesirable genetic effects of exploitation (3.3.4) *(secondary indicator)*
Descriptor 4. Elements of food webs ensure long-term abundance	4.1. Productivity (production per unit biomass) of key	- Performance of key predator species using their production per unit biomass (productivity) (4.1.1)

and reproduction	species or trophic groups	
	4.2. Proportion of selected species at the top of food webs	- Large fish (by weight) (4.2.1) E30+E31
	4.3. Abundance/distribution of key trophic groups/species	- Abundance trends of functionally important selected groups/species (4.3.1)
Descriptor 5. Eutrophication is minimised	5.1. Nutrients levels	- Nutrients concentration in the water column (5.1.1) - Nutrient ratios (silica, nitrogen and phosphorus), where appropriate (5.1.2)
	5.2. Direct effects of nutrient enrichment	- Chlorophyll concentration in the water column (5.2.1) - Water transparency related to increase in suspended algae, where relevant (5.2.2) - Abundance of opportunistic macroalgae (5.2.3) - Species shift in floristic composition such as diatom to flagellate ratio, benthic to pelagic shifts, as well as bloom events of nuisance/toxic algal blooms (e.g. cyanobacteria) caused by human activities (5.2.4)
	5.3. Indirect effects of nutrient enrichment	- Abundance of perennial seaweeds and seagrasses (e.g. fucoids, eelgrass and Neptune grass) adversely impacted by decrease in water transparency (5.3.1) - Dissolved oxygen, i.e. changes due to increased organic matter decomposition and size of the area concerned (5.3.2)
Descriptor 6. The sea floor integrity ensures functioning of the ecosystem	6.1. Physical damage, having regard to substrate characteristics	Type, abundance, biomass and areal extent of relevant biogenic substrate (6.1.1) - Extent of the seabed significantly affected by human activities for the different substrate types (6.1.2)
	6.2. Condition of benthic community	- Presence of particularly sensitive and/or tolerant species (6.2.1) - Multi-metric indexes assessing

		benthic community condition and functionality, such as species diversity and richness, proportion of opportunistic to sensitive species (6.2.2) - Proportion of biomass or number of individuals in the macrobenthos above some specified length/size (6.2.3) - Parameters describing the characteristics (shape, slope and intercept) of the size spectrum of the benthic community (6.2.4)
Descriptor 7. Permanent alteration of hydrographical conditions does not adversely affect the ecosystem	7.1. Spatial characterisation of permanent alterations	- Extent of area affected by permanent alterations (7.1.1)
	7.2. Impact of permanent hydrographical changes	- Spatial extent of habitats affected by the permanent alteration (7.2.1) - Changes in habitats, in particular the functions provided (e.g. spawning, breeding and feeding areas and migration routes of fish, birds and mammals), due to altered hydrographical conditions (7.2.2)
Descriptor 8. Concentrations of contaminants give no effects	8.1. Concentration of contaminants	- Concentration of the contaminants mentioned above, measured in the relevant matrix (such as biota, sediment and water) in a way that ensures comparability with the assessments under Directive 2000/60/EC (8.1.1)
	8.2. Effects of contaminants	- Levels of pollution effects on the ecosystem components concerned, having regard to the selected biological processes and taxonomic groups where a cause/effect relationship has been established and needs to be monitored (8.2.1) - Occurrence, origin (where possible), extent of significant acute pollution events (e.g. slicks from oil and oil products) and their impact on biota physically affected by this pollution (8.2.2)

Descriptor 9. Contaminants in seafood are below safe levels	9.1. Levels, number and frequency of contaminants	- Actual levels of contaminants that have been detected and number of contaminants which have exceeded maximum regulatory levels (9.1.1) - Frequency of regulatory levels being exceeded (9.1.2)
Descriptor 10. Marine litter does not cause harm	10.1. Characteristics of litter in the marine and coastal environment	- Trends in the amount of litter washed ashore and/or deposited on coastlines, including analysis of its composition, spatial distribution and, where possible, source (10.1.1) - Trends in the amount of litter in the water column (including floating at the surface) and deposited on the sea-floor, including analysis of its composition, spatial distribution and, where possible, source (10.1.2) - Trends in the amount, distribution and, where possible, composition of micro-particles (in particular micro-plastics) (10.1.3)
	10.2. Impacts of litter on marine life	- Trends in the amount and composition of litter ingested by marine animals (e.g. stomach analysis) (10.2.1)
Descriptor 11. Introduction of energy (including underwater noise) does not adversely affect the ecosystem	11.1. Distribution in time and place of loud, low and mid frequency impulsive sounds	- Proportion of days and their distribution within a calendar year over areas of a determined surface, as well as their spatial distribution, in which anthropogenic sound sources exceed levels that are likely to entail significant impact on marine animals measured as Sound Exposure Level (in dB re 1μPa^2.s) or as peak sound pressure level (in dB re 1μPa_{peak}) at one metre, measured over the frequency band 10 Hz to 10 kHz (11.1.1)
	11.2. Continuous low frequency sound	- Trends in the ambient noise level within the 1/3 octave bands 63 and 125 Hz (centre frequency) (re 1μPa RMS; average noise level in these octave bands over a year) measured by observation stations and/or with the use of models if appropriate (11.2.1)

In order to achieve its goal, the Directive establishes European marine regions and sub-regions on the basis of geographical and environmental criteria. Four marine region are listed: the Baltic Sea, the North-East Atlantic Ocean, the Mediterranean Sea and the Black Sea, located within the geographical boundaries of the existing Regional Seas Conventions. The Mediterranean Sea, in turn, is divided in three sub-regions: the Western Mediterranean Sea, the Ionian Sea and the Central Mediterranean Sea and the Adriatic Sea (Figure 2).

The Directive established that monitoring programmes should be carried out and implemented on the basis on the initial assessment and be compatible within marine regions or subregions and shall integrate and complement the monitoring requirements imposed by other EU legislation (e.g. Water Framework Directive).Consistency, coherence and comparability within marine regions and subregions should be ensured by coordination of monitoring programmes and methods in the framework of Regional Sea Convention (RSCs) taking into account transboundary features and impacts.

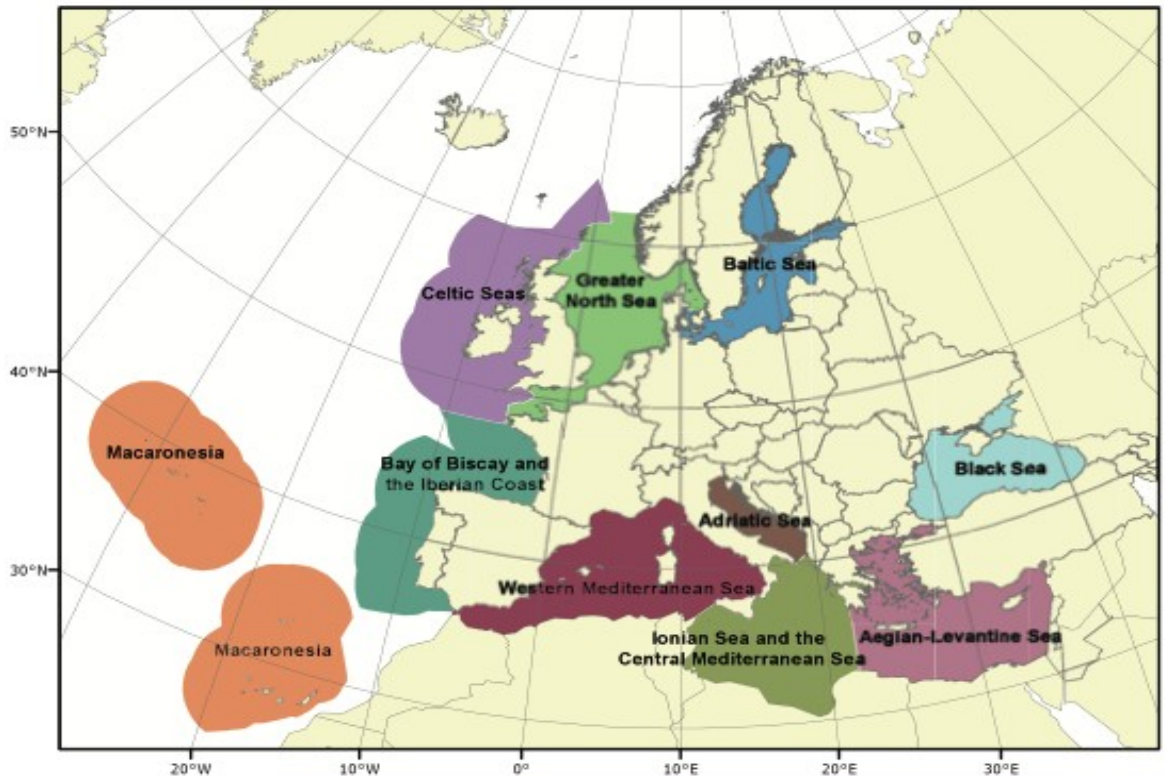

Figure 2 European seas sub-division identified by Marine Strategy Framework Directive.

There are numerous on-going or planned marine monitoring activities in Member States. Still, the MSFD requires additional efforts to be implemented in a meaningful manner and gives an opportunity to review, revise and integrate existing activities. Efforts towards integration have already started and Members States should take them into account when

finalizing and reporting their monitoring programmes and are encouraged to consider cooperation in common cruises and sharing of capacities and know-how. Member States should also make the most of existing monitoring activities, e.g. ensure that monitoring under the DCF serves also to collect data for as many descriptors as possible.

The review of current MSFD related research programmes demonstrated that there is a wealth of on-going research and there are high expectations for delivering applicable outputs. However, gaps in basic knowledge and applied tools will continue to exist in the near future.

Gaps and needs for further research differ between descriptors depending on their level of maturity in respect to the methods, indicators and existing datasets. Some deficits and gaps concerning the majority of descriptors could be grouped as:

- Lack of adequate data and time-series (e.g. on distribution of marine organisms, traceability of seafood, catches and by-catches for a number of non-targeted species, quantitative information on intermediate size litter-particles).
- Lack of baseline knowledge (e.g. information on specific habitats-deep sea, knowledge of biology and ecology of invasive species).
- Gaps on indicators relevant to answer MSFD objectives or describe GES and correspondent monitoring parameters (e.g. indicators for specific habitats and species communities).

The identification of the gaps drives future research on monitoring. Such research could be implemented directly when appropriate methods are available to support monitoring for MSFD. In case of not available methods or data, additional investment and research is required to ensure a medium- or long –term implementation of efficient monitoring. Moreover, investment on common data platforms and on integration of observations from different surveys and sources will be useful in terms of knowledge-sharing, as well as compilation of geo-referenced monitoring data (GIS data) should become self-evident as this is a pre-requisite when applying the ecosystem based approach to planning and management of marine areas.

Infrastructure for Spatial Information in Europe (INSPIRE)

The challenges regarding the lack of availability, quality, organization, accessibility, and sharing of spatial information are common to a large number of policies and activities and

are experienced across the various levels of public authority in Europe. In order to solve these problems it is necessary to take measures of coordination between the users and providers of spatial information. The Directive 2007/2/EC of the European Parliament and of the Council adopted on 14 March 2007 aims at establishing an Infrastructure for Spatial Information in the European Community (INSPIRE) for environmental policies, or policies and activities that have an impact on the environment. INSPIRE is based on the infrastructures for spatial information that are created and maintained by the Member States. To support the establishment of a European infrastructure, Implementing Rules addressing the following components of the infrastructure have been specified: metadata, inter-operability of spatial data sets and spatial data services, network services, data and service sharing, and monitoring and reporting procedures.

INSPIRE does not require collection of new data. However, after the period specified in the Directive (within 5 years) Member States have to make their data available according to the Implementing Rules.

Interoperability in INSPIRE means the possibility to combine spatial data and services from different sources across the European Community in a consistent way without involving specific efforts of humans or machines. It is important to note that "interoperability" is understood as providing access to spatial datasets through network services, typically via Internet. Interoperability may be achieved by either changing (harmonizing) and storing existing datasets or transforming them via services for publication in the INSPIRE infrastructure. It is expected that users will spend less time and efforts on understanding and integrating data when they build their applications based on data delivered in accordance with INSPIRE. In order to benefit from the endeavors of international standardization bodies and organizations established under international law their standards and technical means have been utilized and referenced, whenever possible.

To facilitate the implementation of INSPIRE, it is important that all stakeholders have the opportunity to participate in specification and development. For this reason, the Commission has put in place a consensus building process involving data users and providers together with representatives of industry, research and government. This open and participatory approach was successfully used during phases of decision processing such as the development of data specifications and data themes.

European Marine Observation and Data Network (EMODnet)

An example of effort in terms of marine data collection and sharing is the European Marine Observation and Data Network (EMODnet; Figure 3). It is a long term marine data initiative from the European Commission Directorate-General for Maritime Affairs and Fisheries (DG MARE) underpinning its Marine Knowledge 2020 strategy. EMODnet is a consortium of organizations assembling European marine data, data products and metadata from diverse sources in a uniform way. EMODnet consists of more than 100 organizations assembling marine data, products and metadata.

The main purpose of EMODnet is to unlock fragmented and hidden marine data resources and to make these available to individuals and organizations (public and private), and to facilitate investment in sustainable coastal and offshore activities through improved access to quality-assured, standardized and harmonized marine data which are interoperable and free of restrictions on use.EMODnet is currently in its second development phase with the target to be fully deployed by 2020.

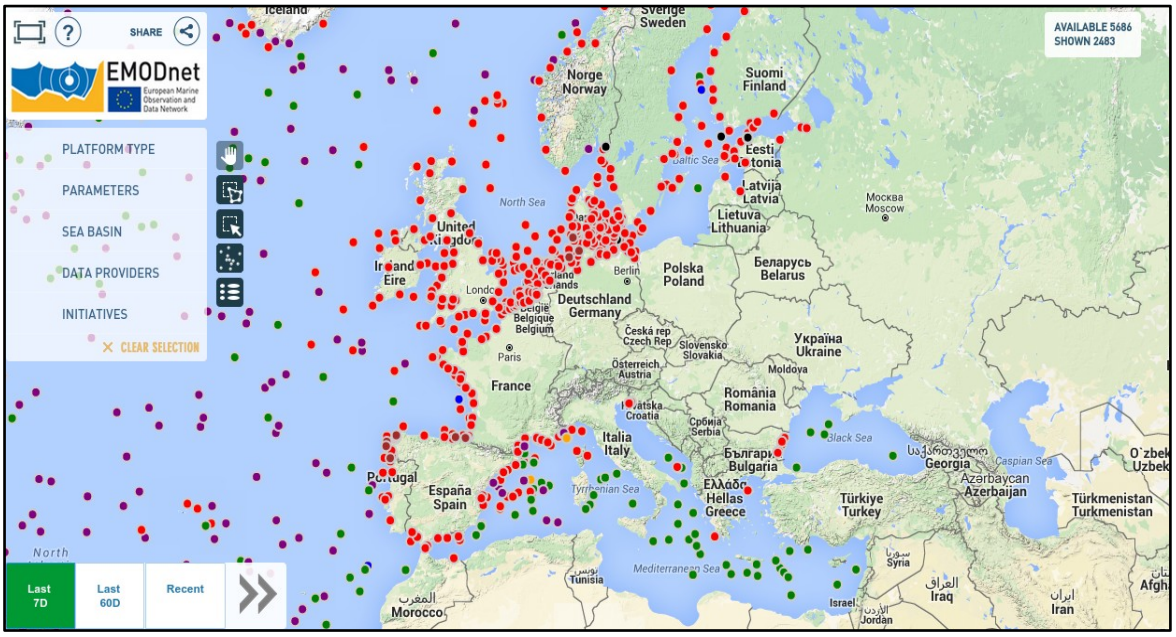

Figure 3 - Example of screenshot from EMODnet platform (www.emodnet.eu).

The EMODnet data infrastructure is developed through a stepwise approach in three major phases. Currently EMODnet is at the end of the 2nd phase of development with seven sub-portals in operation that provide access to marine data from the following themes: bathymetry, geology, physics, chemistry, biology, seabed habitats and human activities. EMODnet development is a dynamic process so new data, products and functionality are

added regularly while portals are continuously improved to make the service more fit for purpose and user friendly with the help of users and stakeholders.

- Phase I (2009-2013) - developed a prototype (so called ur-EMODnet) with coverage of a limited selection of sea-basins, parameters and data products at low resolution;
- Phase II (2013-2016) - aims to move from a prototype to an operational service with full coverage of all European sea-basins, a wider selection of parameters and medium resolution data products;
- Phase III (2015-2020) - will work towards providing a seamless multi-resolution digital map of the entire seabed of European waters providing highest resolution possible in areas that have been surveyed, including topography, geology, habitats and ecosystems; accompanied by timely information on physical, chemical and biological state of the overlying water column as well as oceanographic forecasts.

EMODnet is subdivided into several categories: bathymetry, geology, seabed habitats, chemistry, biology, physics, human activities, coastal mapping.

This PhD thesis has been partially developed within the project EMODnet physics, thanks to the economic support of ETT Ltd, which coordinates such project. Physics portal has been developed under the ur-EMODnet preparatory actions during EMODnet Phase I (2009-2013). In the current phase, EMODnet Physics will enhance and expand existing services to move, together with the six other EMODnet sub-portals, towards an operational service with full coverage of all European sea-basins, a wider selection of parameters and medium resolution data products.

Access to archived and real-time data on the physical conditions of European sea-basins and oceans is important for a wide range of users and for many different reasons; to monitor sea level variability, to make predictions on climate change or for the operation and planning of off-shore activities. Physical parameters include; sea water salinity and temperature, currents, turbidity, wind direction and speed, sea level and ice cover.

Data on the physical state of our sea basins and oceans are currently collected and stored by a myriad of public and private organizations throughout Europe, using fixed measuring stations (e.g. moored buoys, rigs/platforms, coastal stations) or automatic observatories at sea (e.g. profiling floats, drifting buoys, ships of opportunity, research vessels). However,

until recently, there was no coordinated effort to assemble these data into integrated data streams and make them easily available for users at a pan-European scale.

This second phase will strengthen the existing structure and infrastructure of the EuroGOOS ROOSs as the backbone of EMODnet Physics and will improve and expand the data portal in order to:

- Provide better access to additional data not yet in the current system;
- Provide access to additional Ferrybox data;
- Streamline and optimize the data flow;
- Fully exploit opportunities to obtain additional parameters from existing data sites;
- Fill in gaps in time series;
- Assist the work on the completeness of stations, leading to a list of uniform station names that reduces duplication between ROOSs;
- Achieve greater uptime of services and synchronization of data sources between ROOSs and data centers.

The challenge to achieve Good Environmental Status in a changing marine ecosystem due to global climate changes

There is now overwhelming evidence that human activities are driving rapid changes on marine ecosystems. Many of these changes are already occurring within the world's oceans with serious consequences likely over the coming decades. Our understanding of how climate change is affecting marine ecosystems has lagged behind that of terrestrial ecosystems. This is partly due to the size and complexity of the oceans, but also to the relative difficulty of taking measurements in marine environments. Studies on the impacts of climate changes on marine ecosystems revealed that the world oceans are changing rapidly with an increased risk of sudden nonlinear transformations (Hoegh-Guldberg and Bruno, 2010).

Alterations of hydrographical conditions (Descriptor 7) can occur as a consequence of global climate changes or human-related structures and/or activities (e.g. coastal defense structures, discharges of warm/cool waters by industrial plants, wind farms, fish farm).

MSFD does not consider thermohaline and circulation's modifications due to climate changes but only the impact produced by direct anthropogenic pressures. Infrastructures can only affect hydrological conditions at local scales. The alteration of hydrographical conditions has a combined effect on both ecosystem processes and functions which in turn

complicates the assessment of the impact level. For example, changes in currents and waves can in turn induce further changes to sediment transportation, bed forms, salinity and temperature which might lead to further positive or negative impacts on the biota as a result of environmental changes or through food chain effects (Zampoukas et al., 2014).

Changes in thermohaline regime and seawater circulation can have cascading effects on species and community (Descriptor 1 and 4; Table 2): species distribution is strongly related to their thermal tolerance and ability to adapt. Even individual physiological/phenological response depends on temperature regime: demographic changes resulting from alterations to recruitment, growth and survival together with phenological changes lead to potential predator-prey mismatches, along with the increased susceptibility to alien and invasive species (Descriptor 1,2,4; Table 2) ultimately determining ecosystem composition, spatial structure and functioning (Descriptor 1,4,6; Table 2). This will have repercussion on fisheries (Descriptor 3) and conservation management (Descriptor 1, 6). Altered temperature regime can profoundly modify the breeding cycle with consequent competitive advantage/disadvantage and changes in community structure and functioning along with increased growing season and growth rate, that means higher and longer productivity and changes in nutrient budget with symptoms of eutrophication and, once again, repercussion on fisheries and conservation management.

Large scale climatic patterns influence catchment run-off, including nutrients and contaminants, into semi-enclosed seas. Arguably, the greatest challenge in predicting the effects of climate change on the hydrodynamics of a catchment and hence the nutrient inputs to, and response in, enclosed coastal seas is the ability to understand these interlinked relationships (Meier *et al.*, 2011). In particular, nutrient run-off will create the adverse consequences of eutrophication (i.e. Descriptor 5) but this is difficult to predict against a background of inherent variability due to changes in land-use patterns (Elliott *et al.*, 2016).

Table 2 Main topics relating to the marine consequences of climate change and the way in which they influence the Good Environmental Status Descriptors D1-D11 (summarized from Elliott et al., 2016).

Descriptor	D1	D2	D3	D4	D5	D6	D7	D8	D9	D10	D11
Topics											
Altered temperature regime - species re-distribution and community response	•	•	•	•		•					
Altered temperature regime - individual physiological/phenological response	•	•	•	•	•	•					
Increased relative sea level rise-physiographic changes	•		•	•		•	•				
Increased climate variability effects on coastal hydrodynamics	•			•		•	•				
Changes to large scale climatic patterns due to land run-off	•		•	•	•	•	•	•	•		
Increased relative sea level rise changing estuarine hydrodynamics	•			•		•	•				
Increased ocean acidification and seawater physical-chemical changes	•		•	•		•		•	•		
Loss of polar ice cover and global transport repercussion	•	•	•	•	•		•			•	•
Sum categories	8	3	6	8	3	7	5	2	2	1	1

As shown here, climate change produces impediments to implementing the MSFD and achieving GES and there are repercussions of those impediments: (1) the science-base is good on conceptual aspects but is required to give precise links between changes in biota and climate features; the 'so-what?' and what-if?' questions cannot yet be answered. New scientific developments may overcome this during several iterations of the MSFD process. (2) Climate change produces '*shifting baselines*' which need to be accommodated in monitoring, particularly during the assessment of GES and marine management; actions will have to account for '*unbounded boundaries*' given the ecology and climate change-induced

migrations and dispersal of highly-mobile, nekton and plankton species. Hence, long-term and spatially large datasets are essential for signal-noise separation, to identify changes in ecological indicators, detect sudden and gradual ecosystem shifts and regime changes, and provide a baseline against which to interpret future changes. However, given that such datasets do not exist for most components then this may not be achieved. As the MSFD

takes the current conditions as the baseline, predictions are required against current values.(3) The absence of empirical data will increase the use of modelling but the error limits on the models may be large, and increase because of climate change, or even be unknown, thus giving poor predictability. Furthermore, existing models are adequate for scenario and semi-quantitative testing but not for detailed quantitative and accurate predictions.(4) Member States at present are only considering the means of determining GES on a Descriptor-by-Descriptor basis but at some stage before 2020 they need to consider aggregating these to give GES for a regional or sub-regional area (Borja *et al.*, 2014). Hence while assessing climate change on single Descriptors is the first priority, interactions amongst Descriptors and their changes due to climate change need addressing. Unless GES is defined across the Descriptors then ecosystem health will not be determined. However, it is questioned whether the science is adequate to judge changes in health due to climate change and whether any resulting system is regarded as 'unhealthy' ('deteriorated' *à la* MSFD) or just different.(5) The challenges for marine monitoring and management result from having climate change superimposed on the effects of local activities and where climate change may either exacerbate or mask anthropogenic changes in the Descriptors. Detecting change against a greater inherent variability will increase monitoring costs, a challenge in economically difficult times (Borja and Elliott, 2013).(6) Climate-driven spatial and temporal variation should be interrogated including a potential geographic disparity to achieving GES across the marine environment in general and across the regional seas. Raised temperature may have greater effects in northern than southern Europe but these are equivocal. Hence, baselines will have to be revised on a site-specific basis although the evidence needs to be extrapolated to show the short, medium and long-term effects and the speed of environmental response. Modelling is required to indicate how quickly communities can reach a new equilibrium but there is now an urgent need to show adaptation (or the lack of it) over 10s to 100s of generation times for marine organisms.(7) Society will place emphasis on the repercussions of non-achieving GES for the Ecosystem Services and Societal Benefits obtained from the regional seas (e.g. Atkins *et al.*, 2011). The loss of these due both to managed pressures but also climate change has to be determined and emphasized to environmental managers and policymakers (Luisetti *et al.*, 2014; Turner et al, 2014).(8) The failure to meet GES because of climate change has wide-ranging legal repercussions and could lead to a Member State being placed in infraction proceedings. A legal challenge will arise not because of the pressures inside the

waters of a Member State under which they might have some control but because of the external and no controlled pressures. The legal defence, that the failure was the result of third-party actions, natural causes or *force majeure*, would require to be supported by robust science.(9) These lessons are relevant and applicable not only to European seas and the implementation of the MSFD but also to other global areas, for example during the implementation of the Canada Oceans Act and the US Oceans Act 2000 (US Congress 2002). While the latter does not give the same degree of detail as the MSFD in achieving healthy and productive seas and it does not mention climate change in its few pages, determining and managing change due to separating this from other anthropogenic pressures have to be considered.

Objectives

To protect and manage the marine ecosystem it is necessary, first of all, to acquire a deep knowledge of its natural dynamics (deYoung et al., 2008; Giani et al., 2012). At national level, till July 2015 monitoring activities of marine systems carried out by the different Regional Agency for Environmental Protection are restricted to coastal waters (within 3 km far the coastline) and data acquired by scientific institutions in offshore systems are generally spatially and temporally fragmented. Thus, there is a urgent need from one side to integrate the different dataset and from the other to improve the spatial and temporal coverage. To this regard, remote sensing represents a powerful tool to increase the temporal and spatial coverage of environmental information (Barale et al., 2005) providing daily update of data. However, such tool allows only to obtain information on surface layer of the oceans, thus requiring an integration with other tools for the analysis of water masses and biological characteristics below the sea surface. Forecasting systems can help to improve 3D knowledge of marine ecosystems, but the reliability of their outputs should be carefully assessed.

The main objective of this PhD thesis is to integrate data collected by *in situ* measurements, remote sensing and forecasting systems output in order to investigate at different spatial (from local to regional to basin) and temporal (from day, month, season, annual and interannual) scales changes in the main physical and biological variables of the Adriatic Sea related to descriptors 5 (i.e. eutrophication) and 7 (hydrographic alterations) of the MSFD. The variables investigated at the basin scale includes temperature and salinity and chlorophyll-a concentrations (as a proxy of phytoplankton biomass). To better understand spatial patterns, the basin has been divided into four areas on the basis of the bathymetry (Artegiani et al., 1996; Zavatarelli et al., 1998). Moreover, in order to better clarify dynamics occurring at local and regional scale, data on coastal waters of Marche Region have been acquired, thanks to the collaboration of the Agency for Environmental Protection of the Marche Region, along with information on the river outflows (data acquired from the Civil Protection of the Marche Region) and nutrient load.

Given the general spatial and temporal fragmentation of environmental data on the Adriatic Sea and the lack of validated data availability, the final purpose of this thesis is to share acquired data and knowledge by means of EMODnet platform, according to the Marine Strategy Framework Directive objective.

The study area: the Adriatic sea

One of the sub-regions identified by MSFD, and that has been investigated in this thesis, is the Adriatic Sea. The Adriatic Sea (Figure 4) is a complex natural system from both hydrological and biological point of view (Russo and Artegiani, 1996), characterized by a strong human pressure. Such human pressure along with the current global climate changes are strongly affecting the ecosystem health and resilience of the Adriatic Sea.The Adriatic Sea is located in the northern part of the Mediterranean Sea, orientated in northwest-southeast direction from 40°N to 46°N, with an average depth of 250 m and total surface of 138 000 km², which makes $1/20^{th}$ of the entire Mediterranean. This elongated basin (800 km long and 90-200 km wide) is surrounded by Dinaric, Alpine and Apennine mountain chains. Its northern end is very shallow and gently sloping, with an average bottom depth of about 35m. The middle Adriatic is 140 m deep on the average, with the two Pomo Depressions reaching 260 m, situated between the two lines Ancona-Zadar and Gargano-Lastovo. The southern end is characterized by a wide depression deeper than 1200 m, situated between Gargano-Lastovo line and Otranto Channel.

This epicontinental basin, characterized by regular, low and sandy Italian coast on the west and generally high, rocky and torned by channels and islands eastern coast, is connected with the Ionian Sea by the Otranto Strait (800 m deep), where the water exchange with the rest of the Mediterranean Sea takes place suggesting an inflow along the eastern and an outflow along the western coast.

Although strong annual and year-to-year fluctuations of oceanographic properties give the Adriatic Sea a clearly continental aspect, from different points of view it can be considerate a miniature ocean because of its geomorphologic and hydrodynamic characteristics.

River runoff is particularly strong in the northern basin and affects the circulation through buoyancy input and the ecosystem by introducing large amounts of nutrients. Runoff is also responsible for making the Adriatic a dilution basin, with an average fresh water gain of about 1 m, since evaporation and precipitation almost compensate each other (Raicich,1996).

The Po River is the largest Italian river, with average discharge of 1500 m^3/s, flowing trough very large and highly populated industrial and agricultural region that includes large cities like Milan and Torino. In this area intensive agricultural and industrial activities, with consequent nutrient losses, generate nutrient-rich discharges and increase of primary

production in northern Adriatic basin. In fact, although there are important nutrient inputs of Isonzo and Adige rivers, and some other point sources along both coasts, the Po River is responsible for 70% of nutrient input in Adriatic basin (Degobbis and Gilmartin, 1990; Beg Paklar *et al.*, 2001).

Extension of the Po River plume influences granulometry, hydrodynamic and biogeochemical processes of northern and western part of the basin (Russo *et al.*, 2005); the plume evolution depends on seasonality of river discharge that has two maxima, the first one in spring due to snow melting, and the second one in autumn due to strong precipitation (Marchetti, 1984). Other factors that influence the extension of the plume are seasonal meteorological and hydrological conditions: during winter period Po River discharge is confined along the Italian coastline, while in summertime, when stratification of water column is very noticeable, the warmer freshwater remains in the surface layer and spreads in all directions, even towards northern and eastern coasts; the varying wind regime induces further variability of the plume extension. These seasonal and higher frequency fluctuations of river inflow and meteorological and hydrological conditions can cause important biological effects, in particularly in spring and summer when short and relevant inputs could be important for development of mucilage events (Degobbis *et al.*, 1995, 2005).

The Adriatic Sea presents a decreasing trophic gradient from north to south, due to the major nutrient input in northern part and general circulation in entire basin, with eutrophic conditions in northern basin and oligotrophic in central and southern basins (Degobbis and Gilmartin, 1990; Revelante and Gilmartin, 1976a,b, 1995; Zavatarelli *et al.*, 1998). As the Po River discharge is the major source of nutrient input in the Adriatic Sea, the eutrophic coastal waters of northern Adriatic represent the most productive part with high primary productivity, while central and southern basins show oligotrophic characteristics and a lower primary productivity (Degobbis, 1988; Viličić, 1989, 2002; Viličić*et al.,* 1998, 2002; Degobbis and Gilmartin, 1990; Degobbis *et al.*, 1997).

In general, related to the spreading of Po River plume, a west-east decreasing gradient of biomass and production is observed (Smodlaka and Revelante, 1983; Smodlaka, 1986), that reflects climatic and trophic gradients. This eutrophic conditions and a high primary productivity induced by nutrient discharges in the coastal water of northern basin can cause local events of anoxic conditions in bottom water and consequent mass mortality of

benthic organism (Stachowitsch, 1984, 1991; Justić*et al.*, 1987; Justić, 1991; Šimunović*et al.*, 1999; Travizi and Vidaković, 1994; Travizi, 2000; Stachowitsch*et al.* 2007).

Because of its geomorphologic characteristics of epicontinental basin, the Adriatic is subject to highly variable atmospheric forcing, river discharges and air-sea fluxes that play an important role in controlling the dynamics of its waters and variability in circulation and distribution of its water masses, presenting a seasonal variability in the circulation (Artegiani *et al.*, 1997a,b; Cushman-Roisin*et al.*, 2001; Figure 4) and the ecosystem (Zavatarelli *et al.*, 1998). It has been shown that the Adriatic circulation is influenced by morphology and seasonal meteorological changes (Buljan and Zore-Armanda, 1976; Franco *et al.*, 1982) that cause changes in intensity of marine currents (stronger in autumn-winter period and less intensive in spring-summer period), due to stronger wind stress in autumn and winter and weaker one in spring and summer (Budillon *et al.*, 2002).

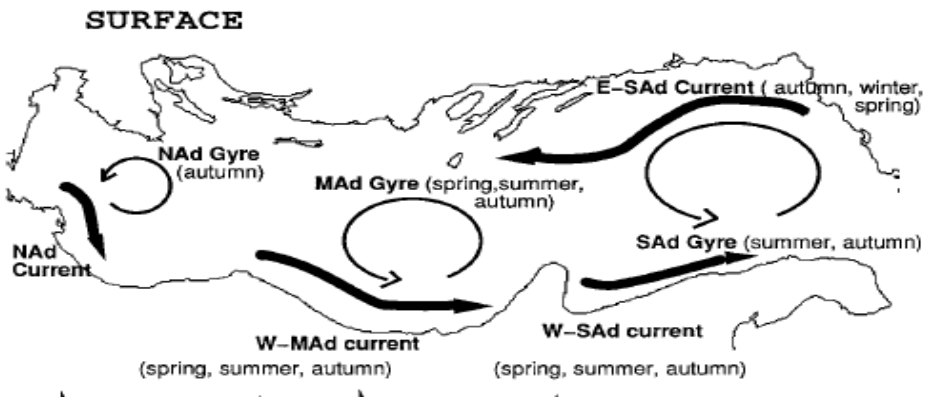

Figure 4 - Schematic picture of the Adriatic Sea surface baroclinic circulation (Artegiani et al. 1997b).

The general circulation in the Adriatic basin is cyclonic with two main circulation currents and three sub-basin gyres (Russo and Artegiani 1996; Artegiani *et al.*, 1997a,b; Bergamasco *et al.*, 1999; Alvera-Azcarate*et al.*, 2005): warmer and more saline Levantine Intermediate Waters (LIW) enter in Adriatic from the Ionian Sea through the Strait of Otranto and flow north-westward along the eastern coast as weak and wide current, called Eastern Adriatic Current (EAC); while western current, called Western Adriatic Current (WAC), flows southward along the western coast exporting to the Ionian Sea water with lower salinity due to the riverine inputs in northern basin (Orlić*et al.*, 1992; Vilibić and Orlić, 2002; Vilibić, 2003; Vilibić*et al.*, 2004; Alvera-Azcarate*et al.*, 2005). Some authors found that the stronger advection of warmer and more saline Mediterranean waters, coincided with higher primary production and higher zooplankton in the Adriatic basin

(Buljan 1957, 1968; Zore-Armanda, 1963; Pucher-Petković, 1970; Vučetić, 1970; Pucher-Petković*et al.*, 1971).

The Adriatic basin shows a seasonal thermal cycle, with winter vertical mixing of the water column induced by surface cooling and wind stress, and formation of seasonal thermocline in spring and summer induced by freshwater input and surface heating that generate a stratifies water column (Franco, 1983, 1989; Franco and Michelato, 1992; Artegiani *et al.*, 1997, 1989; Vested *et al.*, 1998). Winter period is characterized by cooling of the water column, caused by formation of cold and dense water masses stressed by Bora that helps vertical mixing and causes its homogeneity, while summer period is characterized by vertical stratification and horizontal heterogeneity due to intensive heating of the surface and input of freshwater from Po River that generate a seasonal thermocline and halocline. The intensity of three sub-basin cyclonic gyres, generated in every sub-basin, vary due to seasonal conditions and fluctuation of riverine inputs.

On basis of different temperature and salinity profiles it is possible to distinguish three main water masses in Adriatic basin: Surface Water, Adriatic Deep Water (ADW) and Modified Levantine Intermediate Water (MLIW; Figure 5). Surface Water occupies the layer above 100 meter of depth in the southern basin, layer that going toward the north-western end of the basin becomes thinner, up to order of 10 m in the north western most area. Surface Water includes Ionian and possibly Atlantic waters that enter in Adriatic Sea, flow along the eastern coast, as well as waters freshened by Po and other western rivers and outflow to Ionian Sea along western coast (Artegiani *et al.*, 1997). The northern Adriatic Current (NAd current) can be found in front of the Po River mouth and during the winter period extends 100 km to the south along the Italian coast, while in summer period results separated from the current in the middle Adriatic that is called Western-Middle Adriatic Current (Artegiani *et al.*, 1997; Zore-Armanda, 1969).

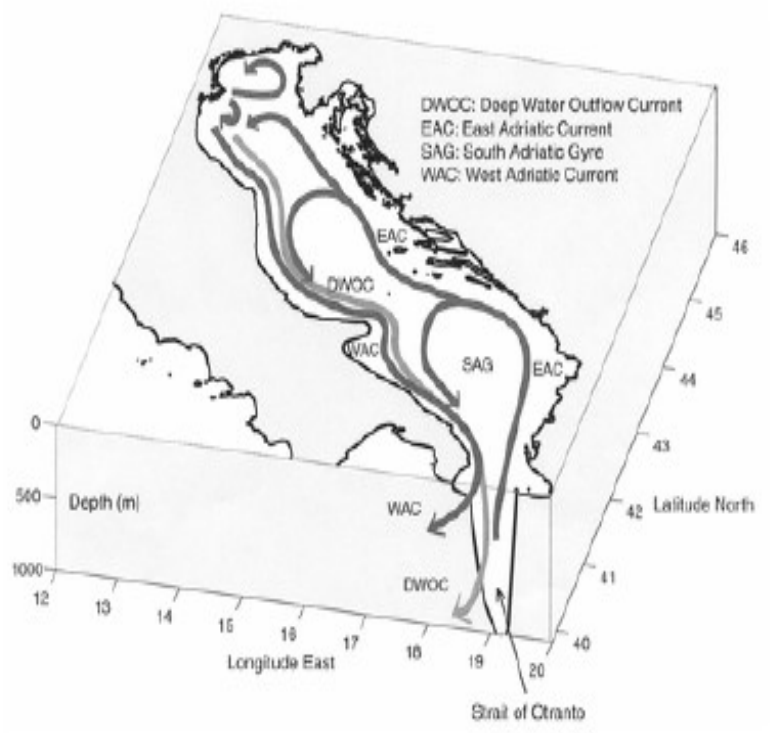

Figure 5 - Schematic picture of general circulation in the Adriatic Sea (Cushman-Roisinet al. 2001)

The Adriatic Sea behaves like a dilution basin due to Po River runoff (Artegiani *et al.*, 1997) and it is one of the site where deep water formation occurs: generated by surface heat losses in the northern basin, the Northern Adriatic Dense Water (NADW) is generated due to strong wind stress of Bora, more pronounced in wintertime, and cool and fresh water which flow along the western coast (Artegiani *et al.*, 1997; Roether and Schlitzer, 1991; Zavatarelli *et al.*, 1998; Bergamasco *et al.*, 1999; Vilibić and Orlić, 2002). Very low winter temperatures and wind stress of cold Bora cause deep water formation and mixing of surface waters with deeper water layers. Besides the formation of dense water in northern Adriatic, its formation has been reported in the southern and even in the middle Adriatic (Zore-Armanda, 1963). This dense water, called Adriatic Deep Water (ADW) spreads through the Strait of Otranto and becomes a component of the Eastern Mediterranean Deep Water (EMDW; Figure 6).

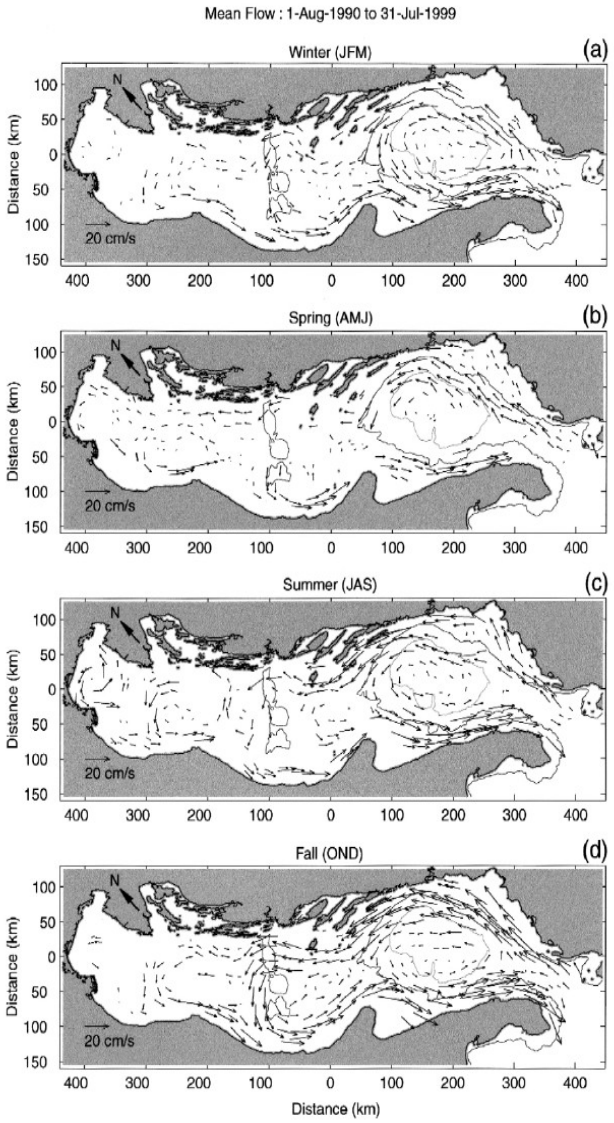

Figure 6 - Seasonal maps of surface mean flow (Poulain, 2001)

The two dominant winds in Adriatic basin are: cold and generally dry wind from northeast direction called Bora, mainly present in winter, spring and autumn; and the south-easterly warm and humid wind called Sirocco, mainly present in autumn and summer (Cavaleri *et al.*, 1996; Bergamasco *et al.*, 1999; Poulain, 1999; Russo *et al.*, 2005; Pullen *et al.*, 2007). Other winds present in Adriatic Sea, with lower frequencies, are north-westerly wind Maestrale and Tramontana. In general, Bora implies advection of cold, dry air, while sirocco usually carries warm, humid air to the Adriatic area, but sometimes there are exceptions to this pattern when "dry Sirocco" and "dark Bora" events occur. Mean wind fields over the Adriatic are weak, but episodes of Bora and Sirocco affect significantly the Adriatic flow field.

The Bora wind is formed when the air pressure in Central Europe is high, especially in wintertime, and the Mediterranean basin is subjected to atmospheric depression that causes low pressure in the Adriatic basin, so that the flux of cold continental air from Central Europe passes through narrow valleys of Dinaric Alps to the Adriatic, increasing in this way the speed of the wind, reaching the maximum speed in eastern coast of Adriatic near Trieste, Senj and Šibenik. Such conditions, depending on different atmospheric configuration can generate both "light Bora" (dry wind) and "dark Bora" (wind with rain and snow). Once arrived in Adriatic basin, Bora wind of is subjected to weakening while proceeds across the Adriatic Sea, which creates the alternation of areas with high and low wind intensity and influences the marine currents, causing stronger current from the Gulf of Trieste and from the Kvarner Bay. Bora winds coming from the northeast, as well as Sirocco from southeast, can raise sea level meters up its mean and drown low. western coastlines This phenomenon generally occurs in autumn-winter period and it is called *aqua alta* (high water in Italian) because of high tides that influence all the Venice Lagoon.

The Sirocco wind blows from south-east and it is generally warm, humid and less strong than Bora, incrementing gradually to the maximum intensity on the east cost of the middle Adriatic and then decreasing toward western and northern coasts. It causes different effects on marine current, generating major intensity of the Eastern Adriatic Current and, in combination with other factors, it can cause inversions in Western Adriatic Current with rare phenomena of upwelling in western coast of middle Adriatic (Poulain *et al.*, 2004). There are two types of Sirocco, one is dry wind associated with anticyclonic atmospheric circulation and with clear sky, while the other one, more frequent, is associated with cyclonic circulation and accompanied by rain.

Biogeochemical characteristics of the Adriatic Sea

Several studies had been carried out in order to characterize Adriatic Sea from biogeochemical point of view. One of the more interesting data collection has been published by Zavatarelli et al. (1998) who consider a large amount of published and available unpublished data relative to the Adriatic Sea in the period 1911-1914 and 1948-1991. Despite data was affected by a certain degree of uncertainty - due to a large intrinsic variability of the properties considered and to the insufficient spatial-temporal coverage- provide a quite clear picture of the biogeochemical characteristics of the Adriatic Sea at basin scale as well as of the factors influencing the nutrients levels.

The nutrient levels in the northern Adriatic are clearly controlled by the river inputs (not only from the Po but also from the other Adriatic rivers) inducing intense phytoplankton development in late winter (due to rain and snow melting in the Alps and Appennines) and autumn, during intense raining events. Thus, in the northern Adriatic Sea the runoff is significantly dependent on interannual oscillations of precipitations, which might be easily affected in the future by climate modifications (Zanchettin et al., 2008; Cozzi et al., 2012). Another factor controlling the nutrient distribution is the assimilative processes of phytoplankton. In fact, during the winter bloom the biological demand for phosphate and silicate is such to determine a horizontal distribution of these two nutrients which is totally different from the distribution of nitrate (which appear more controlled by the advective processes), confirming the nature of the northern Adriatic Sea (NAd) as a phosphorus limited ecosystem (Degobbis, 1990).

The annual external input of nutrients, mostly anthropogenic, is of the same order of magnitude as the regenerated amounts during their seasonal cycle (Degobbis and Gilmartin, 1990). Therefore,small changes of these inputs, combined with changes in the water exchange rate with the central Adriatic, which is strongly influenced by climatic fluctuations, significantly affected the eutrophication pressure in the NAd. Changes of mean surface salinity and temperature in the open NAd during the period 1972-2000 were generally well correlated with Po River flow rates, except during the late 1980s, when salinity was lower and temperatures higher than expected from such correlations (Degobbis et al., 2000; Djakovac,2003). This departure was explained by unusually long periods of meteorological stability, during which freshwater mixing was limited to a thinner surface layer, in which heat accumulation was favored. Higher nutrient concentrations in seawater were measured during 1972-1978 as compared to 1980-1985, despite the increased DIN and PO_4 levels in the Po River waters. This was due to higher flow rates in the earlier period. After 1986, the average flow rate of the Po River was similar to the preceding period, but the seawater concentrations of PO_4 were lower, whereas DIN and SiO_4 concentrations were higher, mainly due to changes in the Po River nutrient composition (Degobbis et al., 2000).

In relation to this, when compared at the same salinity (i.e. same dilution degree, independently from the freshwater discharge rate), the chlorophyll-a concentrations and the primary production rates were higher in periods of higher river PO_4 concentrations, but not of DIN concentrations. The mean Po River flow rate in recent years (2003-2009) was

significantly lower than in the previous period (1972-1999). Consequently, a marked increase in surface salinity and decrease in PO_4 and chlorophyll-a concentrations occurred in the eastern NAd during the more recent period (Djakovac et al., 2012), as well as at the western waters. Concurrently, a significant increasing trend of the DIN/PO_4 ratio occurred. A significant decreasing trend of the PO_4 and chlorophyll-a concentrations and an increasing trend of DIN and of DIN/PO_4 ratio were detected during the last four decades (Giani et al., 2012).

Other analyses over the period 1970-2007 confirmed the aforementioned observations, showing significant decreasing trends for PO_4, ammonium and chlorophyll-a concentrations in the NAd, but not for nitrate and SiO_4 (Solidoro et al., 2009; Mozetic et al., 2010). These changes were marked in the 2000s, particularly in the area directly affected by Po River discharges. In the more oligotrophic eastern coastal waters the decrement was the lowest, while intermediate values were obtained for the Gulf of Trieste, the Gulf of Venice and the central open waters. Related to this, the concentration of surface active organic substances, primarily phytoplankton exudates and their degradation products, also considerably decreased in the upper water column during the period 2003-2010 compared to 1998-2003 (Gasparovic, 2012; Giani et al., 2012).

The organic matter produced sinks to the bottom and undergoes strong bacterial regeneration with high apparent oxygen utilization (AOU), that during stratification periods (spring–summer), determines a sensible reduction of the oxygen concentration and a strong nutrient increase in the bottom layers. This situation is particularly evident on the western side of the basin, the most affected by the river inputs.

The middle Adriatic shows a much reduced influence of the riverine inputs, as the river-diluted, nutrient-rich waters are confined to the coastal areas of the basin during most of the year. Also the phytoplankton biomass is sensibly lower than in the northern Adriatic but it seems to control significantly the nutrient distributions. The Pomo Depressions appear as sites of strong nutrient cycling processes associated to the resident dense water.

Finally, the vertical distributions computed for the southern Adriatic show clearly that the MLIW is characterized by high levels of nitrate in all seasons with a well-defined seasonal cycle affecting also the nutrient concentrations in the deep water. In the surface layers the influence of the general cyclonic circulation on the horizontal distribution of the nutrients can be recognized.

A deficiency of phosphorus arise in both the surface and the deep water in the northern Adriatic and in the deep water of the rest of the basin. For the middle and southern Adriatic surface waters is clear a nitrogen deficiency particularly marked in the southern basin. In accordance with Zavatarelli et al. (1998) this result needs a more accurate analysis and also more information relative to the amount and distribution of phytoplankton biomass in the basin.

All of this information need to be better analyzed, harmonized and made available through a free repository (e.g. EMODnet) in order to be consulted or used by any stakeholder and, overall, for the implementation of descriptors and indicators specified by MSFD in the contest of different criteria identified for the GES. It is also necessary to perform further analyses, starting from both in situ observations (collected by Regional Agencies for the Environmental Protection) and from remote sensing ─ and where no data are available, from forecasting models ─ which keep into account adequate spatial-temporal scales.

The following work represents attempts to integrate and harmonize different sources of data in order to provide information at different spatial and temporal scales in one of the sub-region identified by MSFD, as request by the Directive.

In the first chapter, the output of three operational forecasting systems will be analyzed in order to identify the one with the best performance for the Adriatic Sea. In the second chapter, temporal patterns of key physical and biological parameters at the basin scale has been analyzed on the basis of forecasting models output and validated remote sensing data in order to improve our comprehension on ecosystem dynamics and potential changes related to global climate changes. In the last chapter, the role of nutrient loads related to river outflows on spatial and temporal dynamics of physical-chemical and biochemical variables in a coastal area of the Adriatic Sea (Marche Region) has been investigated.

References

Alvera-Azcarate A., Barth A., Rixen M., Beckers J.M. (2005) Reconstruction of incomplete oceanographic data sets using empirical orthogonal functions: application to the Adriatic Sea surface temperature. *Ocean Modelling* 9: 325–346.

Artegiani A., Azzolini R., Salusti E. (1989) On the dense water in the Adriatic Sea. *Oceanol. Acta*, 12: 151–160.

Artegiani A, Bregant D, Paschini E, Pinardi N, Raicich F, Russo A. 1996. The Adriatic Sea general circulation. Part I: Air-Sea interactions and water mass structure. Journal of Physical Oceanography 27 (8) 1492-1514.

Artegiani A, Bregant D, Paschini E, Pinardi N, Raicich F, Russo A. 1996. The Adriatic Sea general circulation. Part II: Baroclinic circulation structure. Journal of Physical Oceanography 27(8) 1515-1532.

Atkins JP, Burdon D, Elliott M, Gregory AJ. 2011. Management of the Marine Environment:Integrating Ecosystem Services and Societal Benefits with the DPSIR Framework in a SystemsApproach. *Marine Pollution Bulletin,* 62(2): 215-226.

Barale V, Schiller C, Tacchi R, Merachal C. 2005. Trends and interactions of physical and bio-geo-chemical features in the Adriatic Sea as derived from satellite observations. Science of Total Environment 353 (2005) 68-81.

Beg-Paklar G., Isakov V., Korain D., Kourafalou V., Orlić M. (2001) A case study of bora-driven flow and density changes on the Adriatic Shelf (January 1987) *Continental Shelf Research* 21 (16-17): 1751-1783.

Bergamasco A., Oguz T., Malanotte-Rizzoli P. (1999) Modeling dense water mass formation and winter circulation in the northern and central Adriatic Sea. *Journal of Marine Systems* 20: 279–300.

Borja Á, Elliott M. 2013. Marine monitoring during an economic crisis: the cure is worse thanthe disease. *Marine Pollution Bulletin* 68: 1-3.

Budillon G., Grilli F., Ortona A., Russo A., Tramontin M. (2002) An assessment of surface dynamics observed offshore Ancona with HF Radar. P.S.Z.N.: *Marine Ecology*, 23, Supplement 1, 21-37.

Buljan M. (1957) Fluctuation of temperature in the open Adriatic. *Acta Adriatica* 8(7): 1–26.

Buljan M., Zore-Armanda M. (1976) Oceanographical properties of the Adriatic Sea. *Oceanography and marine biology, Aberdeen University Press Ann. Rev.* 14, 11–98.

Cavaleri L., Lavagnini A., Martorelli S. (1996) The wind climatology of the Adriatic Sea deduced from coastal stations, *Nuovo Cimento*, 19: 37–50.

Claussen U, Connor D, de Vrees L, Leppänen JM, Percelay J, Kapari M, Mihail O, Ejdung G, Rendell J. 2011. Common Understanding of (Initial) Assessment, Determination of Good Environmental Status (GES) and Establishment of Environmental Targets (Art. 8, 9 & 10 640 MSFD). WG GES EU MSFD.

Cozzi, S.M., Giani, M. (2011). River water and nutrient discharges in the northern Adriatic Sea: current importance and long term changes. Continental Shelf Research 31:1881-1893

Cushman-Roisin B., Gačić M., Poulain P.M., Artegiani A. (2001) Physical Oceanography of the Adriatic Sea: Past, Present and Future. Kluwer Academic Publishers, Dordrecht/Boston/London.

Degobbis D., Gilmartin M. (1990) Nitrogen, phosphorus, and biogenic silicon budgets for the northern Adriatic Sea. *Oceanologica acta* 13:31-45.

Degobbis D., Fonda Umani S., Franco P., Malej A., Precali R., Smodlaka N. (1995) Changes in the northern Adriatic ecosystem and the hypetrophic appearance of gelatinous aggregates. *The Science of the Total Environment*, 165, pp. 43-58.

Degobbis D., Precali R., Ivančić I., Smodlaka N., Kveder S. (1997) The importance and problems of nutrient flux measurements for study eutrophication of the northern Adriatic. *Periodicum Biologorum* 99, 161-167.

Degobbis D., Precali R., Ferrari C.R., Djaković T., Rinaldi A., Ivančić I., Gismondi M., Smodlaka, N. (2005) Changes in nutrient concentrations and ratios during mucilage events in the period 1999-2002. *Science of the Total Environment* 353, 103-114.

Djakovac T., Degobbis D., Supic N., Precali R. Marked reduction of eutrophication pressure in the northeastern Adriatic in the period 2000-2009. Estuarine, coastal and shelf science 115 (1012) 25-32.

deYoung B, Barange M, Beaugrand G, Harris R, Perry R.I., Scheffer M, Werner F. Regime shift in marine ecosystems: detection, prediction and management. Trends in Ecology and Evolution 23(7) pp. 402-409.

Elliott M, Borja A, McQuatters-Gollop A, Mazik K, Birchenough S, Andersen J.H., Painting S, Peck M. 2016. Force majeure: will climate change affect our ability to attain Good Environmental Status for marine biodiversity?. Marine Pollution Bullettin

Franco P. (1983a) L'Adriatico settentrionale – caratteri oceanografici e problemi. Atti del 5° Congresso AIOL, 1-27.

Franco P. (1983b) Distribuzione verticale della produttività primaria e struttura della colonna d'acqua nell'Adriatico Settentrionale. Atti del 5° Congresso AIOL, 515- 524.

Franco P, Michelato A. (1992) Northern Adriatic Sea: oceanography of the basin proper and of the western coastal zone. *Sci Total Environ* 35–62 [Suppl].

Franco P., Bregant D., Voltolina D. (1982) Oceanography of the middle Adriatic Sea. Data from the cruises December 1970, March–April 1971 and March 1972. *Archo. Oceanol. Limnol*. 20 (suppl. 1): 1–72.

Giani M, Djakovac T, Degobbis D, Cozzi S, Solidoro C, Fonda Umani S. 2012. Recent changes in the marine ecosystems of the northern Adriatic Sea. Estuarine, Coastal and Shelf Science 115 (2012) 1-13.

Hoegh-Guldberg O., Bruno, J.F.. The impact of climate change on the world's marine ecosystems. Science328 (2010) pp.1523-1528.

Justić D. (1991) An analysis of factors affecting oxygen depletion in the northern Adriatic sea. *Acta Adriatica* 32 (2) 741-752.

Justić D., Legović T., Rottini-Sandrini L. (1987) Trends in oxygen content 1911-1984 and occurrence of benthic mortality in the northern Adriatic Sea Estuarine Coastal and Shelf Science 25(4):435-445.

Luisetti T, Turner RK, Jickells T, Andrews J, Elliott M, Schaafsma M, Beaumont N, Malcolm, Burdon D, Adams C, Watts W. 2014. Coastal Zone Ecosystem Services: From science tovalues and decision making; a case study. *Science of the Total Environment* 493: 682–693.

Marchetti R. (1984) Quadro di sintesi delle indagini svolte dal 1978 sul problema dell'eutrofizzazione delle acque costiere dell'Emilia-Romagna. Atti Convegno: Eutrofizzazione dell'Adriatico: Ricerche e linee di intervento. 18-20 Maggio 1983: 37-75.

Meier HEM, Eilola K, Almroth E. 2011. Climate-related changes in marine ecosystemssimulated with a 3-dimensional coupled physical-biogeochemical model of the Baltic Sea.*Climatic Research* 48, 31-55

Orlić M., Gačić M., La Violette P.E. (1992) The currents and circulation of the Adriatic Sea. *Oceanol. Acta* 15: 109-124.

Poulain P.M. (1999) Drifter observations of surface circulation in the Adriatic Sea between December 1994 and March 1996, *J. Mar. Syst.* 20: 231–253.

Poulain P. M. (2001) Adriatic Sea surface circulation as derived from drifter data between 1990 and 1999. *Journal of Marine Systems* 29: 3– 32.

Poulain P. M., Mauri E., Ursella L. (2004) Unusual upwelling event and current reversal off the Italian Adriatic coast in summer 2003. *Geophysical Research Letters*, Vol. 31, L05303, doi: 10.1029/2003GL019121.

Pucher-Petković T. (1963) Rapports quantitatifs entre les divers groupes du phytoplancton en Adriatlque rnoyenne. *Rapp. Comm. lnt Mer Medit*. 17: 479-485.

Pullen J., Doyle J.D., Haack T., Dorman C., Signell R.P., Lee C.M. (2007) Bora event variability and the role of air-sea feedback. *Journal of geophysical research*, 112: C03S18, doi:10.1029/2006JC003726.

RaicichF. (1996) On the fresh water balance of the Adriatic Sea, *Journal of Marine Systems* 9: 305-319.

Revelante N., Gilmartin M. (1976a) The effect of Po river discharge on phytoplankton dynamics in the Northern Adriatic Sea, Mar. Biol., 34, 259-271.

Revelante N. Gilmartin M. (1976b) Temporal succession of phytoplankton in the Northern Adriatic. Neth. J. Sea Res., 10 (3), 377-396.

Revelante N., Gilmartin M. (1995) The relative increase of larger phytoplankton in a subsurface chlorophyll maximum of the Northern Adriatic Sea. *J. Plankton Res.,* 17 (17): 1535-1562.

Roether W., Schlitzer R. (1991) Eastern Mediterranean deep water renewal on the basis of chlorofluoromethane and tritium data. *Dyn. Atmos. Oceans* 15: 333–354.

Russo A, Artegiani A. (1996). Adriatic Sea hydrography. Scientia Marina 60 (2): 33-43.

Russo A., Maccaferri S., Djakovac T., Precali R., Degobbis D., Deserti M., Paschini E., Lyons D.M. (2005) Meteorological and oceanographic conditions in the northern Adriatic Sea during the period June 1999–July 2002: Influence on the mucilage phenomenon, *Science of the Total Environment* 353: 24– 38.

Smodlaka N. (1986) Primary production of the organic matter as an indicator of the eutrophication in the northern Adriatic sea. *The Science of The Total Environment* 56: 211-220.

Smodlaka N., Revelante N. (1983) The trends of phytoplankton production in the Northern Adriatic Sea: A twelve year survey. *Rapp Comm int Mer Médit* 28:89-90.

Stachowitsch M. (1984) Mass mortality in the Gulf of Trieste: The course of community destruction. *P.S.Z.N.I: Mar. Ecol*. 5:243–264.

Stachowitsch M., Riedel B., Zuschin M., Machan R. (2007) Oxygen depletion and benthic mortalities: the first in situ experimental approach to documenting an elusive phenomenon. *Limnol. Oceanogr.: Methods* 5, 344–352.

Šimunović A., Piccinetti C., Zore-Armanda M. (1999) Kill of benthic organisms as a response to an anoxic state in the northern Adriatic: (a critical review). *Acta Adriatica* 40 (1): 37-64.

Travizi A. (2000) Effect of anoxic stress on density and distribution of sediment meiofauna. *Periodicum biologorum* 102 (2): 207-215.

Travizi A., Vidaković J. (1994) An evaluation of eutrophication effects on northern Adriatic meio-and nematofauna communities. *Periodicum biologorum* 96 (4): 469-473.

Turner K, Schaafsma M, Elliott M, Burdon D, Atkins J, Jickells T, Tett P, Mee L, van Leeuwen
S, Barnard S, et al. 2014. UK National Ecosystem Assessment Follow-on. Work PackageReport 4: Coastal and marine ecosystem services: principles and practice. UNEP-WCMC,LWEC, UK.

Vested H.J., Berg P., Uhrenholdt T. (1998) Dense water formation in the Northern Adriatic. *Journal of Marine Systems* 18 (1-3): 135-160.

Viličić D. (1989) Phytoplankton population density and volume as indicators of eutrophication in the eastern part of the Adriatic Sea. *Hydrobiologia* 174: 117-132.

Viličić D. (2002) Fitoplankton Jadranskog mora: biologija i taksonomija. [Phytoplankton of the Adriatic Sea: biology and taxonomy]. Zagreb: Školska knjiga, 247 pp.

Vilibić I. (2003) An analysis of dense water production on the North Adriatic shelf. *Estuarine, Coastal and Shelf Science* 56: 697–707.

Vilibić I., Orlić M. (2002) Adriatic water masses, their rates of formation and transport through the Otranto Strait *Deep-Sea Research I* 49: 1321–1340.

Vilibić I., Grbec B., Supić N. (2004) Dense water generation in the north Adriatic in 1999 and its recirculation along the Jabuka Pit. *Deep-Sea Research I* 51: 1457–1474.

Viličić D., Jasprica N., Carić M., Burić Z. (1998) Taxonomic composition and seasonal distribution of microphytoplankton in Mali Ston Bay (eastern Adriatic). *Acta Botanica Croatica* 57: 29–48.

Viličić D., Marasović I., Mioković D. (2002) Checklist of phytoplankton in the eastern Adriatic Sea. *Acta botanica Croatica* 61 (1): 57-91.

Vučetić T. (1970) Fluktuacije zooplanktona na srednjem Jadranu. *Pomorski zbornik* 8: 867-881.

Zampoukas N, Palialexis A, Duffek A, Graveland J, Giorgi G, Hagebro C, Hanke G,Korpinen S, Tasker M, TOrnero V, Abaza V, Battaglia P, Caparis M, Dekeling R, Frias Vega M, Haarich M, Katsanevakis S, Klein H, krzyminski W, Laamanen M, LeGac J.C, Leppanen J.M, Lips U., Maes T, Magaletti E, Malcolm S, Marques J.M, Mihail O, Moxon R, O'Brein C, Panagiotidis P, Penna M, Piroddi C, Probst W.N, Raicevich S, Trabucco B, Tunesi L, van der Graad S, Weiss A, Wernersoon A.S, Zevenboom W. Technical guidance on monitoring fot the Marine Strategy Framework Directive. Joint Research Center Scientific and policy reports, 2014.

Zanchettin D., Rubino A., Traverso P., Tomasino M (2008). Impact of variations in solar activity on hydrological decadal patterns in northern Italy. Journal of geophysical research, Vol. 113, D12102, doi:10.1029/2007JD009157, 2008.

Zavatarelli M, Raicich F, Bregant D, Russo A, Artegiani A. 1998. Climatological biogeochemical characteristics of the Adriatic Sea. Journal of Marine Systems 18 (1998) 227-263.

Zore-Armanda M. (1963) Les masses d'eau de la mer Adriatique. *Acta Adriat*., 10: 1–94.

Zore-Armanda M. (1969) Water exchange between the Adriatic and the Eastern Mediterranean. *Deep-Sea Res*. 16:171-178.

Chapter 1

Quality check of forecasting system output

Introduction

Ocean physical processes play a crucial role in governing marine dynamics (acoustical, biological and sedimentological). Changes due, for example, to global warming, human pressure, storm events, flash floods, cumulative effect of multiple stressors, and long-term ocean and coastal changes, can have cascading effects in environmental goods and services supplying.

The Adriatic Sea is a complex natural system (Russo and Artegiani, 1996) strongly impacted by human activities and highly vulnerable to global warming (Micheli et al., 2013). Cumulative effects of these two drivers can have synergic effect amplifying degradation processes of coastal-marine system. Understanding of such dynamics can greatly contribute to improve our knowledge about the functioning of marine sub-systems as well as dynamics of the more vulnerable coastal zone (Warner et al., 2010).

Monitoring activities are fundamental to define functioning and variability of marine system. In the Adriatic Sea sampling activities were carried out since the beginning of 19th century, with improvements from the middle of the century (Pollack, 1951; Zore-Armanda, 1956; Zore-Armanda, 1963; Hopkins, 1978)up to recent past and present, where monitoring activities are mainly carried out by Regional Agencies for Environmental Protection. Nevertheless, limitation of observational *in situ* data due to spatial temporal fragmentation makes them not completely suitable for dynamics definition, requiring an integration able to fill spatial-temporal gaps.

By employing observational data, acquired knowledge and increasing capability to predict ocean and coastal processes will increase the ability to effectively manage and prepare for response to marine system changes (Warner et al., 2010).

Operational forecasting of physical ocean fields can greatly contribute in providing an efficient supporting tool for marine environmental management. For several applications such as fisheries management, naval operations, shipping, tourism, administration of marine resources and also for pure scientific purposes, high-resolution ocean forecasts are frequently required for limited regions. Focusing on characteristic scales, processes and dynamics of a limited area, allows devoting particular attention to regionally specific

numerical requirements (i.e. approximations, parameterizations, resolution and numerical techniques). Currently, several numerical models exist based on the same physical assumptions, and each single model shows its specific behavior. Since model results derive from physical laws warped by numerical discretization techniques, the possibility of having several numerical models implemented in the same area increases the confidence in model results (Chiggiato and Oddo, 2008).On the other hand, the increasing complexity of ocean forecasting models require an assessment of their prediction skills aimed to improve numerical simulation capabilities and to quantify their reliability in comprehension of ocean and coastal dynamics.

First part of the PhD work aims to assess the reliability of three principal forecasting system output of the Adriatic Sea in comparison with observational data in order to verify the possibility to employ daily regional scale forecasted data to investigate tridimensional thermohaline conditions and their potential variations over time.Thermohaline conditions play a fundamental role in governing biological dynamics of ecosystems (Stachowicz et al., 2002) such as presence or absence of certain species, their recruitment, migration, introduction and persistence of non-indigenous species. Understanding the effects of short-term fluctuation of these variablesin environmental conditions, especially for temperature, is one approach to developing better predictions regarding also the ecological effects of future climate change.

Materials

In this section, three operational forecasting systems for the Adriatic Sea are described along with observational data employed to check the quality of their output.

AdriaROMS

AdriaROMSis the operational ocean forecast system for the Adriatic Sea running at the Hydro-Meteo-Clima Service (ARPA-SIMC)of Emilia Romagna Region in Bologna (Italy). It is based on the Regional Ocean Modelling System (ROMS, detailed kernel description is in Shchepetkin and McWilliams, 2005; Haidvogel et al., 2008). This Adriatic configuration has a horizontal resolution of 2 km with 20 s-coordinate levels for the vertical. A third order upstream scheme is used for advection (Shchepetkin and McWilliams, 1998); a

Laplacian operator adds a weak grid-size dependent on horizontal diffusivity, while no horizontal viscosity is used. The Mellor and Yamada (1982) 2.5 scheme is used for the vertical mixing, and density Jacobian scheme with spline reconstruction of the vertical profiles is used for the pressure gradient (Shchepetkin and McWilliams, 2003). The model was initialized in September 2004 from the Mediterranean Forecasting System – General Circulation Model (MFS-GCM) fields optimally interpolated onto AdriaROMS grid, then run in pre-operational configuration until June 2005 when the first forecasts were published on the web. A detailed description of AdriaROMS is provided in Russo et al.(2009), with updates in Russo et al. (2013) and Falcieriet al. (2013).Surface forcing is provided by COSMO-I7, the implementation over Italy of the model developed by the Consortium for Small-scale Modeling (COSMO,http://www.cosmo-model.org/)).COSMO-I7 is a non hydrostatic numerical weather prediction model,run operationally by the Italian Air Force Meteo Service and by ARPA-SIMC,with 7 km horizontal resolution providing tri-hourly shortwave radiation, 10 m wind, 2 m temperature, relative humidity, total cloud cover, mean sea level pressure and precipitation. All thecited parameters are used to compute momentum and heat fluxes. Long wave radiation is estimated using Berliand formula (Budyko, 1974), turbulent fluxes following Fairall et al. (1996), while no evaporation precipitation flux was included (added in a later version). MFS-GCM data are used at the open boundary to the south (see Fig. 1) with clamped boundary conditions with superimposed four major tidal harmonics (S2, M2, O1, K1), from the work of Cushman-Roisin and Naimie (2002), following Flather (1976). Forty-eight rivers and springs are included as well, using monthly climatological values from Raicich (1996). Persistence of daily discharge measured one day backward is used for the Po River.

Coupled ocean-atmosphere-wave-sediment transport (COAWST) modeling system

The Coupled Ocean–Atmosphere–Wave–Sediment Transport (COAWST) Modeling System (Warner et al., 2008) is comprised of several components that include models for the ocean, atmosphere, surface waves, sediment transport, a coupler to exchange data fields, and a method for regridding. The Model Coupling Toolkit as the coupler to exchange data fields between the ocean model ROMS, the atmosphere model WRF, the wave model SWAN, and the sediment capabilities of the Community Sediment Transport

Model. These components, improvements to individual components, and the coupling are described below.

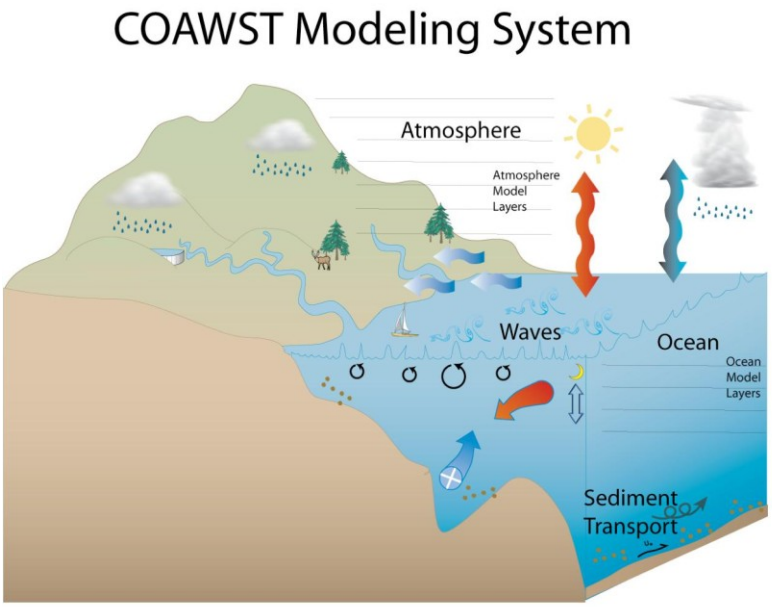

Fig. 1– *The COAWST Modeling System comprising a coupler (MCT) that provides exchange between an ocean model, an atmosphere model, a waves model and a sediment transport model (Warner et al., 2010)*

The ocean model is the previously cited Regional Ocean Modeling System (ROMS), a general class of free surface, terrain-following numerical models that solve the three dimensional Reynolds-averaged Navier–Stokes equations (RANS) using the hydrostatic and Boussinesq approximations. ROMS uses finite-difference approximations on a horizontal curvilinear Arakawa C grid and on a vertical stretched terrain-following coordinate. Momentum and scalar advection and diffusive processes are solved using transport equations and an equation of state computes the density field that accounts for temperature, salinity, and suspended-sediment contributions. ROMS provides a flexible structure that allows multiple choices for many of the model components such as several options for advection schemes (second order, third order, fourth order, and positive definite), turbulence models, lateral boundary conditions, bottom and surface-boundary layer sub-models, air–sea fluxes, surface drifters, a nutrient-phytoplankton-zooplankton model, and an adjoin model for computing model inverses and data assimilation. The code is written in Fortran90 and runs in serial mode on a single processor, or uses either shared or distributed-memory architectures (OpenMP or MPI) to run on multiple processors (Warner et al., 2010).

The atmospheric model component in the coupled system is the Advanced Research Weather Research and Forecasting (WRF) Model (ARW; Skamarock et al., 2005). It is a nonhydrostatic, quasi-compressible atmospheric model with boundary layer physics schemes and a variety of physical parameterizations of sub-grid scale processes for predicting meso- and microscales of motion. The model predicts three-dimensional wind momentum components, surface pressure, dew point, precipitation, surface sensible and latent heat fluxes, longwave and shortwave radiative fluxes, relative humidity, and air temperature on a sigma-pressure vertical coordinate grid.WRF has been used extensively for operational forecasts (http://www.wrf-model.org/plots/wrfrealtime.php) as well as for realistic and idealized research experiments.

The wave model is Simulating WAves Nearshore (SWAN; Booij et al., 1999). It is a spectral wave model specifically designed for shallow water that solves the spectral density evolution equation. SWAN simulates wind wave generation and propagation in coastal waters and includes the processes of refraction, diffraction, shoaling, wave–wave interactions, and dissipation due to white capping, wave breaking, and bottom friction.

The sediment modeling component is developed by the Community Sediment Transport Modeling System (CSTMS; Warner et al., 2008b). The sediment routines consist of algorithms for suspended-sediment transport, bed load transport for current and wave–current forcing, enhanced bottom stress due to surface waves, a multiple bed model to track stratigraphy, morphology, and the ability to transport multiple sediment classes.

All the cited components are integrated into the COAWST modeling system. However they are identified as a separate set of routines and can be extracted as a separate entity. These routines have been demonstrated to simulate a variety of inner shelf and estuarine sediment processes.

The coupler is the Model Coupling Toolkit that allows the transmission and transformation of various distributed data between component models using a parallel coupled approach. MCT is a program written in Fortran90 and works with the MPI communication protocol. It is compiled as a set of libraries, which are linked during the compilation. During model initialization each model decomposes its own domain into sections (or segments) that are distributed to processors assigned for that component. Each grid section on each processor initializes into MCT, and the coupler compiles a global map to determine the distribution of model segments. Each segment also initializes an attribute vector that contains the fields to be exchanged and establishes a router to provide an exchange pathway between model

components. During the run phase of the simulation the models will reach a predetermined synchronization point, fill the attribute vectors with data, and use MCT _send and _receive commands to exchange fields (Warner et al., 2008c).

For the Adriatic Sea, two release of COAWST system were running: the first has been running since 2011 in ARPA-SIMC(COAWST-C from now on), the other one since 2013 in Regione Marche (one of the 20 administrative Regional Institutions of Italy) at Ancona and represents an improved version of the first one (COAWST-D from now on). All forecasts are produced every day for the subsequent 72 hour with hourly resolution for the northern part of the Adriatic Sea at 0.5 × 0.5 km horizontal resolution and 12 s-coordinate vertical level. Details about COAWST-C and COAWST-D, as well as AdriaROMS, can be found in Russo et al. (2013 a,b), Falcieri et al. (2013), Brando et al. (2015), Carpi et al. (2015), Carlson et al. (2016).

Mediterranean forecasting system re-analysis data

The Mediterranean Forecasting System (MFS) physical reanalysis component, is a long term (26 years) reanalysis of temperature, salinity and currents of the Mediterranean Sea.MFS is based ona hydrodynamic model, supplied by the Nucleous for European Modelling of the Ocean (NEMO), with a variational data assimilation scheme (OceanVAR) for temperature and salinity vertical profiles and satellite Sea Level Anomaly along track data. The model horizontal grid resolution is 1/16°(ca. 6-7 km) and the unevenly spaced vertical levels are 72.

The model is implementedin the Mediterranean Basin and also extend into the Atlantic in order to better resolve the exchanges with the Atlantic Ocean at the Strait of Gibraltar. The NEMO model is nested, in the Atlantic, within the monthly mean climatological fields computed from ten years of daily output of the 1/4° x 1/4° degrees global model (Drevillon et al., 2008)

The assimilated data include: sea level anomaly, sea surface temperature, in situ temperature profiles by VOS XBTs, in situ temperature and salinity profiles by ARGO floats, and in situ temperature and salinity profiles from CTD.

The analysis is done weekly using a daily assimilation cycle. This means that in order to produce an analysis, the model is run for 24 hours and the analysis is produced at the end

of the day assimilating all and only the data available in that time window (filter mode). The daily analysis cycle is done once a week, each Tuesday, producing 13 past analyses and the present day analysis. Each day a 10 days forecast is produced starting on Tuesday from an analysis and each of the successive six days from a model simulation. A MFS quality assessment has been performed by Adani et al. (2011) by means of global ocean reanalysis technique in order to produce a consistent three-dimensional estimate of ocean circulation from observations and model simulations. The product of such operation is named re-analysis.

Reanalysis is like an analysis done with a consistent model and data assimilation scheme for the period of interest, yielding to a temporally homogeneous gridded dataset (Glickman 2000; see online at http://amsglossary.allenpress.com/glossary).

In this case, the reanalysis have been initialized with a gridded climatology for Temperature and Salinity computed from in-situ data sampled before 1987 (PRE-TRANSIENT climatology) from SeaDataNet FP6 project. The model has been initialized at the 1st January 1985. The assimilation of the available satellite and in situ data is done since January 1st 1985 too. Two year of spin-up are considered, thus the available data starts in 1987.

The MFS reanalysis are distributed through the Copernicus Marine Environment Monitoring System (CMEMS; http://marine.copernicus.eu).

In situ measurements

Two extensive dataset of CTD measurements (Figure 1) were collected during several ISMAR-CNR (Institute of Marine Sciences of the Italian Council of National Research) oceanographic cruises. First dataset consist of 843 of CTD casts collected in the northern and middle Adriatic Sea from 2011 to 2014, as shown below, and was employed for AdriaROMS and COAWST comparison.

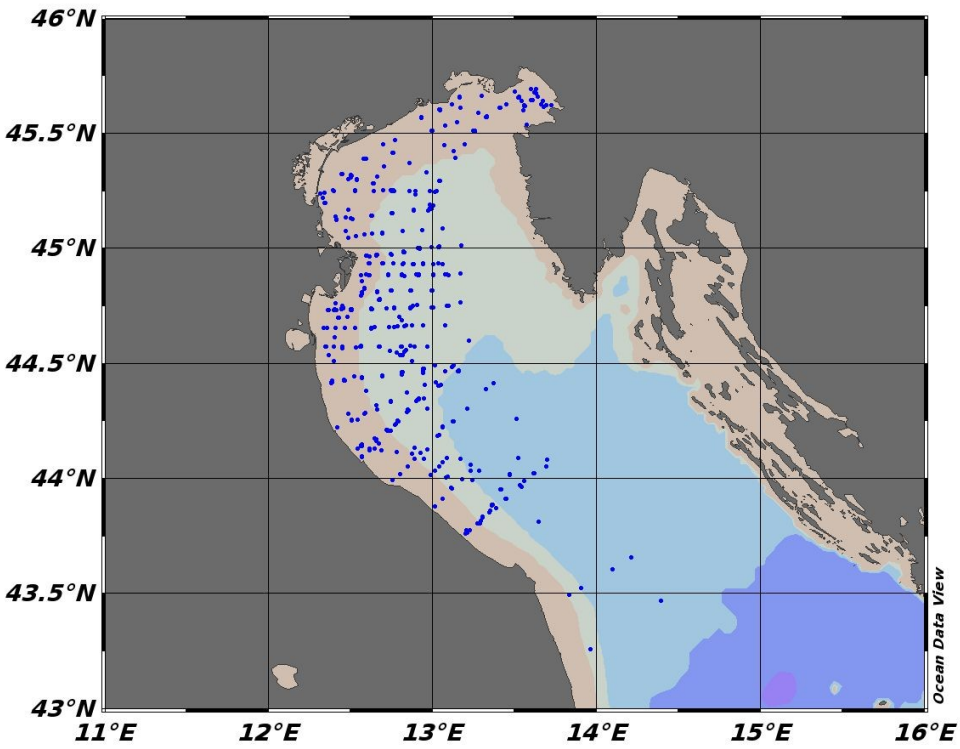

Figure 1– Stations point of CTD measurements exploited in data comparison with AdriaROMS and COAWST output.

A second larger dataset was employed given the wider temporal coverage of MFS re-analysis data. It consists of 17.450 CTD casts measured between 1987 and 2005 as shown in Figure 2.

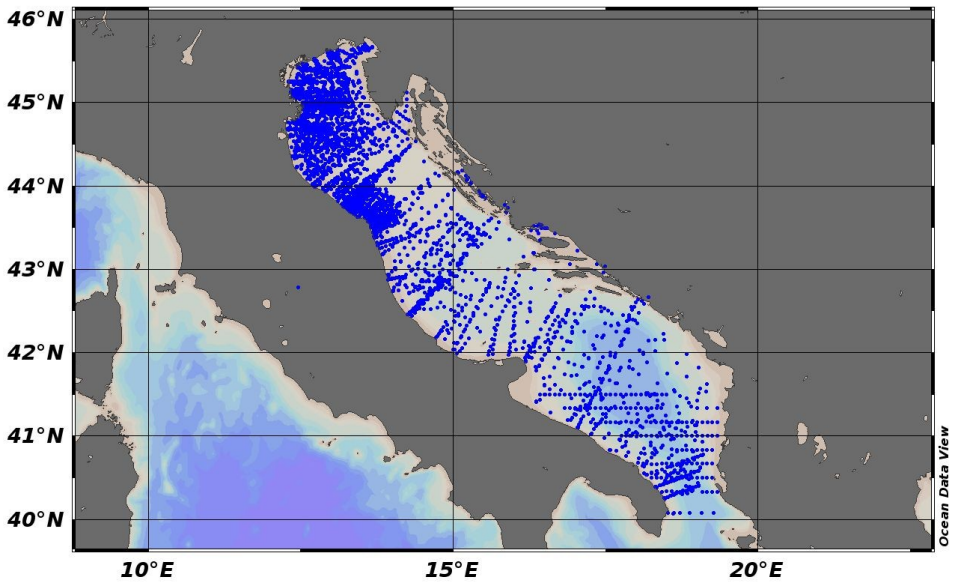

Figure 2 - Stations point of CTD measurements exploited in data comparison with Mediterranean Forecasting System re-analysis data.

Sea surface temperature

In the framework of the CMEMS, different L3S remotely-sensed Sea Surface Temperature (SST) products are operationally produced and distributed in near- real time by the Istituto di Scienze dell'Atmosfera e del Clima - Gruppo di Oceanografia da Satellite (ISAC- GOS) of CNR(Rome, Italy).

A single daily super-collated image (L3S) is obtained by merging different L3P images (if present). However, the SST estimated from one sensor might significantly differ from that retrieved by another, mainly as a consequence of the differences among the sensors (number of bands, spectral resolution, scanning/viewing geometry, etc.) and/or of the different algorithms applied, which, in particular, might correct very differently the atmospheric contribution to the measured brightness temperature. Consequently, a bias adjustment procedure is applied to L3P data before super-collating. Two different algorithms are used in the ISAC-GOSHR and UHR processing, both selecting the best measure available for each pixel.

The HR scheme corrects the biases among the images by adjusting them to a reference SST (which is updated every time a corrected image is added to the merged map). Here, best is defined through a pre-determined sensor validation statistics, and a simple hierarchy of sensors is identified coherently. During the collating procedure, before adding the new data to the merged map, the large scale bias between each new image and the pixels that have already been merged is estimated and removed. In this phase, an additional check on cloud contamination is performed by flagging the pixels that result to be colder (by a fixed threshold) than the previous day value, as measured in the corresponding L3S.

The UHR scheme is based on a different definition of best measure, which keeps into account the continuity of the data present in the single image. The bias is not estimated with respect to the higher accuracy sensor data but between each image and the first guess field, which is build directly from the HR L4 SST (see reference below). This bias is estimated and removed locally (50 km). The best data are then selected basing on a measure of each image data sparseness (spotty/scattered data being qualified as worse; Buongiorno et al., 2012).

Data employed for my purpose had 0.01° spatial resolution (UHR, about 1 km) and daily temporal resolution, starting from November 2011 up to January 2014.

Methods

Data from MFS, AdriAROMS, COAWST and from sampling stations had different format. So, first fundamental step consisted in a standardization of data format on the base of our purpose. For the sake of readability, where necessary, data were exported in text files and re-organized in chronological order, especially for observed datasets. Moreover, a form was establish for all the available data ─ cruise, station, data, time, longitude, latitude ─ excluding all the unnecessary information. Finally, data affected by recording errors were corrected or, most often, removed.

All the analysis described below was made in a LINUX operative system by means of its shell, and employing MATLAB® (release R2007b and R2012b) and Ocean Data View (ODV; Schiltzer, 2013) software (release 4.5.3).

Qualitative comparison

Preliminary investigation on data mismatching has been performed using a qualitative approach. Visual comparison provides a quick preliminary tri-dimensional idea of major mismatching between observations and models output.

First, Sea Surface Temperature from satellite measurement were plotted for each day by means of *mapping toolbox* in MATLAB.

The first discriminatory variable was the cloud cover: if the number of pixels with no values ─ cloud covered ─was higher than 50% of the entire basin (e.g. Fig. 3), daily data was rejected, otherwise observed data were plotted along with models SST output for the same day (Fig. 4).

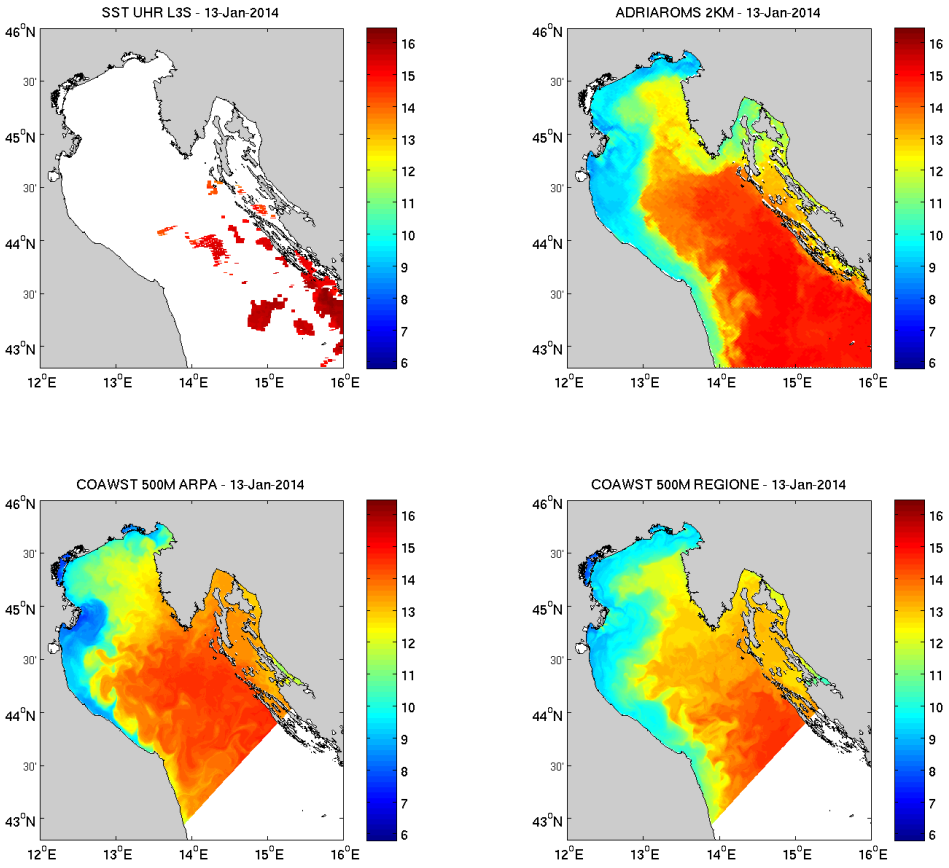

Figure 3 – Example of rejected satellite Sea Surface Temperature data (high-left corner) because of the extensive cloud cover.

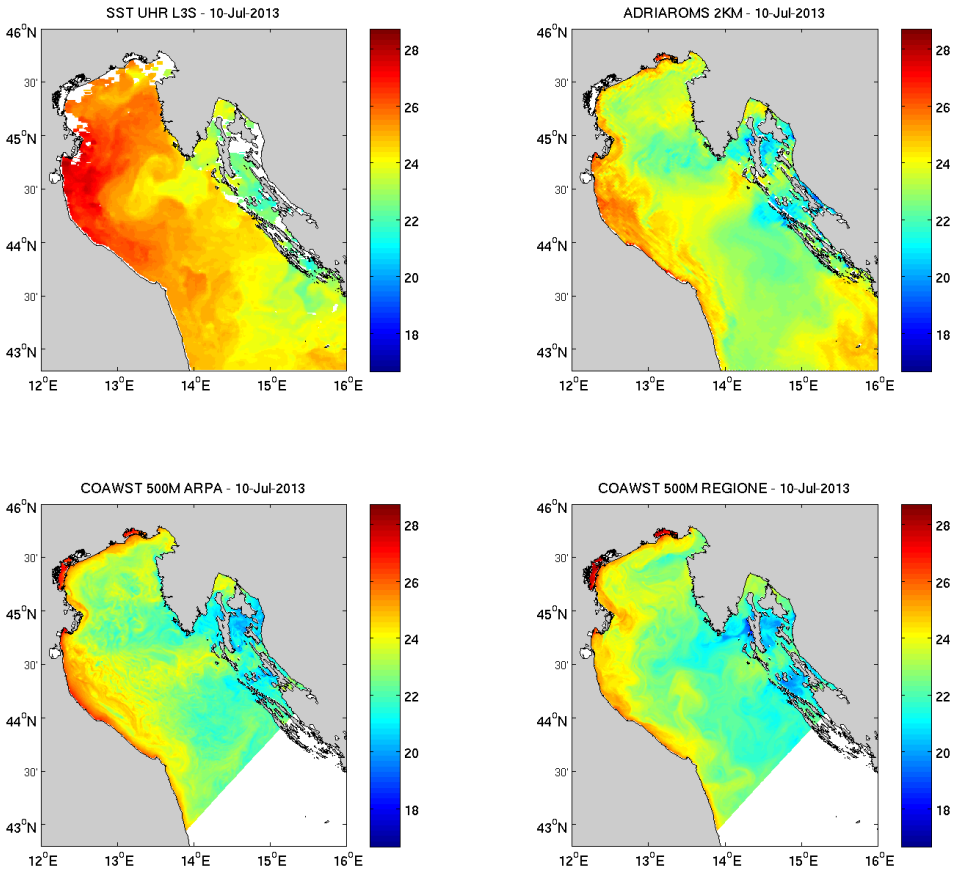

Figure 4 – Example of Ultra High Resolution (UHR) Sea Surface Temperature (SST) plotted in a representative day in summer 2013. Satellite data are reported in higher left corner, followed by the three forecasting systems.

In order to highlight vertical behavior of forecasting models, observed *in situ* CTD profiles were compared with models output using ODV to generate plots. Given the spatial and temporal fragmentation of CTD measures, a temporal selection was made along with spatial interpolation. In this case it was possible to obtain information on temperature and salinity mismatching.

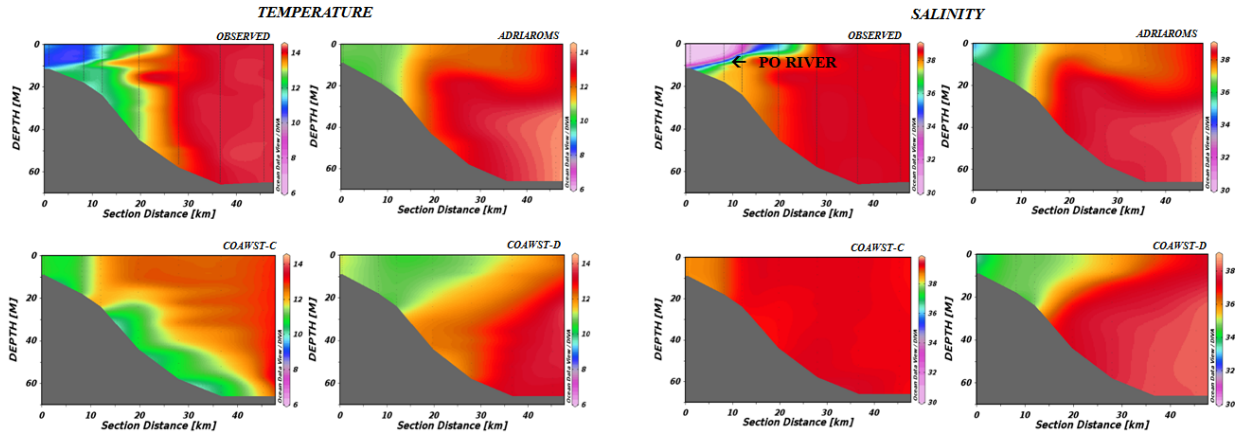

Figure 5 – Example of vertical profiles plot. The transect was taken at Po river mount.

Quantitative comparison

In order to quantify effective mismatching between simulations output and observations, only *in situ* measurements were employed.

A procedure was created for each one of the three forecasting systems. Given the data format, the procedure created for AdriaROMS and COAWST systems will be described together, while the one created for MFS re-analysis data will be considered apart.

After data importing, a standardization of time in MATLAB format was made along with the adjustment of threshold values of 30 minutes for the comparison of the time steps.

Observed vertical profiles were separated on the basis of depth and a progressive number was assigned to each one of them. Models vertical profiles were easier detectable given the standardization of the vertical levels.

A very important step consists in interpolation of depth of the forecasted variables (temperature and salinity) on the depths of observed profiles. In this way we can perform a more correct vertical comparison. Mean values, standard deviations and variance were computed for observed and forecasted variables. Given the differences between depths, it is possible that some model values are not valid (*not a number, NaN*) in the upper and deeper layers. In order to avoid *NaN* values, first and last values from surface and bottom model profile, respectively, were duplicated.

For each interpolated depth of each profile mean bias, mean absolute error, root mean square error and cross correlation for both temperature and salinity were computed (Figg. 6-7). Finally, profile metadata were updated.

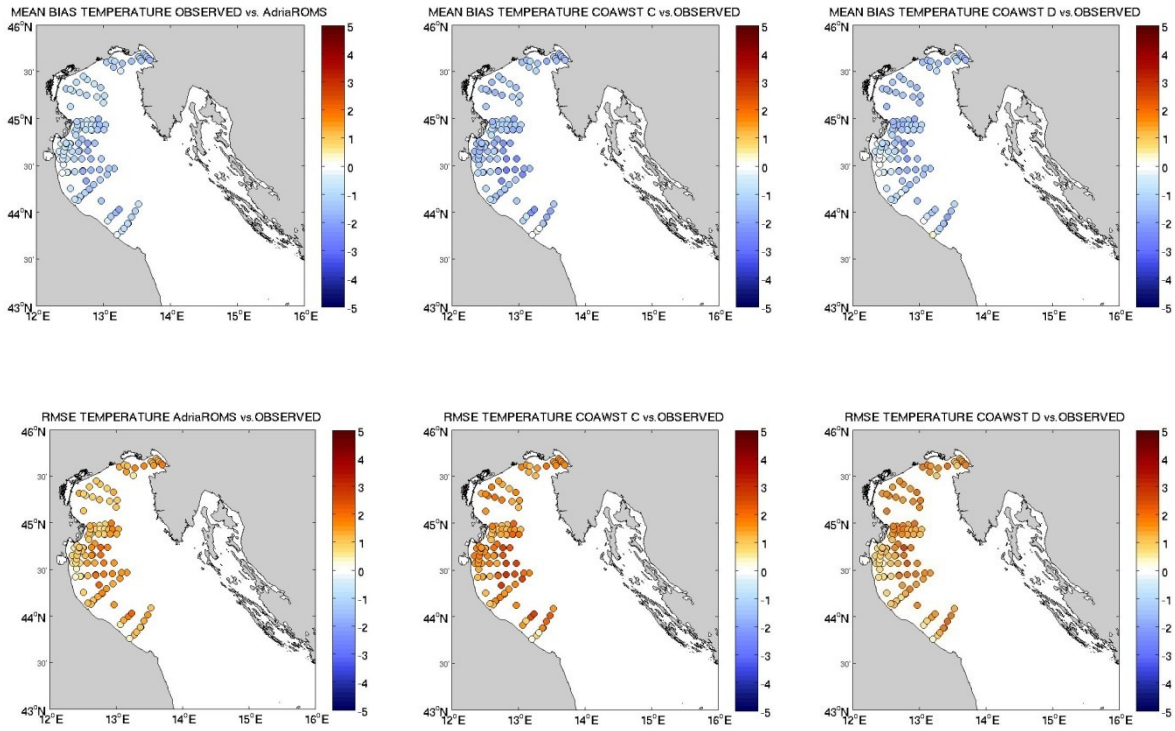

Figure 6 – Example of mean bias (first row) and root mean square error (secondo row) between observed data and AdriaROMS (first column), COAWST-C (second column) and COAWST-D (third column) for temperature values.

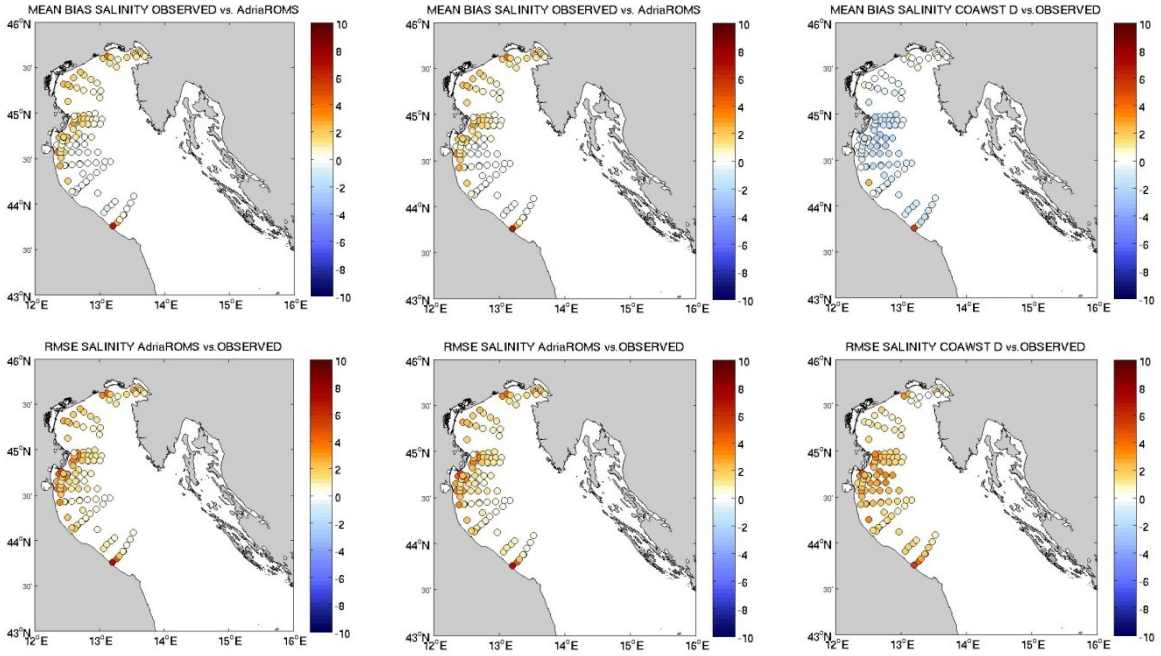

Figure 7 – Example of mean bias (first row) and root mean square error (second row) between observed data and AdriaROMS (first column), COAWST-C (second column) and COAWST-D (third column) for salinity values.

To better highlight the mismatching between observations and models, a Taylor diagram was plotted (Fig. 8) for temperature and salinity.

Given the structure of the created script, particular attention is necessary for the last profile. Basically, it must be treated separately but with the same procedure. A similar procedure was created for MFS re-analysis data, with difference in data import method (Fig. 9).

Results

In this section, results from AdriaROMS and the two releases of COAWST output quality check are discussed together, followed by discussion about MFS re-analysis data comparison. Reported statistics are relative to the entire water column and are spatial-temporal averaged, allowing to have a general comprehensive idea of models performance.
Hydrodynamic forecasting system AdriaROMS and two release of coupled wave-current COAWST systems output were compared with measured data of the Adriatic Sea for the period 2010-2014. The main objectives was to check models capability in reproducing thermohaline regime of the Adriatic Sea in order to understand at wider spatial-temporal scale its dynamics.
Although all the three systems require a detailed bias correction, AdriaROMS demonstrated a better performance for both temperature and salinity (Table 1), followed by the second release of COAWST, as shown in Table 1. Smaller values of mean bias (MB) and root mean square error (RMSE), especially for temperature, and higher value of cross correlation (CC)for COAWST-D in comparison with AdriaROMS could be partially explained by the higher spatial resolution (0.5×0.5 km^2 vs. 2×2 km^2) of the former and by the fact that it takes into account effects of waves on the currents; aspects that in principle would allow for a better reproduction of the dynamics. On the other hand, the performance of the first release of COAWST was unsatisfactory, especially for salinity.
Temperature values predicted by the models were generally underestimated probably due to a not correct computation of heat content derived by the systems initialization and the horizontal diffusion problems that arise where cold coastal waters spread inside the basin (Oddo et al., 2005). A possible overestimation of Bora wind blowing predicted by COSMO model could also cause heat losses higher than the real ones.
Analyzing the general performance on salinity, all the systems have larger MB and RMSE in coastal zones. This is easily explained by the difficulty to simulate the exact salinity in the western coastal current, since the models are anyway using climatological data for all rivers except the Po River. In fact, errors decrease going toward deeper locations. Based on MB, RMSE and CC, AdriaROMS is generally the most accurate and provides, in any case, a wider spatial coverage necessary for the purpose of this work. Moreover, these results expand previous findings using the same forecasting system outputs (Tonani et al., 2009; Chiggiato and Oddo, 2008) confirming the correctness of the procedure created for the

purpose, and point out the need to improve such systems before they can be effective in monitoring of temperature and salinity or in correct reproduction of past dynamics. The available temporal scale can only partially satisfy the comprehension of long term water mass circulation in the Adriatic Sea, but it can be anyway considered a starting point for such kind of analysis.

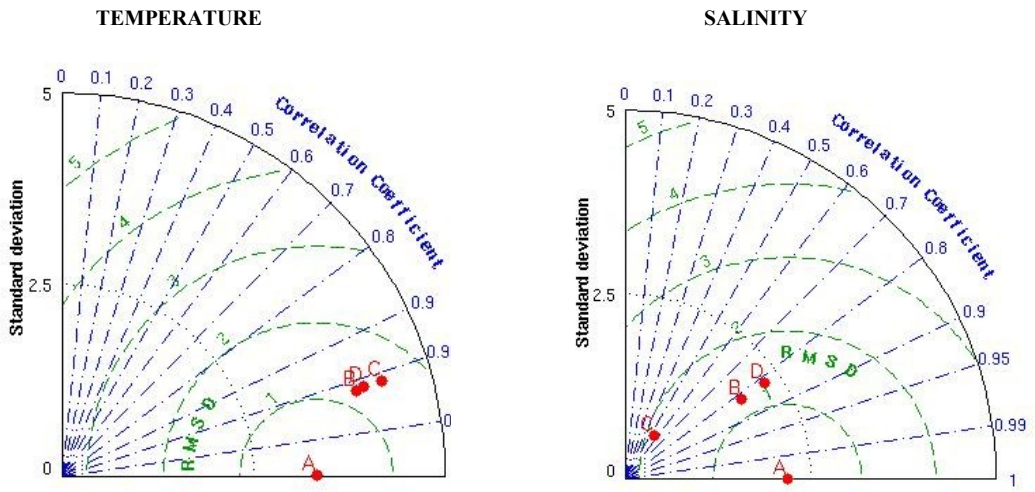

Figure 8– Temperature and salinity mismatching between observations A, AdriaROMS B, COAWST first release C (ARPA-SIMC) and COAWST second release D (Marche Region).

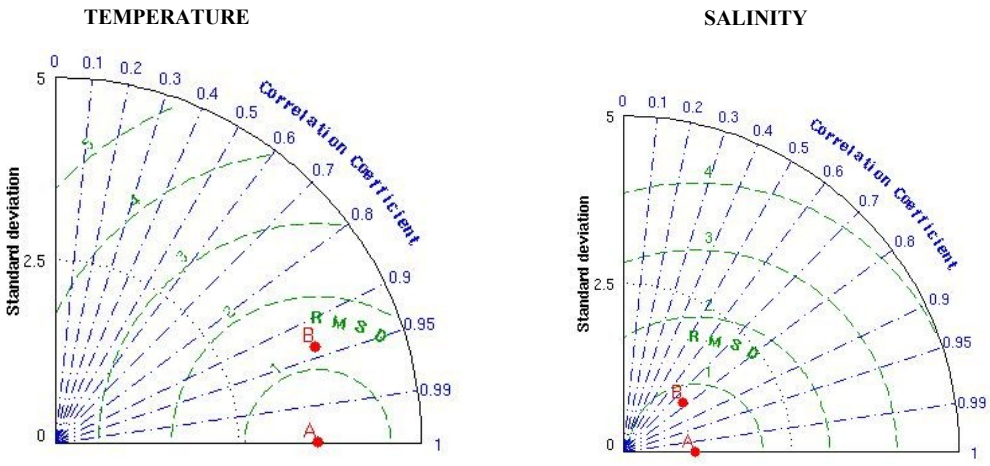

Figure 9 – Temperature and salinity mismatching between observations (A) and Mediterranean Forecasting System re-analysis data (B).

TEMPERATURE					
	MB	MAE	STD	RMSE	CC
AdriaROMS	-0.5775	1.2002	±3.2654	1.3851	0.9056
COAWST-C	-0.9293	1.5653	± 4.0644	1.7455	0.9069
COAWST-D	-0.4751	1.0288	± 4.1022	1.3133	0.9592
SALINITY					
	MB	MAE	STD	RMSE	CC
AdriaROMS	0.8857	1.1568	± 1.4635	1.2519	0.7502
COAWST-C	2.4177	2.4197	± 0.6856	1.7831	0.5009
COAWST-D	-0.8251	1.1640	±2.2819	1.3362	0.8218

Table 1 – Statistics of temperature and salinity values mismatching between observed data and AdriaROMS, COAWST-C and COAWST-D forecasting system output.

Mediterranean Forecasting System re-analysis data were compared with measured data in order to check its skills in reproducing thermohaline conditions of the Adriatic Sea from 1987 to 2012 at high spatial-temporal resolution. Although the spatial-temporal completeness of this dataset appears appropriate for this purpose, its robustness was checked through a comparison with observational data. A much larger observational dataset available for the Adriatic Sea was used, given the greater temporal coverage of the Mediterranean Forecasting System compared to the other models used. The results of this comparison indicate a very good agreement of re-analysis data with the available in situ measurements, as shown in Table 2. AdriaROMS had actually a similar good performance and its spatial resolution is even better than the MFS re-analysis data, but the temporal coverage of the latter is more suitable for reconstruction of past thermohaline conditions of the Adriatic Sea. So, MFS re-analysis data appears sufficiently appropriate to be used as a tool for investigating patterns up to decadal time scales of the physical dynamics of the Adriatic.

TEMPERATURE					
	MB	MAE	STD	RMSE	CC
MFS re-analysis data	0.3079	0.7861	±3.7734	1.3143	0.9375
SALINITY					
	MB	MAE	STD	RMSE	CC
MFS re-analysis data	-0.0331	0.3168	±1.1394	0.7425	0.7763

Table 2 – Statistics of temperature and salinity values mismatching between observed data and Mediterranean Forecasting System re-analysis data.

Conclusions

Three regional operational forecasting systems, namely AdriaROMS, COAWST (two releases) and the Mediterranean Forecasting System (MFS) have been presented and assessed. The performances of these operational systems have been evaluated by means of standard statistics. Available observations posed limitations to the assessment which is based on temperature and salinity only, not including any analysis on currents or other quantities.

Although all the three regional systems require a detailed bias correction, AdriaROMS demonstrated a better performance for both temperature and salinity, followed by the second release of COAWST. The performance of the first release of COAWST was unsatisfactory, especially for salinity. This can be due (i) to different s-coordinate level computation and (ii) differences in systems implementation (an updated version was used for the second release). Moreover, salinity misfits in coastal areas can be partially attributed to the lack of real-time observed values for river discharge: only Po river discharge measurements are given in input to the systems, while only climatological values are considered for the other rivers. On the other hand also temperature values predicted by the models were generally underestimated probably due to a not correct computation of radiative fluxes, and to the lack of data assimilation. Overall these results expand previous findings using the same forecasting system outputs (Tonani et al., 2009; Chiggiato and Oddo, 2008) and point out the need to improve such systems before they can be effective in monitoring of temperature and salinity.

The results of comparison between MFS re-analysis data and in situ measurements indicate a very good agreement of re-analysis data with available observations for both temperature and salinity, so that this dataset of Mediterranean Forecasting System appears sufficiently appropriate to be used as a tool for investigating patterns at decadal time scales of physical dynamics at Adriatic basin scale, needed to disentangle the natural variability from potential man-made and/or climate-induced changes.

References

N. Booij, R.C. Ris and L.H. Holthuijsen (1999). A third-generation wavemodel for coastal regions. Part.I – Model description and validation. J.Geophys. Res., 104, 7649–7666.

Brando,V.E., F. Braga, L. Zaggia, C. Giardino, M. Bresciani, E. Matta, D. Bellafiore, C. Ferrarin, F. Maicu,A. Benetazzo, D. Bonaldo, F. M. Falcieri, A. Coluccelli, A. Russo, and S. Carniel (2015).High-resolution satellite turbidity and sea surface temperatureobservations of river plume interactions during asignificant flood event. Ocean Sci., 11, 909–920, doi:10.5194/os-11-909-2015.

Buongiorno Nardelli B., C.Tronconi, A. Pisano, R.Santoleri, 2013: High and Ultra-High resolution processing of satellite Sea Surface Temperature data over Southern European Seas in the framework of MyOcean project, Rem. Sens. Env., 129, 1-16, doi:10.1016/j.rse.2012.10.012.

Carlson DF, Griffa A, Zambianchi E, Suaria G, Corgnati L, Magaldi MG, PoulainP-M, Russo A, Bellomo L, Mantovani C, Celentano P, Molcard A, BorghiniM (2016).Observed and modeled surface Lagrangian transport betweencoastal regions in the Adriatic Sea with implications for marine protectedareas. Cont Shelf Res, 118:23–48

Carpi, P. , M. Martinelli , A. Belardinelli , A. Russo , E. Arneri , A. Coluccelli , and A. Santojanni . 2015. Coupling an oceanographic model to a fishery observing system through mixed models: the importance of fronts for anchovy in the Adriatic Sea. Fisheries Oceanography 24:521–532.

Chiggiato J, Oddo P. Operational ocean models in the Adriatic Sea: a skill assessment. Ocean Science, 4, 61-71, 2008.

Falcieri, F.M., Benetazzo, A., Sclavo, M., Russo, A. and Carniel,S, (2013).Po River plume pattern variability investigated from model data. Cont. Shelf Res., 87:84–95 doi:10.1016/j.csr.2013.11.001.

Hopkins, T. S. – 1978. Physical processes in Mediterranean Estuaries. In: B. Kjerfue (ed.): Transport processe in Estuarine Environments, pp. 269-310. Seventh Bell W. Baruch Institute Marine Biology and Coastal Research Symposium, Georgetown, South Carolina.

Micheli F, Halpern BS, Walbridge S, Ciriaco S, Ferretti F, et al. (2013) Cumulative Human Impacts on Mediterranean and Black Sea Marine Ecosystems: Assessing Current Pressures and Opportunities. PLoS ONE 8(12): e79889. doi:10.1371/journal.pone.0079889

Pinardi, N., I. Allen, P. De Mey, G. Korres, A. Lascaratos, P.Y. Le Traon, C. Maillard, G. Manzella and C. Tziavos, 2003. The Mediterranean ocean Forecasting System: first phase of implementation (1998-2001). Ann. Geophys., 21, 1, 3-20

Pollak, M.J. – 1951. The sources of deep water of the Eastern Mediterranean Sea. J. Mar. Res., 10: 128-152.

Raicich F. (1996) On the fresh water balance of the Adriatic Sea, *Journal of Marine Systems* 9: 305-319.

Russo A, Artegiani A. Adriatic Sea hydrography. Scientia Matina 60 (Supl.2) 33-43.

Shchepetkin, A. F., and J. C. McWilliams (2005), The Regional Ocean Modeling System: A split-explicit, free-surface, topography following coordinates ocean model, Ocean Modelling, 9, 347-404.

Russo,A.,Coluccelli,A.,Iermano,I.,Falcieri,F.,Ravaioli,M.,etal.,2009.An operational system for forecasting hypoxic events in the northern Adriatic Sea. Geofizika 26,191–213.

Russo,A.,Coluccelli,A.,Carniel,S.,Benetazzo,A.,Valentini,A.,Paccagnella,T.,Ravaioli,M.,Bortoluzzi,G.,2013a.Operationalmodelshierarchyforshorttermmarine predictions:theAdriaticSeaexample.In:OCEANS-Bergen,2013MTS/IEEE, pp.1–6.

Russo, A.,Carniel,S.,Benetazzo,A.,2013b.Support for ICZM and MSP in the AdriaticSea region. SeaTechnol., 54,27–35.

Stachowicz J.J, Fried H, Osman R.W., Whitlatch R.B. (2002). Biodiversity, invasion resistance and marine ecosystem function: reconciling pattern and process. Ecology, 83(9), 2002, pp. 2575-2590

Warner, J.C., Perlin, N., Skyllingstad, E., 2008c. Using the Model Coupling Toolkit to couple earth system models. Environmental Modelling and Software 23, 1240–1249.

Warner J.C., Armstrong B., He R., Zombon J.B (2010). Development of a coupled ocean-atmosphere-wave-sediment transport (COAWST) modeling system. Ocean Modelling 35 (2010), 230-244.

Zore M. (1956) On gradient currents in the Adriatic Sea. Acta Adriatica 8:1-38.

Zore-Armanda M. (1963) Les masses d'eau de la mer Adriatique. *Acta Adriat*., 10: 1–94.

CHAPTER 2

Spatial and temporal analysis of thermohaline conditions and chlorophyll-α concentration in the Adriatic basin

Introduction

Rising atmospheric greenhouse gas concentrations have increased global temperatures by~ 0.2°C per decade over the past 30 years. Most of the added energy is being absorbed by the world's oceans. In addition, the oceans have absorbed approximately one-third of the carbon dioxide produced by human activities. There is now overwhelming evidence that human activities are driving rapid changes on marine ecosystems. The anthropogenic CO_2, for example, has acidified the surface layers of the ocean, with a steady decrease of 0.02 pH units over the past 30 years (Hoegh-Guldberg and Bruno, 2010). Moreover, an extremely rapid surface warming has been observed in the enclosed and semi-enclosed European Sea surrounded by major industrial/population agglomerations (Belkin, 2009). Studies on satellite Sea Surface Temperature of the Mediterranean Sea in 1992-2005 reveal a rise at a rate of 0.061°C/year (Criado-Aldeanueva et al., 2005), consistent with the study of Belkin where satellite SST of Mediterranean Sea in 1978-2003 period reveal a rising rate of 0.56°C/decade, or 4 times the global rate, with a general SST increase of 0.71°C for the period 1982-2006. This may have been caused by both terrestrial warming directly affecting the adjacent coastal areas and direct impacts of human activities (Belkin, 2009).

The maintenance of a good environmental status in European seas and coastal areas is a primary concern embodied in European regulations (Marine Strategy Framework Directive, Directive 2008/56/EC of the European Parliament and of the Council, ''establishing a framework for community action in the field of marine environmental policy'') (Mélin et al., 2011).

The Mediterranean Sea is a natural system highly affected by multiple drivers' impact (Coll et al., 2011; Micheli et al., 2013). Drivers associated with climate change (Sea Surface Temperature, UV increase, ocean acidification among others), demersal fisheries and maritime transport have a large impact on the Mediterranean Sea. These drivers, along with coastal hypoxia, were found to exert the greatest impact within the territorial waters followed by coastal pollution density, invasive species, land-based pollution (inorganic pollution, pesticide and fertilizer runoff) and modification of the coastline through coastal

erosion and engineering (Micheli et al., 2013). Drivers categories differ in their distribution across the Mediterranean Sea, but climatic drivers are the broadly distributed ones and have the greatest contribution to the average cumulative impacts.

Moreover, among the European waters, the ecosystems of the Adriatic Sea, and particularly its northern part, are recognized as degraded and under severe pressure (Lotze et al., 2006; Diaz and Rosenberg, 2008; Halpern et al., 2008; Coll et al., 2009). In the Adriatic Sea the major contribution to system degradation derive from demersal fishing, hypoxia and pollution from land-based activities, so that it results to be one of the most impacted areas on the Mediterranean. Moreover, in the Adriatic Sea the most impacted areas overlap with vulnerable habitats, especially the central Adriatic (Micheli et al., 2013). Climatic modification on the Adriatic area triggered a decline of atmospheric precipitation followed by a reduction in rivers runoff and, consequently, a significant decrease of the phytoplankton abundances concurrently with cascade effects on higher trophic levels. Changes in species composition and changes in the zooplankton community were observed, along with decrease of demersal fishes, top predators and small pelagic fishes ascribed to both overfishing and demise of eutrophication. Moreover, the correlation observed between introduced species recruitment and interannual temperature variation suggests that, over longer time periods (e.g. decades), ocean warming will facilitate the establishment and spread of alien species, particularly those from warmer climates (Stachowicz et al., 2002). It is clear how these changes widely affects marine ecosystems' goods and services, with consequences in economic activities.

Several studies already investigated on conditions of the northern part of the Adriatic Sea, but less has been done to analyze the entire basin from physical and biological point of view at different temporal scales.

To better assess basin features, and to detect potential anomalies useful to plan mitigation actions, it is necessary to perform more detailed and long term analysis. In that context, remote sensing has a role to play both as a monitoring tool and for understanding ecological dynamics by providing information on observed water properties and biological component concentrations (Mélin et al., 2011). On the other hand, remote sensing information must be integrated on the water column. Although *in situ* measurements are the most reliable data for this kind of assessment, it is clear that their fragmentation in time and space represents a limit in understanding the whole water mass. In this sense, a great contribution can be provided by forecasting systems output, because of their high spatial

temporal resolution, even if the quality and reliability of such product must be carefully checked– e.g. by means of comparison with observational data – before their employment.

A lot has been done so far to investigate physical and biological conditions of the Adriatic Sea, especially for the northern part of the basin (Artegiani et al., 1996a/b, Giani et al., 2012, Simoncelli et al., 2011) but often they were based on small datasets of *in situ* data with not sufficient spatial temporal coverage.

In this chapter, a multiple approach was employed to understand spatial-temporal dynamics of thermohaline conditions and phytoplankton biomass regimes using temperature, salinity and chlorophyll-α concentration – as proxy of algae biomass – data, respectively. The analysis of daily data was performed starting from 1987 in the whole Adriatic Sea. Four sub-areas were distinguished on the basis of thermohaline and physiographic characteristics, including the water column depth (Artegiani et al., 1998), in order to better discriminate several processes depending on these features. Temporal means were computed to obtain annual, seasonal and monthly patterns of each variable.

Materials

MFS re-analysis data

Given the reliability in reproducing thermohaline conditions of the Adriatic Sea – as demonstrated in previous chapter - , re-analysis data of the Mediterranean Forecasting System had been employed in time series analysis of temperature and salinity patterns. It is important to point out that the assumption that the models output is the best estimate of the reality instead of an independent observation is mainly due to the fact that the aim of this work is to evaluate the overall dynamics and changes in thermohaline conditions of the Adriatic Sea and not only in those few positions where data are available (Pinardi et al., 2009).

The dataset covers 25 years from 1987 to 2012, with daily time step, at about 7 km horizontal resolution (1/16°) and 72 unevenly spaced vertical levels. The assimilated data include: sea level anomaly, sea surface temperature, *in situ* temperature profiles by VOS XBTs, *in situ* temperature and salinity profiles by ARGO floats, and *in situ* temperature and salinity profiles from CTD. In this chapter, temperature and salinity information was employed. Data were selected as described in the previous chapter and analyzed in order to investigate potential changes in their patterns.

Given the vertical subdivision adopter with this model, it was not possible to correctly extract different layers on the basis of water masses features, so only surface and bottom layers were considered and analyzed.

Remote sensing chlorophyll-α concentration

Given the spatial resolution improvement in estimating chlorophyll-α concentration from satellites, two different dataset were employed, the first one at 4 km spatial resolution from 1997 to July 2012,and the second one at 1km spatial resolution from August 2012 to September 2015. Their description follows.

For the Mediterranean Sea, the ESA-CCI input Remote Sensing Reflectance (Rrs) spectrum is used to compute surface Chlorophyll (mg m-3) 4 km resolution via regional ocean color algorithm (MedOC4, Volpe et al., 2007). This algorithm was developed and used for near real time, delayed time and re-analysis of SeaWiFS data by the Group for

Satellite Oceanography (GOS-ISAC) of the Italian National Research Council (CNR), in Rome. ESA-CCI Rrs results from the merging of SeaWiFS, MODIS-Aqua and MERIS sensors.

Ocean color technique exploits the emerging electromagnetic radiation from the sea surface in different wavelengths. The spectral variability of this signal defines the so called ocean color which is affected by the presence of phytoplankton. ESA-CCI Rrs data, provided by Plymouth Marine Laboratory, are converted to chlorophyll concentration via ad hoc IDL script (IDL v8.2.3). The entire data set is consistent and processed in one-shot mode (with unique software version and identical configurations). This product is remapped at 4 km spatial resolution using cylindrical equirectangular projection. The chlorophyll product is obtained by means of the MedOC4 algorithm (Mediterranean Ocean Color 4 bands, Volpe et al., 2007). MedOC4 is an empirical ocean color algorithm for chlorophyll retrieval and is most suited for the Mediterranean Case 1 waters. Units are expressed in mg m-3. It uses the blue-to-green Reflectance ratio. In particular, it uses, on a pixel-by-pixel basis, the Maximum among Rrs443/Rrs555, Rrs490/Rrs555 and Rrs510/Rrs555, where Rrs443, Rrs490, Rrs510 and Rrs555 are the Remote Sensing Reflectances at 443, 490, 510 and 555 nm, respectively. This product identifies the average chlorophyll content of the surface layer as defined by the first optical depth (roughly one fifth of the euphotic depth).Time interval of this dataset goes from 4th September 1997 to 31thjuly 2012.

For the Mediterranean Sea, Surface Chlorophyll concentration (mg m-3) 1 km spatial resolution is operationally produced using regional ocean color algorithms (Figure 1). The Group for Satellite Oceanography (GOS-ISAC) of the Italian National Research Council (CNR), in Rome, uses an updated version of the algorithm reported in Santoleri et al. (2008) for Case 1 waters for near real time and delayed time data from MODIS-Aqua and NPP-VIIRS sensors.

Ocean color technique exploits the emerging electromagnetic radiation from the sea surface in different wavelengths. The spectral variability of this signal defines the so called ocean color which is affected by the presence of phytoplankton.

Current available OC sensor Level-1 data are routinely processed up to Level-3 with the SeaWiFS Data Analysis System (SeaDAS) software package available from NASA website (Volpe et al., 2012).

The Group for Satellite Oceanography (GOS) collects Level-1 data from the upstream providers as soon as they are available (Near Real Time). Delayed Time processing mode is performed some days after satellite overpasses as soon as ancillary data are made available for downloading. Standard masking criteria for detecting clouds or other contamination factors are routinely applied, i.e., land, cloud, sun glint, atmospheric correction failure, high total radiance, large solar zenith angle (70deg), large spacecraft zenith angle (56deg), coccolithophores, negative water leaving radiance, and normalized water leaving radiance at 555 nm 0.15 Wm-2 sr-1 (McClain et al., 1995).

All datasets belonging to this product are remapped at 1 km spatial resolution using cylindrical equirectangular projection.

Datasets are obtained by means of the Mediterranean Ocean Color algorithms. These are empirical ocean color algorithms for chlorophyll retrieval for the Mediterranean Case 1 or Case 2 waters. Units are expressed in mg m-3. They use the blue-to-green Maximum Reflectance ratio. In particular, they use two or three (depending on the sensor) Remote Sensing Reflectances in the blue part of the spectrum and the Remote Sensing Reflectances near 550nm.

The merged Case1-Case2 datasets are obtained using the empirical Mediterranean algorithm for Case 1 waters and the AD4 algorithm for Case 2 waters type (DAlimonte and Zibordi, 2003). Discrimination between the two water types is performed by comparing the satellite spectrum at pixel-by-pixel level with the average water type spectral signature from *in situ* measurements for both water types (the MedOC4 (Volpe et al., 2007) for Case 1, and CoASTS (Berthon et al., 2002) for Case 2). Merging of Case 1 and Case 2 information is performed following D'Alimonte et al. (2003).

This product identifies the average chlorophyll content of the surface layer as defined by the first optical depth (roughly one fifth of the euphotic depth).

Time interval of this second dataset goes from 1st August 2012 to 31th August 2015.

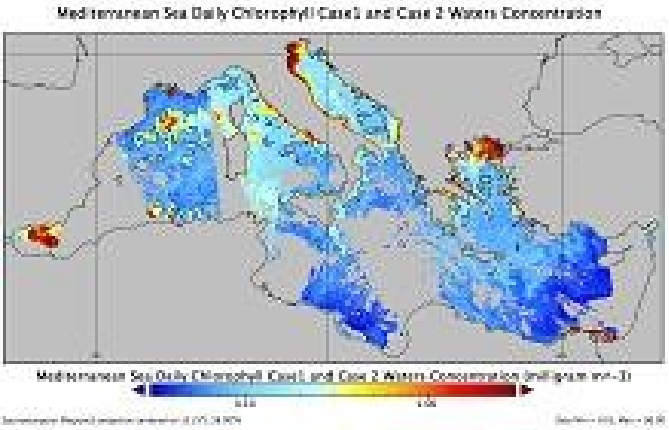

Figure 1- Example of 1 km spatial resolution chlorophyll product from SeaWiFS data processing (source: www.myocean.com)

Methods

Despite different data sources, it was possible to adopt some analogous methodologies to analyze the three datasets. Natural processes, and biological ones especially, are strongly influenced by water masses characteristics, so the Adriatic basin has been divided into four sub-areas, following Artegiani et al.(1997) and Zavatarelli et al.(1998), to better understand basin dynamics from both physical and biological point of view (Figure 2). Annual, seasonal and monthly means were computed in order to specifically point out potential changes over time.

First of all, three masks had been created for 7 km, 4 km and 1 km spatial resolution data using the reference bathymetry *Adria15* from USGS (see Annex II). Then, polygons related to first and second area (from north to south) were edited in order to exclude the complex orography of Istrian coasts. Then, the horizontal grid (longitude, latitude) has been extracted from one of the satellite data and interpolated with bathymetry. The land/sea/areas mask has been generated in order to exclude land points, Tyrrhenian Sea and Ionian Sea. Finally, a value from 1 to 4 as been assign to every pixel of each area, respectively, from north to south.

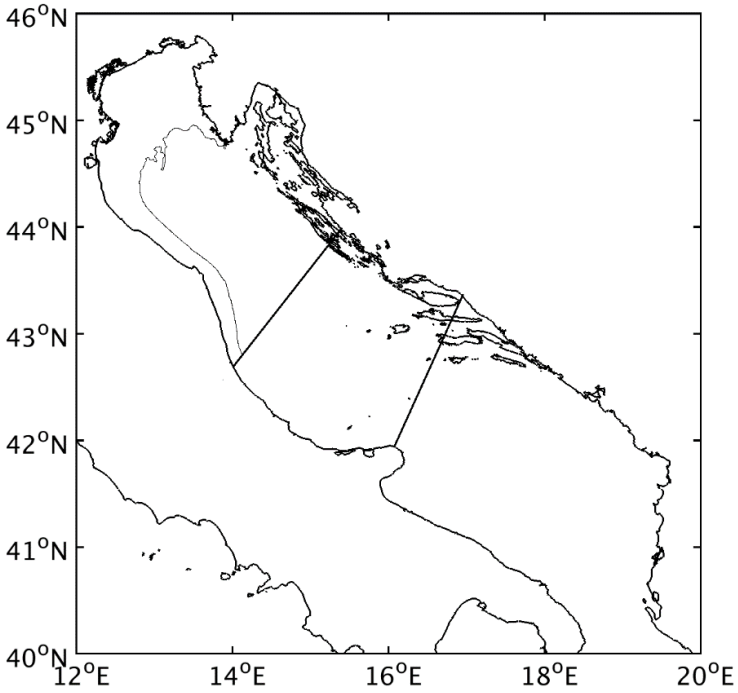

Figure 2– Subdivision of the Adriatic Sea in four sub-areas base on bathymetry (Artegiani et al., 1997; Zavatarelli et al., 1998).

From every file (corresponding to one day of measurements), longitude, latitude, time and the respective variables (temperature, salinity and chlorophyll-α concentration) had been extracted in loop. Appling the mask, spatial average has been computed for every area, followed by the computation of their monthly, seasonal and annual means, standard deviation and standard error.

Several kind of seasonal temporal subdivisions were use in literature up to now. In this work was chosen to follow seasonality of water masses so, starting from the first day of the month:

- Winter: December –January – February
- Spring: March – April – May
- Summer: June – July – August
- Autumn: September – October – November

Statistical analysis were effectuated by calculating trends using the Microsoft Excel template MAKESENS, (**Ma**nn-**Ke**ndall test for trend and **Sen's** slope estimates) developed by Salmi *et al.* (2002) for detecting and estimating trends in the time series of annual values of temperature, salinity and chlorophyll-a concentration. The MAKESENS software uses the nonparametric Sen's linear estimate for the slope of the trend line and the nonparametric Mann-Kendall test to evaluate whether that slope is statistically different from zero (no trend), performing two types of statistical analyses:

1) nonparametric Mann-Kendall test for detecting the presence of a monotonic increasing or decreasing trend, applicable in cases where the trend may be assumed to be monotonic, with no seasonal or other cycle is present in the data; and

2) nonparametric Sen's method for detecting the magnitude of the trend, using a linear model to estimate the slope of the trend, with the variance of the residuals that should be constant in time.

In MAKESENS test there are four significance levels α : 0.1, 0.05, 0.01 and 0.001; and for the four tested significance levels the following symbols are used:

***	if trend at α = 0.001 level of significance
**	if trend at α = 0.01 level of significance
*	if trend at α = 0.05 level of significance
+	if trend at α = 0.1 level of significance

If the cell is blank, the significance level is greater than 0.1.

The smallest significance level α with which the test shows that the null hypothesis of no trend should be rejected. If n is 9 or less, the test is based to the S statistic and if n is at least 10, the test is based to the Z statistic (normal approximation).
Missing values are allowed in MAKESENS test and the number of annual values in the studied data series (n) can thus be smaller than the number of years in the studied time series. For time series with less than 10 data points the S test is used, while for time series with 10 or more data points the normal approximation test is used, where the presence of a statistically significant trend is evaluated using the Z value. A positive (negative) value of Z indicates an upward (downward) trend. If there are several tied values (i.e. equal values) in the time series, it may reduce the validity of the normal approximation when the number of data values is close to 10. All time series analyzed in this research have much more than 10 data values. The minimum values of n with which the four significance levels can be reached:

Significance level α	required n
0.1	≥ 4
0.05	≥ 5
0.01	≥ 6
0.001	≥ 7

The significance level 0.001 means that there is a 0.1% probability that the values x_i are from a random distribution and with that probability we make a mistake when rejecting the null hypothesis of no trend. Thus the significance level 0.001 means that the existence of a monotonic trend is very probable, while the significance level 0.1 means that there is a 10% probability that we make a mistake when rejecting the null hypothesis.
Sen's slope estimate (Q) is the Sen's estimator for the true slope of linear trend i.e. change per unit time period (in this case a year).
Statistical analysies of atmosphere forcings, Po River inflow, marine physical, biogeochemical and biological data

It is important to highlight that the processing level chosen for satellite data (L3S) allows to obtain the highest level of data correctness with no interpolation over time and space. On the other hand, cloudy cover especially in winter period was reason of data incompleteness so that some results are not well representative of natural phytoplankton

processes. In order to partially fix this missing, histograms were produced in order to quantify the number of data available in each area and period (Annex II).

Results

In this section only significant outputs are reported. For the complete tables see Annex II.

Temperature

The analysis of mean interannual surface temperature of the Adriatic Sea from Mediterranean Forecasting System re-analysis data (Figure 3) highlights a strongly significant (<0.0008) increase of temperature values, from 1987 to 2012, of 0.94°C (±0.21) in the northern area down to 0.89°C(±0.23) in the southern one.

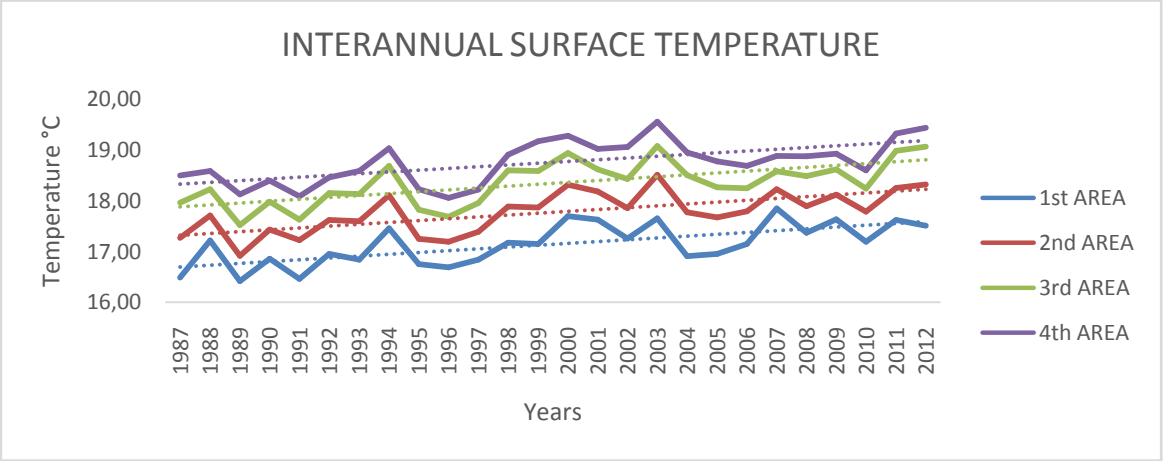

Figure 3 - Interannual surface temperature for the four areas of the Adriatic Sea from 1987 to 2012.

INTERANNUAL SURFACE TEMPERATURE °C

	R2	P level	ΔT(± err)	ΔT 26years(± err)
AREA 1	0,4456	0,0002	0,0360 (±0,0082)	0,94 (± 0.21)
AREA2	0,4508	0,0002	0,0363 (±0,0082)	0,94 (± 0.21)
AREA3	0,4223	0,0003	0,0371 (±0,0089)	0,97 (± 0.23)
AREA4	0,3825	0,0008	0,0343 (±0,0089)	0,89(± 0.23)

Table 1 - Significant interannual surface temperature oscillations in the four areas.

Investigating at seasonal time scale (Table 2) in the whole basin the major increasing temperature values are shown in summer season followed by spring and winter. In the shallower area, after summer and spring, major increasing temperature are measured in autumn instead of winter. This can be attributed to cold winter Bora wind (ENE or NE)

that generate cooling of the water column, contributing to dense water formation phenomenon (Bergamasco et al., 1999) and contrasting water column warming.

SEASONAL SURFACE TEMPERATURE °C

AREA 1

	R2	P level	ΔT(± err)	ΔT 26years(± err)
WINTER	0.1305	0.0698	0.0191 (± 0.0100)	0.50 (± 0.26)
SPRING	0.1397	0.0600	0.0385 (± 0.0195)	1.00 (± 0.51)
SUMMER	0.3341	0.0020	0.0575 (± 0.0166)	1.49 (± 0.43)
AUTUMN	0.1522	0.0488	0.0289 (± 0.0139)	0.75 (± 0.36)

AREA 2

	R2	P level	ΔT (± err)	ΔT 26years(± err)
WINTER	0.1656	0.0391	0.0198 (± 0.0091)	0.51 (± 0.24)
SPRING	0.2542	0.0086	0.0452 (± 0.0158)	1.17(± 0.41)
SUMMER	0.3614	0.0012	0.0640 (± 0.0174)	1.66 (± 0.45)
AUTUMN	0.0410	0.3214	0.0158 (± 0.0156)	0.41 (± 0.40)

AREA 3

	R2	P level	ΔT (± err)	ΔT 26years(± err)
WINTER	0.1484	0.0519	0.0177 (± 0.0086)	0.46 (± 0.22)
SPRING	0.2951	0.0041	0.0429 (± 0.0135)	1.11 (± 0.35)
SUMMER	0.3747	0.0009	0.0701 (± 0.0185)	1.82 (± 0.48)
AUTUMN	0.0435	0.3063	0.0174 (± 0.0167)	0.45 (± 0.43)

AREA 4

	R2	P level	ΔT (± err)	ΔT 26years(± err)
WINTER	0.2188	0.0160	0.0201 (± 0.0078)	0.52 (± 0.20)
SPRING	0.3495	0.0015	0.0415 (± 0.0116)	1.08 (± 0.30)
SUMMER	0.3446	0.0016	0.0580 (± 0.0163)	1.51 (± 0.42)
AUTUMN	0.0423	0.3136	0.0173 (± 0.0168)	0.45 (± 0.44)

Table 2 - Seasonal variations of temperature and their significant level in surface layer for the four areas.

Downscaling at monthly time step (Table 3), significative increases can be find all over the basin from April to July with higher ones in June, when it is reported an increase > 2°C in

26 years. For the whole basin, in these four months, temperature increases are never lower than 1.12 °C.

MONTHLY SURFACE TEMPERATURE °C				
AREA 1				
	R2	**P level**	**ΔT(± err)**	**ΔT 26years(± err)**
APRIL	0.1936	0.0245	0.0479 (±0.0200)	1.25 (±0.52)
MAY	0.1763	0.0327	0.0644 (± 0.0284)	1.67(± 0.74)
JUNE	0.2665	0.0069	0.0836 (± 0.0283)	2.17 (± 0.74)
JULY	0.3177	0.0027	0.0636 (± 0.0190)	1.65 (± 0.49)
AREA 2				
	R2	**P level**	**ΔT (± err)**	**ΔT 26years(± err)**
APRIL	03275	0.0022	0.0531 (± 0.0155)	1.38 (± 0.40)
MAY	0.2058	0.0199	0.0707 (± 0.0283)	1.84 (± 0.74)
JUNE	0.2990	0.0038	0.0904 (± 0.0283)	2.35 (± 0.73)
JULY	0.3922	0.0006	0.0732 (± 0.0186)	1.90 (± 0.48)
AREA 3				
	R2	**P level**	**ΔT (± err)**	**ΔT 26years (± err)**
APRIL	0.3770	0.0008	0.00508 (± 0.0133)	1.32 (± 0.35)
MAY	0.2101	0.0185	0.0659 (± 0.0261)	1.71 (± 0.68)
JUNE	0.3102	0.0031	0.0916 (± 0.0279)	2.38 (± 0.72)
JULY	0.4115	0.0004	0.0811 (± 0.0198)	2.11 (± 0.51)
AREA 4				
	R2	**P level**	**ΔT (± err)**	**ΔT 26years (± err)**
APRIL	0.3579	0.0012	0.0432 (± 0.0118)	1.12 (± 0.31)
MAY	0.2629	0.0074	0.0682 (± 0.0233)	1.77 (± 0.61)
JUNE	0.3510	0.0014	0.0905 (± 0.0251)	2.35 (± 0.65)
JULY	0.3429	0.0017	0.0634 (± 0.0179)	1.65 (± 0.47)

Table 3 - Monthly variations of temperature and their significant level in surface layer for the four areas.

Even in the bottom layer, temperature shows increasing trend (Figure 4) with significant values in first and fourth area of 0.81°C and 0.27°C, respectively (Table 4). No significative values were found for second and third areas. If it can be plausible, for the shallower area, a general warming of the water column, it is interesting to note the increase

of 0.27°C in the bottom layer of the fourth area having a mean deep of 800m. This large increase for such a deep area can be related to the Eastern Mediterranean Transient, during which Adriatic Dense Water production stopped. The lack of supply of dense and cold waters is likely to be the main cause of such a large increment of deep Adriatic waters temperature. This finding is consistent with recent oceanographic studies in deep-sea that showed dynamic temperature changes even over periods as short as decades or a few years. Moreover, rapid deep-water warming (~0.1°C per decade) over the last ~50 years is known in the western Mediterranean (Bethoux et al., 1990; Yasuhara and Danovaro, 2014).

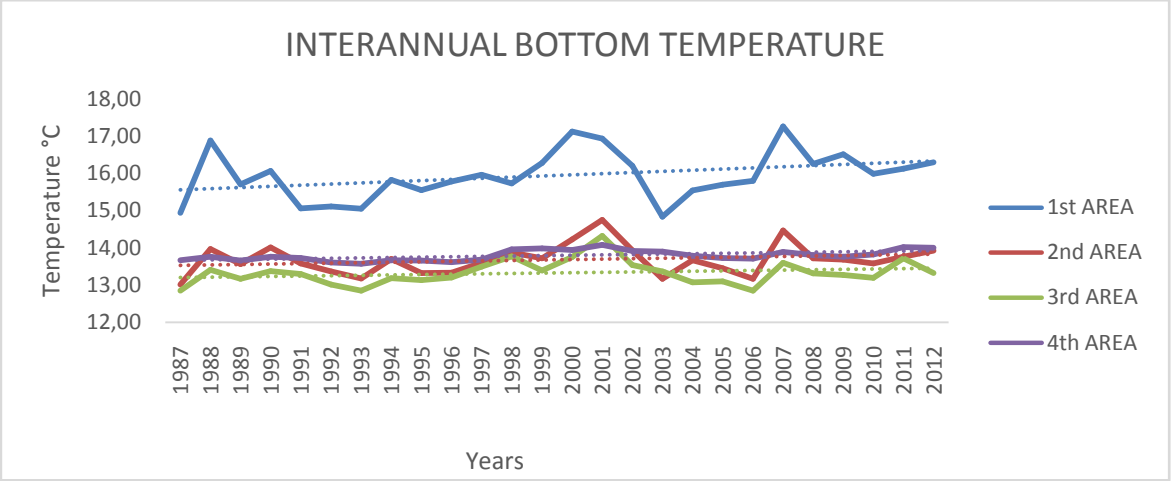

Figure 4 - Interannual bottom temperature for the four areas of the Adriatic Sea.

INTERANNUAL BOTTOM TEMPERATURE °C				
	R2	**P level**	**ΔT(± err)**	**ΔT 26years(± err)**
AREA 1	0,1307	0,0695	0,0312 (±0,0164)	0,81 (± 0.43)
AREA 4	0,3068	0,0033	0,0104 (±0,0032)	0,27 (± 0.08)

Table 4 - Interannual bottom temperature in first and fourth areas

Investigating at seasonal scale (Table 5), significant increases are shown in summer and autumn for the shallower area, when general conditions of irradiation and air temperature are naturally higher and influence water temperature. Previous increasing values are confirmed for the bottom layer of deeper area with significant increasing values in all seasons with no relevant distinctions among them. Inspecting the different behavior of bottom water temperatures in area 1 and 4, it appears that MFS is able to reproduce the winter dense water formation occurring in the shallow area 1, while in area 4 MFS mostly

relies on assimilation of available data (which are sparse in space and time, especially in the deeper part). The latter fact is in agreement with MFS model characteristics, which does not allow to correctly reproduce winter deep convection.

SEASONAL BOTTOM TEMPERATURE °C

AREA 1

	R2	P level	ΔT(± err)	ΔT 26years (± err)
SUMMER	0.2677	0.0068	0.0678 (± 0.0229)	1.76 (± 0.59)
AUTUMN	0.2585	0.0080	0.0537 (± 0.0186)	1.40 (± 0.48)

AREA 4

	R2	P level	ΔT (± err)	ΔT 26years (± err)
WINTER	0.3042	0.0035	0.0101 (± 0.0031)	0.26 (±0.08)
SPRING	0.2592	0.0079	0.0109 (± 0.0038)	0.28 (± 0.10)
SUMMER	0.2810	0.0053	0.0107 (± 0.0035)	0.28 (± 0.09)
AUTUMN	0.1765	0.0326	0.0100 (± 0.0044)	0.26 (± 0.11)

Table 5 - Significant seasonal temperature variations and their significant level in first and fourth areas

Downscaling at monthly level (Table 6), significant temperature increase for the shallower area are recorded in September, followed by July.

This can be attributed to longer persistence of warm air masses after the merely summer season due to global warming (Alcamo et al., 2007; IPCC 2007) and water mass inertia in heat content exchange at air-sea interface.

MONTHLY BOTTOM TEMPERATURE °C				
AREA 1				
	R2	**P level**	**ΔT (± err)**	**ΔT 26 years (± err)**
JUNE	0.188	0.027	0.063 (± 0.027)	1.64 (± 0.69)
JULY	0.310	0.003	0.077 (± 0.023)	1.99 (± 0.61)
AUGUST	0.233	0.013	0.064 (± 0.024)	1.65 (± 0.61)
SEPTEMBER	0.400	0.001	0.085 (± 0.021)	2.20 (± 0.55)
AREA 4				
	R2	**P level**	**ΔT (± err)**	**ΔT 26years (± err)**
APRIL	0.2870	0.0048	0.0116 (± 0.0037)	0.30 (± 0.10)
MAY	0.3143	0.0029	0.0121 (± 0.0037)	0.32 (± 0.10)
JUNE	0.3524	0.0014	0.0132 (± 0.0036)	0.34 (± 0.09)
JULY	0.2933	0.0043	0.0114 (± 0.0036)	0.30 (± 0.09)

Table 6 - Significant monthly temperature variations and their significant levels in bottom layer for first and fourth areas.

Salinity

Salinity interannual mean values (Figure 5) highlight an increasing trend of 0.83 in 26 years only in the surface layer of the shallower area, the most influenced by river discharge. One of the freshwater characteristics is, indeed, the buoyancy so it was not surprising to find any significant salinity trends in bottom layers or in areas where scarce or any influence from riverine waters persists.

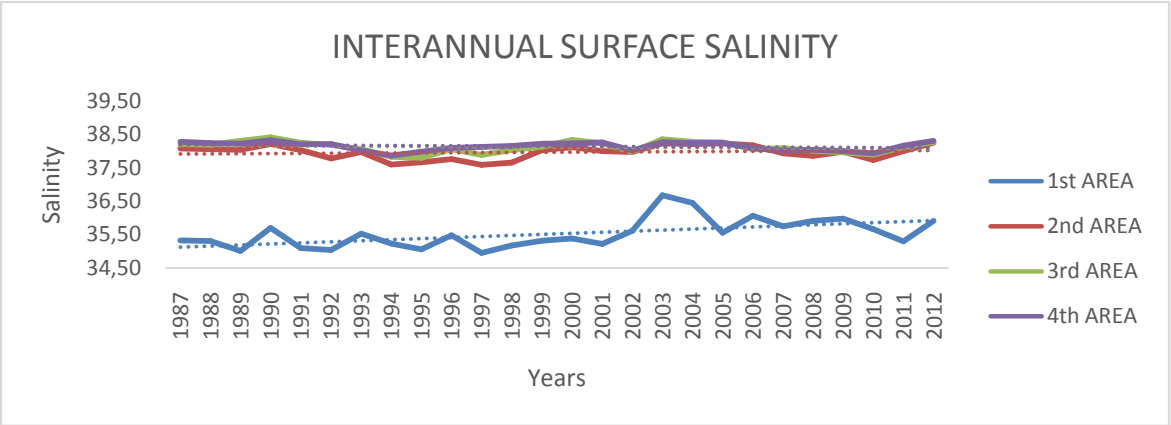

Figure 5 - Interannual surface salinity for the four areas of the Adriatic Sea from 1987 to 2012.

Analyzing seasonal behavior of salinity in shallower area, the higher increases are shown in summer (+0.98 ±0.22) followed by autumn (+0.92 ±0.37) and winter (+0.75 ±0.22) with only + 0.64 (± 0.29) in spring. Higher concentration of salinity will increase water density (decrease its volume). This effect, termed "haline contraction", plays a very important role in the annual cycle of steric sea height (combined effect of thermal expansion and haline contraction on sea level) and in maintaining the ocean thermohaline circulation. Changes in salinity can be an indicator of changes in local and global hydrological cycles (Antonov et al., 2002)

These findings are confirmed by several other studies on general physical conditions of the Mediterranean basin and Adriatic Sea. The already mentioned increase in air temperature (IPCC, 2015) has been associated to decreased precipitations (35-40%), especially in southern Europe, including snow over the Alps and, consequently, the runoff in the northern Adriatic watersheds. A recent sharpening of extreme discharges was reported for Po together with an increase of the frequency of prolonged droughts after 1940's due to the concomitant downward shift of precipitation and upward shift of evaporation (Cozzi and Giani, 2011; Zanchettin et al., 2008). The annual runoff of Po River, in particular, showed relevant oscillations on multidecadal time scale. During the dry years 2005-2007, a strong reduction of river water flows and nutrient loads was experienced by the north Adriatic ecosystem with respect to years characterized by medium-high regimes. An increased frequency of similar drought periods, due to ongoing climate changes or to a larger human usage of continental waters, would be easily able to significantly change the biogeochemistry of this basin (Cozzi and Giani, 2011).

Chlorophyll-*a*

The last part of the work investigates the primary production dynamics in the surface layer of the Adriatic basin from 1997 to 2015, employing chlorophyll-α concentration as proxy of phytoplankton biomass.

At interannual time scale, a general increase of chlorophyll-α concentration (mg/m^3) was measured all over the basin (Figure 6), except for deeper northern Adriatic Sea (Area 2) where no significative values are reported. Higher values are reached in shallower area with a mean increase of 2.24 mg/m^3(±0.71) in 19 years.

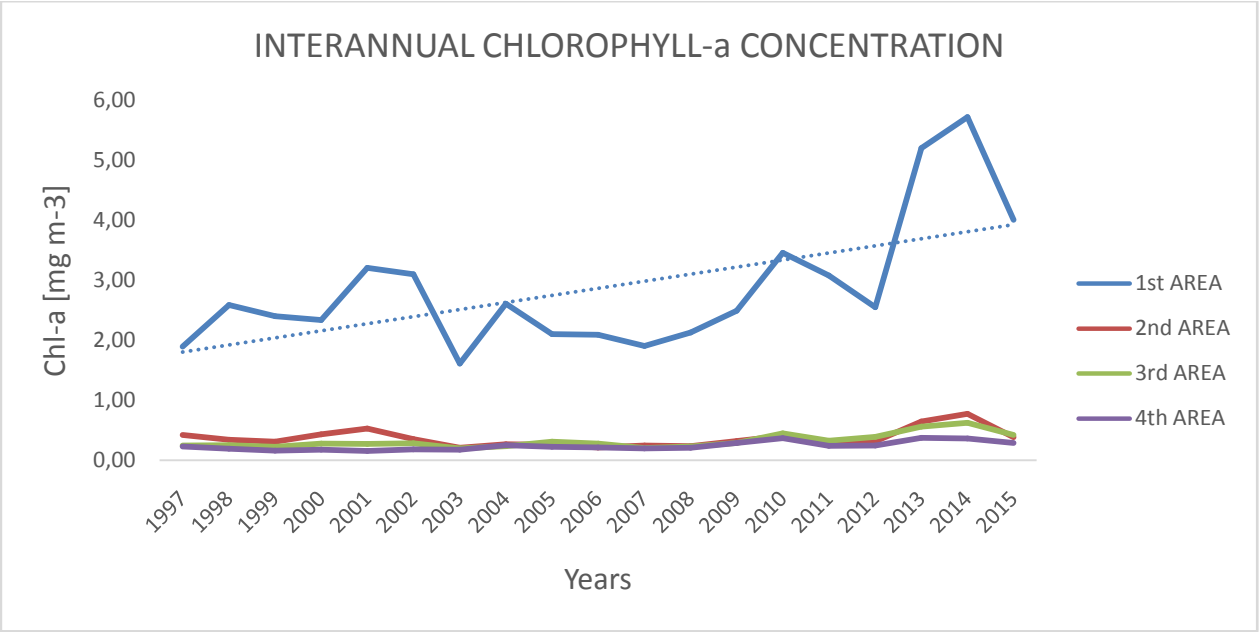

Figure 6 – Interannual chlorophyll-a concentration [mg m-3] in the entire basin for the period 1997-2015.

INTERANNUAL SURFACE CHLOROPHYLL-α CONCENTRATION [mg/m^3]

	R2	P level	ΔC(± err)	ΔC19 years(± err)
AREA1	0.3690	0.0058	0.1180 (± 0.0374)	2.24 (± 0.71)
AREA 2	0.0757	0.2544	0.0072 (± 0.0061)	0.14 (± 0.12)
AREA 3	0.5239	0.0005	0.0153 (± 0.0035)	0.29 (± 0.07)
AREA4	0.5577	0.0002	0.0092 (± 0.0020)	0.17 (± 0.04)

Table 6 - Interannual variations in chlorophyll concentration and their significant level.

Interesting data were found at seasonal scale (Table 7). For the shallower area the most significative increases were registered in spring and summer, likely related to an increased river runoff in spring-summer season. In the middle Adriatic, although concentration increases were quite lower than in the previous area, significance level of such dataset is high enough to make it strongly reliable. Major increases were encountered in winter, spring and summer. Finally, for the southern Adriatic small increases in chlorophyll-α concentration were measured in all the four seasons, with higher values in winter followed by spring.

SEASONAL SURFACE CHLOROPHYLL-α CONCENTRATION [mg/m^3]

AREA 1

	R2	P level	ΔC(± err)	ΔC19 years (± err)
AUTUMN	0.1308	0.1282	0.0466 (± 0.0291)	0.89 (± 0.55)
WINTER	0.1866	0.0648	0.0786 (± 0.0398)	1.49 (± 0.76)
SPRING	0.2347	0.0416	0.1698 (± 0.0767)	3.06 (± 1.38)
SUMMER	0.4116	0.0041	0.1555 (± 0.0465)	2.80 (± 0.84)

AREA 3

	R2	P level	ΔC (± err)	ΔC19 years (± err)
AUTUMN	0.072	0.7296	0.0015 (±0.0042)	0.03 (±0.08)
WINTER	0.3656	0.0061	0.0323 (±0.0103)	0.61 (±0.20)
SPRING	0.4145	0.0039	0.0241 (±0.0072)	0.43 (±0.13)
SUMMER	0.3441	0.0105	0.0061 (±0.0021)	0.11 (±0.04)

AREA 4

	R2	P level	ΔC(± err)	ΔC19 years (± err)
AUTUMN	0.2338	0.0360	0.0045 (±0.0020)	0.09 (±0.04)
WINTER	0.4306	0.0023	0.0215 (±0.0060)	0.41 (±0.11)
SPRING	0.4174	0.0038	0.0107 (±0.0032)	0.19 (±0.06)
SUMMER	0.4414	0.0026	0.0041 (±0.0011)	0.07 (±0.02)

Table 7 - Seasonal variations in chlorophyll concentration and their significant level.

Investigation in monthly mean (Table 8) behavior reveal, for the shallower area, main peaks in June, July, March and September. March is the month with most significative increasing values even for middle and southern Adriatic followed by, for the former June, December, May, February, August and April, while for the latter almost every month is recorded a significative increase with the exception of October and November and cases with lower significance level in July, August and January. The order of magnitude of the increase in smaller from the northern to the southern areas.

MONTHLY SURFACE CHLOROPHYLL-α CONCENTRATION [mg/m3]				
AREA 1				
	R2	**P level**	**ΔC(± err)**	**ΔC 19years (± err)**
SEPTEMBER	0.3858	0.0045	0.1053 (± 0.0322)	2.00 (±0.61)
MARCH	0.2484	0.0353	0.2030 (± 0.0882)	3.65 (±1.59)
JUNE	0.3871	0.0058	0.2481 (± 0.0781)	4.47 (± 1.41)
JULY	0.4133	0.0040	0.1230 (± 0.0366)	2.21 (± 0.66)
AREA 3				
	R2	**P level**	**ΔC (± err)**	**ΔT 19years (± err)**
DECEMBER	0.3053	0.0174	0.0648 (±0.0244)	1.17 (±0.44)
FEBRUARY	0.2787	0.0243	0.0289 (±0.0116)	0.52 (±0.21)
MARCH	0.5017	0.0010	0.0350 (±0.0087)	0.63 (±0.16)
APRIL	0.2119	0.0546	0.0159 (±0.0077)	0.29 (±0.14)
MAY	0.2999	0.0186	0.0207 (±0.0079)	0.37 (±0.14)
JUNE	0.3688	0.0075	0.0146 (±0.0048)	0.26 (±0.09)
AUGUST	0.2498	0.0347	0.0027 (±0.0012)	0.05 (±0.02)
AREA 4				
	R2	**P level**	**ΔC (± err)**	**ΔC19years (± err)**
SEPTEMBER	0.4228	0.0023	0.0043 (±0.0012)	0.08 (±0.02)
DECEMBER	0.3940	0.0053	0.0327 (±0.0101)	0.59 (±0.18)
JANUARY	0.3355	0.0118	0.0268 (±0.0094)	0.48 (±0.17)
FEBRUARY	0.3721	0.0072	0.0149 (±0.0048)	0.27 (±0.09)
MARCH	0.4560	0.0021	0.0121 (±0.0033)	0.22 (±0.06)
APRIL	0.2340	0.0420	0.0093 (±0.0042)	0.17 (±0.08)
MAY	0.4187	0.0037	0.0111 (±0.0033)	0.20 (±0.06)
JUNE	0.4045	0.0046	0.0072 (±0.0022)	0.13 (±0.04)
JULY	0.3262	0.0133	0.0032 (±0.0011)	0.06 (±0.02)
AUGUST	0.3344	0.0119	0.0020 (±0.0007)	0.04 (±0.01)

Table 8 - Monthly variations in chlorophyll concentration and their significant level .

These results does not fit with findings of other past studies that highlight strong decreases in chl-*a* concentration especially in northern Adriatic Sea. Mozetic et al. (2010) for example, according to Zanchettin et al. (2008) and Comici and Bussani (2007), describe a decrease in chl-*a* levels in the period 1998-2007. This phenomenon was explained by reduced freshwater discharges especially for Po and Isonzo Rivers, together with

phosphorus banning by Italian law in the mid-1980s. This, along with the general improvement in sewage treatment, could have had a strong influence on nutrient concentrations in the coastal area where both phosphorus and ammonia have decreased significantly over the last 30 years.

Actually, the behavior of chlorophyll-α concentration in first area can be attributed to natural rivers discharge oscillations that influence phytoplankton biomass dynamics but, on the other hand, the increased values reported for the rest of the surface basin must be attributed to other causes. One hypothesis is that the aforementioned increased water temperature can have triggered a stronger re-mineralization of inorganic matter making available major quantity of nutrient employed in metabolic processes of phytoplankton biomass. Finally, the decreasing concentrations of chlorophyll-α going from north to south of the basin can be explain first of all by the contribution of rivers discharge, influenced more than ever by changes in precipitation regime (increasing flash flood events followed by drought periods) and, secondly, by the different circulation regime that characterized each one of the four areas.

Comparing surface patterns of the three variables investigated (Table 9), it can be noted correspondence in periods of increasing values, especially for temperature and chlorophyll-α concentration. At interannual time scale, in the shallower area can be observed the increase of all the three variables, middle and southern Adriatic shown increases only in temperature and chlorophyll-α concentration.

In the last ~20 years, first area present correspondent increase in temperature and chlorophyll-α concentration in summer season. Similar patterns are shown in deeper northern, middle and southern Adriatic Sea where in summer and also in spring ─ although with weaker significance level ─ temperature and chlorophyll-α concentration increase.

Investigating at monthly level, in the shallower area July is the most affected by temperature and phytoplankton biomass increases followed by June, when correspondent increases in the two variables are highlighted in third and fourth areas. In this last case, significative level of increasing values are shown in July and May.

AREA 1				
	R2	**P level**	**Δvar (± err)**	**Δvar 26years (± err)**
TEMP	0.4456	0.0002	0.0360 (±0.0082)	0.9366 (±0.2132)
SALT	0.3062	0.0034	0.0318 (±0.0098)	0.8262 (±0.2539)
CHL-a	0.3690	0.0058	0.1180 (±0.0374)	2.2416 (±0.7109)

Table 9 - Variation of the three variables in 26 years for the first area.

Conclusions

Thermohaline conditions and phytoplankton biomass dynamics were investigated during the past 25 years. Time series were extracted from the re-analysis data of the Mediterranean Forecasting System and from daily satellite observation at high (4×4 km) and very high (1 ×1 km) spatial resolution. Discriminations based on sub-basins and bathymetry was necessary in order to better understand different mechanisms and dynamics of a complex system such as the Adriatic Sea. Mann-Kendall test (Mann 1945, Kendall 1975, Gilbert 1987) has been used to highlight the presence of a significant temporal trend at monthly, seasonal and inter-annual time scales. From 1987, temperature values show a general increase throughout the whole water column in all of the four sub-areas of the Adriatic Sea, with a major increase in surface waters (up to 2°C). The stronger increase of temperature occurred in summer season, especially from 2003 and it is consistent along the entire water column especially in shallower areas.

Time series analysis of salinity revealed a significant increase starting from 2003 in the shallower areas. This is probably due to heat wave event of summer 2003, when the high temperature and absence of cloudy cover were associated to a prolonged drought; severe droughts happened also in following years. Smaller inter-annual differences of salinity are shown in areas not directly affected by river discharge: the deeper northern area show a decreasing trend in autumn until 1997 and a reverse behavior up to 2012 (+0.5). Middle and southern Adriatic highlight only decreasing values in spring in the entire investigated period.

Chlorophyll-a concentrations displayed higher values especially in coastal area most influenced by river discharge but a general increase was observed in the whole basin especially from 2008 up to present; the lower values in the 2003-2008 are likely related to the drought occurred in that period. Past studies on trophic conditions of the Adriatic Sea (e.g. Mozetic et al., 2010) report a global tendency towards chl-a reduction in the period 1970-2007 (-0.11 mg m-3 y-1), more marked in the eutrophic area under the influence of the Po River while in the rest of the basin no long-term changes were detected. The decade 1997-2007 was characterized by a stronger decrease because of reduction in ammonia and phosphate loads from inland activities.

Results obtained in this study demonstrated a reverse trend after 2008. The unusual increment in chlorophyll-*a* concentration it is likely to be related with the aforementioned increase in water temperature which can have triggered an intense re-mineralization of

inorganic matter, making available major quantity of nutrient employed in metabolic processes of phytoplankton biomass.

These findings highlight how rapidly is changing thermohaline conditions of the Adriatic Sea, not only under direct anthropogenic pressure as described by MSFD, but especially because of climate change. Thermohaline condition of ecosystems represent a fundamental driver influencing marine biodiversity, food web structure, distribution of non indigenous species as well as eutrophication processes thus the knowledge on the potential changes of thermohaline condition at basin scale potentially related to global climate change can have a major consequences for biodiversity maintenance related to descriptor one, the potential spreading non indigenous species (descriptor 2), food web structure (descriptor 4) and to potential distrophic events due to eutrophication processes (descriptor 5). At the same time changes of biological productivity related to photosynthetic biomass production can have an important effect on biodiversity and ecosystem functioning and thus on the sustainable maintenance on the provisioning of marine ecosystems' good and services for human wellbeing.

These results highlight the need of strong monitoring activities even in offshore water to better investigate this trend and to adopt strategies to avoid negative impact on seawater. If this rapid change will reveal to be actual, it will be necessary to plan and rapidly adopt adaptive strategies for the possible consequences of ocean warming on human activities and marine resources exploitation.

.

References

Antonov J.I, Levitus S, Boyer T.P. Steric sea level variations during 1957-1994: importance of salinity. journal of geophysical research: Oceans. 2002 DOI:10.1029/2001JC000964

Artegiani A, Bregant D, Paschini E, Pinardi N, Raicich F, Russo A. 1996. The Adriatic Sea general circulation. Part I: Air-Sea interactions and water mass structure. Journal of Physical Oceanography 27 (8) 1492-1514.

Artegiani A, Bregant D, Paschini E, Pinardi N, Raicich F, Russo A. 1996. The Adriatic Sea general circulation. Part II: Baroclinic circulation structure. Journal of Physical Oceanography 27(8) 1515-1532.

Belkin I.M. Rapid warming of large marine ecosystems. Progress in oceanography 81(2009) 207-213.

Coll M, Libralato S, Tudela S, Palomera I, Pranovi F (2009) Ecosystem overfishing in the ocean. PlosOne 3: e3881. doi:10.1371/journal.pone.0003881.

Comici, C., and A. Bussani. "Analysis of the River Isonzo discharge (1998–2005)." *Applicata* 48 (2007): 435-454.

Criado - Aldeanueva F., Del Rio J., Garcia-Lafuente J. 2008. Steric and mass - induced Mediterranean sea level trends from 14 years of altimetry data. Global and planetary change 60(3-4) 563-575.

Diaz R.J. and Rosenberg R. Spreading dead zones and consequences for marine ecosystems. Science vol. 321 (2008), Issue 5891, pp. 926-929.

D'Alimonte D. and Zibordi G. (2003). Phytoplankton determination in an optically complex coastal region using a multilayer perceptron neural network. IEEE rans. Geoscience Remote sensing, vol 41, pp. 286.

D'Alimonte D., Mèlin F., Zibordi G and Berthon J.F (2003). Use of the novelty detection technique to identify the range of applicability of the empirical ocean color algorithms. IEEE trans. Geoscience Remote sensing, 41, 2833-2843.

Grilli F, Marini M, Book J.W, Campanelli A, Paschini E, Russo A. Flux of nutrients between the middle and southern Adriatic Sea (Gargano-Split section). Marine Chemistry 153 (2013) 1-14.

Giani M, Djakovac T, Degobbis D, Cozzi S, Solidoro C, Fonda Umani S. 2012. Recent changes in the marine ecosystems of the northern Adriatic Sea. Estuarine, Coastal and Shelf Science 115 (2012) 1-13

Hoegh-Guldberg O., Bruno, J.F.. The impact of climate change on the world's marine ecosystems. Science328 (2010) pp.1523-1528.

Lotze H.K, Lenihan H.S., Bourgue B.J., Jackson J.B.C. 2006. Depletion, degradation and recovery potential of estuaries and coastal seas. Science 312(5781):1806-9.

McClain C.R., Arrigo K.R., Esaias W., Darzi M., Patt F.S., Evans R.H., et al (1995). SeaWiFS Algorithms Part1. NASA Tech. Memo. 104566, Vol 28. Greenbelt, Maryland: NASA Goddard Space Flight Center

Melin F, Vantrepotte V, Clerici M, D'Alimonte A, Zibordi G, Berthon J.F, Canuti E. Multi-sensor satellite time series of optical properties and chlorophyll-a concentration in the Adriatic Sea. Progress in Oceanography 91 (2011) 229-244.

Micheli F., Halpern B.S., Walbridge S., Ferretti F., Fraschetti S., Lewison R., Nykjaer L., Rosenberg A.A. Cumulative human impacts on Mediterranean and Black Sea marine ecosystems: assessing current pressures and opportunities. PLoS ONE 8(12): e79889. doi:10.1371/journal.pone.0079889.

Mozetic P, Solidoro C, Cossarini G, Socal G, precali R, Francé J, Bianchi F, De Vittor C, Smodlaka N, Fonda Umani S. Recent trends towards oligotrophication of the Northern Adriatic: evidence from chlorophyll a time series. Estuaries and Coasts (2010) 33: 362-375.

Pinardi, N., I. Allen, P. De Mey, G. Korres, A. Lascaratos, P.Y. Le Traon, C. Maillard, G. Manzella and C. Tziavos, 2003. The Mediterranean ocean Forecasting System: first phase of implementation (1998-2001). Ann. Geophys., 21, 1, 3-20.

Salmi T., Määttä A., Anttila P., Ruoho-Airola T., Amnell T. (2002) Detecting trends of annual values of atmospheric pollutants by the Mann-Kendall test and Sen's slope estimates - The Excel template application MAKESENS. *Publications on air quality* No. 31 Finnish Meteorological Institute, Helsinki.

Santoleri R., et al (2008). Open waters remote sensing of the Mediterranean Sea, in Remote sensing of the European Seas, edited by V. Barale and M. Gade pp. 103-116. Springer.

Simoncelli S, Pinardi N, Oddo P, Mariano A.J, Montanari G, Rinaldi A, Deserti M. Coastal rapid environmental assessment in the northern Adriatic Sea. Dynamics of the Atmospheres and Oceans (2011).

Stachowicz J.J., Fried H., Osman R.W., Whitlatch R.B. Biodiversity, invasion resistance, and marine ecosystem funcion: reconciling pattern and process. Ecology 83(9), 2002, pp. 2575-2590.

Volpe G, Santoleri R., Vellucci V., Ribera d Acalà M., Marullo S. and D Ortenzio F. (2007). The colour of the Mediterranean Sea: Global versus regional bio-optical algorithms evaluation and implication for satellite chlorophyll esistems. Remote Sensing of Environment, 107, 625-638.

Volpe G., Colella S., Forneris V., Tronconi C. and Santoleri R (2012). The Mediterranean Ocean Colour observing system development and product validation. Ocean Science, 8 , 869-883.

Zanchettin D., Rubino A., Traverso P., Tomasino M (2008). Impact of variations in solar activity on hydrological decadal patterns in northern Italy. Journal of geophysical research, Vol. 113, D12102, doi:10.1029/2007JD009157, 2008.

Zavatarelli M, Raicich F, Bregant D, Russo A, Artegiani A. Climatological biogeochemical characeristics of the Adriatic Sea. Journal of Marine Systems 1998.

CHAPTER 3

Spatial and temporal changes of thermohaline and biogeochemical characteristics of coastal marine systems at local scale (Marche region) and interactions with river outflows

Introduction

Among the European waters, the ecosystems of the Adriatic Sea, and particularly its northern part, are recognized to be severely affected by different human pressures including fishing and pollution from land-based activities (Lotze et al., 2006; Diaz and Rosenberg, 2008; Halpern et al., 2008; Coll et al., 2009), which can determine important impact also on different vulnerable habitats (Micheli et al., 2013). The north-western side of the Adriatic basin is characterized by important river inputs which, by collecting nutrient loads from zootechnical and agricultural activities, can be main drivers of eutrophication phenomena. Such events are recognized as one of the major threats in coastal areas (Gladan et al., 2015) and, as such, need to be monitored and managed by European directives. Moreover, preservation and restoration of coastal areas is fundamental in order to ensure long term sustainability of ecosystem's good and services from recreational, economic and environmental point of view. Since the beginning of the 19th century, from North to South, the basin appears characterized by progressively reduced nutrient concentrations in the surface layer, and by a decrease of the seasonal cycle amplitude in the middle and southern parts of the basin. After 1970 significant changes of trophic status of the northern Adriatic ecosystem occurred (Giani et al., 2012). In particular, a gradual increase of eutrophication occurred during 1970's until mid-1980's, followed by a reverse trend particularly marked in the 2000s due to the combination of reduction in phosphorus loads from human activities and modification in climate features. It is worth to note that the Po River outflow has been particularly low after 2002, especially in 2003, 2005 and 2006 (Zanchettin et al., 2008). This, together with decreased nutrient release, might explain the decrease in phosphate and ammonia concentrations in the northern Adriatic in the recent past (Solidoro et al., 2009). These factors can determine major effects on phytoplankton assemblages in terms of overall biomass, species composition and phenology (Mélin et al., 2011).

So far, several studies investigated dynamics and impacts triggered by rivers runoff in northern Adriatic Sea, but few investigations have been carried out to understand patterns at local scale. Given the influence of hydrodynamic features, different bathymetry level, and the rivers contribution, spatial and temporal dynamics of the Adriatic Sea at basin level not always reflect small scale phenomena.

To provide new insights on dynamics occurring at local spatial scale, this chapter of the PhD thesis has analyzed spatial and temporal patterns of temperature, salinity, inorganic nutrients and phytoplankton biomass in relation with river outflows and nutrient load transported along the entire coastal area of the Marche Region. This because it is known that continental transport of nutrients coming from different anthropogenic sources (wastewaters, zoo technical and agricultural activities; Nincevic-Gladan et al., 2015), can have significant effects on the biogeochemistry of receiving coastal waters (e.g. inducing eutrophication phenomenon). To do so, two different sources of *in situ* data were exploited deriving i) from Regional Agency for Environmental Protection (A.R.P.A.M.) which made available data acquired at monthly basis in 56 stations at two different distances from the coastline (500 and 3000 meters) and at the river mouth since 2003; ii) from Regional Civil Protection which made available data on daily mean river outflow for different rivers of the Marche Region.

Materials and methods

Study area

The Marche Region occupies about 9.365,86 km² of the Italian territory and are located on middle-Adriatic side, with an elongated shape developed from NW to SE (Figure 1). It is extended from Conca to Tronto Rivers from north to south, and it's limited by Appennino umbro-marchigiano in the west side. The 173 km of coastline has a straight tendency, with sandy or gravelly beaches. The coastline is interrupted, in the middle, by Monte Conero promontory that divides the coast in two different sides, the northern one with NW-SE orientation, and the southern one with NE-SW orientation. This entails a stronger influence of the Po River on the coastal waters of northern side of the region, while the south side dynamics are more related to regional river outflows. Rivers rise from Apennines, have a typical torrential features and maintain a parallel course till the coastline. The longest one is Metauro (121 km), followed by Tronto (115 km), Potenza (95 km), Chienti (91 km) and Esino (85 km).

Rainfall regimes are usually higher in spring and autumn, but in the last four decade it has been recorded a decreasing trend, with an enhancement of drought periods started from 1980. It has been also observed a moderate drought in November, February and during summer, followed by extreme drought in December and January, in contrast with spring when rainfall regime is higher than standard.

Figure 1 - Marche Region.

Data mining from ARPAM

The Marine Directive 2000/60/CE has introduced a strong innovation in the monitoring of surface and hypogeum water bodies, and defines a reference framework to community actions related to water protection, including coastal marine waters. The Directive aims to guarantee protection and restoration of marine ecosystems in European seas and to ensure the ecologic fairness of economic activities linked to marine environment, to prevent qualitative and quantitative deterioration of water bodies, improving water conditions and ensuring a sustainable exploitation of water resources.

The national law n.152/2006 transpose the European Directive and successive implementation decrees dictating the criteria to planning monitoring activities, perform the analysis and elaborate results.

The Marche Region, along with other Adriatic regions, is elaborating its own "marine strategy" as defined in 2008/56/CE Directive. In this perspective, monitoring activities which are carried out by the Agency for the Environmental Protection of Marche Region (ARPAM) provide key information on the ecological status of coastal marine environment.

Sampling activities in the Marche Region are carried out once a month during the year and twice a month in June-September period. In the Marche Region, monitoring grid consists of 35 stations (Tab. 1) located along transects of stations, located at different distance from the shorelines (i.e. from the mouth of the main rivers up to 3000 m far the shorelines; Table 1; Figure 2).

In this study only the datasets collected at the mouth of the major rivers and at 500 and 3000 m from the coastline were considered since they displayed the wide temporal and spatial coverage. In particular, data of temperature and salinity and of chlorophyll-a, phosphate, total phosphorus, nitrate, nitrite and ammonia concentrations collected from March 2003 up to August 2014 were considered. Data underwent first a deep quality check and then they were used for elaborations.

NOME	CODICE STAZIONE	COMUNE	PROV.	DISTANZA DA RIVA
S.Bartolo 500	0021	Pesaro	PU	500 m
S.Bartolo 3000	3021	Pesaro	PU	3000 m
Viale Berna	015	Pesaro	PU	100 m
Fosso Sejore 500	0022	Pesaro	PU	500 m
Fosso Sejore 3000	3022	Pesaro	PU	3000 m
Metauro 500	0003	Fano	PU	500 m
Metauro 3000	3003	Fano	PU	3000 m
Sud Metauro	076	Fano	PU	100 m
Misa 500	0006	Senigallia	AN	500 m
Misa 3000	3006	Senigallia	AN	3000 m
Rotonda Senigallia	008	Senigallia	AN	10 m
Casello 190	026	Montemarciano	AN	10 m
Esino 500	0007	Falconara Marittima	AN	500 m
Esino 3000	3007	Falconara Marittima	AN	3000 m
Trave	051	Ancona	AN	10m
Conero 500	0009	Ancona	AN	500 m
Conero 3000	3009	Ancona	AN	3000 m
Palombina	040	Ancona	AN	10 m
Musone riva	001	Porto Recanati	MC	10 m
Musone 500	0010	Porto Recanati	MC	500 m
Musone 3000	3010	Porto Recanati	MC	3000 m
Sud Fiumarella	009	Porto Recanati	MC	10m
Potenza 500	0011	Porto Recanati	MC	500 m
Potenza 3000	3011	Porto Recanati	MC	3000 m
Fosso Maranello	047	Civitanova Marche	MC	10 m
Chienti 500	0012	Civitanova Marche	MC	500 m
Chienti 3000	3012	Civitanova Marche	MC	3000 m
Tenna 500	0015	Porto San Giorgio	FM	500 m
Tenna 3000	3015	Porto San Giorgio	FM	3000 m
Rio Vallescura	0089	Fermo	FM	200 m
Aso 500	0017	Pedaso	FM	500 m
Aso 3000	3017	Pedaso	FM	3000 m
Sud Tesino	0080	Grottammare	AP	10 m
Tronto 500	0020	San Benedetto del Tronto	AP	500 m
Tronto 3000	3020	San Benedetto del Tronto	AP	3000 m

Table 1 - Name, station code, municipality, district and distance from the coast of each monitored station.

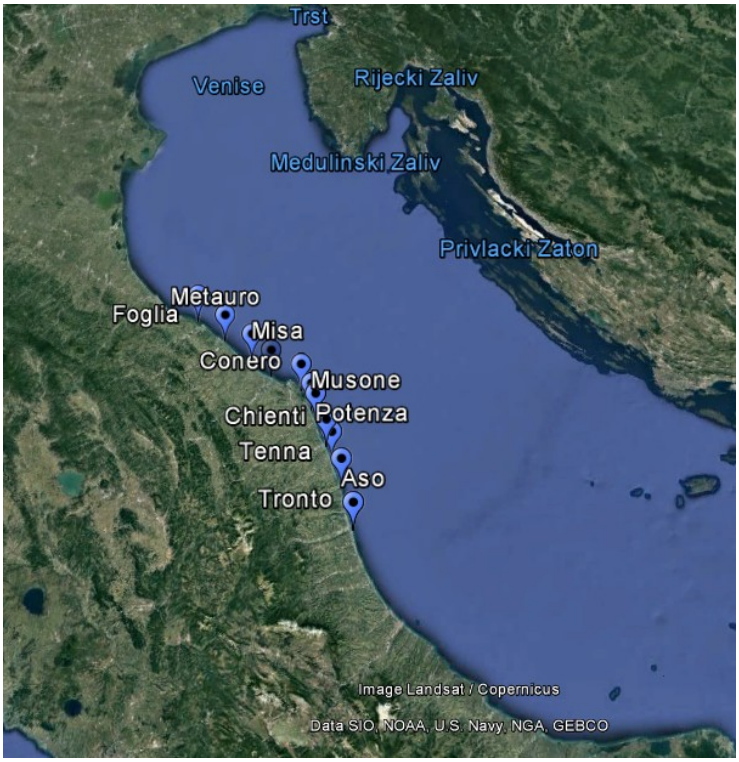

Figure 2 - Map of ARPAM monitored stations (Google Earth).

Data mining from Regional Civil Protection of the Marche Region

Regional system of Civil Protection and Local Safety has realized an extended real time monitoring network for principal meteorological (precipitation, temperature, humidity, wind, etc.) and hydrological (rivers hydrometric level) parameters in order to forecast and prevent hydrological risks in Marche Region. Main objectives of Regional Civil Protection are the constant monitoring and protection of territory by means of (i) real time observations of precipitation and hydrometric level of rivers (ii) measurements, elaboration, storage and visualization of meteorological and hydrological data and their real time spreading and (iii) to made available validated data to produce hydrological annals and data sharing in several fields such as hydrology, hydrogeology, environmental studies and management of water and environmental resources.

Real time monitoring of river inputs is performed by means of specific sensors which, at regular time interval, measures and stores hydrometric level. In Marche Region, such activity is performed by hydrometric stations of Meteo-Hydro-Pluvio regional network. Data are transmitted and made available on Civil Protection website. From these measures, and on the basis of known river section (included in the monitoring activities), river inputs can be quantify.

In this study, river inputs (as daily mean m^3/s) were selected and analyzed on the basis of their temporal robustness. Eight rivers were chosen: Foglia (12°53'51.75571", 43°54'27.19793"), Cesano (13°10'15.79037", 43°44'58.76164"), Misa (13°9'53.99683", 43°39'45.57611"), Esino (13°19'57.21226", 43°35'59.39171"), Musone (13°34'0.09826", 43°29'38.40011"), Potenza (13°39'5.82206", 43°24'55.1146"), Tenna (13°46'20.65858", 43°13'57.63727"), Tronto (13°53'47.7096", 42°53'31.6608").

Data elaborations

Several kind of elaborations were performed with the two datasets. For the first part of the work, we considered data of surface waters collected at 500 and 3000 meters from the coastline in different areas (Foglia, Cesano, Misa, Esino, Conero, Musone, Potenza, Chienti, Tenna, Aso and Tronto) from 2003 to 2014. Before data elaborations a deep quality check has been carried out. First, a conversion in *.csv* format allowed to convert excel boxes where text does not correspond to the format cell - incorrect visualization- especially for date. Other punctual errors had been corrected semi-automatically by means

of *sed* command from the Linux shell. Finally, using *AWK* programming language, a script has been created ad hoc in order to erase the spikes - usually due to refuses -, define lower and upper threshold, modify punctual not valid values and re-organized data in a unique text file easily readable from MATLAB® software.

A second script was created in MATLAB® to organize data in structure arrays in order to derive information about temporal pattern of each variable for each station. A structure array is a data type that groups related data using data containers called fields. Each field can contain any type of data or other fields. In our case, for example, the field *Foglia* contained six fields carrying information on distances from the coastline, date, variables. Mann-Kendall test (Mann, 1945; Kendall 1975) was performed to statistically assess if there is a monotonic upward or downward trend of the variable of interest in the period under investigation, followed by computation of regression index R^2.

Time series were first plotted for each station at 500 and 3000 m from the coast for each variable in order to have an overall preview about quality, reliability and spatial-temporal robustness of the ARPAM dataset, along with preliminary knowledge of variables' dynamics over time.

During the period under investigation and, in particular after 2008, some modifications were introduced by ARPAM for sampling stations selection. Only the most complete ones were taken into account (see Annex III for the whole results).

Assembling stations at the same distance from the coast, monthly means of each variables were computed and a regression analysis were performed for the entire region and then sub-dividing the dataset in northern and southern part of the region.

Finally, to highlight spatial dynamics over time, temporal average was computed for each station at 500 and 3000 m from the coast, at interannual and seasonal scale.

In order to highlight the potential causes of system variability over space and time, rivers outflow data were considered. A script was created to find spatial and temporal matching between ARPAM measures and river discharge data from Civil Protection. In this phase several data were discarded because of no correspondence in time and/or space. As such spatial-temporal correspondences were found only for the following rivers outflow: Misa, Esino, Musone, Potenza and Tronto at both distances from the coast.

Results

At both 500 m and 3000 m distance from the coastline, values of temperature were characterized by significant interannual changes, with decreasing values from 2003 to 2014 both in the northern and in the southern sector of the Marche Region (Figure 3). Similar patterns were also observed for salinity values which significantly decreased (Table 2) during the investigated period (Figure 4).

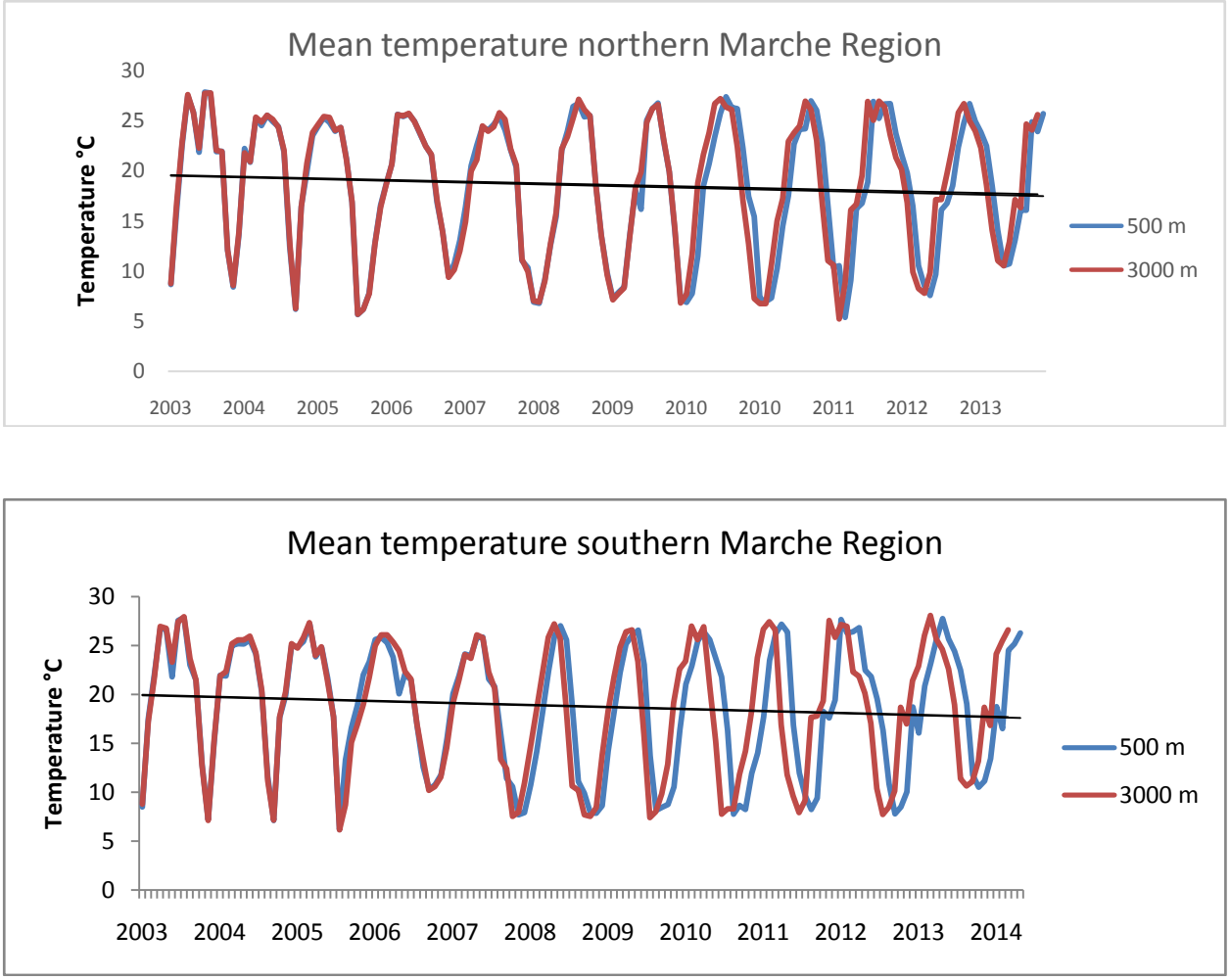

Figure 3- Interannual temperature variations at 500 m (blue line) and 3000 m (orange line) from the coast of the northern and the southern sector of the Marche Region

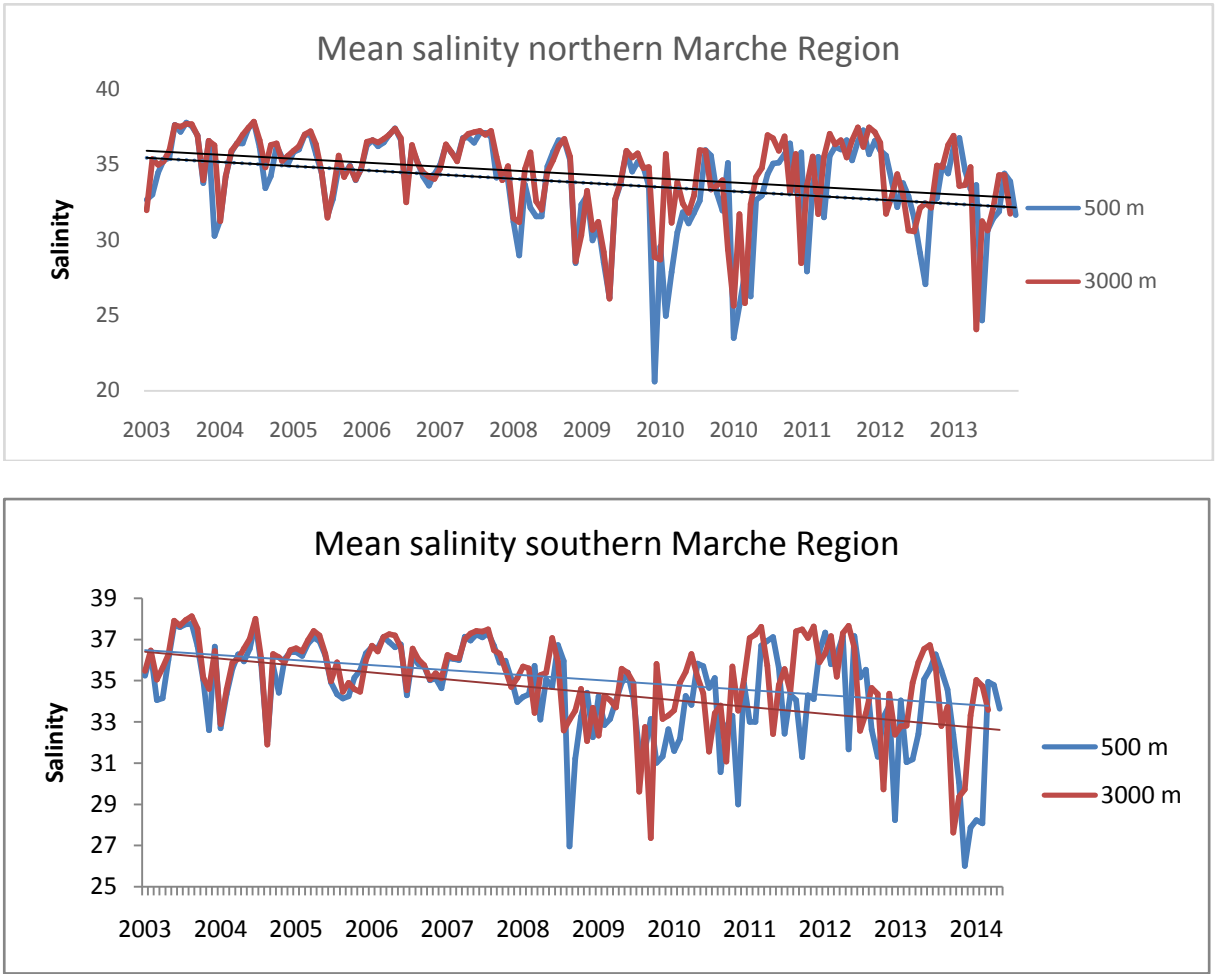

Figure 4 - Interannual salinity variations at 500 m (blue line) and 3000 m (red line) from the coast of the northern and the southern sector of the Marche Region

No clear inter-annual changes were observed for chlorophyll-a concentrations both in the northern and in the southern sector of the Marche Region, although higher values were found in the northern part of the region (Figure 5).

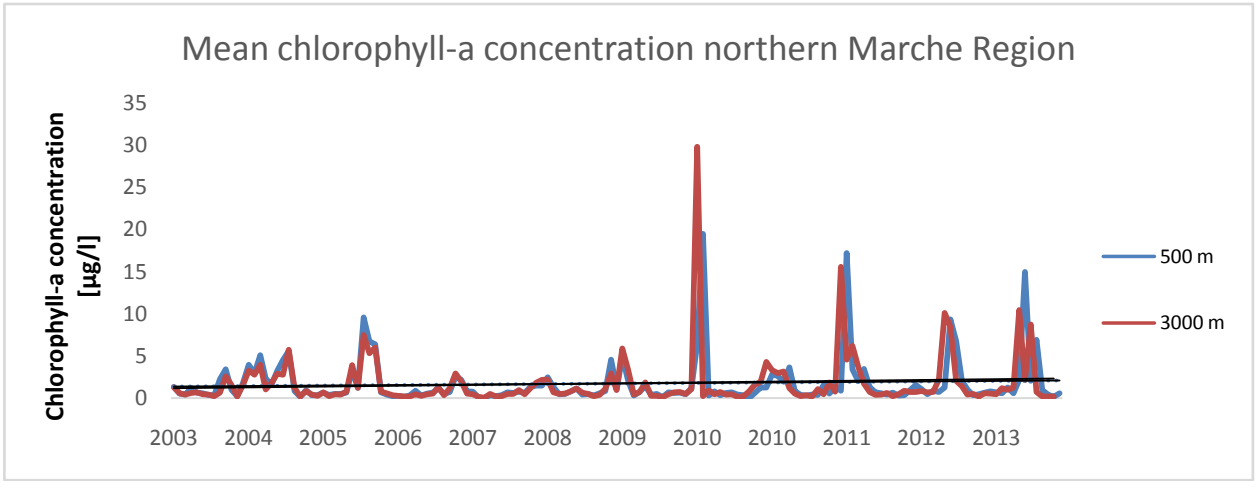

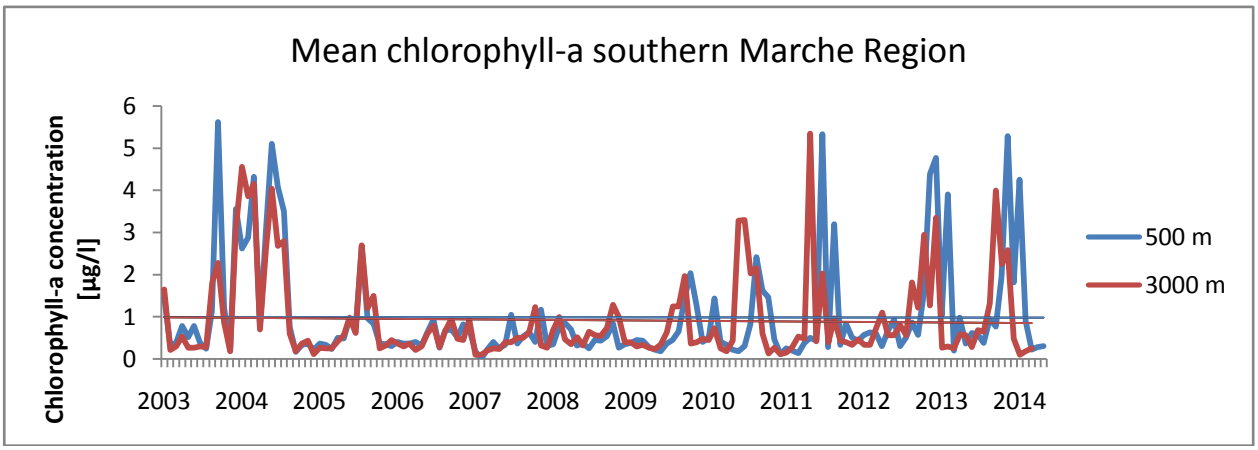

Figure 5 - Interannual chlorophyll-a variations at 500 m (blue line) and 3000 m (orange line) from the coast of the northern and the southern sector of the Marche Region

Conversely to what observed for temperature and salinity, total phosphorus concentrations in surface waters of both the northern and southern sector of the Marche Region significantly increased, with a more pronounced increase at 500 m than at 3000 m far the coastline (Figure 6).

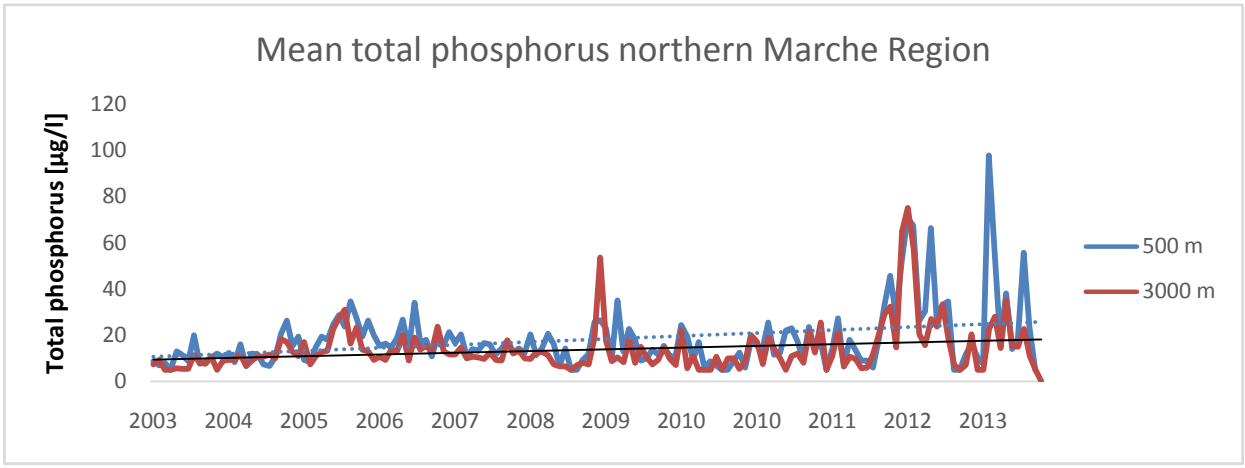

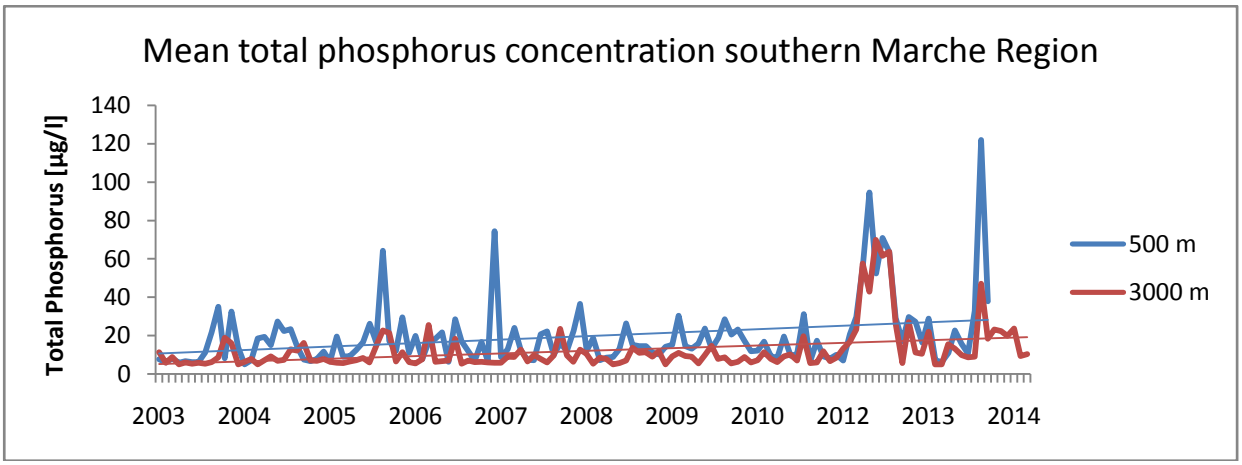

Figure. 6 - Interannual total phosphorus variations at 500 m (blue line) and 3000 m (orange line) from the coast of the northern and the southern sector of the Marche Region

Also nitrate concentrations were characterized by major inter-annual changes with an increasing pattern, although not always consistent, from 2003 to 2014 (Figure 7).

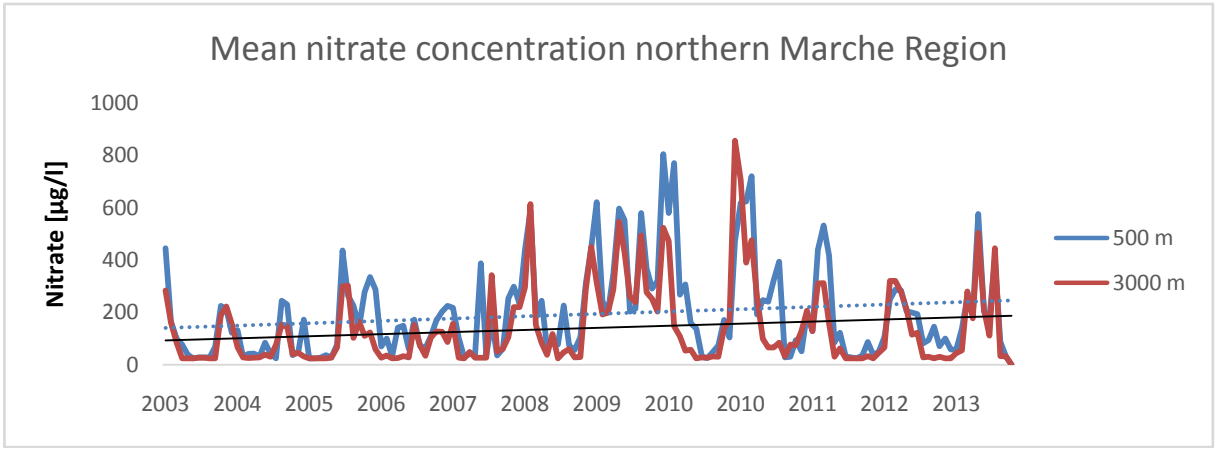

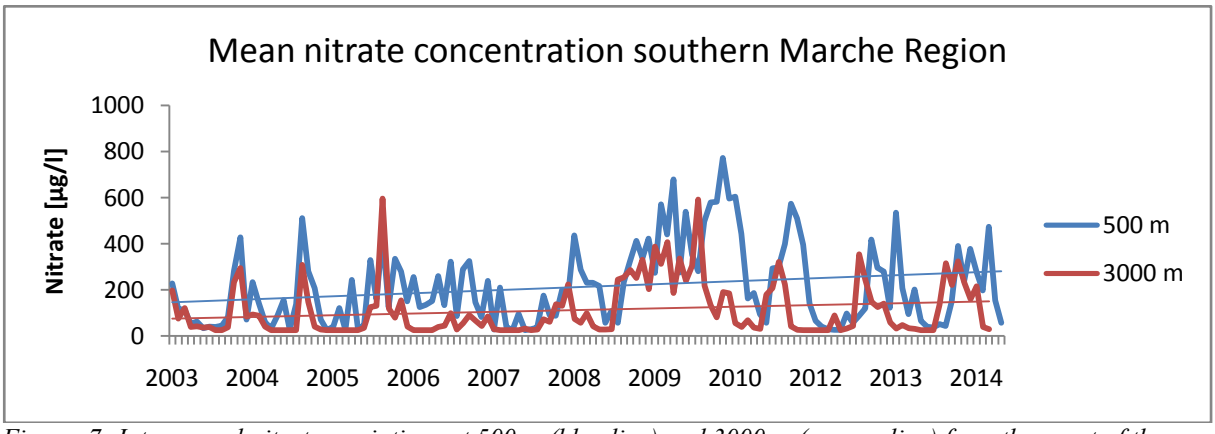

Figure. 7- Interannual nitrate variations at 500 m (blue line) and 3000 m (orange line) from the coast of the northern and the southern sector of the Marche Region

	500 m		3000 m	
	H	**Test Z**	**H**	**p value**
Northern Temperature	0	-1.44	0	-1.30
Southern temperature	0	-1.30	0	-1.03
Northern salinity	0.1	-1.85	0.01	-2.67
Southern salinity	0.01	-2.81	0.05	-2.54
Northern chlorophyll-a concentration	0	1.17	0	1.17
Southern chlorophyll-a concentration	0	0.89	0	0.75
Northern total phosphorus concentration	0.05	2.26	0	1.44
Southern total phosphorus concentration	0.1	1.87	0.1	1.71
Northern nitrate concentration	0.1	1.71	0.1	1.85
Southern nitrate concentration	0	1.56	0	1.56

Table 2 - Results from MAKESENS analysis, significance level (H) and the presence of a statistically significant trend (Z value). A positive (negative) value of Z indicates an upward (downward) trend.

In order to provide information on the spatial variability of the investigated variables among the different sites, mean values of the investigated variables calculated from the entire sampling periods were compared. Both temperature and salinity values were rather homogenous across the sampling sites, with the exception of the Metauro site which was characterized by lower salinity values (Figure 8).

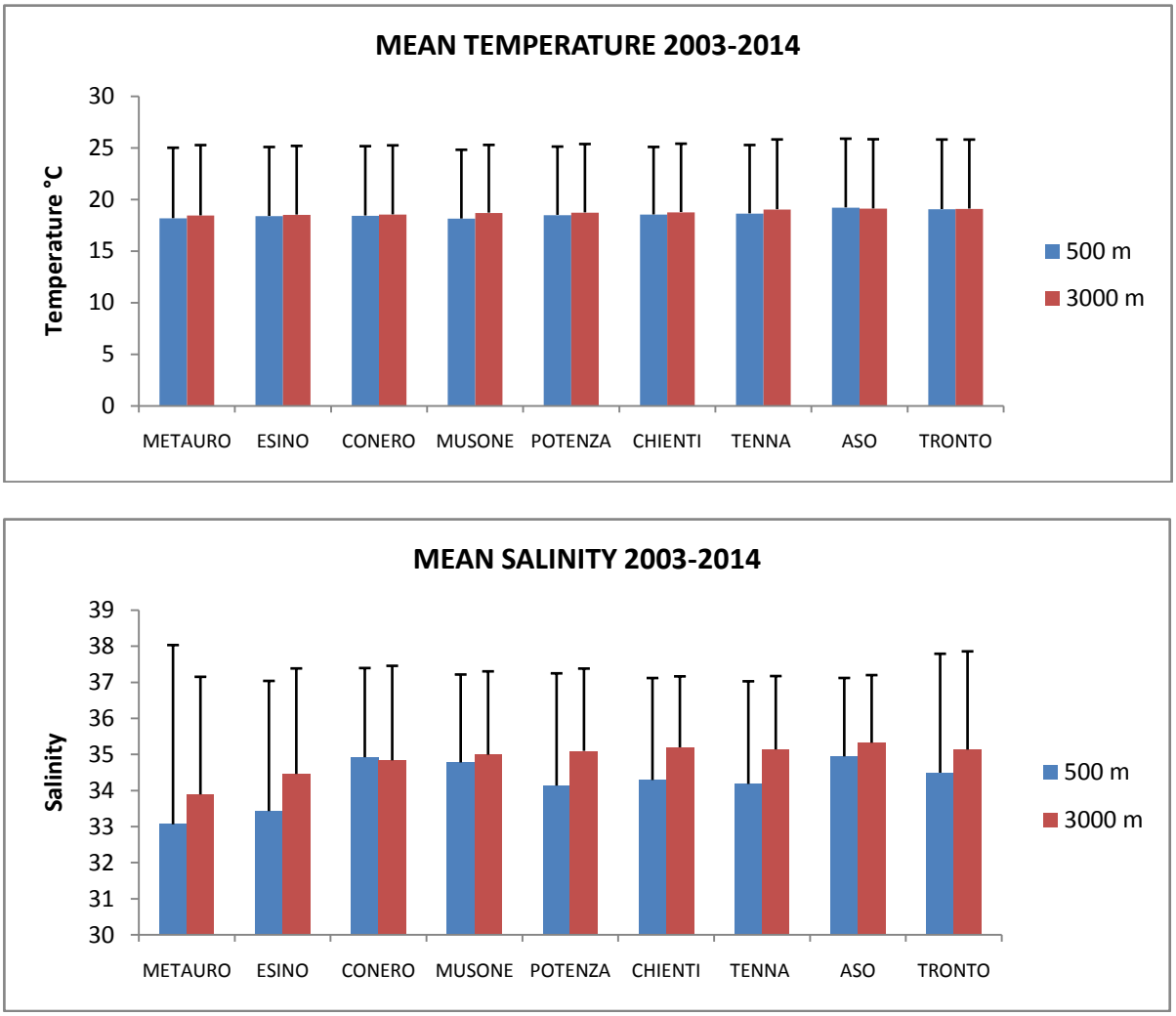

Figure. 8 - Mean values and standard deviations of temperature and salinity at 500 and 3000 m far at each sampling site

Chlorophyll-a concentrations were higher at sites located in the northern part of the Marche Region, whereas no clear spatial patterns were observed for total phosphorus and nitrate concentrations (Figure 9).

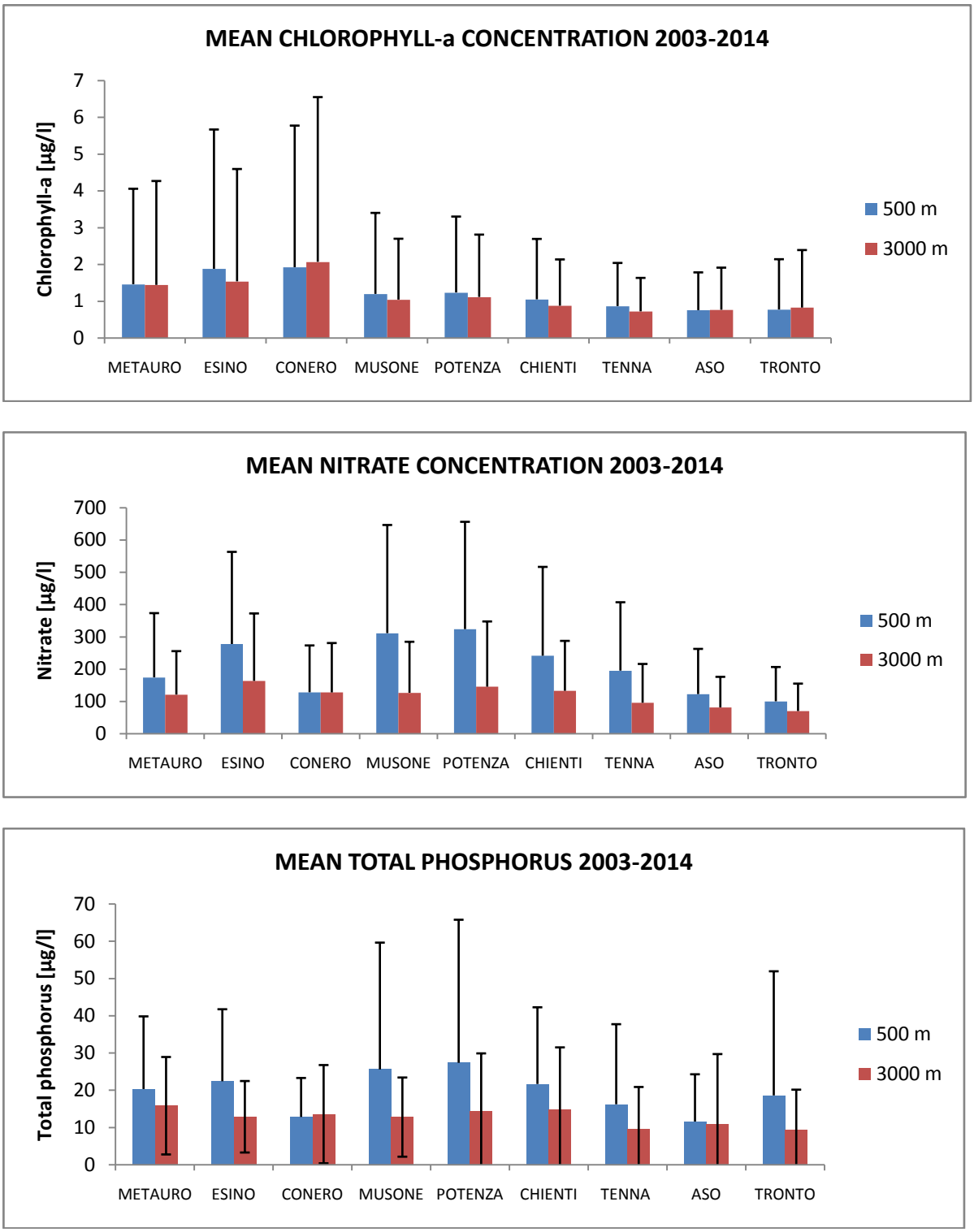

Figure. 9 - Mean values of chlorophyll-a, nitrate and phosphorus concentration at 500 and 3000 m far at each sampling site.

The investigated variables were also analyzed in order to highlight their seasonal variability across the different costal sites. In particular higher chlorophyll-a concentrations were reported in the northern sites during winter/spring season (Figure 10).

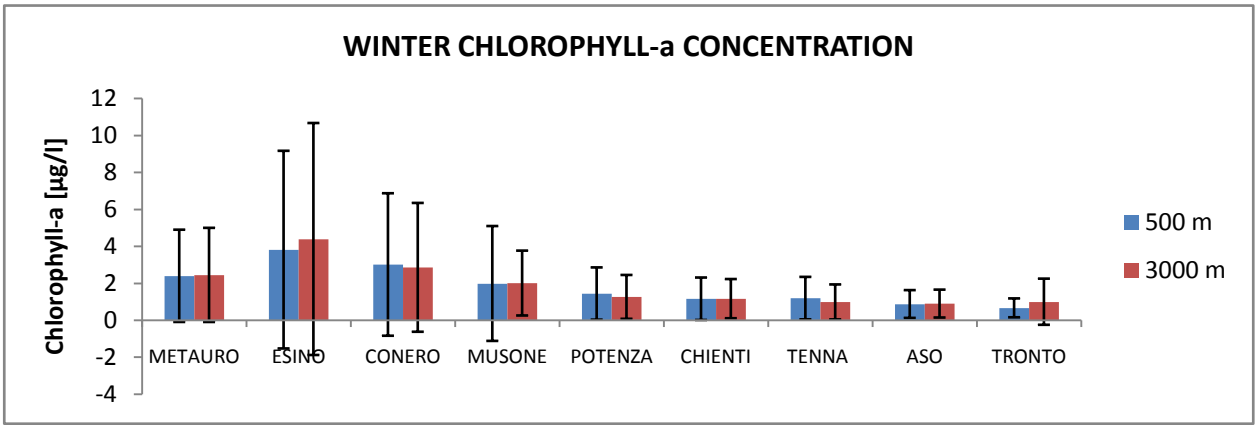

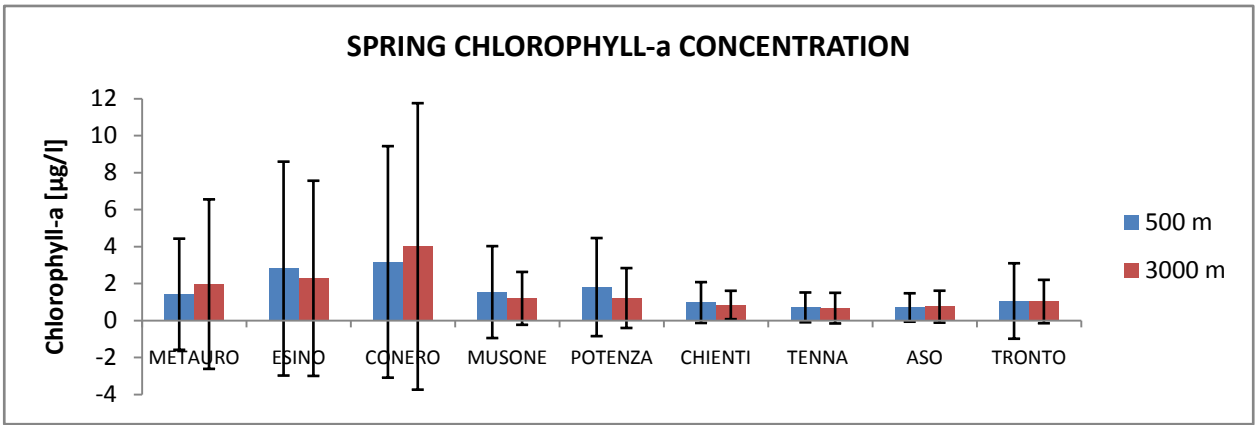

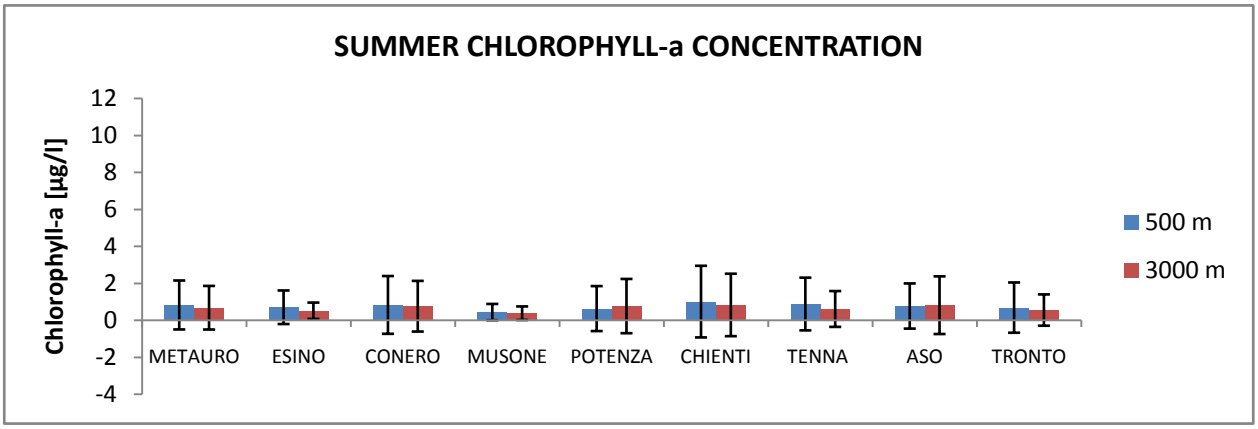

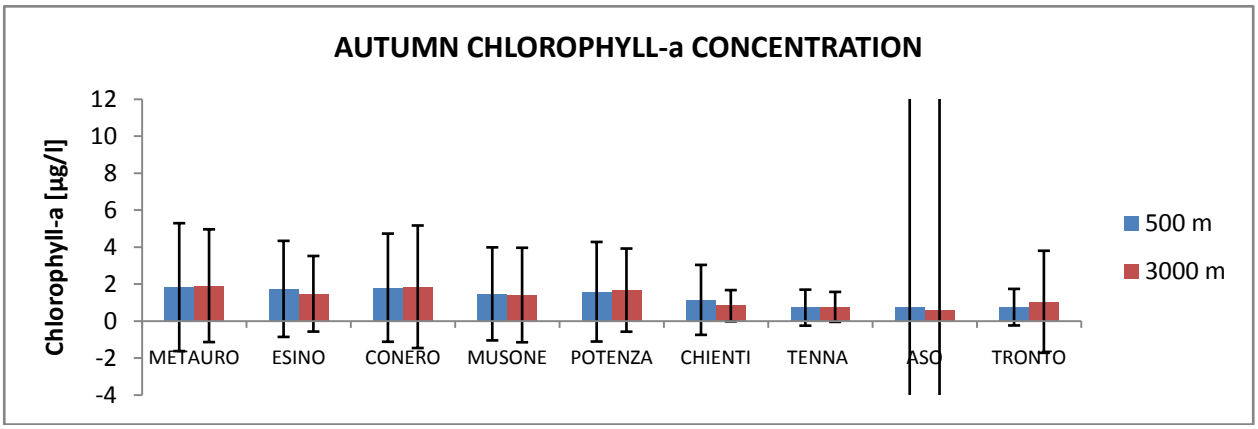

Figure. 10 - Seasonal mean values and standard deviations of chlorophyll concentrations at 500 and 3000 m far each sampling site.

Total phosphorus concentrations were characterized by seasonal changes with values lower in summer and higher in winter/spring (Figure 11).

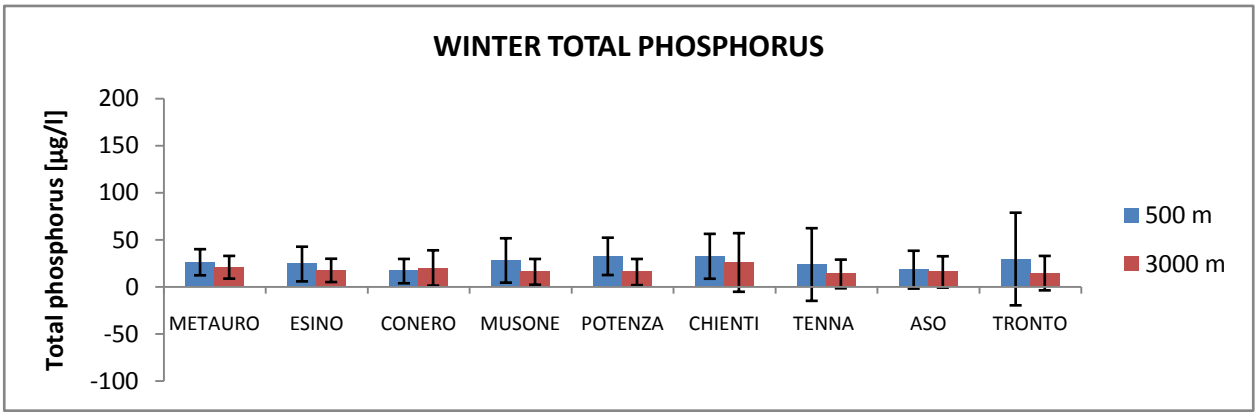

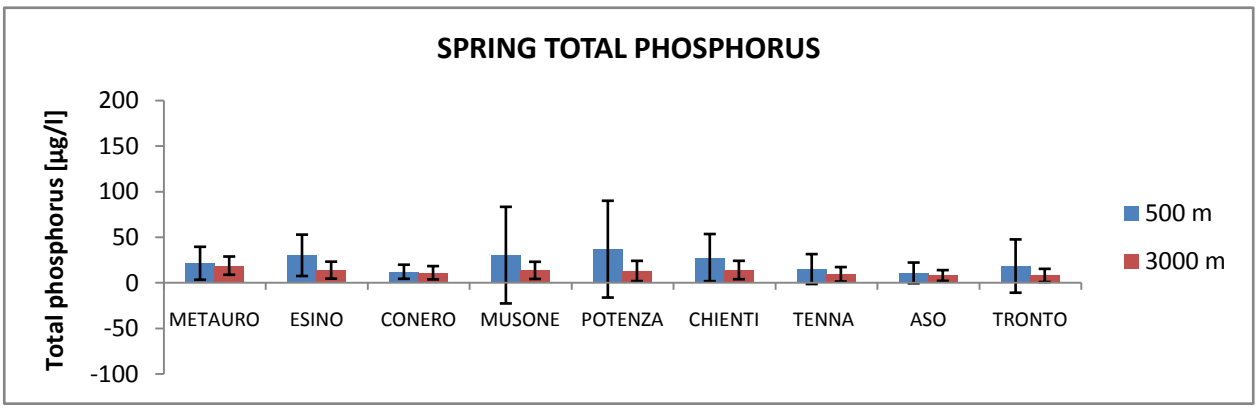

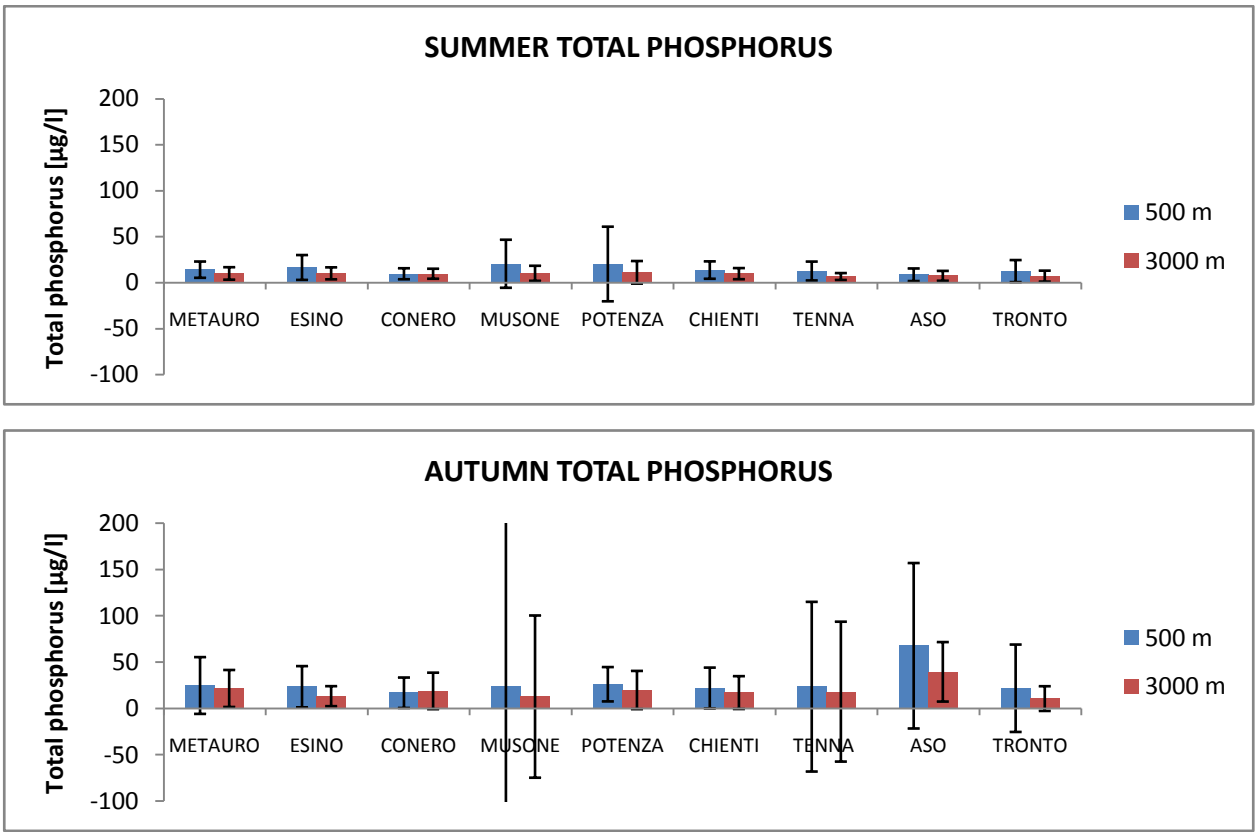

Figure. 11 - Seasonal mean values and standard deviations of total phosphorus e at 500 and 3000 m far each sampling site.

Also nitrate concentrations were characterized by similar seasonal changes (Figure 12).

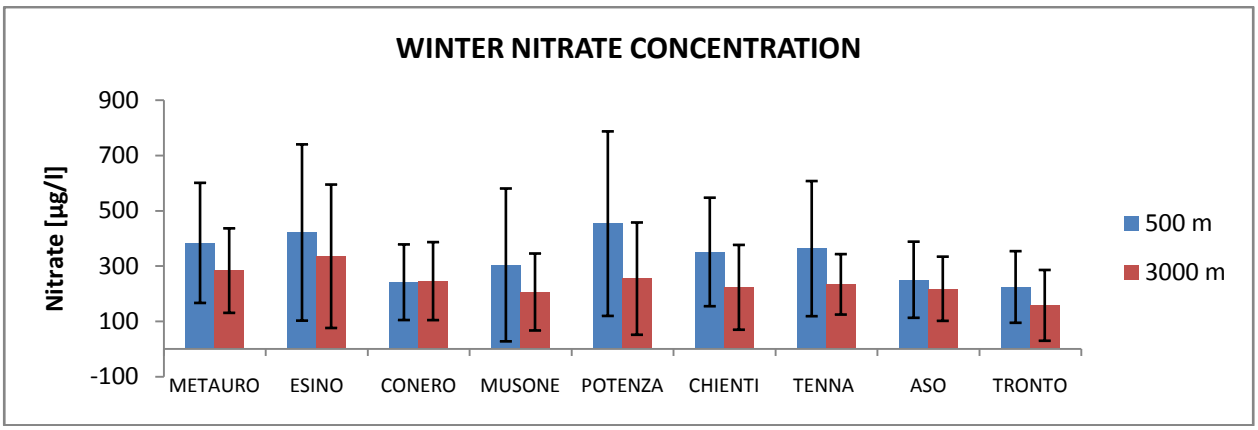

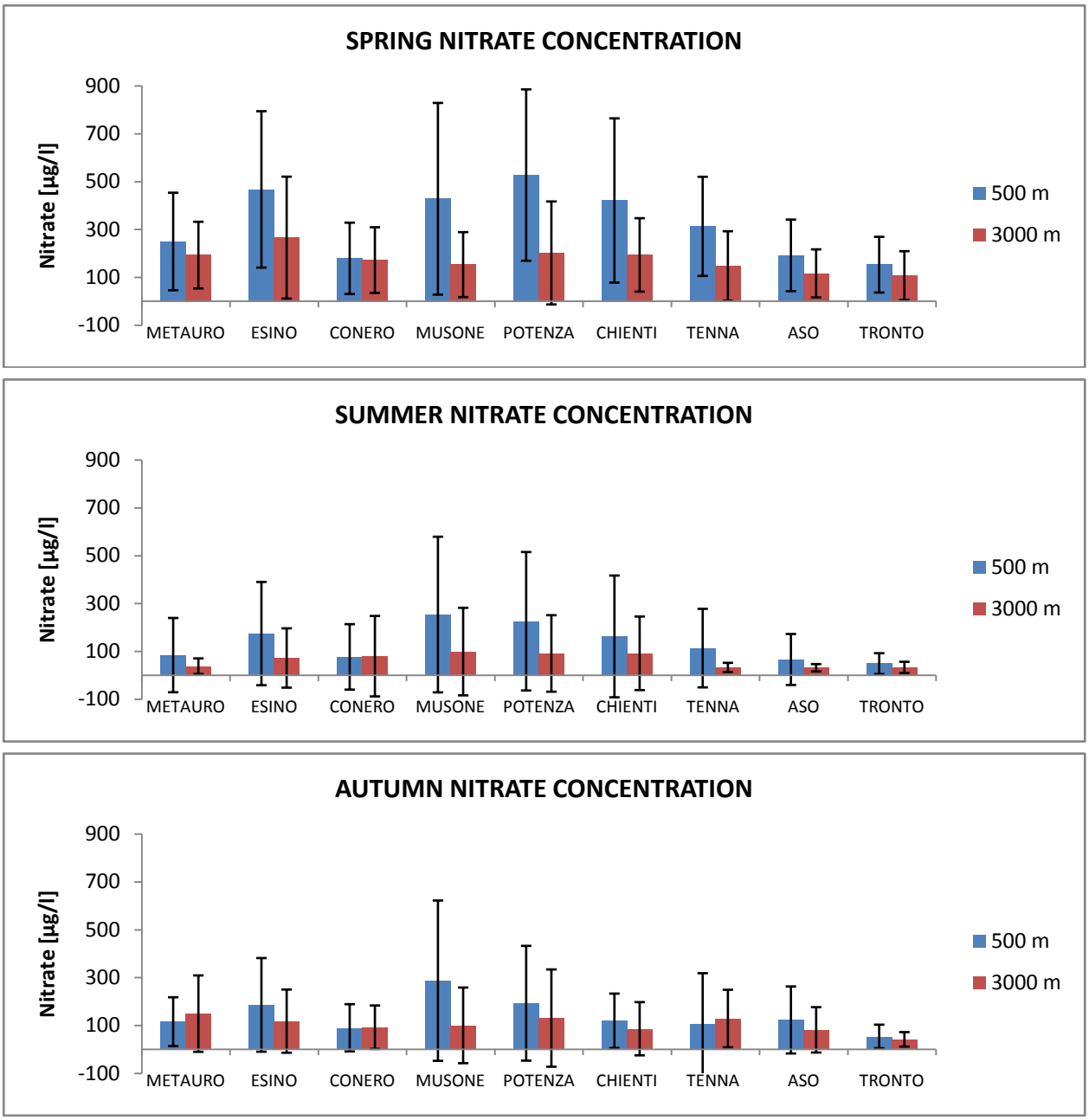

Figure. 12 - Seasonal mean values and standard deviations of nitrate concentrations at 500 and 3000 m far each sampling site.

In order to provide insights on the potential drivers influencing the spatial and temporal patterns of the investigated variables, we investigated river outflows and nutrient loads entering the coastal marine system. To do this, we utilized only data in which data of nutrient concentrations at the river mouth from ARPAM and data of river outflows from Civil Protection matched in time or space.

Our findings indicate the river outflows were the major responsible of changes of thermohaline conditions of coastal seawater, as indicated by the significant correlations we

found (Figure 13). Independently from the site considered, temperature and salinity of surface coastal waters were inversely related with freshwater inputs. Such an effect was more evident at stations closer to the coastline (i.e. at 500 m far).

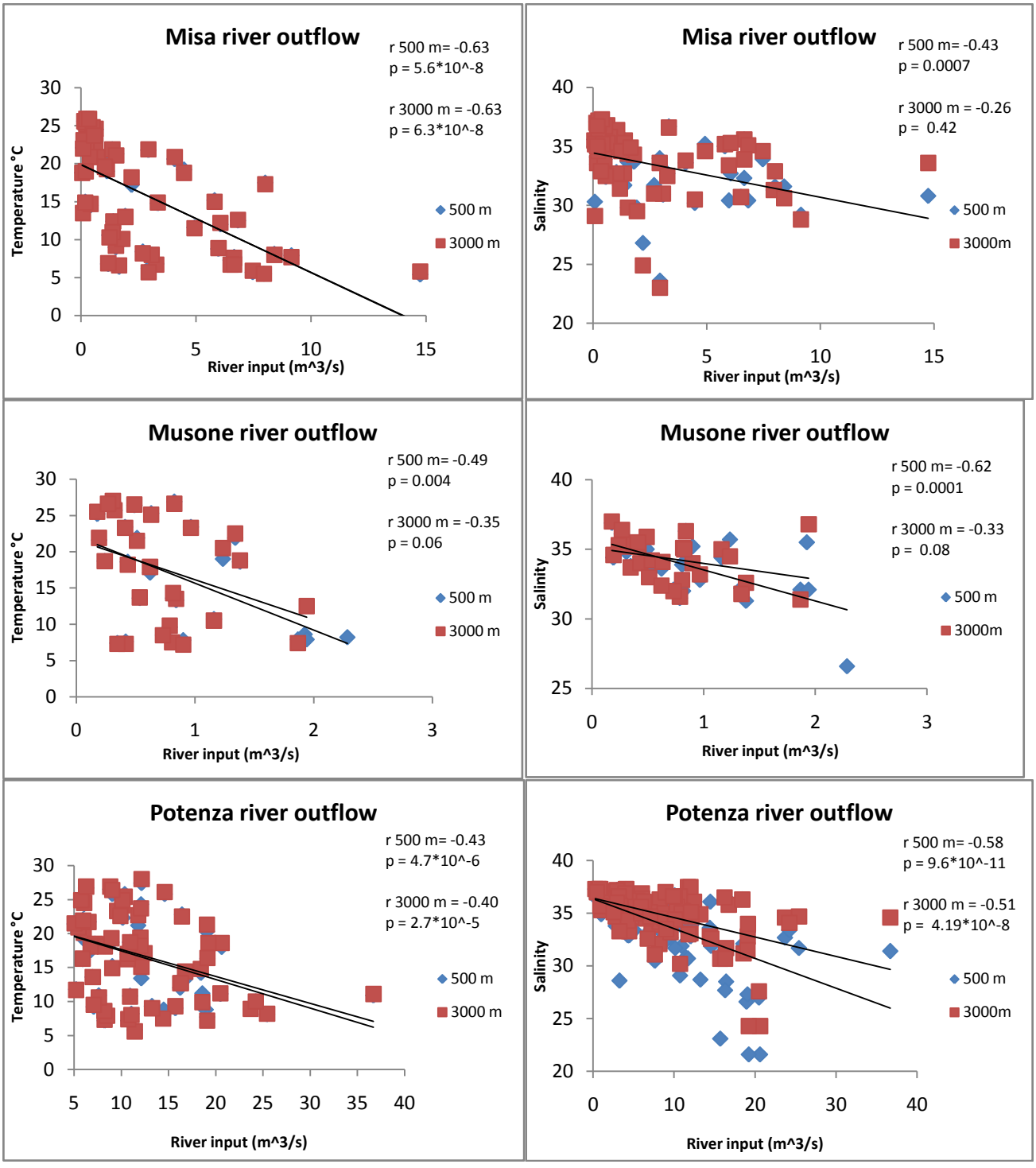

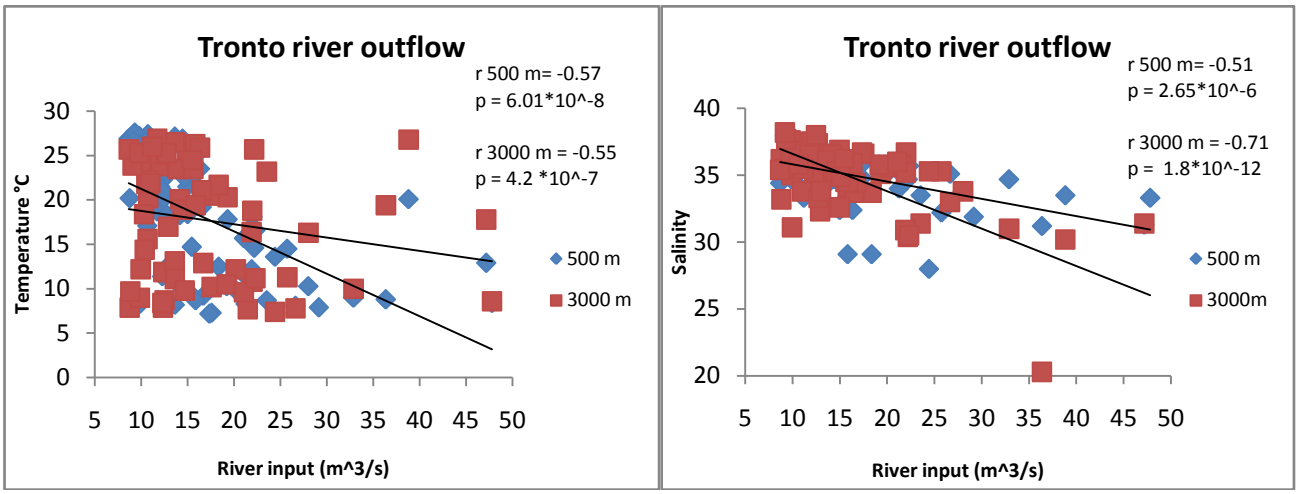

Figure.13 – Relationships between temperature and salinity determined in surface waters of different coastal marine sites and their relative river outflows. In the right corner are reported values of correlation (r) and its significant level (p).

By combining total phosphorus, nitrate, nitrite and ammonia concentrations with river outflows we estimated the annual nutrient loads entering the marine coastal ecosystems of the Marche Region (Figure 14).

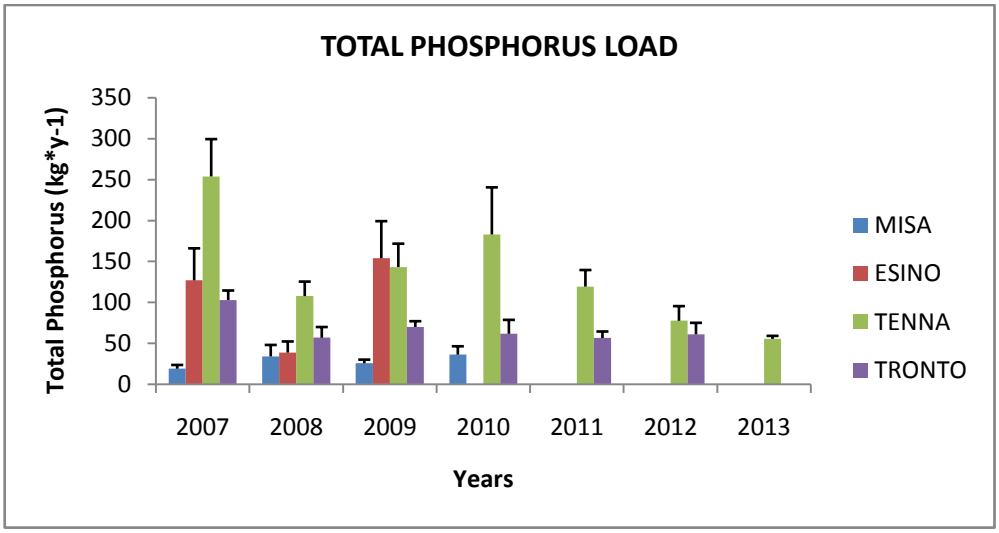

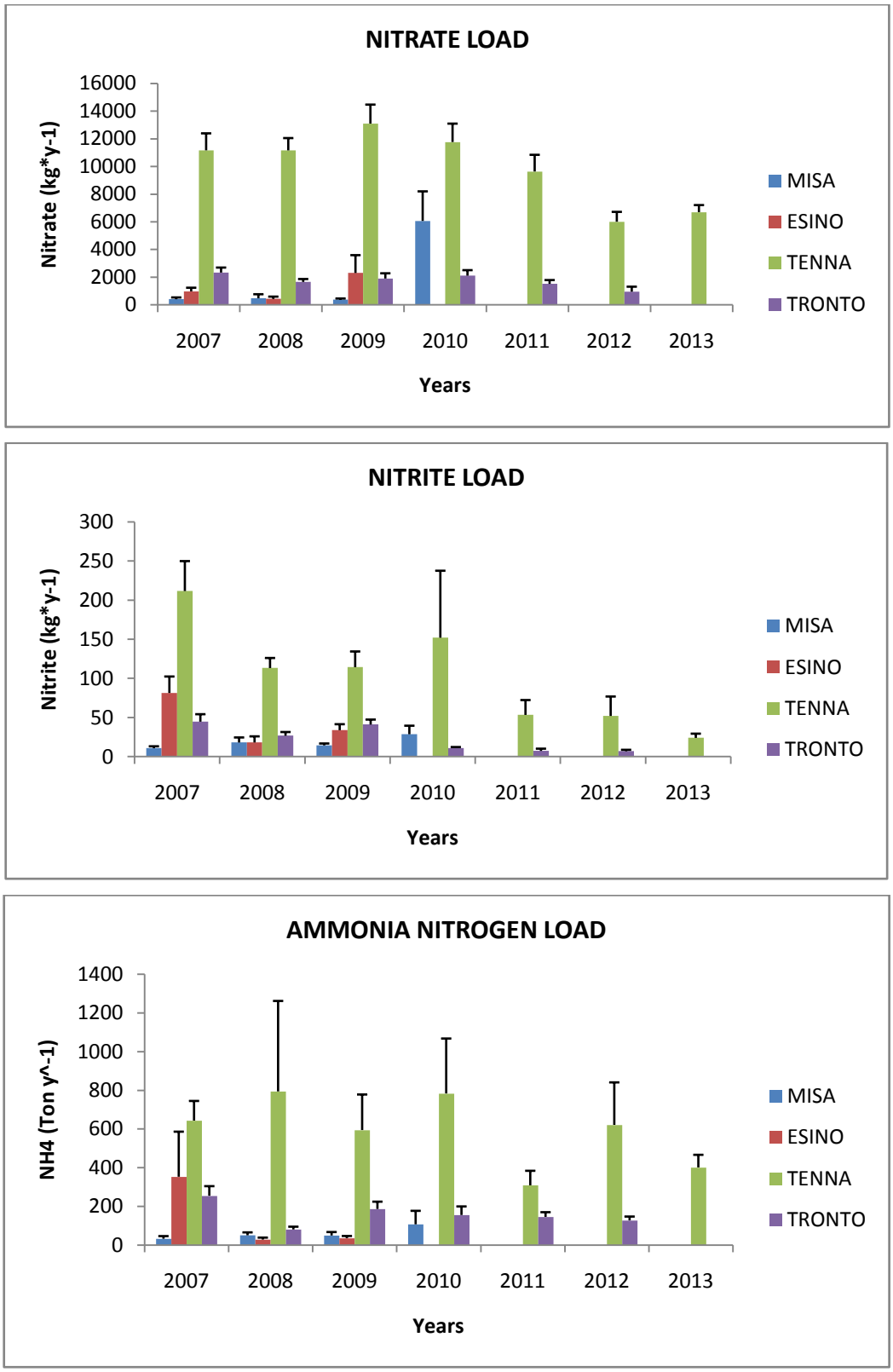

Figure. 14 - Nutrient load entering the marine system estimated at river mouth of Misa, Esino, Tenna and Tronto rivers.

This analysis revealed a wide spatial and inter-annual variability of the nutrient loads entering the coastal marine system of the Marche Region, with much higher values related

to Tenna's inputs. Independent from the coastal sites considered (belonging to the northern or southern sector of the Marche Region), the biogeochemical features of marine coastal waters in terms of inorganic nutrient concentrations and phytoplankton biomass (expressed ad chlorophyll-a concentrations) were significantly and positively related with inorganic nutrient loads from river outflows (Figure 15).

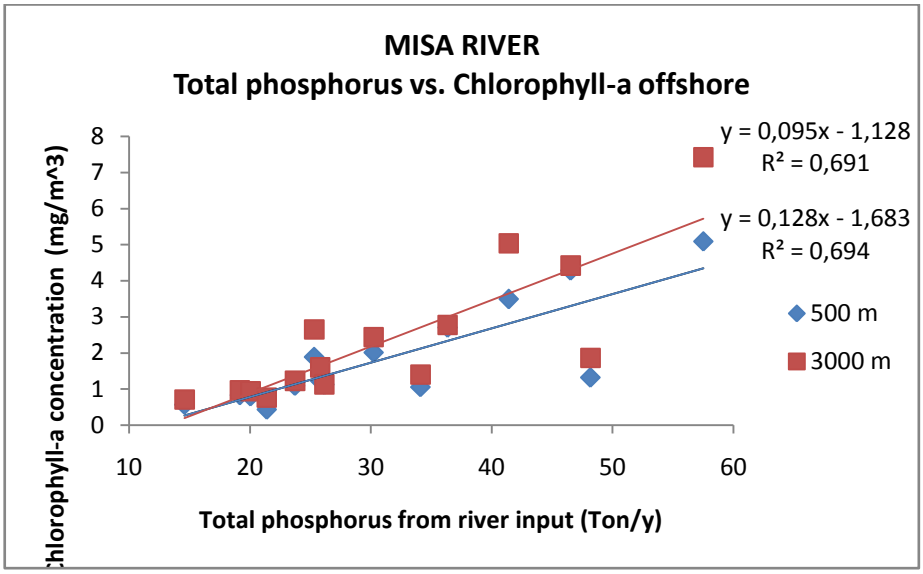

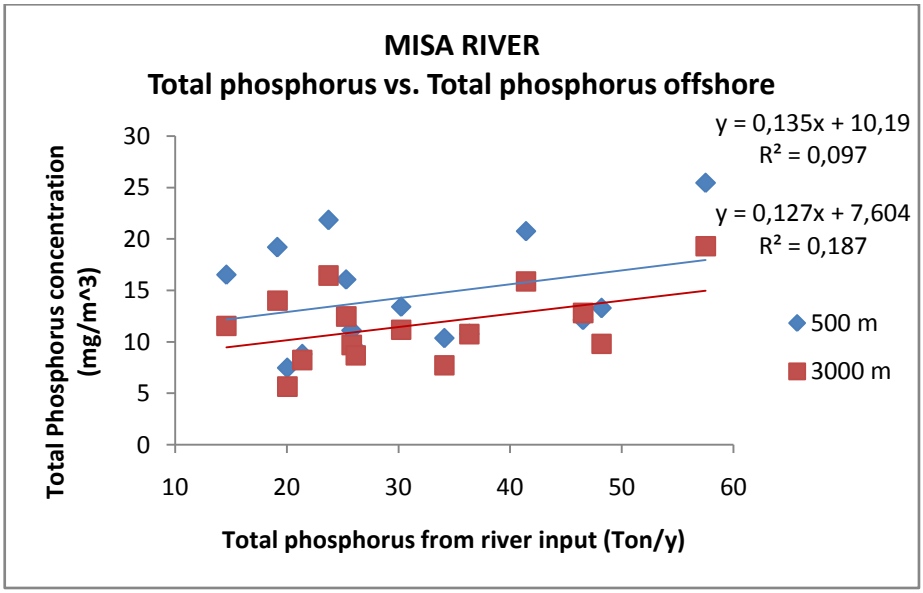

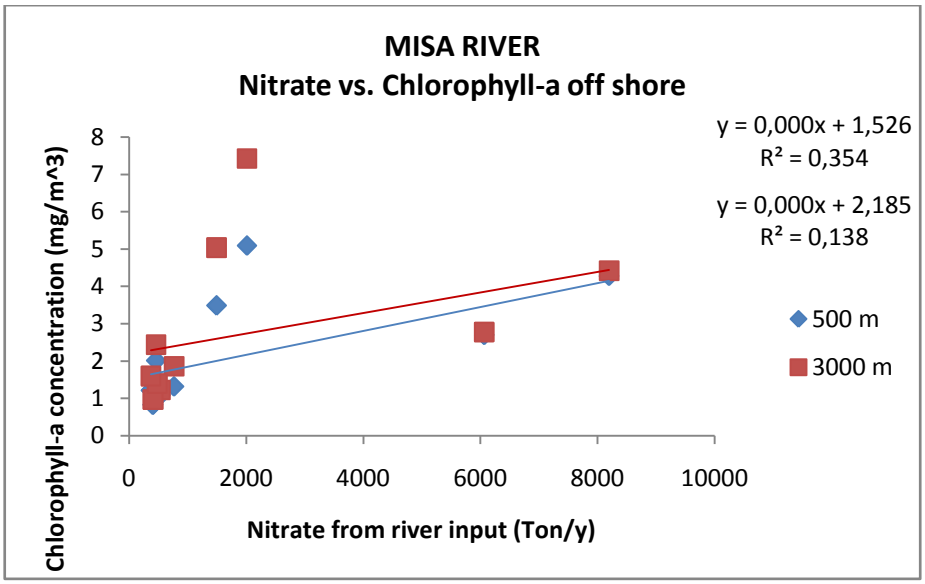
MISA RIVER
Nitrate vs. Chlorophyll-a off shore
y = 0,000x + 1,526
R² = 0,354
y = 0,000x + 2,185
R² = 0,138
500 m
3000 m
Chlorophyll-a concentration (mg/m^3)
Nitrate from river input (Ton/y)
0
1
2
3
4
5
6
7
8
0
2000
4000
6000
8000
10000

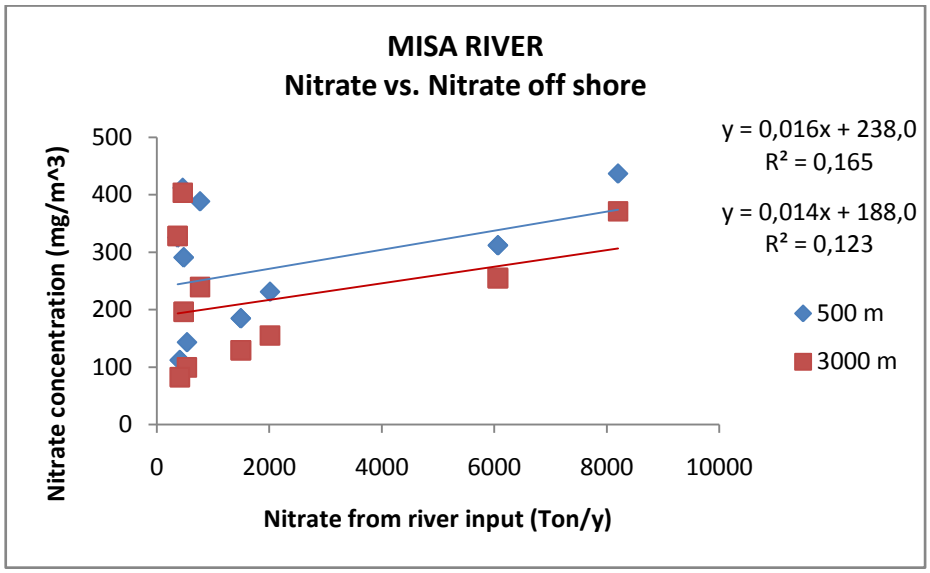
MISA RIVER
Nitrate vs. Nitrate off shore
y = 0,016x + 238,0
R² = 0,165
y = 0,014x + 188,0
R² = 0,123
500 m
3000 m
Nitrate concentration (mg/m^3)
Nitrate from river input (Ton/y)
0
100
200
300
400
500
0
2000
4000
6000
8000
10000

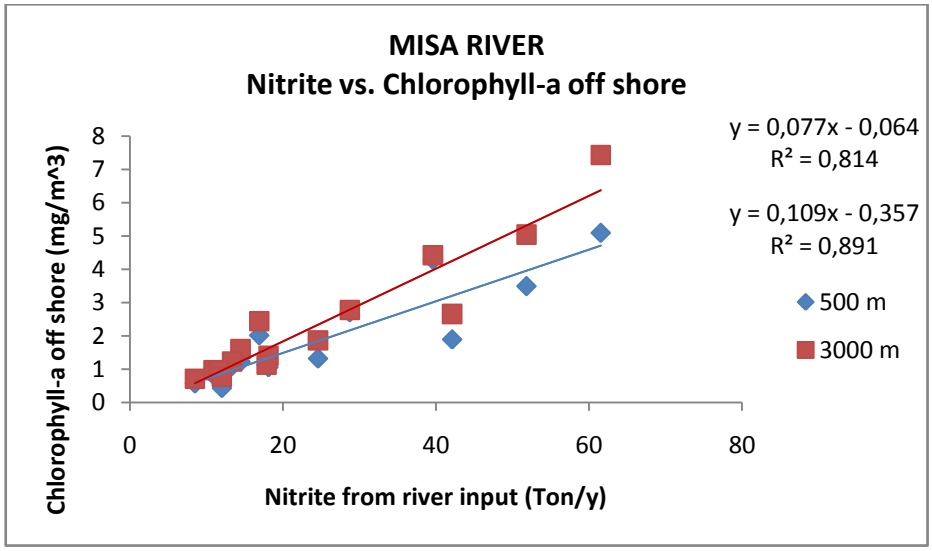
MISA RIVER
Nitrite vs. Chlorophyll-a off shore
y = 0,077x - 0,064
R² = 0,814
y = 0,109x - 0,357
R² = 0,891
500 m
3000 m
Chlorophyll-a off shore (mg/m^3)
Nitrite from river input (Ton/y)
0
1
2
3
4
5
6
7
8
0
20
40
60
80

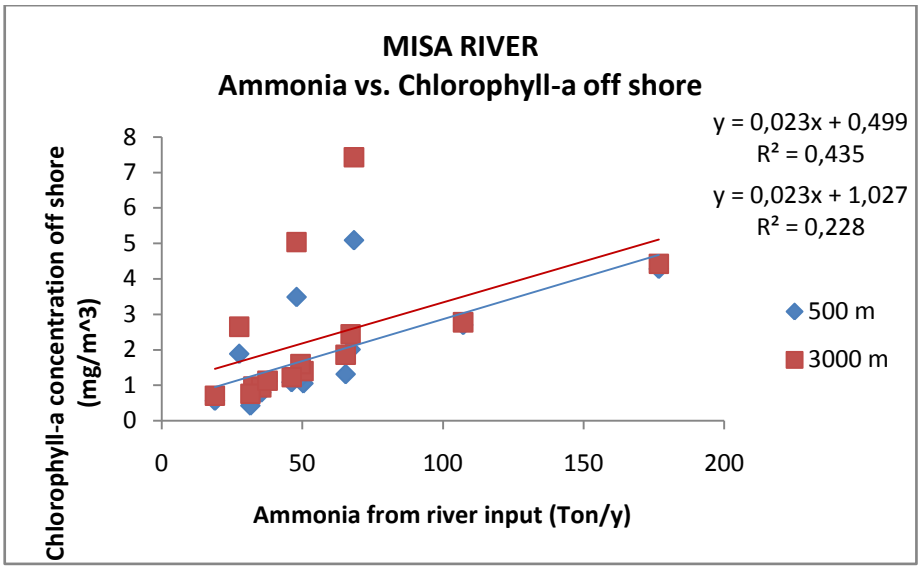
MISA RIVER
Ammonia vs. Chlorophyll-a off shore
y = 0,023x + 0,499
R² = 0,435
y = 0,023x + 1,027
R² = 0,228
500 m
3000 m
Chlorophyll-a concentration off shore (mg/m^3)
Ammonia from river input (Ton/y)
0
1
2
3
4
5
6
7
8
0
50
100
150
200

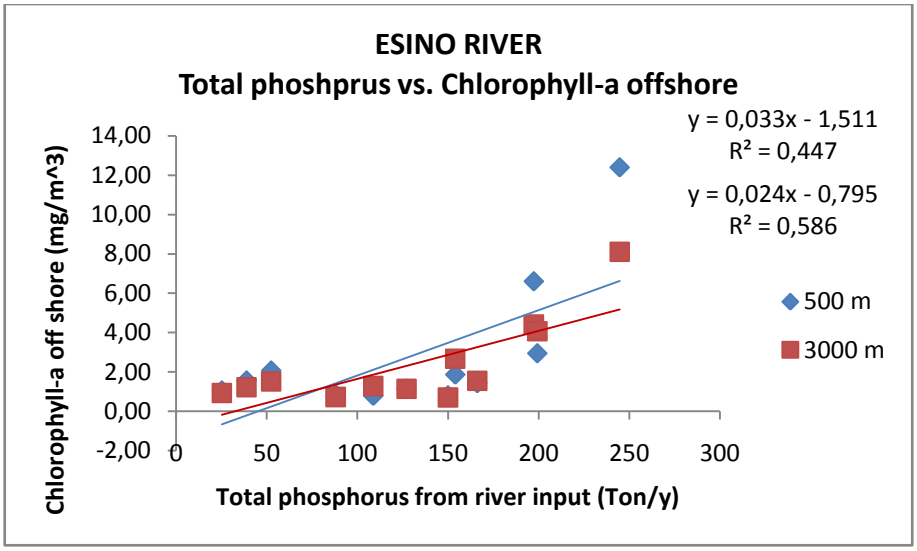
ESINO RIVER
Total phoshprus vs. Chlorophyll-a offshore
y = 0,033x - 1,511
R² = 0,447
y = 0,024x - 0,795
R² = 0,586
500 m
3000 m
Chlorophyll-a off shore (mg/m^3)
Total phosphorus from river input (Ton/y)
14,00
12,00
10,00
8,00
6,00
4,00
2,00
0,00
-2,00
0
50
100
150
200
250
300

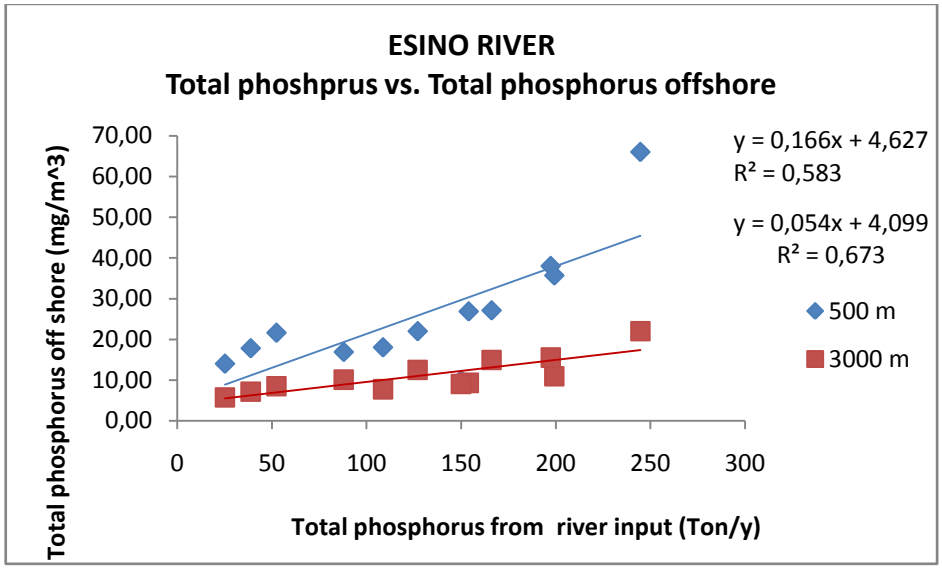
ESINO RIVER
Total phoshprus vs. Total phosphorus offshore
y = 0,166x + 4,627
R² = 0,583
y = 0,054x + 4,099
R² = 0,673
500 m
3000 m
Total phosphorus off shore (mg/m^3)
Total phosphorus from river input (Ton/y)
70,00
60,00
50,00
40,00
30,00
20,00
10,00
0,00
0
50
100
150
200
250
300

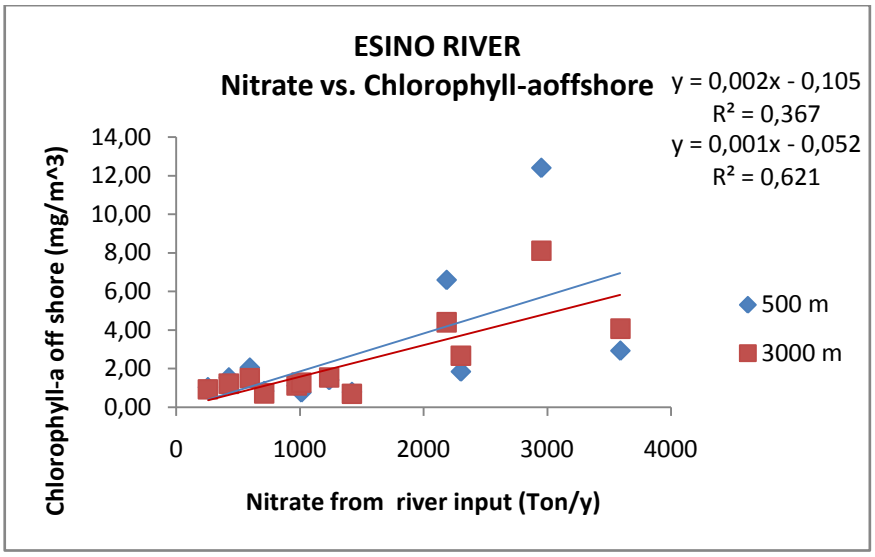
ESINO RIVER
Nitrate vs. Chlorophyll-aoffshore
y = 0,002x - 0,105
R² = 0,367
y = 0,001x - 0,052
R² = 0,621
Chlorophyll-a off shore (mg/m^3)
14,00
12,00
10,00
8,00
6,00
4,00
2,00
0,00
0
1000
2000
3000
4000
Nitrate from river input (Ton/y)
500 m
3000 m

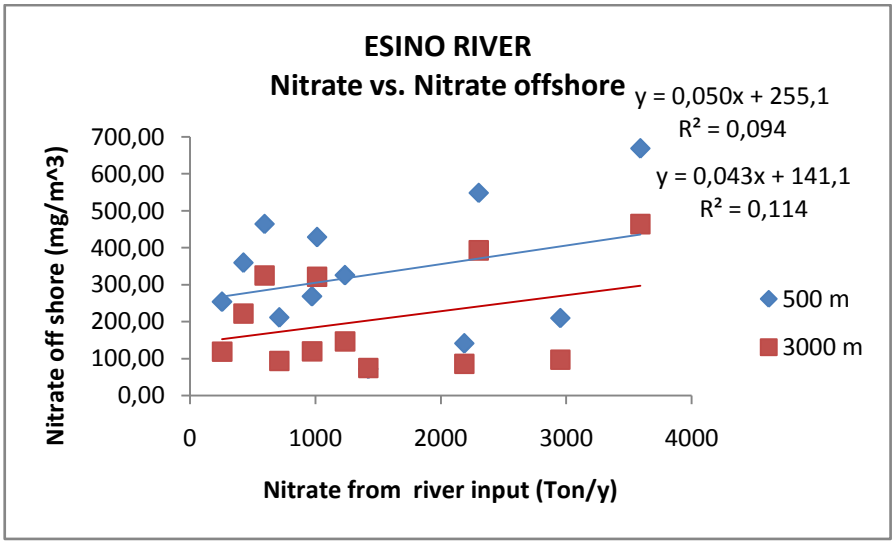
ESINO RIVER
Nitrate vs. Nitrate offshore
y = 0,050x + 255,1
R² = 0,094
y = 0,043x + 141,1
R² = 0,114
Nitrate off shore (mg/m^3)
700,00
600,00
500,00
400,00
300,00
200,00
100,00
0,00
0
1000
2000
3000
4000
Nitrate from river input (Ton/y)
500 m
3000 m

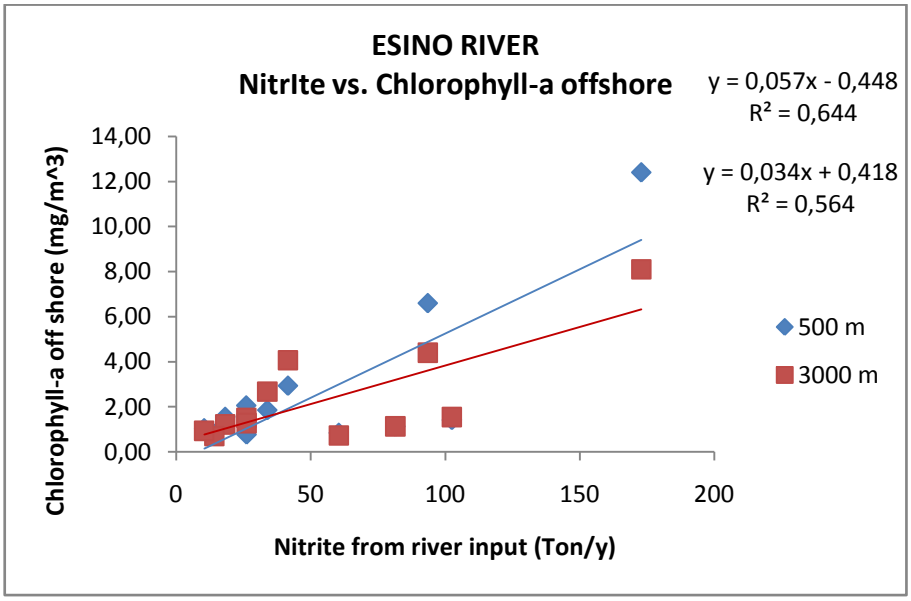
ESINO RIVER
NitrIte vs. Chlorophyll-a offshore
y = 0,057x - 0,448
R² = 0,644
y = 0,034x + 0,418
R² = 0,564
Chlorophyll-a off shore (mg/m^3)
14,00
12,00
10,00
8,00
6,00
4,00
2,00
0,00
0
50
100
150
200
Nitrite from river input (Ton/y)
500 m
3000 m

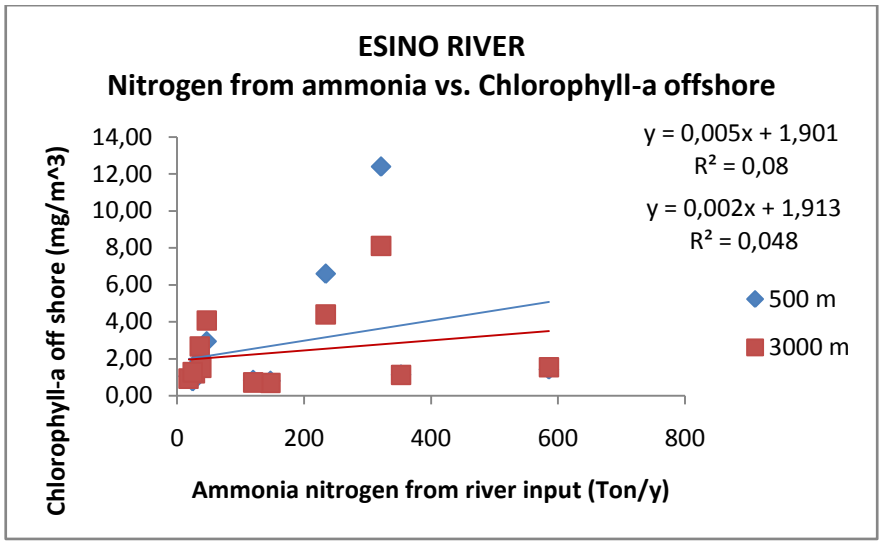
ESINO RIVER
Nitrogen from ammonia vs. Chlorophyll-a offshore
y = 0,005x + 1,901
R² = 0,08
y = 0,002x + 1,913
R² = 0,048
500 m
3000 m
Chlorophyll-a off shore (mg/m^3)
14,00
12,00
10,00
8,00
6,00
4,00
2,00
0,00
0
200
400
600
800
Ammonia nitrogen from river input (Ton/y)

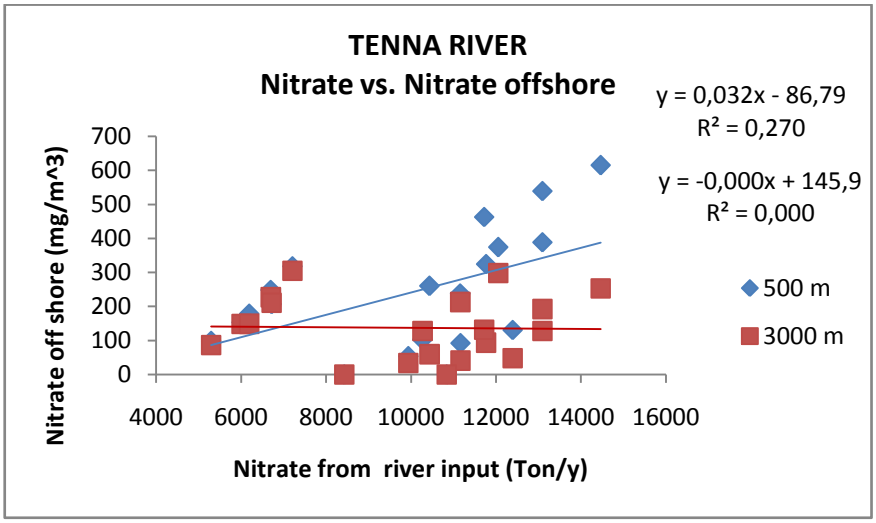
TENNA RIVER
Nitrate vs. Nitrate offshore
y = 0,032x - 86,79
R² = 0,270
y = -0,000x + 145,9
R² = 0,000
500 m
3000 m
Nitrate off shore (mg/m^3)
700
600
500
400
300
200
100
0
4000
6000
8000
10000
12000
14000
16000
Nitrate from river input (Ton/y)

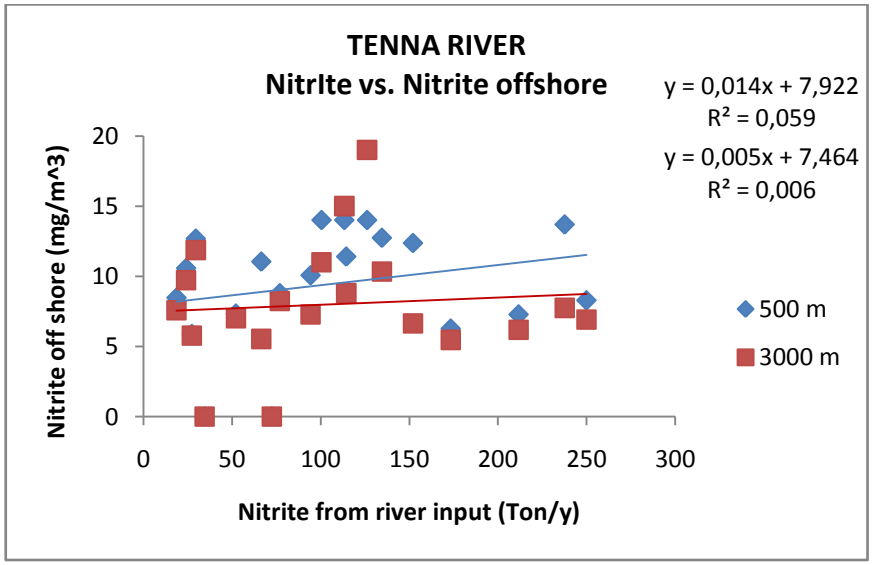
TENNA RIVER
NitrIte vs. Nitrite offshore
y = 0,014x + 7,922
R² = 0,059
y = 0,005x + 7,464
R² = 0,006
500 m
3000 m
Nitrite off shore (mg/m^3)
20
15
10
5
0
0
50
100
150
200
250
300
Nitrite from river input (Ton/y)

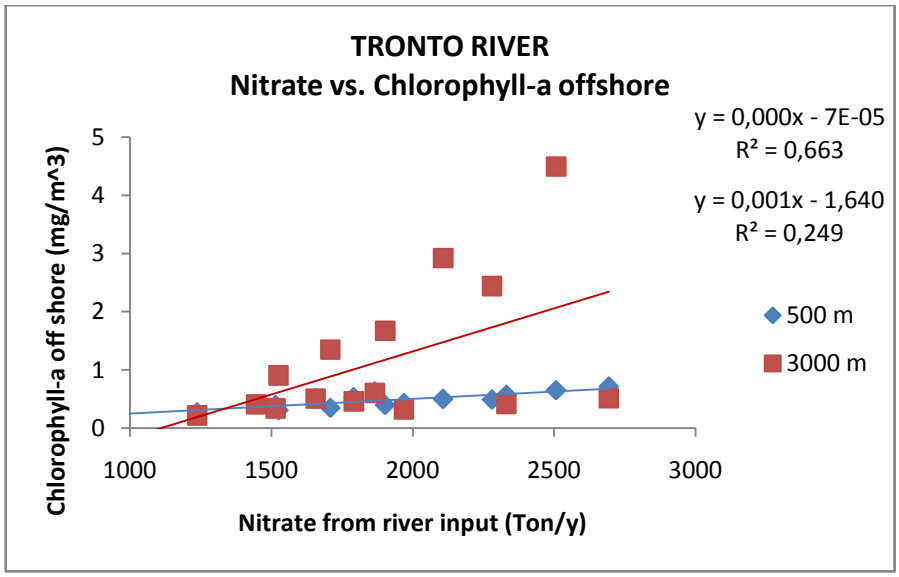
TRONTO RIVER
Nitrate vs. Chlorophyll-a offshore
y = 0,000x - 7E-05
R² = 0,663
y = 0,001x - 1,640
R² = 0,249
500 m
3000 m
Chlorophyll-a off shore (mg/m^3)
Nitrate from river input (Ton/y)
0
1
2
3
4
5
1000
1500
2000
2500
3000

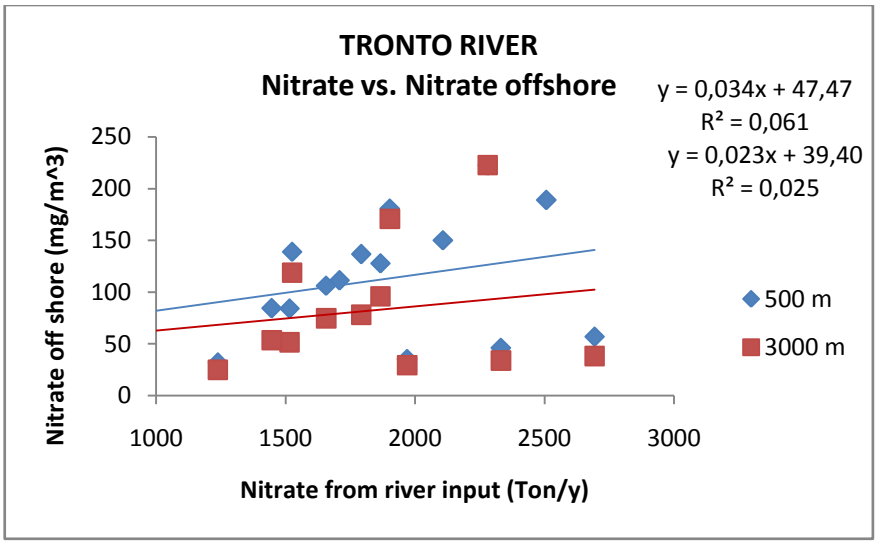
TRONTO RIVER
Nitrate vs. Nitrate offshore
y = 0,034x + 47,47
R² = 0,061
y = 0,023x + 39,40
R² = 0,025
500 m
3000 m
Nitrate off shore (mg/m^3)
Nitrate from river input (Ton/y)
0
50
100
150
200
250
1000
1500
2000
2500
3000

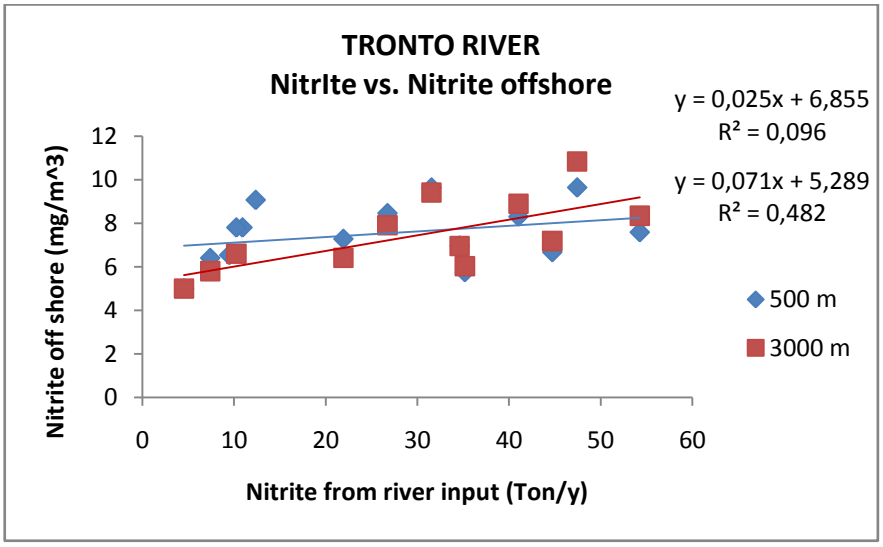
TRONTO RIVER
NitrIte vs. Nitrite offshore
y = 0,025x + 6,855
R² = 0,096
y = 0,071x + 5,289
R² = 0,482
500 m
3000 m
Nitrite off shore (mg/m^3)
Nitrite from river input (Ton/y)
0
2
4
6
8
10
12
0
10
20
30
40
50
60

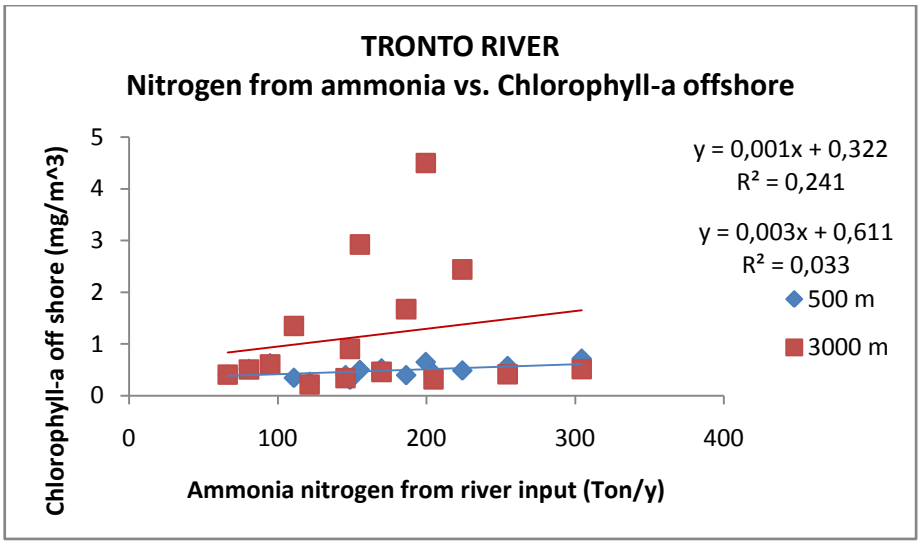

Figure. 15 - Correlation between continental nutrient loads (from river inputs) and nutrient or chlorophyll-a concentrations at 500 and 3000 m far from rivers mouth (Misa, Esino, Tenna and Tronto river).

In order to better understand potential modifications in the composition of nutrient inputs entering the marine system, we calculated the ratio of nitrogen to phosphorus (N/P) at the mouth of the different rivers On the basis of the available information, lower N/P ratios were observed at the mouth of rivers located in the northern sector of the Marche Region when compared to the southern ones (Figure 16).

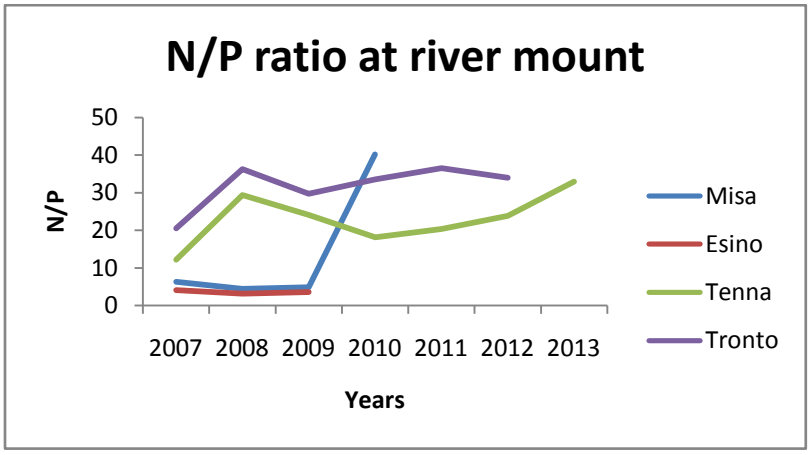

Figure. 16 – Nitrogen to phosphorus ratios estimated at river's mouth,

Conclusions

The analysis of the spatial and temporal changes of thermohaline conditions and biogeochemical characteristics in shallow coastal waters at local scale can improve our understanding on factors and processes which can lead to detrimental effects on coastal marine ecosystems such as dystrophic events due to hypoxia phenomena as well as the spreading of harmful algal blooms. Harmful algal blooms (due to *Ostreopsis cf. ovata*) has been documented in shallow coastal areas of the Marche Region, but factors triggering their temporal evolution and spreading need to be fully clarified yet (Accoroni et al., 2015). In this chapter we provide evidence that temporal patterns of thermohaline conditions and biogeochemical characteristics in shallow coastal waters at local scale do not reflect dynamics occurring at the basin scale (i.e. of the entire Adriatic Sea). Temperature and salinity values along the entire coastal areas of the Marche Region, indeed, decreased over the time period investigated, whereas an opposite pattern was observed at basin scale, especially in surface waters.

The distribution of phytoplankton biomass (as chlorophyll-a concentrations) at local scale revealed higher values in the northern sector when compared to the southern one. Such a decreasing gradient from the north to the south has been repeatedly reported also at basin scale as a consequences of the high nutrient loads entering in the North Adriatic Sea through river inputs (Solidoro et al., 2009). In the present study, also major blooming periods has been observed following similar seasonal dynamics reported in the Adriatic basin (higher values in winter/spring and lower values in summer; Bernardi Aubry et al. 2012). However, respect to the basin scale, no clear patterns on a decadal scale of phytoplankton biomass was observed. Conversely inorganic nutrient concentrations of surface waters of the Marche Region showed an increase over the time scale considered, suggesting an un-coupling between trophic state (as inorganic nutrient concentrations) and biological responses of phytoplankton assemblages.

In this study we also observed a major influence of freshwater inputs and related inorganic nutrient loads on the thermohaline and biogeochemical characteristics of the coastal marine systems of the Marche Region. Indeed, both in the north and south sector of the Marche Region temperature and salinity values of the marine coastal waters were inversely related to the river flows. Such an influence of the river flows was more evident, as expected at stations closer to the river mouths. Also the biogeochemical characteristics of the coastal

marine systems of the Marche Region was influenced by river inputs as revealed by the significant and positive relationships between continental inorganic nutrient loads and nutrient and chlorophyll-a concentrations in surface sea waters. In particular, a strong correlation was found with the nitrate loads (which represent the major inorganic nutrients transported by rivers in the Marche Region), reinforcing previous findings at local scale on the role of this element in influencing the biogeochemical characteristics at sub-basin scale (i.e North Adriatic Sea; Degobbis et al., 2000, Cozzi and Giani 2011).

Although results of this study need to be better refine in space and time, findings reported here suggest that changes in river flows associated with changes in precipitation regimes due to also climate change and modifications of nutrient inputs due to changes in land uses can have important influences on the trophic status of coastal marine ecosystems with cascade effects on the pelagic food webs at local spatial scale. Presently, as requested by the MSFD, monitoring activities of marine ecosystems routinely carried out by the Regional Environmental Protection Agencies (ARPA) have been extended up to 12 nm, instead of 3 nm from the coastline. We conclude that river dynamics should be systematically monitored and integrated within the current monitoring programs for a better understanding of changes of the ecological status of coastal marine systems over time.

References

Accoroni, S. Glibert, P.M., Pichierri, S., Romagnoli, T., Marini, M., Totti, C. (2015) A conceptual model of annual *Ostreopsis cf. ovata* blooms in the northern Adriatic Sea based on the synergic effects of hydrodynamics, temperature, and the N:P ratio of water column nutrients. Harmful Algae 45:14-25

Bernardi Aubry F., Cossarini G., Acri F., Bastianini M., Bianchi F., Camatti E., De Lazzari A., Pugnetti A., Solidoro C., Socal G. (2012) Plankton communities in the northern Adriatic Sea: Patterns and changes over the last 30 years. Estuarine, Coastal and Shelf Science 115:125-137

Coll M, Libralato S, Tudela S, Palomera I, Pranovi F (2009) Ecosystem overfishing in the ocean. PlosOne 3: e3881. doi:10.1371/journal.pone.0003881.

Cozzi, S.M., Giani, M. (2011). River water and nutrient discharges in the northern Adriatic Sea: current importance and long term changes. Continental Shelf Research 31:1881-1893

Degobbis, D., Precali, R., Ivancic, I., Smodlaka, N., Fuks, D., Kveder, S. (2000). Long term changes in the northern Adriatic ecosystem related to anthropogenic eutrophication. International Journal of Environment and Pollution 13:495-533.

Djakovac T., Degobbis D., Supic N., Precali R. Marked reduction of eutrophication pressure in the northeastern Adriatic in the period 2000-2009. Estuarine, coastal and shelf science 115 (1012) 25-32.

Diaz R.J. and Rosenberg R. Spreading dead zones and consequences for marine ecosystems. Science vol. 321 (2008), Issue 5891, pp. 926-929.

Giani M, Djakovac T, Degobbis D, Cozzi S, Solidoro C, Fonda Umani S. 2012. Recent changes in the marine ecosystems of the northern Adriatic Sea. Estuarine, Coastal and Shelf Science 115 (2012) 1-13.

Gladan Z. N, Bu˘zan˘ci´c M, Ku˘spili´c G., Grbec B., Matijevi´c S., Skeji´c S., Marasovi´c I., Morovi´c M. 2015. The response of phytoplankton community to anthropogenic pressure gradient in the coastal waters of the eastern Adriatic Sea. *Ecological indicators* 56 (2015) 106-115.

Halpern B.S., Walbridge S., Selkoe K.A., Kappel C.V., Micheli F., D'Agrosa C., Bruno J.F., Casey K.S., Ebert C., Fox H.E., Fujita R., Heinemann D., Lenihan H.S., Madin

E.M.P., Perry M.T., Selig E.R., Spalding M., Steneck R., Watson R. A global map of human impact on marine ecosystems. Science vol. 319 (2008), Issue 5865, pp. 948-952.

Lotze H.K, Lenihan H.S., Bourgue B.J., Jackson J.B.C. 2006. Depletion, degradation and recovery potential of estuaries and coastal seas. Science 312(5781):1806-9.

Melin F, Vantrepotte V, Clerici M, D'Alimonte A, Zibordi G, Berthon J.F, Canuti E. Multi-sensor satellite time series of optical properties and chlorophyll-a concentration in the Adriatic Sea. Progress in Oceanography 91 (2011) 229-244.

Micheli F., Halpern B.S., Walbridge S., Ferretti F., Fraschetti S., Lewison R., Nykjaer L., Rosenberg A.A. Cumulative human impacts on Mediterranean and Black Sea marine ecosystems: assessing current pressures and opportunities. PLoS ONE 8(12): e79889. doi:10.1371/journal.pone.0079889.

Ninčević Gladan Ž., M. Bužančić, G. Kušpilić, B. Grbec, S. Matijević, S. Skejić, I. Marasović, M. Morović. The response of phytoplankton community to anthropogenic pressure gradient in the coastal waters of the eastern Adriatic Sea. Ecol. Indic., 56 (2015), pp. 106–115 http://dx.doi.org/10.1016/j.ecolind.2015.03.018

Solidoro, C., Bastianini, M., Bandelj, V., Codermatz, R., Cossarini, G., Melaku Canu, D., Ravagnan, E., Salon, S., Trevisan, S. (2009). Current state, scales of variability, and trends of biogeochemical properties in the northern Adriatic Sea. Journal of Geophysical Research 114, doi:10.1029/2008JC004838.

Zanchettin D., Rubino A., Traverso P., Tomasino M (2008). Impact of variations in solar activity on hydrological decadal patterns in northern Italy. Journal of geophysical research, Vol. 113, D12102, doi:10.1029/2007JD009157, 2008.

Final remarks and needs for further researches

Results of this work allowed us to improve knowledge on changes of trophic and thermohaline conditions occurring on a multi-annual temporal scale and to identify patterns useful for a better assessment of GES in the Adriatic Sea. Our findings allowed us also to improve knowledge at regional scale on temporal variability of rivers outflows (and related inorganic nutrient loads) and their influence on coastal marine ecosystem highlighting the need, in the definition of GES, to take in consideration not only changes deriving from anthropogenic activities, but also those potentially related to the current climate changes. The descriptor 5 ─ eutrophication ─ is expected to have negative effects only if phytoplankton biomass reaches values above to which detrimental effects of marine ecosystems occur (e.g. due to hypoxia/anoxia leading to mortality of organisms). Despite our findings do not allow to identify thresholds above which detrimental effects can be expected, changes of phytoplankton biomass reported in this study should be considered as they can have a major effect on the entire marine food web and therefore on other descriptors included in the MSFD (i.e., descriptor 1 -biodiversity, descriptor 3 -population of commercial species- and descriptor 4 - food web structure). Besides tools and strategies used in the present study, additional improvement of monitoring strategies can include the development and application of tools for the *in situ* detection of harmful algae and the analysis of changes of phytoplankton community composition that can occur as a consequence of changes of inorganic nutrient loads and modifications of thermohaline conditions even related to climate changes. It can be also useful to develop regional algorithms that allows to reduce the uncertainty in the satellite assessment of chlorophyll-a from global algorithms as well as algorithms for phytoplankton composition identification using remote sensing. Finally, efforts should be devoted to integrate such tools in future monitoring plans of marine environments.

The descriptor 7 of the MSFD takes into account hydrological alterations directly generated by anthropogenic activities (e.g. industrial plants for energy production, harbors, coastal defense) and not those induced by climate changes. However, current climate changes can represent a main constraint for the achievement and the maintenance of GES. In this study, we show the utility of different models to investigate hydrographic conditions at different spatial scales. Thus, these models, if adequately improved, can be useful to detect alterations of hydrological conditions both on a local spatial scale as a consequence

of direct anthropogenic activities and/or on a wide spatial scale also due to current climate changes. Moreover, in this study by analyzing thirty years' time series of physical properties of water masses of the Adriatic Sea, we detected important changes of temperature and salinity likely dependent on the current climate changes. Such modifications should be adequately taken into account for a better interpretation of ecological dynamics occurring in the Adriatic basin and continuously monitored to eventually revise in the future the thresholds of environmental quality.

ANNEX I

Following plots represent the mismatching, in terms of mean bias (MB) and root mean square error (RMSE), between observed data from several oceanographic cruises (temperature and salinity data) and three operational forecasting systems AdriaROMS, COAWST-ARPA and COAWST-REGIONE_MARCHE.

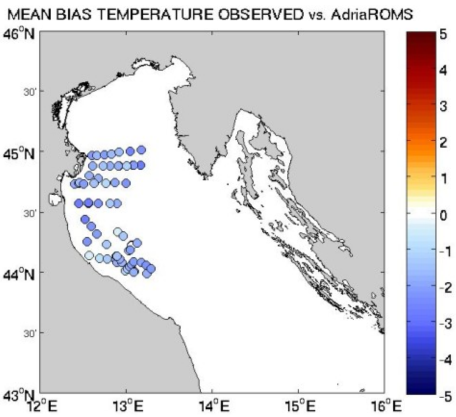

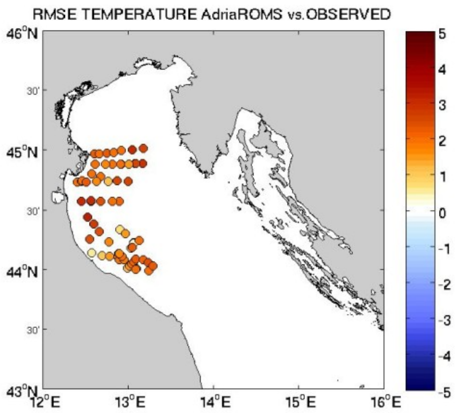

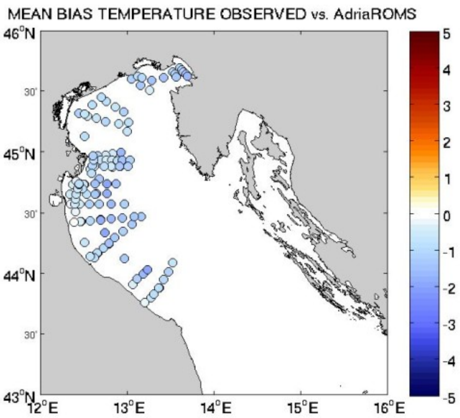

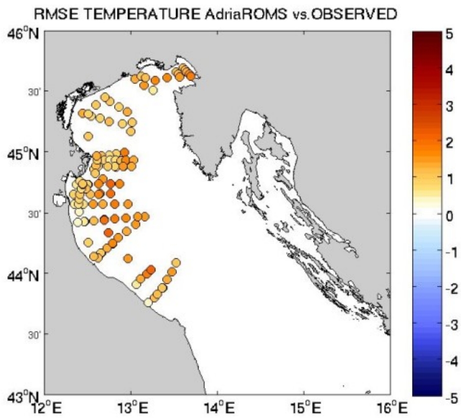

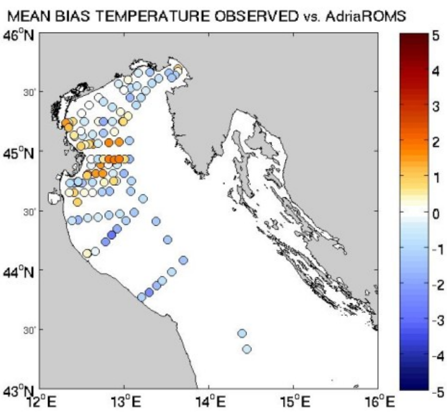

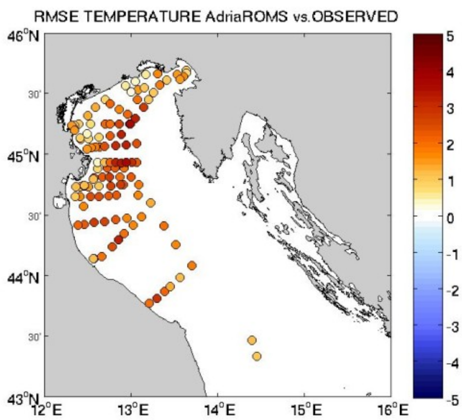

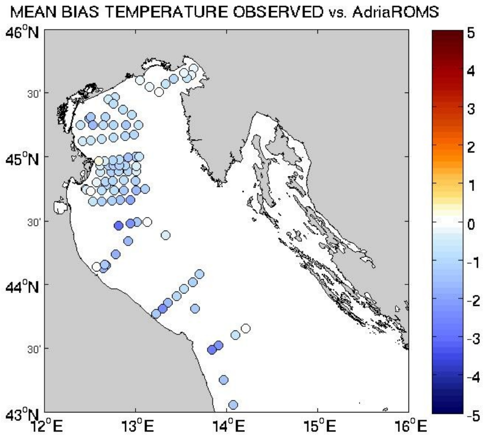
MEAN BIAS TEMPERATURE OBSERVED vs. AdriaROMS
46°N
30'
45°N
30'
44°N
30'
43°N
12°E
13°E
14°E
15°E
16°E
5
4
3
2
1
0
-1
-2
-3
-4
-5

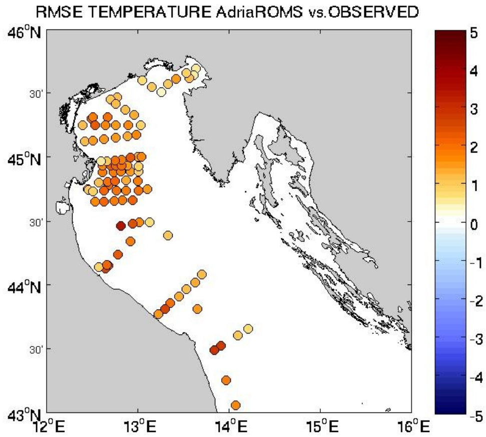
RMSE TEMPERATURE AdriaROMS vs.OBSERVED
46°N
30'
45°N
30'
44°N
30'
43°N
12°E
13°E
14°E
15°E
16°E
5
4
3
2
1
0
-1
-2
-3
-4
-5

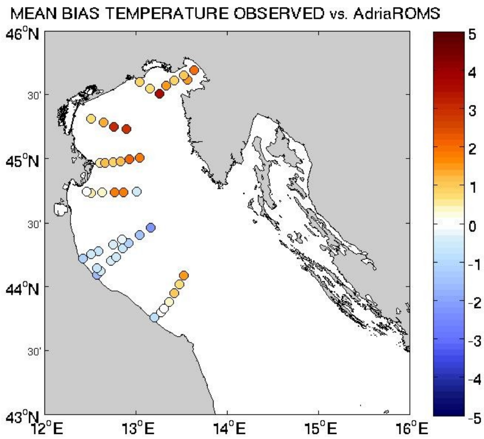
MEAN BIAS TEMPERATURE OBSERVED vs. AdriaROMS
46°N
30'
45°N
30'
44°N
30'
43°N
12°E
13°E
14°E
15°E
16°E
5
4
3
2
1
0
-1
-2
-3
-4
-5

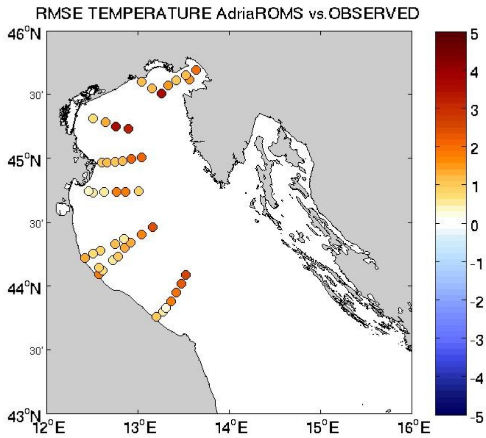
RMSE TEMPERATURE AdriaROMS vs.OBSERVED
46°N
30'
45°N
30'
44°N
30'
43°N
12°E
13°E
14°E
15°E
16°E
5
4
3
2
1
0
-1
-2
-3
-4
-5

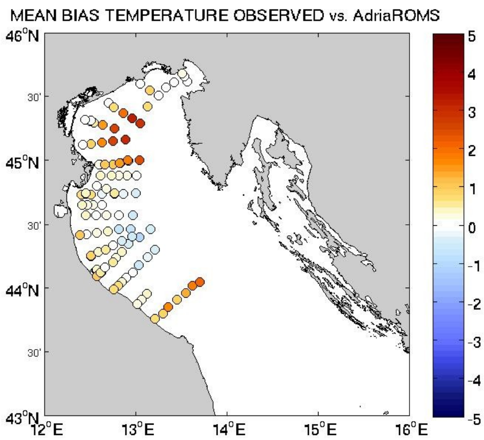
MEAN BIAS TEMPERATURE OBSERVED vs. AdriaROMS
46°N
30'
45°N
30'
44°N
30'
43°N
12°E
13°E
14°E
15°E
16°E
5
4
3
2
1
0
-1
-2
-3
-4
-5

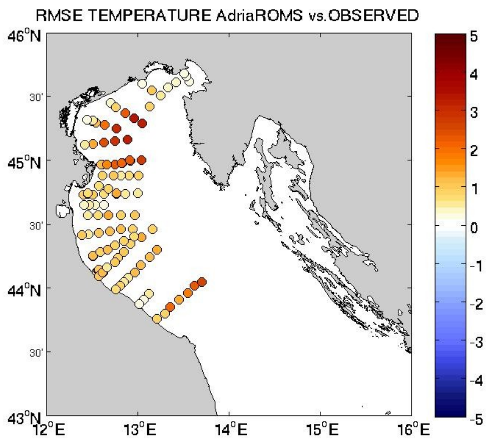
RMSE TEMPERATURE AdriaROMS vs.OBSERVED
46°N
30'
45°N
30'
44°N
30'
43°N
12°E
13°E
14°E
15°E
16°E
5
4
3
2
1
0
-1
-2
-3
-4
-5

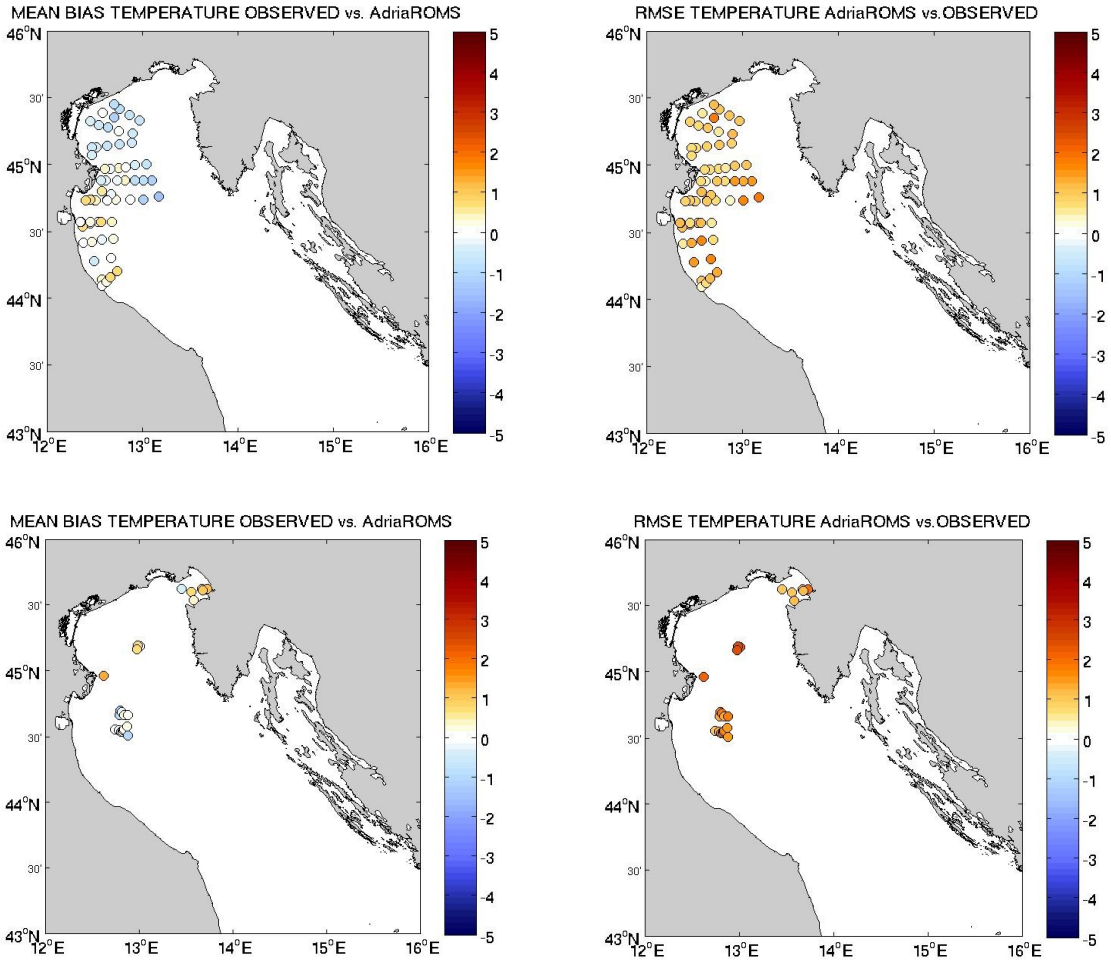

Fig. 1.1. - MB and RMSE between observed and forecasted temperature values by AdriaROMS.

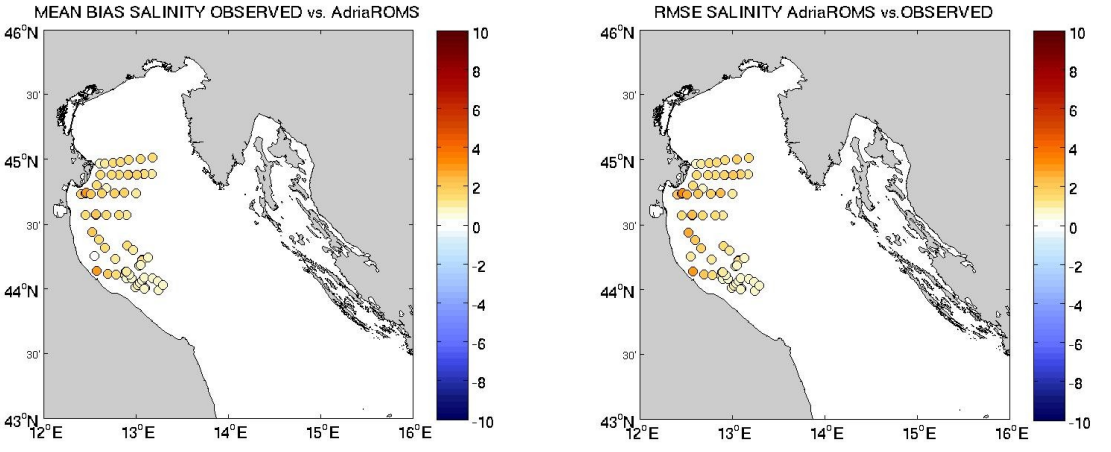

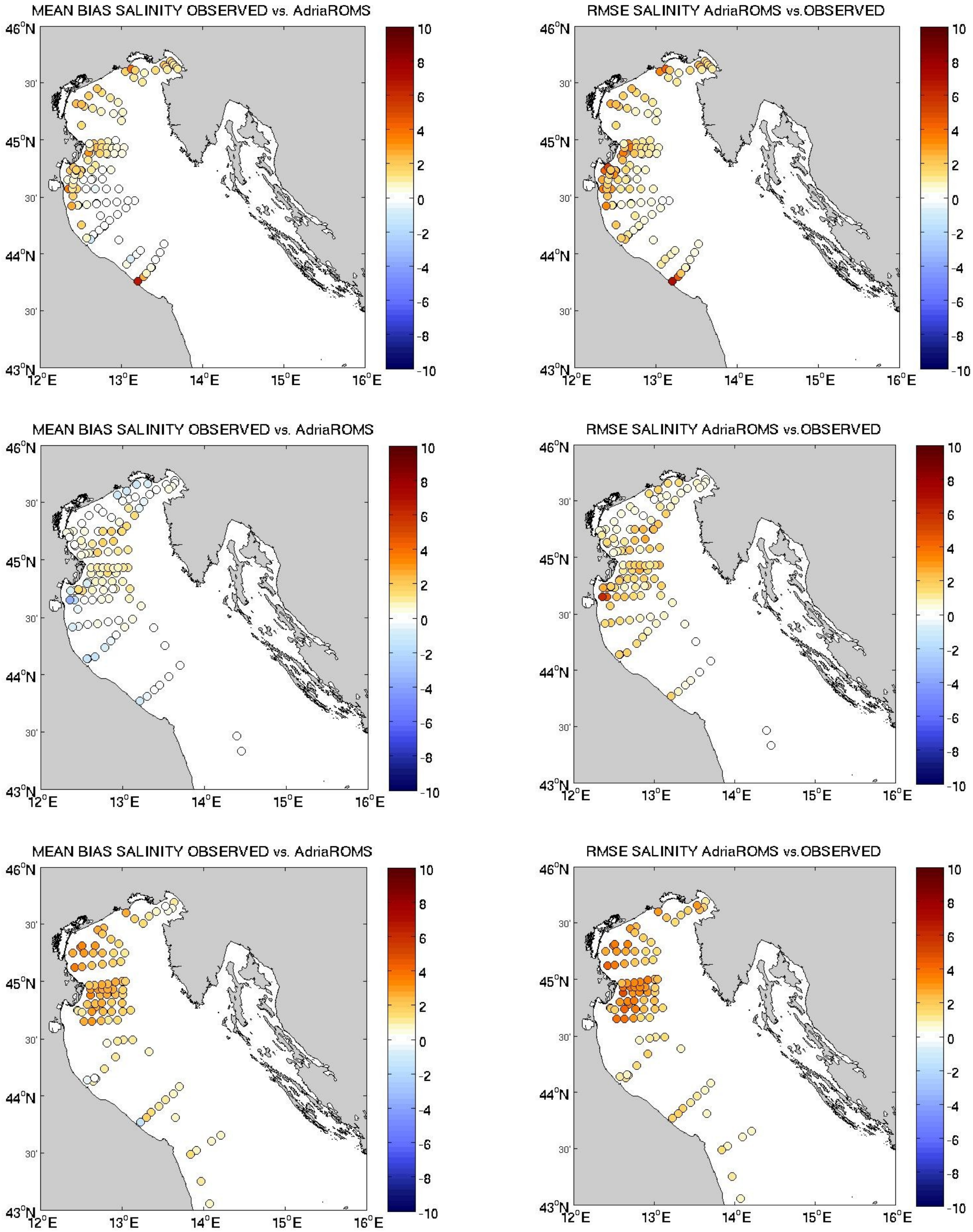
MEAN BIAS SALINITY OBSERVED vs. AdriaROMS
RMSE SALINITY AdriaROMS vs.OBSERVED
MEAN BIAS SALINITY OBSERVED vs. AdriaROMS
RMSE SALINITY AdriaROMS vs.OBSERVED
MEAN BIAS SALINITY OBSERVED vs. AdriaROMS
RMSE SALINITY AdriaROMS vs.OBSERVED
46°N
30'
45°N
30'
44°N
30'
43°N
12°E
13°E
14°E
15°E
16°E
10
8
6
4
2
0
-2
-4
-6
-8
-10

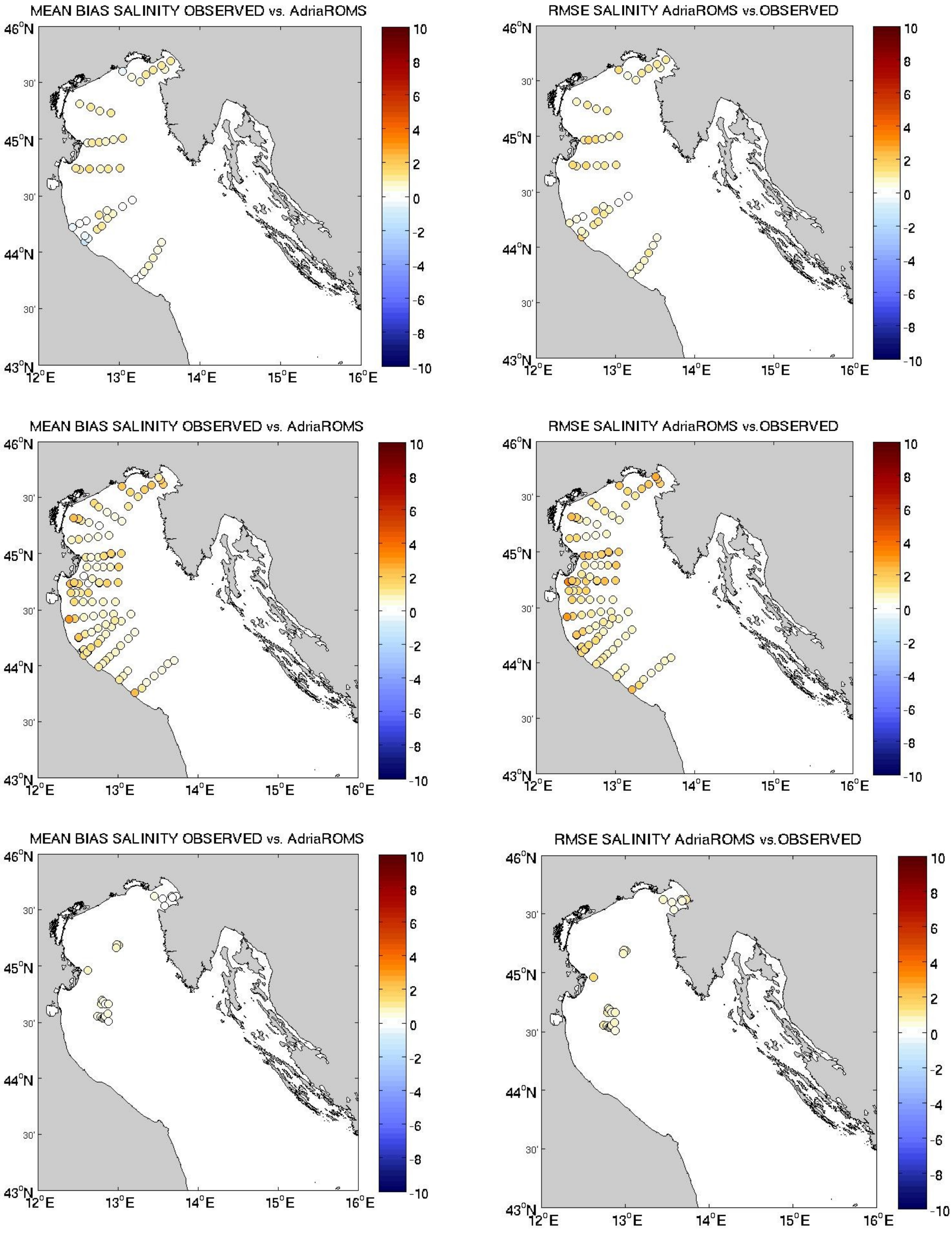
MEAN BIAS SALINITY OBSERVED vs. AdriaROMS
RMSE SALINITY AdriaROMS vs.OBSERVED
MEAN BIAS SALINITY OBSERVED vs. AdriaROMS
RMSE SALINITY AdriaROMS vs.OBSERVED
MEAN BIAS SALINITY OBSERVED vs. AdriaROMS
RMSE SALINITY AdriaROMS vs.OBSERVED
46°N
45°N
44°N
43°N
30'
12°E
13°E
14°E
15°E
16°E
10
8
6
4
2
0
-2
-4
-6
-8
-10

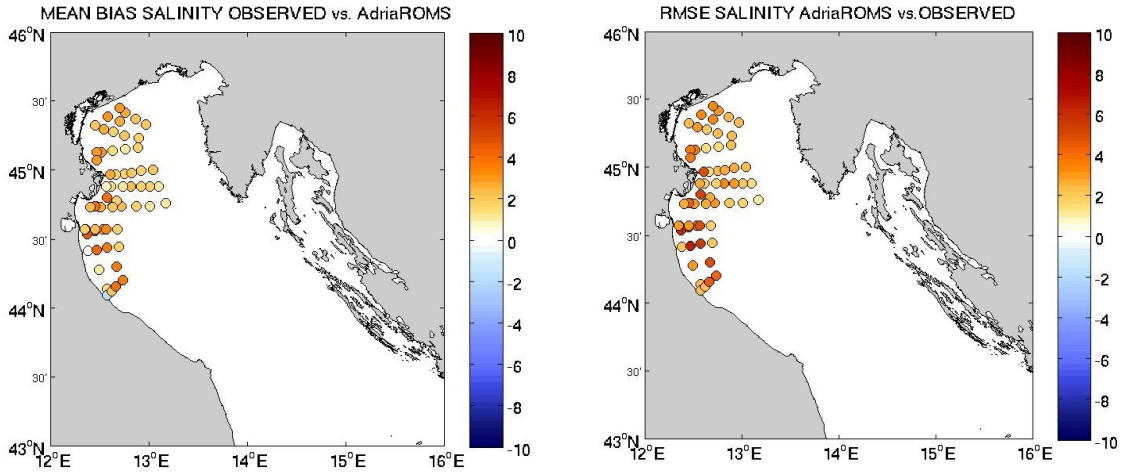

Fig. 1.2. - MB and RMSE between observed and forecasted salinity values by AdriaROMS.

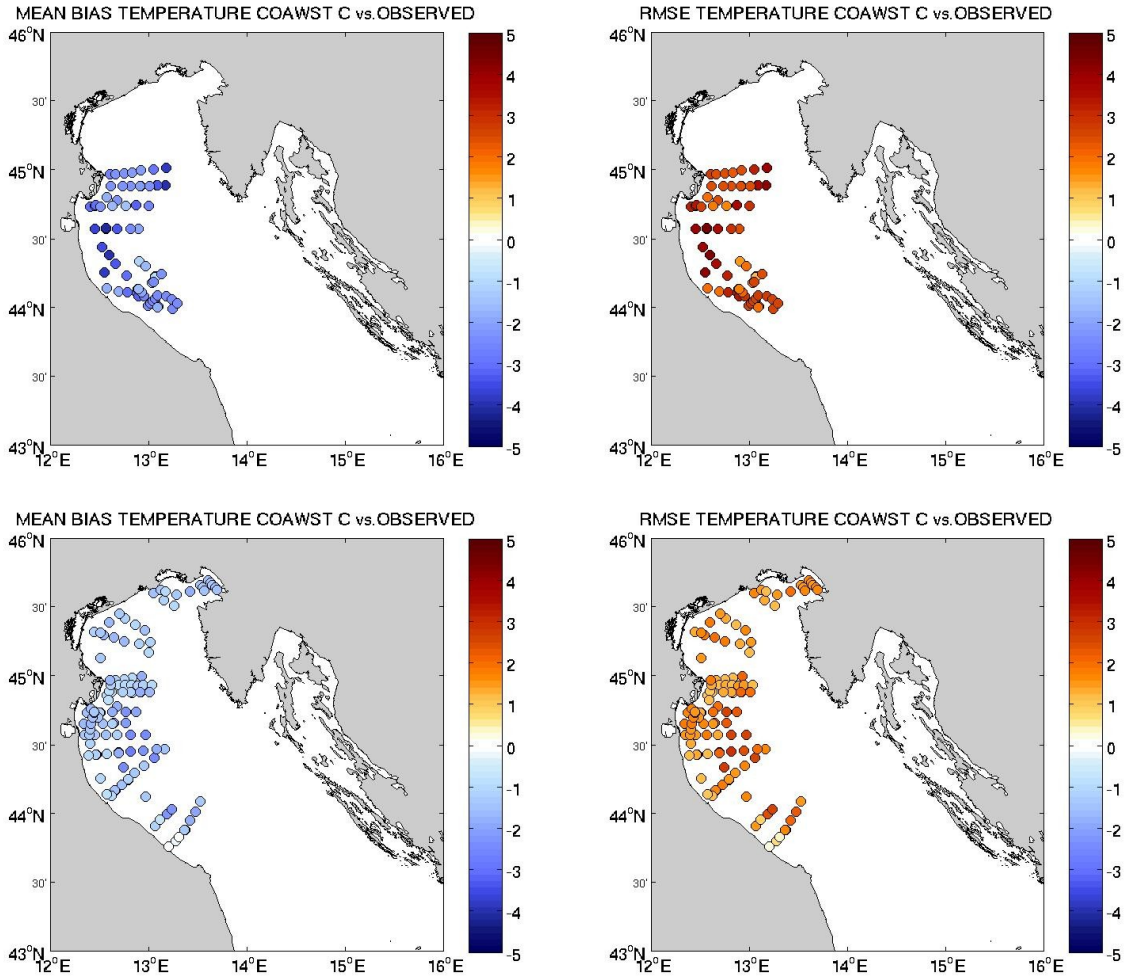

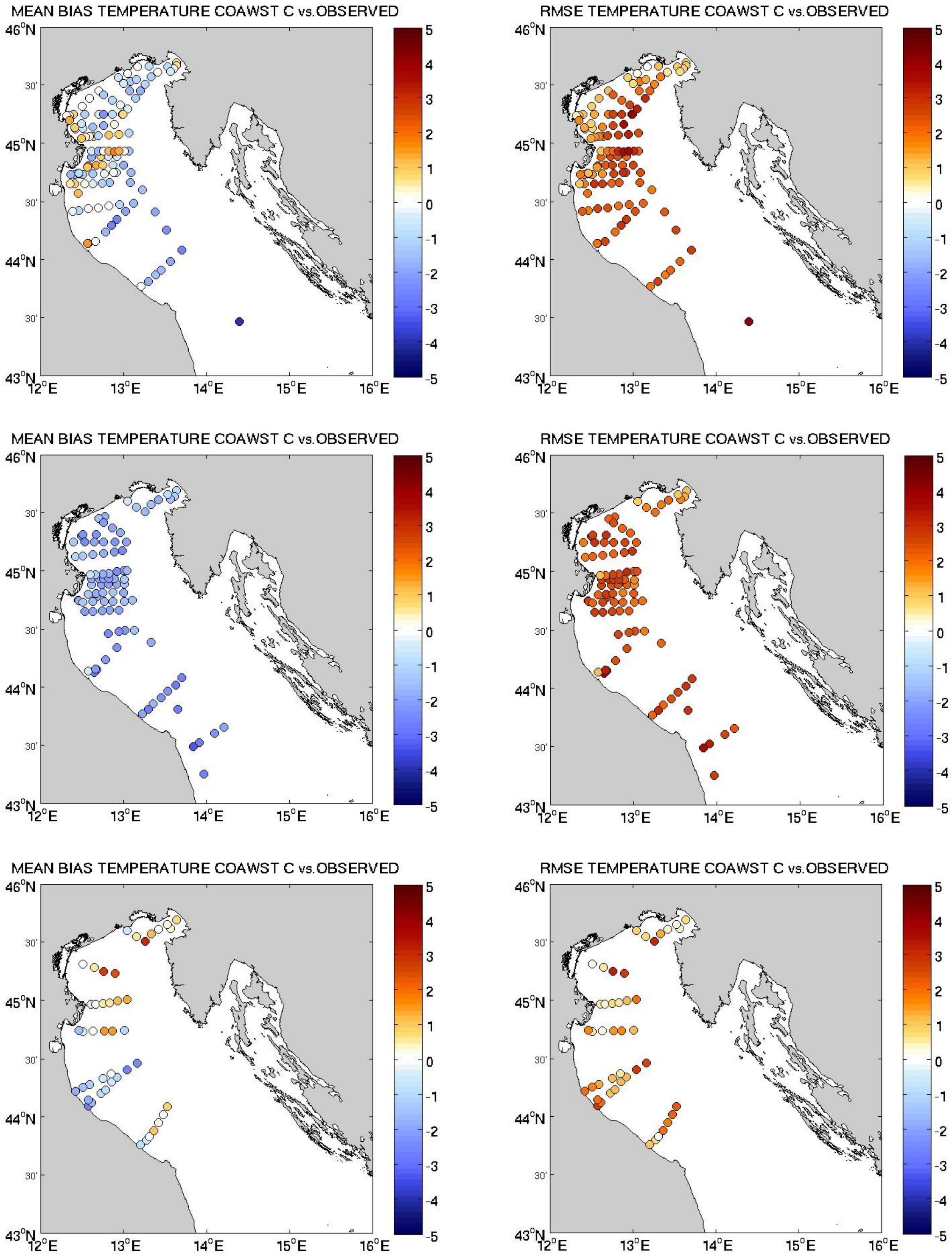
MEAN BIAS TEMPERATURE COAWST C vs.OBSERVED
RMSE TEMPERATURE COAWST C vs.OBSERVED
MEAN BIAS TEMPERATURE COAWST C vs.OBSERVED
RMSE TEMPERATURE COAWST C vs.OBSERVED
MEAN BIAS TEMPERATURE COAWST C vs.OBSERVED
RMSE TEMPERATURE COAWST C vs.OBSERVED
46°N
30'
45°N
30'
44°N
30'
43°N
12°E
13°E
14°E
15°E
16°E
5
4
3
2
1
0
-1
-2
-3
-4
-5

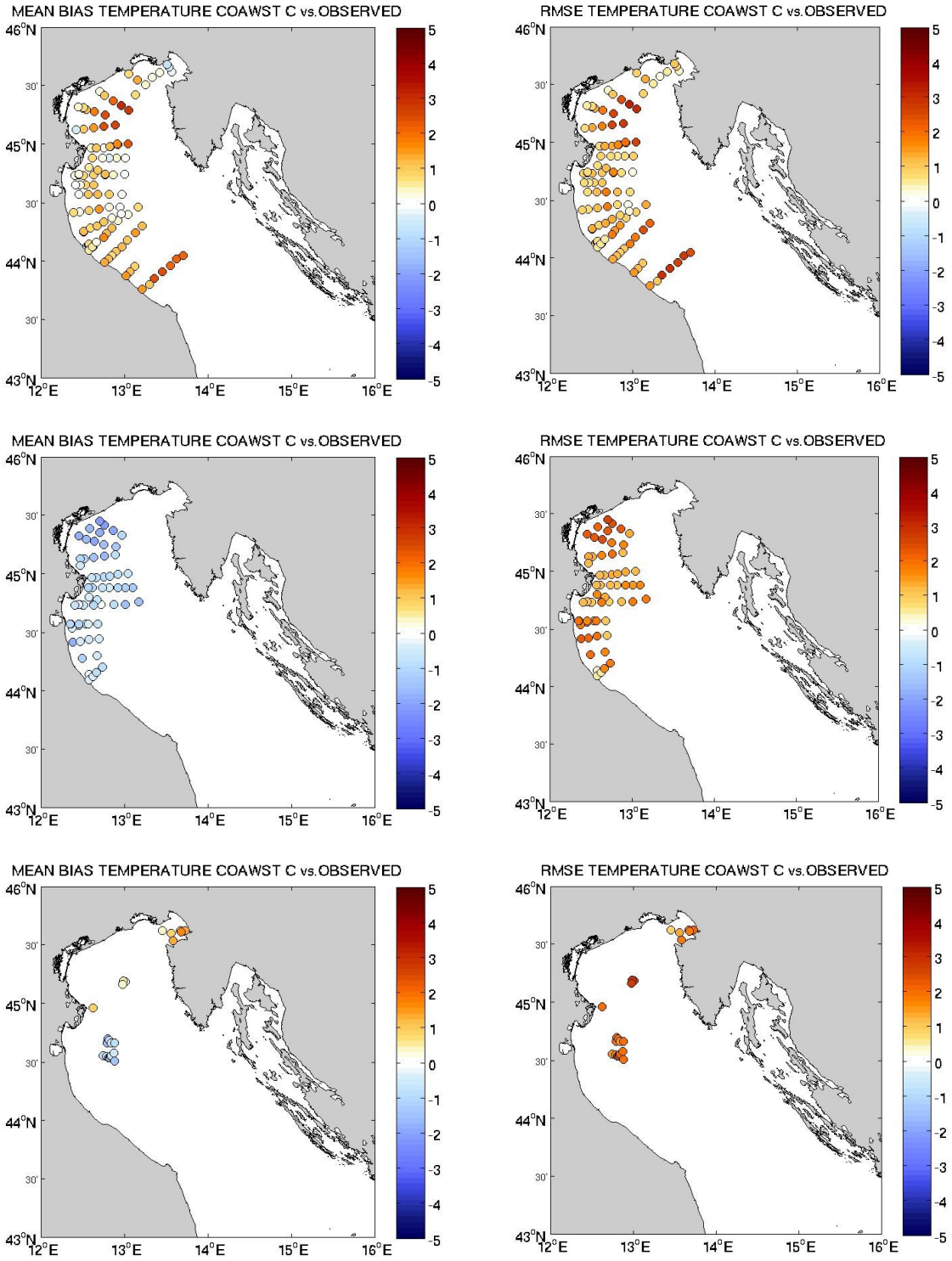

Fig. 1.3. - MB and RMSE between observed and forecasted temperature values by COAWST-C.

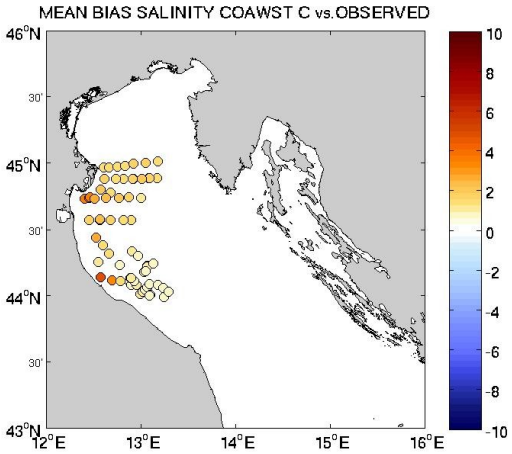
MEAN BIAS SALINITY COAWST C vs.OBSERVED
46°N
45°N
44°N
43°N
12°E
13°E
14°E
15°E
16°E
10
8
6
4
2
0
-2
-4
-6
-8
-10

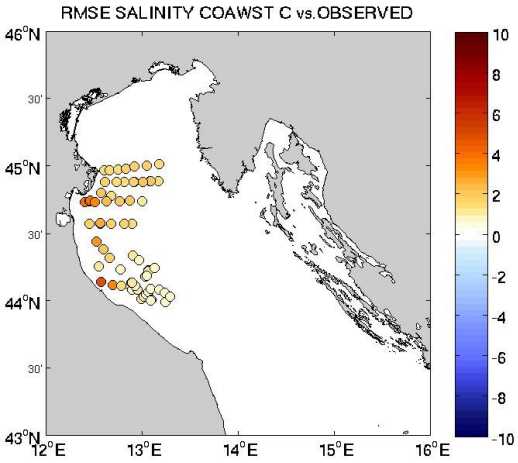
RMSE SALINITY COAWST C vs.OBSERVED
46°N
45°N
44°N
43°N
12°E
13°E
14°E
15°E
16°E
10
8
6
4
2
0
-2
-4
-6
-8
-10

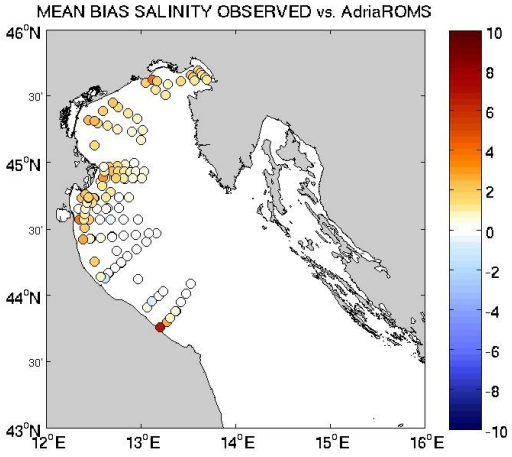
MEAN BIAS SALINITY OBSERVED vs. AdriaROMS
46°N
45°N
44°N
43°N
12°E
13°E
14°E
15°E
16°E
10
8
6
4
2
0
-2
-4
-6
-8
-10

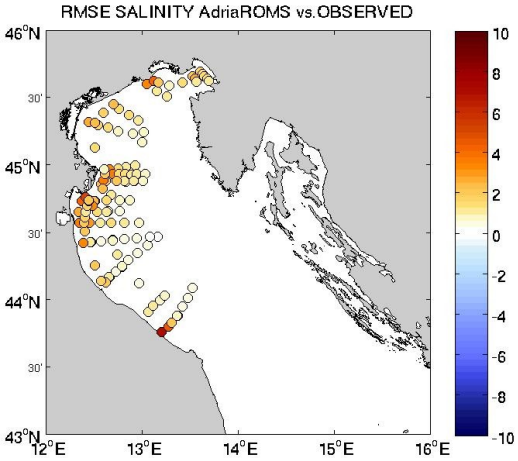
RMSE SALINITY AdriaROMS vs.OBSERVED
46°N
45°N
44°N
43°N
12°E
13°E
14°E
15°E
16°E
10
8
6
4
2
0
-2
-4
-6
-8
-10

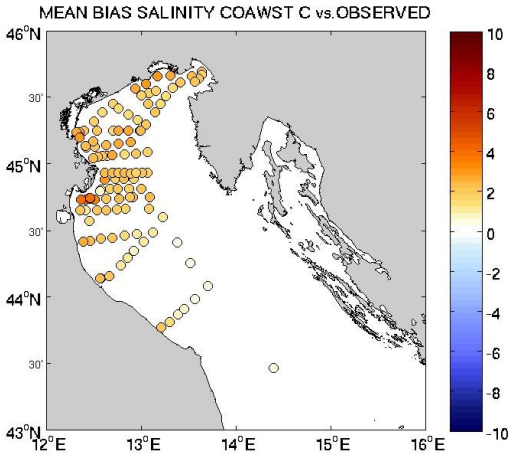
MEAN BIAS SALINITY COAWST C vs.OBSERVED
46°N
45°N
44°N
43°N
12°E
13°E
14°E
15°E
16°E
10
8
6
4
2
0
-2
-4
-6
-8
-10

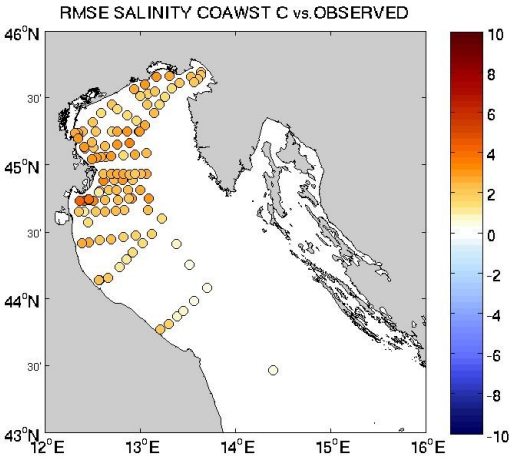
RMSE SALINITY COAWST C vs.OBSERVED
46°N
45°N
44°N
43°N
12°E
13°E
14°E
15°E
16°E
10
8
6
4
2
0
-2
-4
-6
-8
-10

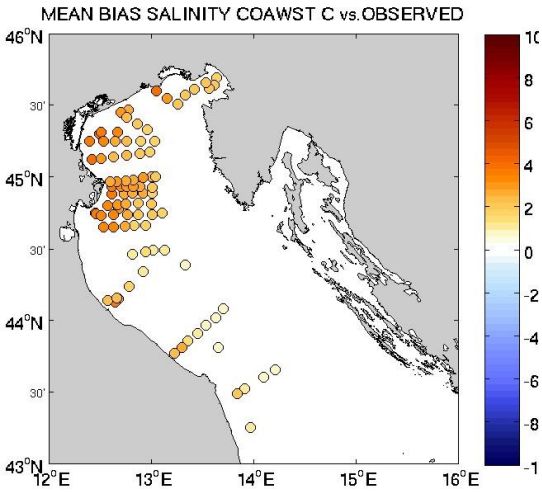
MEAN BIAS SALINITY COAWST C vs.OBSERVED
46°N
45°N
44°N
43°N
12°E
13°E
14°E
15°E
16°E

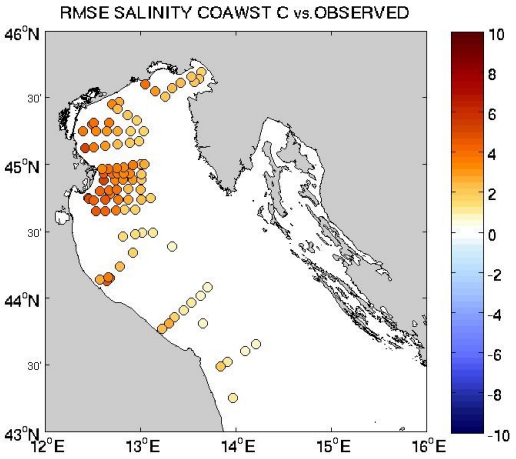
RMSE SALINITY COAWST C vs.OBSERVED
46°N
45°N
44°N
43°N
12°E
13°E
14°E
15°E
16°E
10
8
6
4
2
0
-2
-4
-6
-8
-10

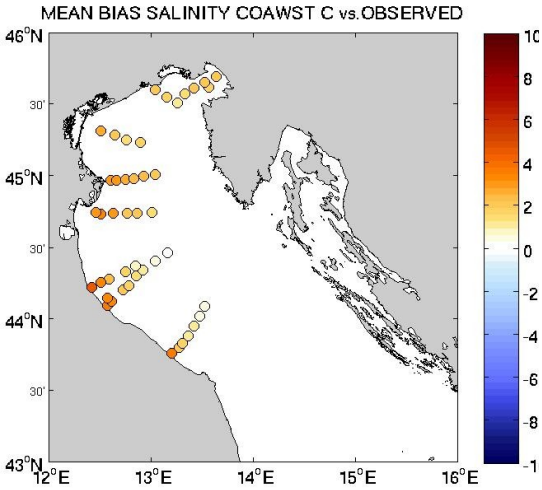
MEAN BIAS SALINITY COAWST C vs.OBSERVED
46°N
45°N
44°N
43°N
12°E
13°E
14°E
15°E
16°E

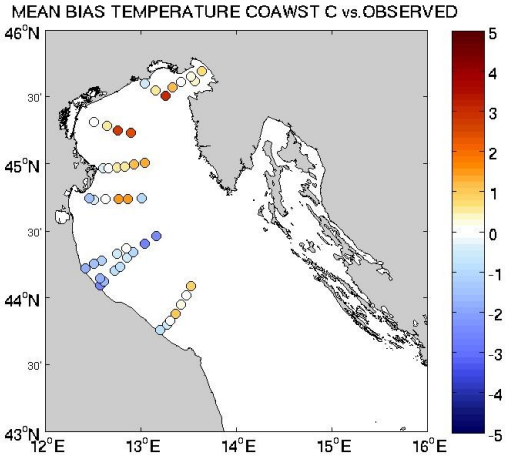
MEAN BIAS TEMPERATURE COAWST C vs.OBSERVED
46°N
45°N
44°N
43°N
12°E
13°E
14°E
15°E
16°E
5
4
3
2
1
0
-1
-2
-3
-4
-5

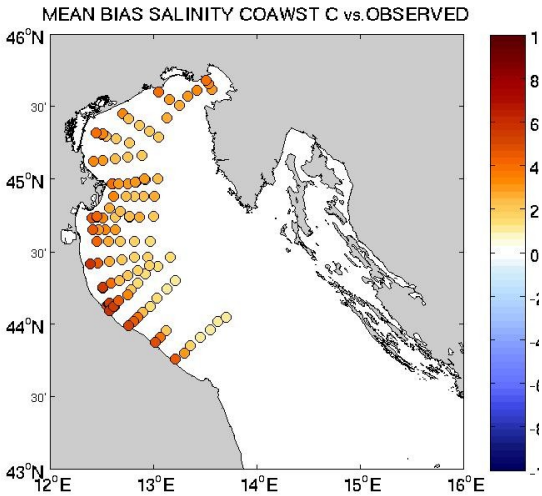
MEAN BIAS SALINITY COAWST C vs.OBSERVED
46°N
45°N
44°N
43°N
12°E
13°E
14°E
15°E
16°E

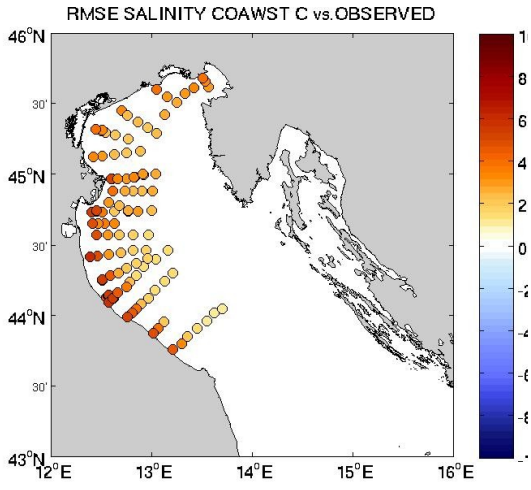
RMSE SALINITY COAWST C vs.OBSERVED
46°N
45°N
44°N
43°N
12°E
13°E
14°E
15°E
16°E

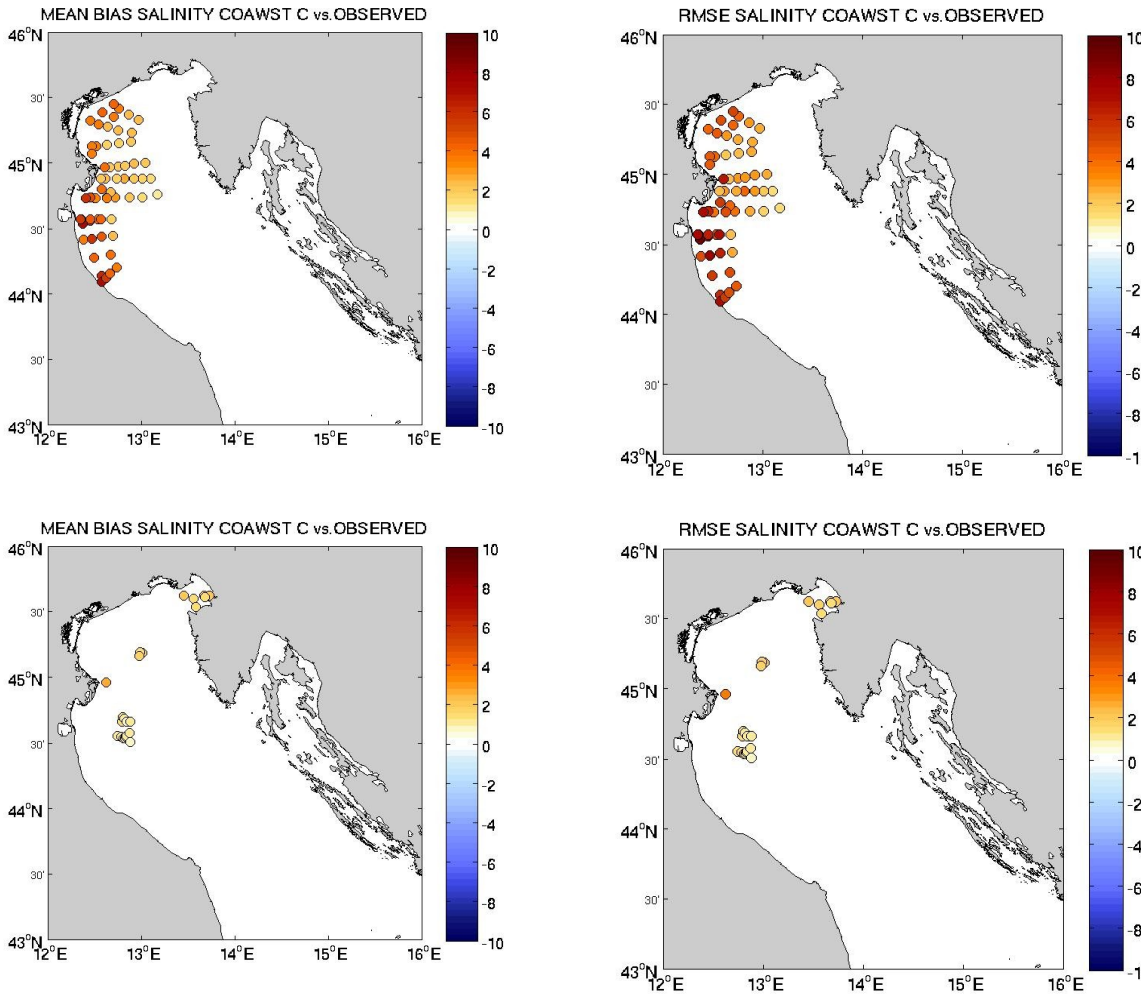

Fig. 1.4. - MB and RMSE between observed and forecasted salinity values by COAWST-C.

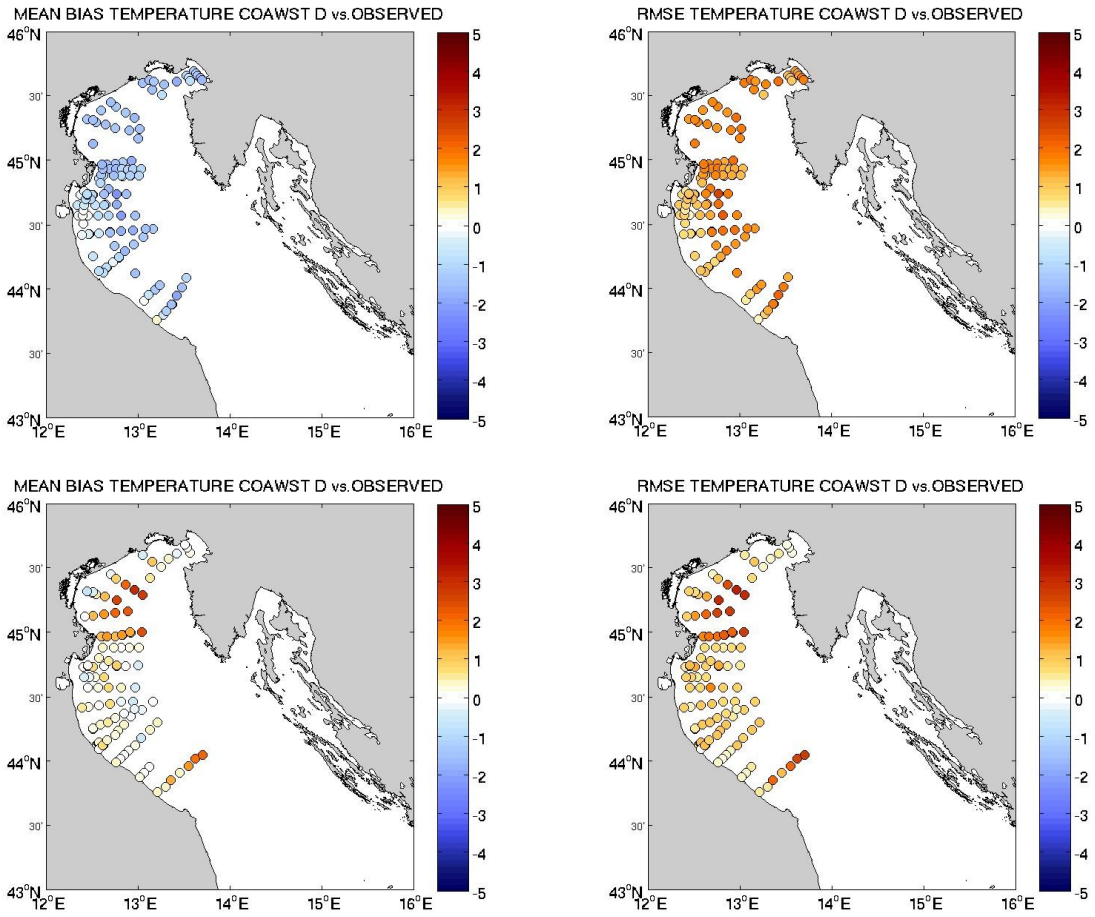

Fig. 1.5. - MB and RMSE between observed and forecasted temperature values by COAWST-D.

ANNEX II

Following histograms show the number of valid pixels from each one of the four areas during the investigated period, first computed day by day (Fig.2.1), then for each season (2.2).

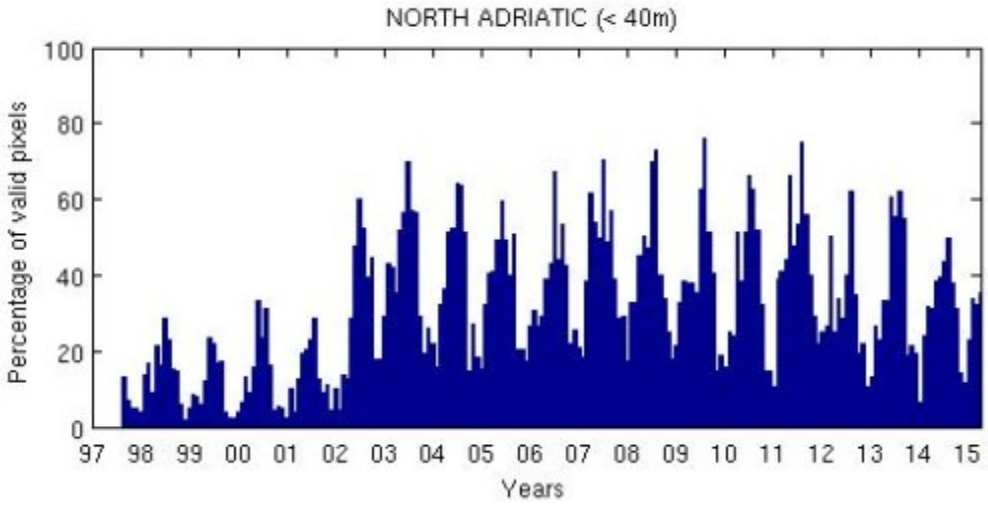

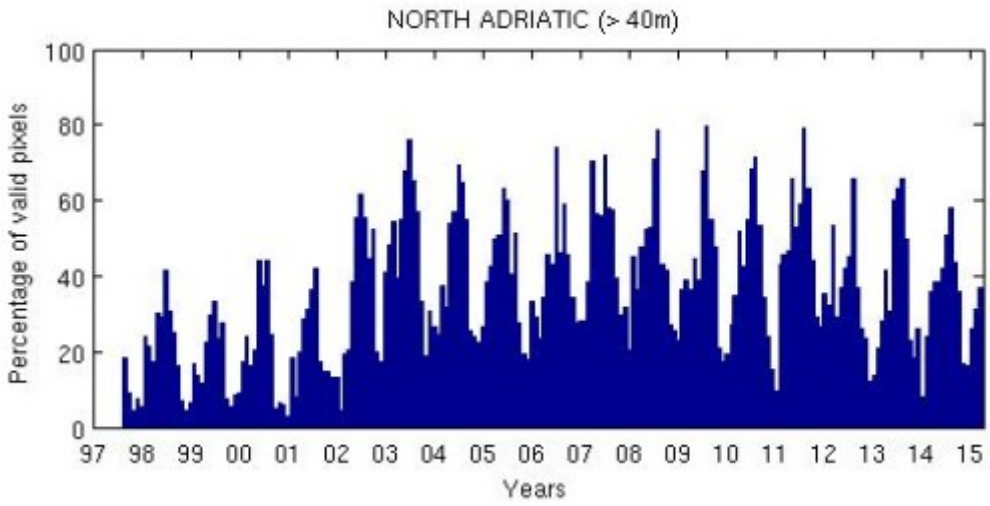

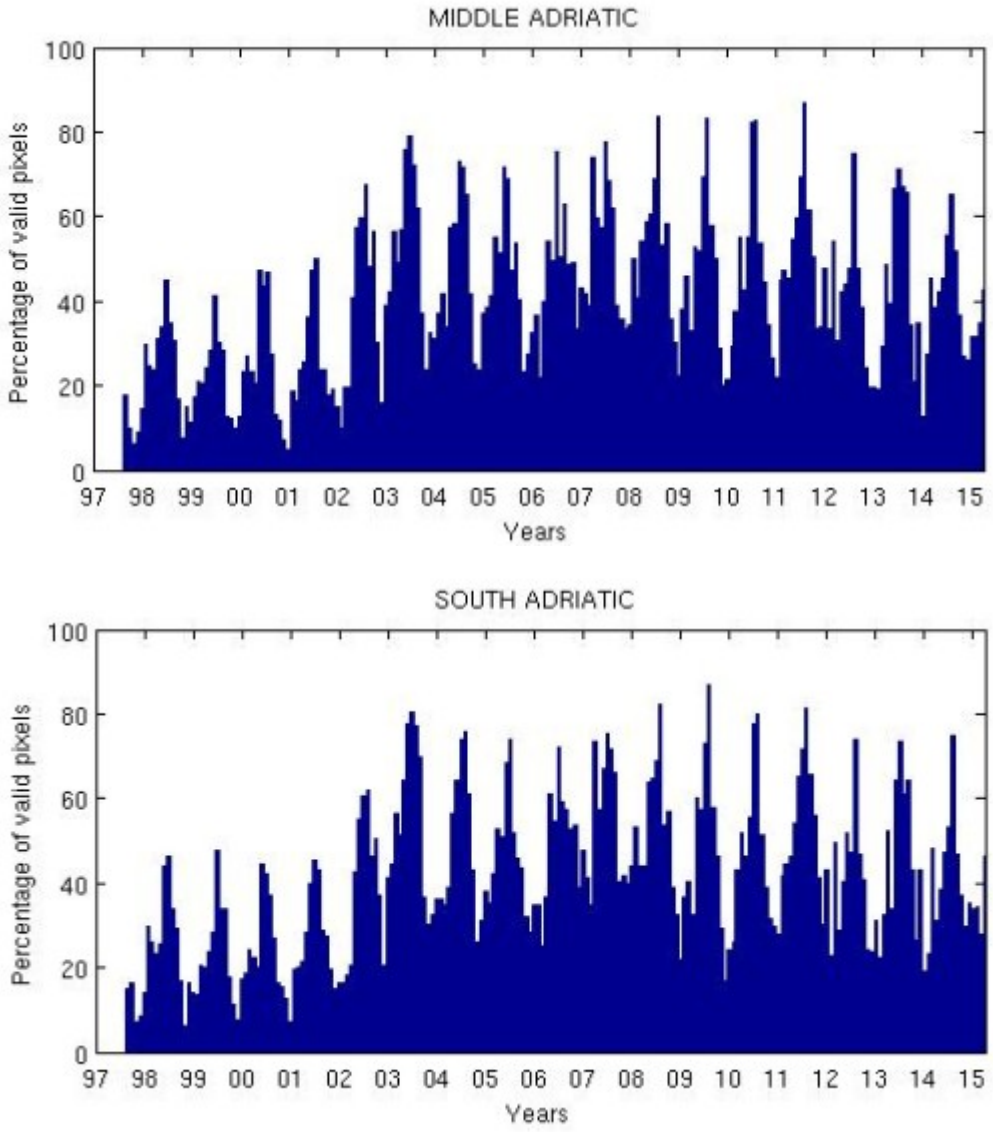

Figure 2.1. - Daily valid pixels from 1997 to 2015.

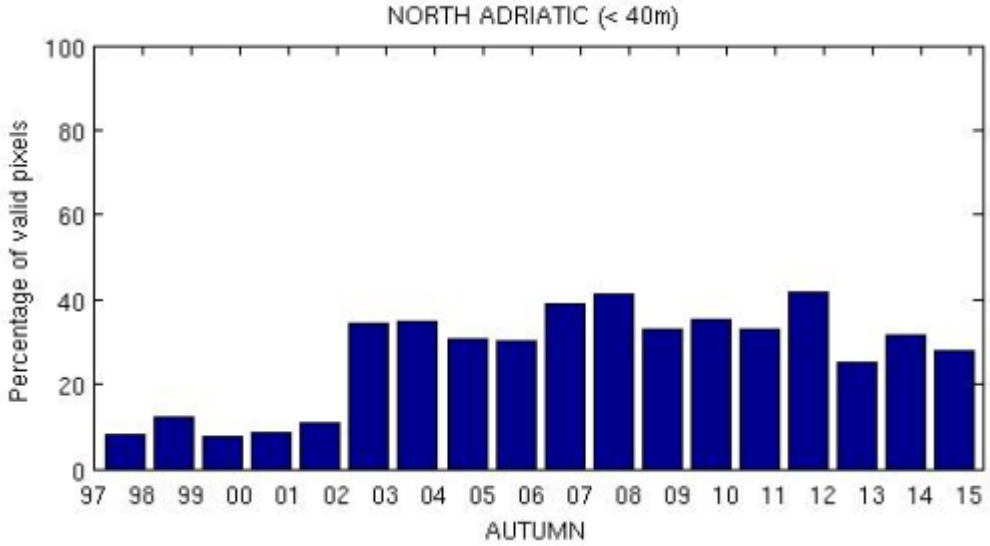

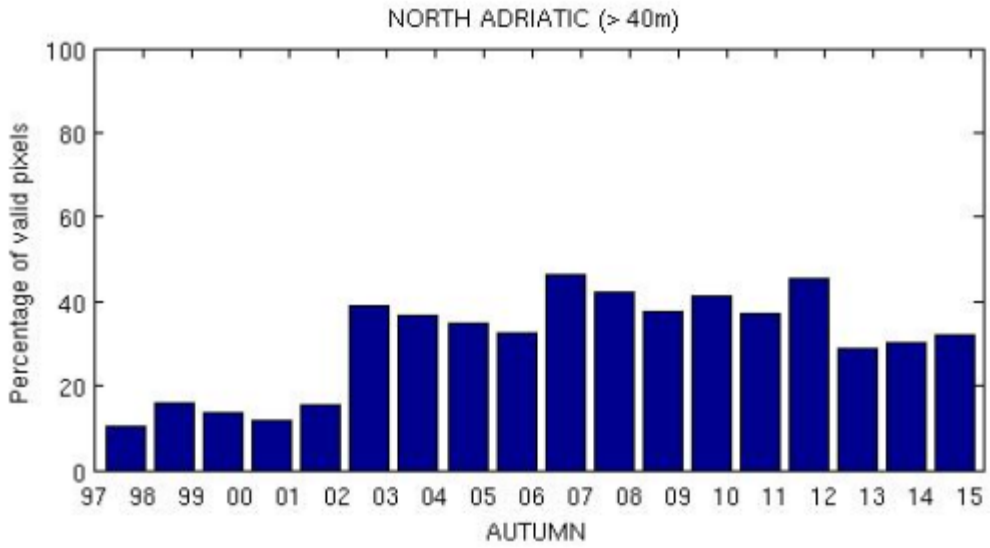
NORTH ADRIATIC (> 40m)
Percentage of valid pixels
100
80
60
40
20
0
97 98 99 00 01 02 03 04 05 06 07 08 09 10 11 12 13 14 15
AUTUMN

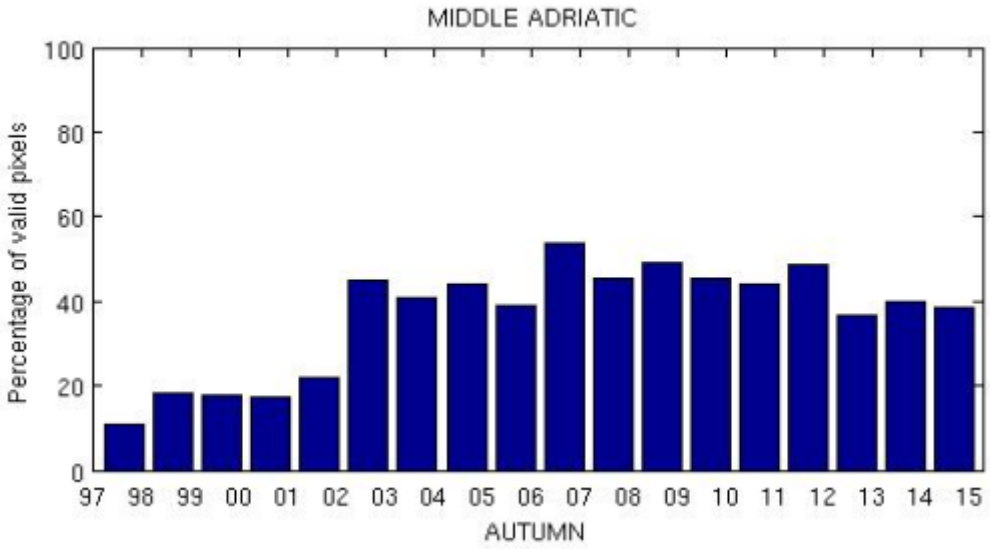
MIDDLE ADRIATIC
Percentage of valid pixels
100
80
60
40
20
0
97 98 99 00 01 02 03 04 05 06 07 08 09 10 11 12 13 14 15
AUTUMN

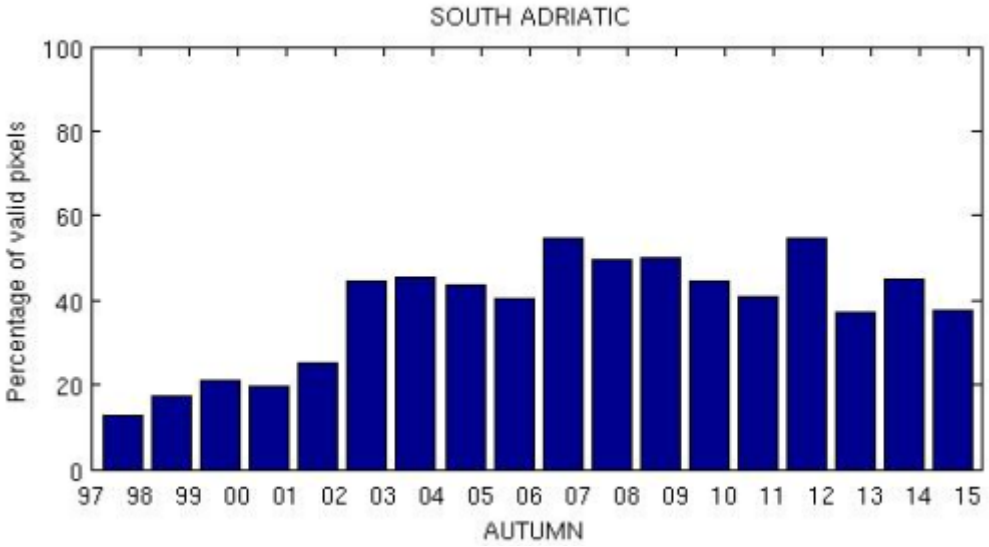
SOUTH ADRIATIC
Percentage of valid pixels
0
20
40
60
80
100
97 98 99 00 01 02 03 04 05 06 07 08 09 10 11 12 13 14 15
AUTUMN

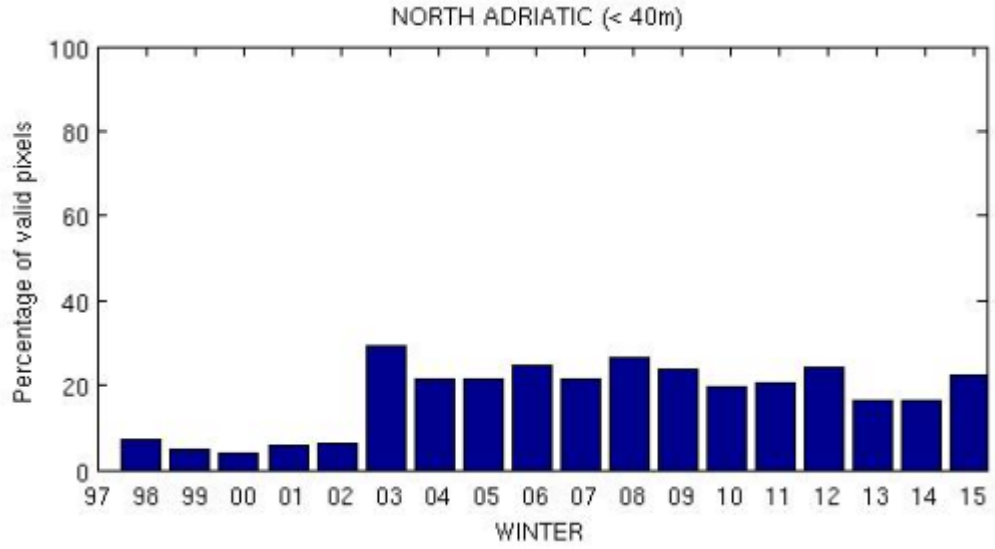
NORTH ADRIATIC (< 40m)
Percentage of valid pixels
0
20
40
60
80
100
97 98 99 00 01 02 03 04 05 06 07 08 09 10 11 12 13 14 15
WINTER

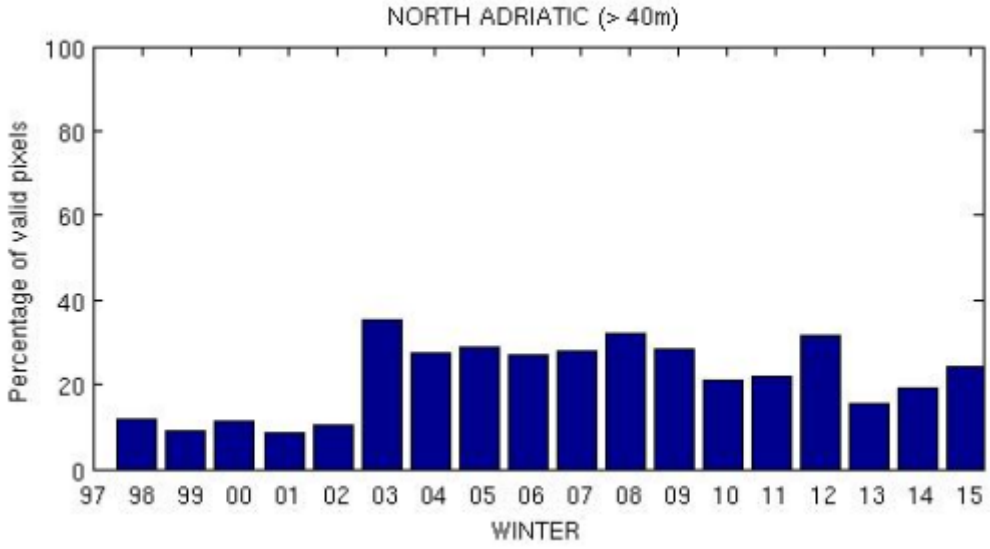
NORTH ADRIATIC (> 40m)
Percentage of valid pixels
0
20
40
60
80
100
97 98 99 00 01 02 03 04 05 06 07 08 09 10 11 12 13 14 15
WINTER

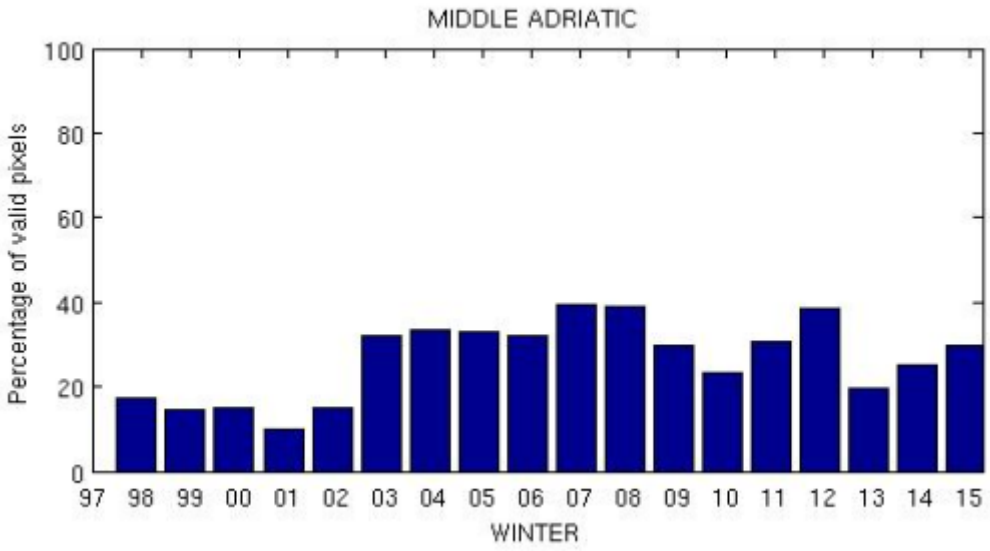
MIDDLE ADRIATIC
Percentage of valid pixels
100
80
60
40
20
0
97 98 99 00 01 02 03 04 05 06 07 08 09 10 11 12 13 14 15
WINTER

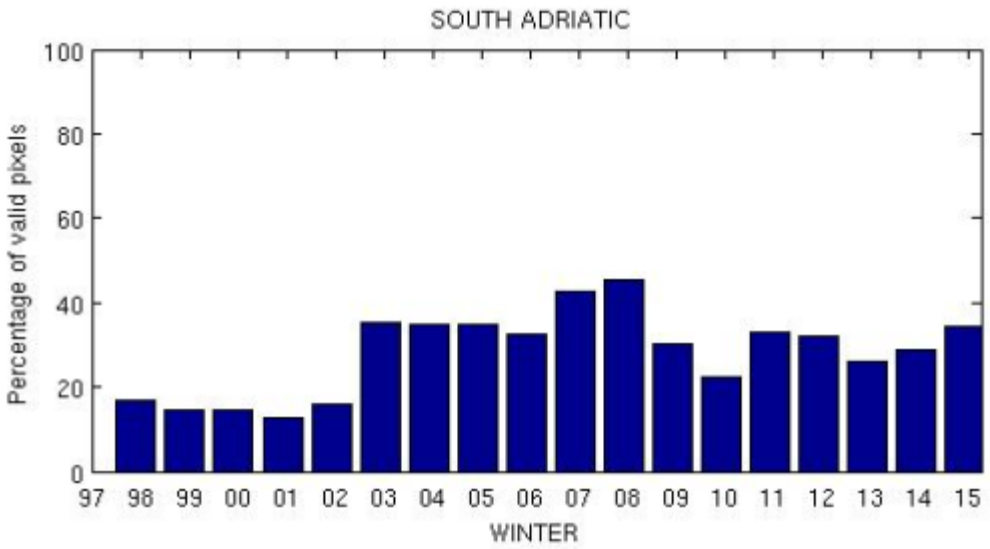
SOUTH ADRIATIC
Percentage of valid pixels
0
20
40
60
80
100
97 98 99 00 01 02 03 04 05 06 07 08 09 10 11 12 13 14 15
WINTER

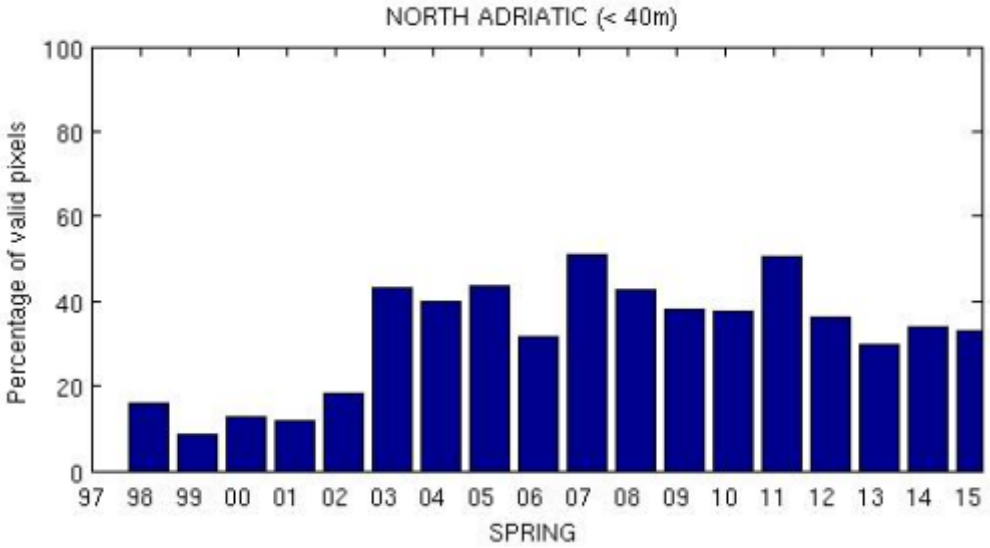
NORTH ADRIATIC (< 40m)
Percentage of valid pixels
0
20
40
60
80
100
97 98 99 00 01 02 03 04 05 06 07 08 09 10 11 12 13 14 15
SPRING

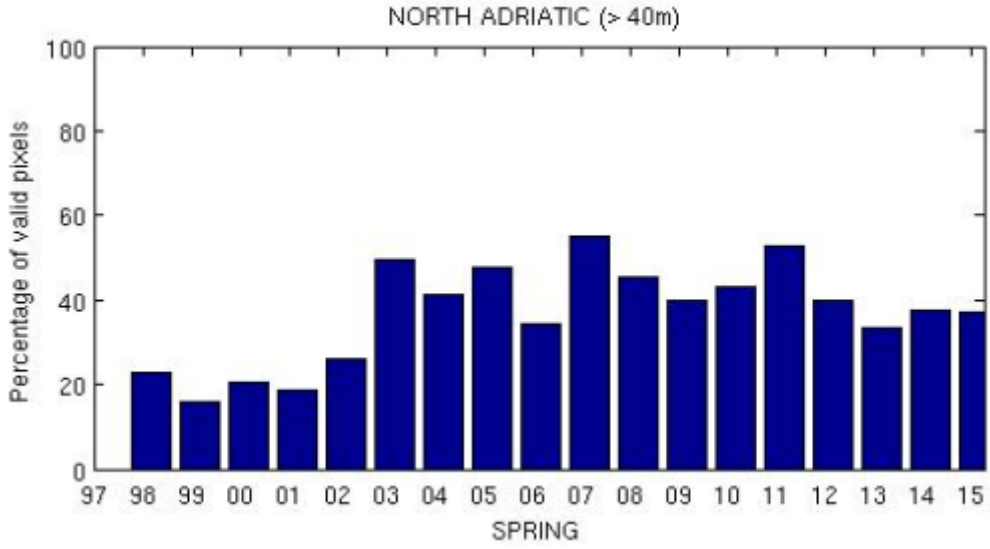
NORTH ADRIATIC (> 40m)
Percentage of valid pixels
0
20
40
60
80
100
97 98 99 00 01 02 03 04 05 06 07 08 09 10 11 12 13 14 15
SPRING

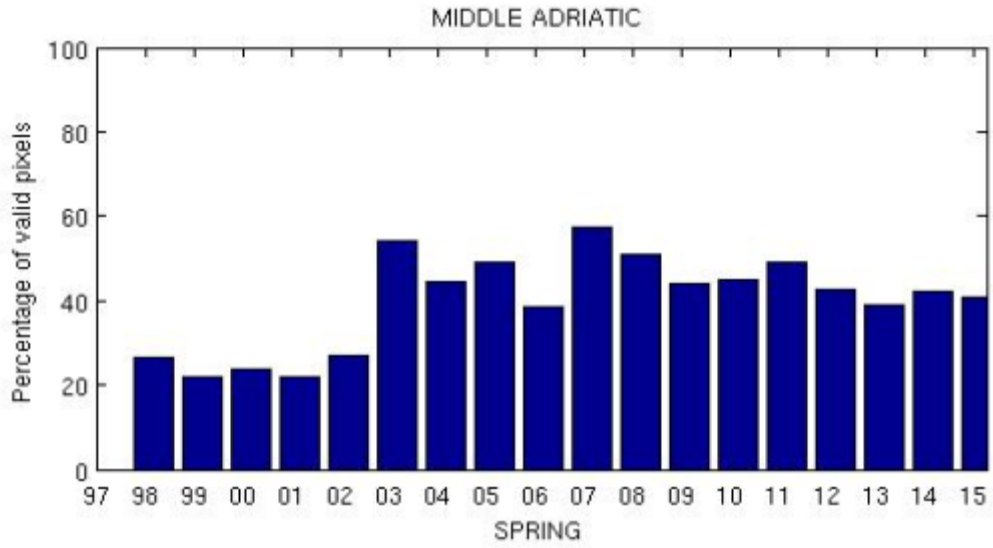
MIDDLE ADRIATIC
Percentage of valid pixels
0
20
40
60
80
100
97 98 99 00 01 02 03 04 05 06 07 08 09 10 11 12 13 14 15
SPRING

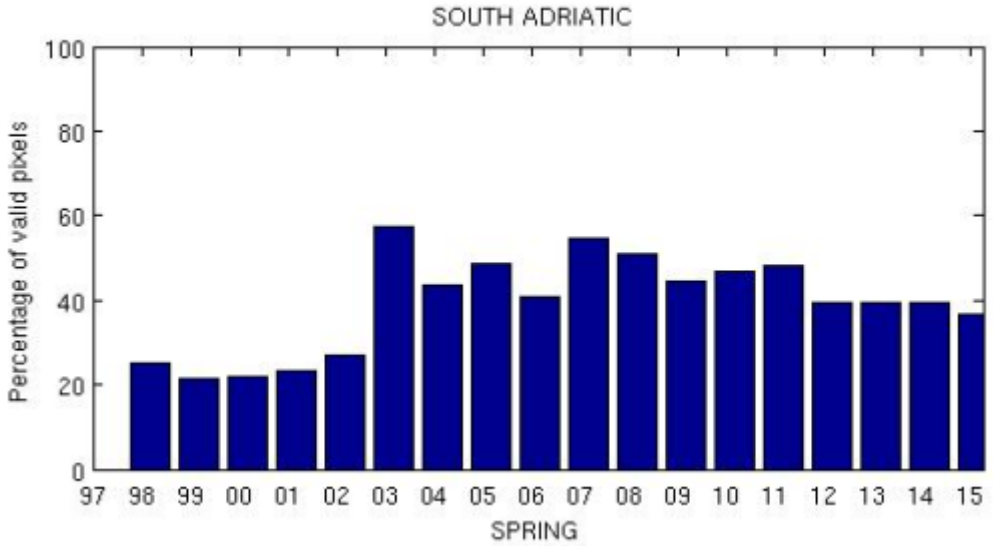
SOUTH ADRIATIC
Percentage of valid pixels
0
20
40
60
80
100
97 98 99 00 01 02 03 04 05 06 07 08 09 10 11 12 13 14 15
SPRING

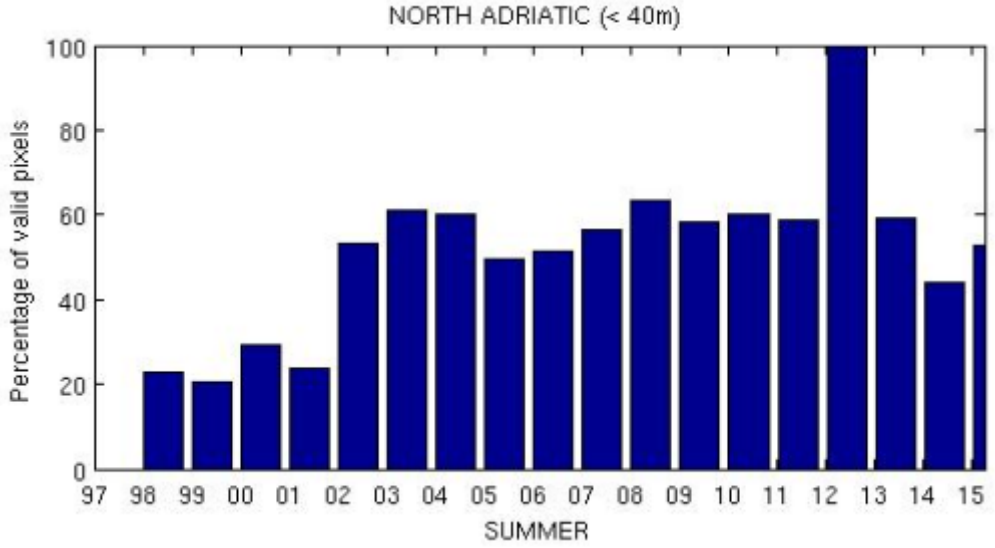
NORTH ADRIATIC (< 40m)
Percentage of valid pixels
0
20
40
60
80
100
97 98 99 00 01 02 03 04 05 06 07 08 09 10 11 12 13 14 15
SUMMER

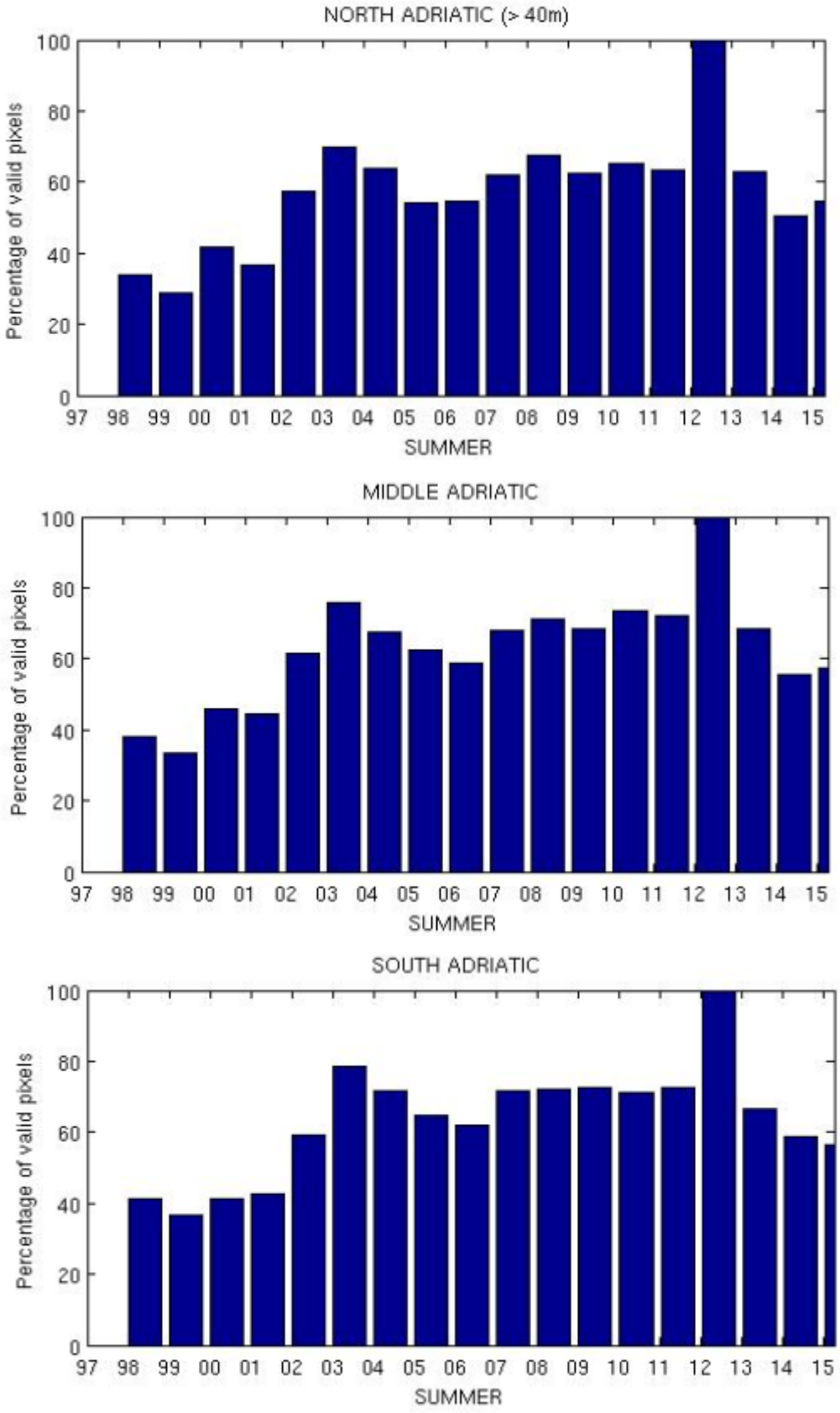

Figure 2.2. - Daily valid pixels for each season from 1997 to 2015.

In the following graphs are reported values of linear regression and its significance level, along with variables increment in one and 26 years. Variables investigated - temperature, salinity and chlorophyll-a concentration - has been analyzed at interannual, seasonal and monthly time scale for each one of the four areas.

Temperature

INTERANNUAL SURFACE TEMPERATURE °C

	R2	P level	ΔT(± err)	ΔT 26years(± err)
AREA1	0,4456	0,0002	0,0360 (±0,0082)	0,94 (± 0.21)
AREA2	0,4508	0,0002	0,0363 (±0,0082)	0,94 (± 0.21)
AREA3	0,4223	0,0003	0,0371 (±0,0089)	0,97 (± 0.23)
AREA4	0,3825	0,0008	0,0343 (±0,0089)	0,89(± 0.23)

SEASONAL SURFACE TEMPERATURE °C

AREA 1

	R2	P level	ΔT(± err)	ΔT 26years(± err)
WINTER	0.1305	0.0698	0.0191 (± 0.0100)	0.50 (± 0.26)
SPRING	0.1397	0.0600	0.0385 (± 0.0195)	1.00 (± 0.51)
SUMMER	0.3341	0.0020	0.0575 (± 0.0166)	1.49 (± 0.43)
AUTUMN	0.1522	0.0488	0.0289 (± 0.0139)	0.75 (± 0.36)

AREA 2

	R2	P level	ΔT (± err)	ΔT 26years(± err)
WINTER	0.1656	0.0391	0.0198 (± 0.0091)	0.51 (± 0.24)
SPRING	0.2542	0.0086	0.0452 (± 0.0158)	1.17(± 0.41)
SUMMER	0.3614	0.0012	0.0640 (± 0.0174)	1.66 (± 0.45)
AUTUMN	0.0410	0.3214	0.0158 (± 0.0156)	0.41 (± 0.40)

AREA 3

	R2	P level	ΔT (± err)	ΔT 26years(± err)
WINTER	0.1484	0.0519	0.0177 (± 0.0086)	0.46 (± 0.22)
SPRING	0.2951	0.0041	0.0429 (± 0.0135)	1.11 (± 0.35)
SUMMER	0.3747	0.0009	0.0701 (± 0.0185)	1.82 (± 0.48)
AUTUMN	0.0435	0.3063	0.0174 (± 0.0167)	0.45 (± 0.43)

AREA 4

	R2	P level	ΔT (± err)	ΔT 26years(± err)
WINTER	0.2188	0.0160	0.0201 (± 0.0078)	0.52 (± 0.20)
SPRING	0.3495	0.0015	0.0415 (± 0.0116)	1.08 (± 0.30)
SUMMER	0.3446	0.0016	0.0580 (± 0.0163)	1.51 (± 0.42)
AUTUMN	0.0423	0.3136	0.0173 (± 0.0168)	0.45 (± 0.44)

MONTHLY SURFACE TEMPERATURE °C

AREA 1

	R2	P level	ΔT(± err)	ΔT 26years (± err)
JANUARY	0.0465	0.2902	0.0248 (± 0.0229)	0.65 (± 0.60)
FEBRUARY	0.0054	0.7212	-0.0077 (± 0.0214)	-0.20 (± 0.56)
MARCH	0.0008	0.8898	0.0034 (± 0.0244)	0.09 (± 0.64)
APRIL	0.1936	0.0245	0.0479 (± 0.0200)	1.25 (± 0.52)
MAY	0.1763	0.0327	0.0644 (± 0.0284)	1.67 (± 0.74)
JUNE	0.2665	0.0069	0.0836 (±0. 0283)	2.17 (± 0.74)
JULY	0.3177	0.0027	0.0636 (± 0.0190)	1.65 (± 0.49)
AUGUST	0.0492	0.2763	0.0260 (± 0.0233)	0.68 (± 0.61)
SEPTEMBER	0.1056	0.1053	0.0351 (± 0.0209)	0.91 (± 0.54)
OCTOBER	0.0703	0.1906	0.0223 (± 0.0166)	0.58 (± 0.43)
NOVEMBER	0.0884	0.1403	0.0296 (± 0.0194)	0.77 (± 0.50)
DECEMBER	0.0890	0.1388	0.0381 (± 0.0249)	0.99 (± 0.65)

AREA 2

	R2	P level	ΔT (± err)	ΔT 26years(± err)
JANUARY	0.0557	0.2372	0.0231 (± 0.0191)	0.60 (± 0.50)
FEBRUARY	0.0052	0.7273	0.0055(± 0.0155)	0.14 (± 0.40)
MARCH	0.0195	0.4964	0.0121 (± 0.0175)	0.31 (± 0.45)
APRIL	0.3275	0.0022	0.0531 (± 0.0155)	1.38 (± 0.40)
MAY	0.2058	0.0199	0.0707 (± 0.0283)	1.84 (± 0.74)
JUNE	0.2990	0.0038	0.0904(± 0.0283)	2.35 (± 0.73)
JULY	0.3922	0.0006	0.0732 (± 0.0186)	1.90 (± 0.48)
AUGUST	0.0585	0.2339	0.0291 (± 0.0239)	0.76 (± 0.62)
SEPTEMBER	0.0416	0.3176	0.0238 (± 0.0233)	0.62 (± 0.61)
OCTOBER	0.0082	0.6606	0.0075 (± 0.0169)	0.20 (± 0.44)
NOVEMBER	0.0316	0.3849	0.0162 (± 0.0183)	0.42 (± 0.48)

DECEMBER	0.0783	0.1662	0.0299 (± 0.0209)	0.78 (± 0.54)

AREA 3

	R2	P level	ΔT (± err)	ΔT 26years (± err)
JANUARY	0.0536	0.2552	0.0174(± 0.0149)	0.45(± 0.39)
FEBRUARY	0.0113	0.6058	0.0062(± 0.0119)	0.16(± 0.31)
MARCH	0.0322	0.3802	0.0122(± 0.0136)	0.32(± 0.35)
APRIL	0.3770	0.0008	0.0508(± 0.0133)	1.32(± 0.35)
MAY	0.2101	0.0185	0.0659(± 0.0261)	1.71(± 0.68)
JUNE	0.3102	0.0031	0.0916(± 0.0279)	2.38(± 0.72)
JULY	0.4115	0.0004	0.0811(± 0.0198)	2.11(± 0.51)
AUGUST	0.0954	0.1247	0.0385(± 0.0242)	1.00(± 0.63)
SEPTEMBER	0.0705	0.1897	0.0330(± 0.0245)	0.86(± 0.64)
OCTOBER	0.0079	0.6649	0.0080(± 0.0183)	0.21(± 0.48)
NOVEMBER	0.0173	0.5220	0.0115(± 0.0177)	0.30(± 0.46)
DECEMBER	0.0866	0.1445	0.0287(± 0.0190)	0.75(± 0.49)

AREA 4

	R2	P level	ΔT (± err)	ΔT 26years (± err)
JANUARY	0.0834	0.1524	0.0163(± 0.0110)	0.42(± 0.29)
FEBRUARY	0.0541	0.2527	0.0098(± 0.0084)	0.25(± 0.22)
MARCH	0.0647	0.2097	0.0132(± 0.0102)	0.34(± 0.27)
APRIL	0.3579	0.0012	0.0432(± 0.0118)	1.12(± 0.31)
MAY	0.2629	0.0074	0.0682(± 0.0233)	1.77(± 0.61)
JUNE	0.3510	0.0014	0.0905(± 0.0251)	2.35(± 0.65)
JULY	0.3429	0.0017	0.0634(± 0.0179)	1.65(± 0.47)
AUGUST	0.0397	0.3292	0.0211(± 0.0212)	0.55(± 0.55)
SEPTEMBER	0.0486	0.2794	0.0243(± 0.0219)	0.63(± 0.57)
OCTOBER	0.0023	0.8162	0.0046(± 0.0197)	0.12(± 0.51)
NOVEMBER	0.0680	0.1983	0.0235(± 0.0178)	0.61(± 0.46)
DECEMBER	0.1761	0.0328	0.0336(± 0.0148)	0.87(± 0.39)

INTERANNUAL BOTTOM TEMPERATURE °C

	R2	P level	ΔT (± err)	ΔT 26years(± err)
AREA1	0,1307	0,0695	0,0312 (±0,0164)	0,81 (± 0.43)
AREA 2	0.0511	0.2666	0.0120 (±0.0105)	0.31 (±0.27)
AREA 3	0.0525	0.2600	0.0098 (±0.0085)	0.26 (±0.22)
AREA 4	0,3068	0,0033	0,0104 (±0,0032)	0,27 (± 0.08)

SEASONAL BOTTOM TEMPERATURE °C

AREA 1

	R2	P level	ΔT(± err)	ΔT 26years (± err)
WINTER	0.0030	0.7916	-0.0036 (± 0.0136)	-0.09 (± 0.35)
SPRING	0.0021	0.8260	0.0061 (± 0.0272)	0.16 (± 0.71)
SUMMER	0.2677	0.0068	0.0678 (± 0.0229)	1.76 (± 0.59)
AUTUMN	0.2585	0.0080	0.0537 (± 0.0186)	1.40 (± 0.48)

AREA 2

	R2	P level	ΔT (± err)	ΔT 26years(± err)
WINTER	0.0841	0.1506	0.0140 (± 0.0094)	0.36 (± 0.24)
SPRING	0.0071	0.6819	0.0072 (± 0.0174)	0.19 (± 0.45)
SUMMER	0.0442	0.3025	0.0178(± 0.0169)	0.46 (± 0.44)
AUTUMN	0.0228	0.4620	0.0089 (± 0.0119)	0.23 (± 0.31)

AREA 3

	R2	P level	ΔT (± err)	ΔT 26years (± err)
WINTER	0.1172	0.0869	0.0136 (± 0.0076)	0.35 (± 0.20)
SPRING	0.0504	0.2704	0.0122 (± 0.0108)	0.32 (± 0.28)
SUMMER	0.0159	0.5395	0.0065 (± 0.0104)	0.17 (± 0.27)
AUTUMN	0.0263	0.4283	0.0072 (± 0.0089)	0.19 (± 0.23)

AREA 4

	R2	P level	ΔT (± err)	ΔT 26years (± err)
WINTER	0.3042	0.0035	0.0101(± 0.0031)	0.26 (± 0.08)
SPRING	0.2592	0.0079	0.0109 (± 0.0038)	0.28 (± 0.10)
SUMMER	0.2810	0.0053	0.0107(± 0.0035)	0.28 (± 0.09)
AUTUMN	0.1765	0.0326	0.0100(± 0.0044)	0.26 (± 0.11)

MONTHLY BOTTOM TEMPERATURE °C

AREA 1

	R2	P level	ΔT(± err)	ΔT 26years (± err)
JANUARY	0.000	0.943	-0.002 (± 0.025)	-0.05(± 0.65)
FEBRUARY	0.066	0.205	-0.039 (± 0.030)	-1.01(± 0.78)
MARCH	0.024	0.448	-0.025 (± 0.032)	-0.64(± 0.83)
APRIL	0.006	0.700	0.010(± 0.025)	0.25(± 0.65)
MAY	0.060	0.226	0.033(± 0.027)	0.86(± 0.70)
JUNE	0.188	0.027	0.063(± 0.027)	1.64(± 0.69)
JULY	0.310	0.003	0.077(± 0.023)	1.99(± 0.61)
AUGUST	0.233	0.013	0.064(± 0.024)	1.65(± 0.61)
SEPTEMBER	0.400	0.001	0.085(± 0.021)	2.20(± 0.55)
OCTOBER	0.136	0.064	0.045(± 0.023)	1.17(± 0.60)
NOVEMBER	0.069	0.196	0.032(± 0.024)	0.82(± 0.62)
DECEMBER	0.046	0.291	0.028(± 0.026)	0.73(± 0.68)

AREA 2

	R2	P level	ΔT (± err)	ΔT 26years(± err)
JANUARY	0.0368	0.3479	0.0185(± 0.0193)	0.48(± 0.50)
FEBRUARY	0.0003	0.9293	0.0015(± 0.0172)	0.04(± 0.45)
MARCH	0.0015	0.8519	0.0034(± 0.0180)	0.09(± 0.47)
APRIL	0.0056	0.7158	0.0066(± 0.0180)	0.17(± 0.47)
MAY	0.0188	0.5043	0.0116(± 0.0172)	0.30(± 0.45)
JUNE	0.0370	0.3464	0.0164(± 0.0171)	0.43(± 0.44)
JULY	0.0462	0.2917	0.0191(± 0.0178)	0.50(± 0.46)
AUGUST	0.0421	0.3147	0.0179(± 0.0174)	0.47(± 0.45)
SEPTEMBER	0.0464	0.2905	0.0168(± 0.0156)	0.44(± 0.40)
OCTOBER	0.0002	0.9456	0.0009(± 0.0127)	0.02(± 0.33)
NOVEMBER	0.0137	0.5685	0.0093(± 0.0161)	0.24(± 0.42)
DECEMBER	0.0520	0.2626	0.0218(± 0.0190)	0.57(± 0.49)

AREA 3

	R2	P level	ΔT (± err)	ΔT 26years (± err)
JANUARY	0.1099	0.0981	0.0187(± 0.0109)	0.49(± 0.28)
FEBRUARY	0.0431	0.3088	0.0106(± 0.0102)	0.28(± 0.27)
MARCH	0.0477	0.2838	0.0124(± 0.0113)	0.32(± 0.29)
APRIL	0.0622	0.2192	0.0134(± 0.0107)	0.35(± 0.28)

MAY	0.0400	0.3273	0.0107(± 0.0107)	0.28(± 0.28)
JUNE	0.0169	0.5266	0.0070(± 0.0109)	0.18(± 0.28)
JULY	0.0162	0.5356	0.0066(± 0.0105)	0.17(± 0.27)
AUGUST	0.0139	0.5666	0.0058(± 0.0100)	0.15(± 0.26)
SEPTEMBER	0.0267	0.4252	0.0074(± 0.0091)	0.19(± 0.24)
OCTOBER	0.0037	0.7690	0.0028(± 0.0094)	0.07(± 0.24)
NOVEMBER	0.0519	0.2629	0.0114(± 0.0100)	0.30(± 0.26)
DECEMBER	0.0565	0.2425	0.0116(± 0.0097)	0.30(± 0.25)

AREA 4

	R2	**P level**	**ΔT (± err)**	**ΔT 26years (± err)**
JANUARY	0.1623	0.0413	0.0098(± 0.0045)	0.25(± 0.12)
FEBRUARY	0.0804	0.1605	0.0063(± 0.0044)	0.16(± 0.11)
MARCH	0.1555	0.0462	0.0090(± 0.0043)	0.23(± 0.11)
APRIL	0.2870	0.0048	0.0116(± 0.0037)	0.30(± 0.10)
MAY	0.3143	0.0029	0.0121(± 0.0037)	0.32(± 0.10)
JUNE	0.3524	0.0014	0.0132(± 0.0036)	0.34(± 0.09)
JULY	0.2933	0.0043	0.0114(± 0.0036)	0.30(± 0.09)
AUGUST	0.1581	0.0443	0.0075(± 0.0036)	0.20(± 0.09)
SEPTEMBER	0.1461	0.0539	0.0089(± 0.0044)	0.23(± 0.11)
OCTOBER	0.1423	0.0575	0.0091(± 0.0045)	0.24(± 0.12)
NOVEMBER	0.1889	0.0265	0.0120(± 0.0051)	0.31(± 0.13)
DECEMBER	0.2915	0.0044	0.0142(± 0.0045)	0.37(± 0.12)

Salinity

INTERANNUAL SURFACE SALINITY

	R2	P level	ΔT (± err)	ΔT 26years(± err)
AREA1	0.3062	0.0034	0,0318 (±0,0098)	0,83 (± 0.25)
AREA 2	0.0258	0.4333	0.0043(±0,0054)	0.11 (± 0.14)
AREA 3	0.0263	0.4285	-0.0036(±0.0044)	-0.09 (± 0.12)
AREA4	0.0479	0.2829	-0.0036 (±0,0033)	-0.09 (± 0.09)

SEASONAL SURFACE SALINITY

AREA 1

	R2	P level	ΔT(± err)	ΔT 26years (± err)
WINTER	0.3233	0.0024	0.0290(± 0.0086)	0.75(± 0.22)
SPRING	0.1707	0.0359	0.0247(± 0.0111)	0.64(± 0.29)
SUMMER	0.2705	0.0065	0.0379(± 0.0127)	0.98(± 0.33)
AUTUMN	0.2091	0.0188	0.0355(± 0.0141)	0.92(± 0.37)

AREA 2

	R2	P level	ΔT (± err)	ΔT 26years(± err)
WINTER	0.0238	0.4514	0.0034(± 0.0045)	0.09(± 0.12)
SPRING	0.0001	0.9628	-0.0003(± 0.0059)	-0.01(± 0.15)
SUMMER	0.0271	0.4218	0.0060(± 0.0074)	0.16(± 0.19)
AUTUMN	0.0586	0.2335	0.0080(± 0.0066)	0.21(± 0.17)

AREA 3

	R2	P level	ΔT (± err)	ΔT 26years (± err)
WINTER	0.0067	0.6910	-0.0015(± 0.0038)	-0.04(± 0.10)
SPRING	0.1259	0.0753	-0.0071(± 0.0038)	-0.19(± 0.10)
SUMMER	0.0272	0.4208	-0.0053(± 0.0064)	-0.14(± 0.17)
AUTUMN	0.0001	0.9609	-0.0003(± 0.0059)	-0.01(± 0.15)

AREA 4

	R2	P level	ΔT (± err)	ΔT 26years (± err)
WINTER	0.0001	0.9624	-0.0002(± 0.0034)	0.00(± 0.09)
SPRING	0.0887	0.1396	-0.0055(± 0.0036)	-0.14(± 0.09)

SUMMER	0.0992	0.1170	-0.0068(± 0.0042)	-0.18(± 0.11)
AUTUMN	0.0090	0.6449	-0.0020(± 0.0043)	-0.05(± 0.11)

MONTHLY SURFACE SALINITY

AREA 1

	R2	**P level**	**ΔT(± err)**	**ΔT 26years (± err)**
JANUARY	0.1570	0.0451	0.0248(± 0.0117)	0.64(± 0.30)
FEBRUARY	0.2404	0.0110	0.0345(± 0.0125)	0.90(± 0.33)
MARCH	0.1649	0.0395	0.0231(± 0.0106)	0.60(± 0.28)
APRIL	0.1024	0.1110	0.0206(± 0.0124)	0.54(± 0.32)
MAY	0.1612	0.0420	0.0301(± 0.0140)	0.78(± 0.36)
JUNE	0.2935	0.0043	0.0423(± 0.0134)	1.10(± 0.35)
JULY	0.2171	0.0164	0.0379(± 0.0147)	0.99(± 0.38)
AUGUST	0.1966	0.0233	0.0336(± 0.0139)	0.87(± 0.36)
SEPTEMBER	0.1923	0.0250	0.0371(± 0.0155)	0.97(± 0.40)
OCTOBER	0.1926	0.0246	0.0379(± 0.0159)	0.99(± 0.41)
NOVEMBER	0.1731	0.0345	0.0314(± 0.0140)	0.82(± 0.36)
DECEMBER	0.1638	0.0403	0.0282(± 0.0130)	0.73(± 0.34)

AREA 2

	R2	**P level**	**ΔT (± err)**	**ΔT 26years(± err)**
JANUARY	0.0039	0.7610	0.0018(± 0.0060)	0.05(± 0.16)
FEBRUARY	0.0210	0.4802	0.0035(± 0.0049)	0.09(± 0.13)
MARCH	0.0409	0.3220	0.0062(± 0.0061)	0.16(± 0.16)
APRIL	0.0026	0.8055	0.0017(± 0.0070)	0.05(± 0.18)
MAY	0.0391	0.3327	-0.0087(± 0.0088)	-0.23(± 0.23)
JUNE	0.0025	0.8084	0.0021(± 0.0085)	0.05(± 0.22)
JULY	0.0298	0.3992	0.0064(± 0.0075)	0.17(± 0.19)
AUGUST	0.0508	0.2684	0.0095(± 0.0084)	0.25(± 0.22)
SEPTEMBER	0.0531	0.2572	0.0105(± 0.0091)	0.27(± 0.24)
OCTOBER	0.0927	0.1304	0.0104(± 0.0066)	0.27(± 0.17)
NOVEMBER	0.0137	0.5685	0.0032(± 0.0055)	0.08(± 0.14)
DECEMBER	0.0404	0.3250	0.0049(± 0.0049)	0.13(± 0.13)

AREA 3

	R2	**P level**	**ΔT (± err)**	**ΔT 26years (± err)**
JANUARY	0.0175	0.5195	-0.0027(± 0.0042)	-0.07(± 0.11)

FEBRUARY	0.0372	0.3449	-0.0038(± 0.0040)	-0.10(± 0.10)
MARCH	0.0969	0.1217	-0.0067(± 0.0042)	-0.17(± 0.11)
APRIL	0.1233	0.0786	-0.0071(± 0.0039)	-0.18(± 0.10)
MAY	0.0909	0.1343	-0.0076(± 0.0049)	-0.20(± 0.13)
JUNE	0.0611	0.2233	-0.0087(± 0.0070)	-0.23(± 0.18)
JULY	0.0168	0.5284	-0.0045(± 0.0071)	-0.12(± 0.18)
AUGUST	0.0054	0.7211	-0.0026(± 0.0073)	-0.07(± 0.19)
SEPTEMBER	0.0020	0.8265	-0.0017(± 0.0078)	-0.05(± 0.20)
OCTOBER	0.0003	0.9291	0.0006(± 0.0062)	0.01(± 0.16)
NOVEMBER	0.0001	0.9553	0.0003(± 0.0050)	0.01(± 0.13)
DECEMBER	0.0074	0.6752	0.0018(± 0.0042)	0.05(± 0.11)

AREA 4

	R2	**P level**	**ΔT (± err)**	**ΔT 26years (± err)**
JANUARY	0.0019	0.8345	-0.0008(± 0.0037)	-0.02(±)
FEBRUARY	0.0078	0.6684	-0.0015(± 0.0035)	-0.04(±)
MARCH	0.0199	0.4918	-0.0025(± 0.0036)	-0.07(±)
APRIL	0.0784	0.1659	-0.0055(± 0.0038)	-0.14(±)
MAY	0.1722	0.0350	-0.0085(± 0.0038)	-0.22(±)
JUNE	0.2091	0.0188	-0.0100(± 0.0040)	-0.26(±)
JULY	0.0728	0.1824	-0.0065(± 0.0047)	-0.17(±)
AUGUST	0.0261	0.4301	-0.0039(± 0.0049)	-0.10(±)
SEPTEMBER	0.0144	0.5586	-0.0030(± 0.0051)	-0.08(±)
OCTOBER	0.0086	0.6520	-0.0020(± 0.0044)	-0.05(±)
NOVEMBER	0.0019	0.8312	-0.0009(± 0.0044)	(±)
DECEMBER	0.0070	0.6853	0.0017(± 0.0042)	(±)

INTERANNUAL BOTTOM SALINITY

	R2	**P level**	**ΔT (± err)**	**ΔT 26years(± err)**
AREA1	0.0904	0.1355	0.0084(± 0.0055)	0.22(± 0.14)
AREA 2	0.0013	0.8618	0.0006(± 0.0034)	0.02(± 0.09)
AREA 3	0.0250	0.4403	-0.0021(± 0.0026)	-0.05(± 0.07)
AREA4	0.2347	0.0121	0.0027(± 0.0010)	0.07(± 0.03)

SEASONAL BOTTOM SALINITY [mg/m3]

AREA 1

	R2	P level	ΔT(± err)	ΔT 26years (± err)
WINTER	0.0198	0.4934	0.0042(± 0.0060)	0.11(± 0.16)
SPRING	0.0367	0.3486	0.0054(± 0.0057)	0.14(± 0.15)
SUMMER	0.1114	0.0956	0.0099(± 0.0057)	0.26(± 0.15)
AUTUMN	0.1265	0.0746	0.0142(± 0.0076)	0.37(± 0.20)

AREA 2

	R2	P level	ΔT (± err)	ΔT 26years(± err)
WINTER	0.0004	0.9255	-0.0003(± 0.0032)	-0.01(± 0.08)
SPRING	0.0036	0.7712	0.0011(± 0.0038)	0.03(± 0.10)
SUMMER	0.0022	0.8183	0.0008(± 0.0035)	0.02(± 0.09)
AUTUMN	0.0020	0.8277	0.0007(± 0.0034)	0.02(± 0.09)

AREA 3

	R2	P level	ΔT (± err)	ΔT 26years (± err)
WINTER	0.0276	0.4173	-0.0022(± 0.0026)	-0.06(± 0.07)
SPRING	0.0260	0.4316	-0.0023(± 0.0028)	-0.06(± 0.07)
SUMMER	0.0229	0.4606	-0.0020(± 0.0027)	-0.05(± 0.07)
AUTUMN	0.0200	0.4913	-0.0018(± 0.0026)	-0.05(± 0.07)

AREA 4

	R2	P level	ΔT (± err)	ΔT 26years (± err)
WINTER	0.2046	0.0203	0.0030(± 0.0012)	0.08(± 0.03)
SPRING	0.1478	0.0525	0.0023(± 0.0011)	0.06(± 0.03)
SUMMER	0.2124	0.0178	0.0022(± 0.0009)	0.06(± 0.02)
AUTUMN	0.2895	0.0046	0.0032(± 0.0010)	0.08(± 0.03)

Chlorophyll-a

INTERANNUAL SURFACE CHLOROPHYLL-a CONCENTRATION[mg/m^3]

	R2	P level	ΔT (± err)	ΔT 19years(± err)
AREA1	0.3690	0.0058	0.1180 (± 0.0374)	2.24 (± 0.71)
AREA 2	0.0757	0.2544	0.0072 (± 0.0061)	0.14 (± 0.12)
AREA 3	0.5239	0.0005	0.0153 (± 0.0035)	0.29 (± 0.07)
AREA4	0.5577	0.0002	0.0092 (± 0.0020)	0.17 (± 0.04)

SEASONAL SURFACE CHLOROPHYLL-a CONCENTRATION [mg/m^3]

AREA 1

	R2	P level	ΔT(± err)	ΔT 19years (± err)
AUTUMN	0.1308	0.1282	0.0466 (± 0.0291)	0.89 (± 0.55)
WINTER	0.1866	0.0648	0.0786 (± 0.0398)	1.49 (± 0.76)
SPRING	0.2347	0.0416	0.1698 (± 0.0767)	3.06 (± 1.38)
SUMMER	0.4116	0.0041	0.1555 (± 0.0465)	2.80 (± 0.84)

AREA 2

	R2	P level	ΔT (± err)	ΔT 19years(± err)
AUTUMN	0.1970	0.0570	-0.0169 (± 0.0083)	-0.32 (± 0.16)
WINTER	0.1984	0.0559	0.0340 (± 0.0166)	0.65 (± 0.31)
SPRING	0.1544	0.1067	0.0186 (± 0.0109)	0.34 (± 0.20)
SUMMER	0.0648	0.3082	0.0053 (± 0.0051)	0.10 (± 0.09)

AREA 3

	R2	P level	ΔT (± err)	ΔT 19years (± err)
AUTUMN	0.072	0.7296	0.0015 (± 0.0042)	0.03 (± 0.08)
WINTER	0.3656	0.0061	0.0323 (± 0.0103)	0.61 (± 0.20)
SPRING	0.4145	0.0039	0.0241 (± 0.0072)	0.43 (± 0.13)
SUMMER	0.3441	0.0105	0.0061 (± 0.0021)	0.11 (± 0.04)

AREA 4

	R2	P level	ΔT (± err)	ΔT 19years (± err)
AUTUMN	0.2338	0.0360	0.0045 (± 0.0020)	0.09 (± 0.04)
WINTER	0.4306	0.0023	0.0215 (± 0.0060)	0.41 (± 0.11)

SPRING	0.4174	0.0038	0.0107 (± 0.0032)	0.19 (± 0.06)
SUMMER	0.4414	0.0026	0.0041 (± 0.0011)	0.07 (± 0.02)

MONTHLY SURFACE CHLOROPHYLL-a CONCENTRATION [mg/m3]

AREA 1

	R2	**P level**	**ΔT(± err)**	**ΔT 19years (± err)**
SEPTEMBER	0.3858	0.0045	0.1053 (±0.0322)	2.00(± 0.61)
OCTOBER	0.1370	0.1306	-0.0692 (±0.0434)	-1.31(± 0.82)
NOVEMBER	0.1055	0.1884	0.1020 (±0.0743)	1.94(± 1.41)
DECEMBER	0.1824	0.0771	0.1302 (±0.0689)	2.47(± 1.31)
JANUARY	0.0002	0.9512	-0.0029 (±0.0470)	-0.05(± 0.85)
FEBRUARY	0.0551	0.3483	0.0529 (±0.0548)	0.95(± 0.99)
MARCH	0.2484	0.0353	0.2030 (±0.0882)	3.65(± 1.59)
APRIL	0.1565	0.1042	0.1443 (±0.0837)	2.60(± 1.51)
MAY	0.1579	0.1024	0.1586 (± 0.0915)	2.85(± 1.65)
JUNE	0.3871	0.0058	0.2481 (± 0.0781)	4.47(± 1.41)
JULY	0.4133	0.0040	0.1230 (± 0.0366)	2.21(± 0.66)
AUGUST	0.1484	0.1144	0.0997 (± 0.0597)	1.79(± 1.08)

AREA 2

	R2	**P level**	**ΔT (± err)**	**ΔT 19years(± err)**
SEPTEMBER	0,0108	0,6725	-0,0020 (± 0,0046)	-0.04(± 0.09)
OCTOBER	0,1752	0,0838	-0.0235(± 0.0127)	-0.42(± 0.23)
NOVEMBER	0,1096	0,1797	-0.0338(± 0.0241)	-0.61(± 0.43)
DECEMBER	0,2784	0,0244	-0.0270(± 0.0109)	0.49(± 0.20)
JANUARY	0,0317	0,4798	0.005(± 0.069)	0.09(± 0.12)
FEBRUARY	0,1372	0,1302	0.0768(± 0.0482)	1.38(±0.87)
MARCH	0,0952	0,2129	0.0134(± 0.0103)	0.24(± 0.19)
APRIL	0,0411	0,4196	0.0092(± 0.0112)	0.17(± 0.20)
MAY	0,1611	0,0988	0.0311(± 0.0178)	0.56(± 0.32)
JUNE	0,0928	0,2190	0.0174(± 0.0136)	0.31(± 0.25)
JULY	0,0523	0,3614	-0.0023(± 0.0024)	-0.04(± 0.04)
AUGUST	0,0106	0,6838	0.0015(± 0.0036)	0.03(± 0.06)

AREA 3

	R2	**P level**	**ΔT (± err)**	**ΔT 19years (± err)**

SEPTEMBER	0,0482	0,3665	0.0028(± 0.003)	0.05(± 0.06)
OCTOBER	0,0015	0,8769	-0.0010(± 0.0067)	-0.02(± 0.12)
NOVEMBER	0,0859	0,2379	0.0097(± 0.0079)	0.17(± 0.14)
DECEMBER	0,3053	0,0174	0.0648(± 0.244)	1.17(± 0.44)
JANUARY	0,0302	0,4906	0.0075(± 0.0106)	0.13(± 0.19)
FEBRUARY	0,2787	0,0243	0.0289(± 0.0116)	0.52(± 0.21)
MARCH	0,5017	0,0010	0.0350(± 0.0087)	0.63(± 0.16)
APRIL	0,2119	0,0546	0.0159(± 0.0077)	0.29(± 0.14)
MAY	0,2999	0,0186	0.0207(± 0.0079)	0.37(± 0.14)
JUNE	0,3688	0,0075	0.0146(± 0.0048)	0.26(± 0.09)
JULY	0,0360	0,4510	0.0014(± 0.0018)	0.03(± 0.03)
AUGUST	0,2498	0,0347	0.0027(± 0.0012)	0.05(± 0.02)

AREA 4

	R2	**P level**	**ΔT (± err)**	**ΔT 19years (± err)**
SEPTEMBER	0,4288	0,0023	0.0043(± 0.0012)	0.08(± 0.02)
OCTOBER	0,1247	0,1506	0.0034(± 0.0022)	0.06(± 0.04)
NOVEMBER	0,2000	0,0628	0.0113(± 0.0057)	0.20(± 0.10)
DECEMBER	0,3940	0,0053	0.0327(± 0.0101)	0.59(± 0.18)
JANUARY	0,3355	0,0118	0.0268(± 0.0094)	0.48(± 0.17)
FEBRUARY	0,3721	0,0072	0.0149(± 0.0048)	0.27(± 0.09)
MARCH	0,4560	0,0021	0.0121(± 0.0033)	0.22(± 0.06)
APRIL	0,2340	0,0420	0.0093(± 0.0042)	0.17(± 0.08)
MAY	0,4187	0,0037	0.0111(± 0.0033)	0.20(± 0.06)
JUNE	0,4045	0,0046	0.0072(± 0.0033)	0.13(± 0.04)
JULY	0,3262	0,0133	0.0032(± 0.0011)	0.06(± 0.02)
AUGUST	0,3344	0,0119	0.0020(± 0.0007)	0.04(± 0.01)

ANNEX III

Following tables report values from regression analysis of the principal variables analyzed from ARPAM dataset at regional level and for the northern and southern part. Values' increase or decrease, significative or not, are reported for one single year and for the whole investigated period (12 years).

MARCHE REGION COASTAL WATERS

500 m

	R2	P level	Δ(± err)	Δ12 years (± err)
Temperature	0.0015	0.6707	-0.0801(0.1880)	0.9617(2.2565)
Salinity	0.1580	0.0000	-0.3046(0.0636)	-3.6551(0.7638)
Chlorophyll-a [µg/l]	0.0001	0.9250	0.0048(0.0507)	0.0575(0.6090)
Total Phosphorus [µg/l]	0.1303	0.0000	1.4609(0.3431)	17.5303 (4.1173)
Nitrate [µg/l]	0.0404	0.0258	11.0383(4.8911)	132.46(58.6937)

3000 m

	R2	P level	Δ(± err)	Δ12 years (± err)
Temperature	0.0015	0.6693	-0.0812(0.1896)	-0.9741(2.2749)
Salinity	0.1390	0.0000	-0.2702(0.0609)	-3.2423(0.7305)
Chlorophyll-a [µg/l]	0.0017	0.6508	0.0229(0.0505)	0.2750(0.6060)
Total Phosphorus [µg/l]	0.1381	0.0000	1.1958(0.2715)	14.3491(3.2583)
Nitrate [µg/l]	0.0389	0.0289	8.6359(3.9048)	103.63(46.8578)

NORTHERN MARCHE REGION COASTAL WATERS

500 m

	R2	P level	Δ(± err)	Δ12 years (± err)
Temperature	0.0158	0.1188	-0.2581(0.1645)	-3.0975(1.97)
Salinity	0.1146	0.0000	-0.3235(0.0727)	-3.8826(0.87)
Chlorophyll-a [µg/l]	0.0085	0.2543	0.0788(0.0689)	0.9457(0.83)
Total Phosphorus [µg/l]	0.1027	0.0001	1.3457(0.3238)	16.1489(3.89)
Nitrate [µg/l]	0.0443	0.0091	11.5117(4.3535)	138.1402(52.24)

3000 m

	R2	P level	Δ(± err)	Δ12 years (± err)
Temperature	0.0110	0.1946	-0.2174(0.1669)	-2.6093(2.00)

Salinity	0.1228	0.0000	-0.2895(0.0627)	-3.4738(0.75)
Chlorophyll-a [µg/l]	0.0132	0.1555	0.1127(0.0790)	1.3527(0.95)
Total Phosphorus [µg/l]	0.0621	0.0019	0.8036(0.2542)	9.6433(3.05)
Nitrate [µg/l]	0.0379	0.0159	9.2380(3.7896)	110.8563(45.48)

SOUTHEN MARCHE REGION COASTAL WATERS

500 m

	R2	P level	Δ(± err)	Δ12 years (± err)
Temperature	0.0164	0.1210	-0.2517(0.1614)	-3.0200(1.94)
Salinity	0.2360	0.0000	-0.3448(0.0514)	-4.1378(0.62)
Chlorophyll-a [µg/l]	0.0000	0.9912	0.0003(0.0303)	0.0040(0.36)
Total Phosphorus [µg/l]	0.1162	0.0001	1.8639(0.4457)	22.3666(5.35)
Nitrate [µg/l]	0.0496	0.0094	11.4334(4.3406)	137.2006(52.09)

3000 m

	R2	P level	Δ(± err)	Δ12 years (± err)
Temperature	0.0160	0.1279	-0.2519(0.1645)	-3.0234(1.97)
Salinity	0.1675	0.0000	-0.2495(0.0464)	-2.9941(0.56)
Chlorophyll-a [µg/l]	0.0009	0.7142	-0.0095(0.0259)	-0.1139(0.31)
Total Phosphorus [µg/l]	0.1385	0.0000	1.2495(0.2723)	14.9942(3.27)
Nitrate [µg/l]	0.0339	0.0339	6.3520(2.9615)	76.2238(35.54)

Correlation values between river discharge data (from Marche Region Civil Protection) and nutrient concentration are reported in table below, with distinction between 500 and 3000 meters from the coast. All the variables provided by A.R.P.A.M. will be shown.

500 m from MISA RIVER								
River discharge		**Temperature °C**	**Salinity**	**pH**	**Dissolved Oxygen (%)**	**Chl-a [µg/l]**	**Phosphate [µg/l]**	**Total Phosphorus [µg/l]**
r	Same day	-0,6620	-0,4342	0,1918	0.0665	0.5050	-0.1018	0.2651
	Previous day	-0,6096	-0,4085	0,1601	0.0490	0.4242	-0.0848	0.2083
	Previous month	-0,6374	-0,4264	0,2008	0.0695	0.5913	-0.0308	0.4073
p	Same day	1.1312242809 1472e-08	0.0006	0.1456	0.6169	4.51564977 207442e-05	0.4390	0.0407
	Previous day	2.9869125073 3008e-07	0.0013	0.2258	0.7124	0,0008	0.5230	0.1134
	Previous month	5.6731278452 7374e-08	0.0008	0.1273	0.6010	8.1955371 1006726e-07	0.8168	0.0014

500 m from MISA RIVER									
River dischange		**Nitrate [µg/l]**	**Nitrite [µg/l]**	**Ammonia [µg/l]**	**Inorganic nitrogen [µg/l]**	**Total nitrogen [µg/l]**	**Silicate [µg/l]**	**Reactive silica [µg/l]**	**Trasparency (m)**
r	Same day	0.4477	-0.0945	0.1722	0.4954	0.1836	NaN	0.0809	-0.3980
	Previous day	0.5096	-0.0808	0.2626	0.5707	0.2411	NaN	0.1243	-0.3651
	Previous month	0.4220	0.1147	0.0385	0.4420	0.1061	NaN	-0.0695	-0.4398
p	Same day	0.0003	0.4727	0.1882	0.0003	0.5890	NaN	0.5806	0.0062
	Previous day	3.7489 832147 0196e-05	0.5429	0.0445	2.2782268 6044155e-05	0.4751	NaN	0.3999	0.0126
	Previous month	0.0009	0.3871	0.7725	0.0017	0.7561	NaN	0.6390	0.0022

3000 m from MISA RIVER								
River discharge		**Temperature °C**	**Salinity**	**pH**	**Dissolved Oxygen (%)**	**Chl-a [µg/l]**	**Phosphate [µg/l]**	**Total Phosphorus [µg/l]**
r	Same day	-0.6643	-0.3062	0.1845	0.1168	0.4910	0.2611	0.2559
	Previous day	-0.6110	-0.2559	0.1578	0.1051	0.4175	0.2228	0.1864
	Previous month	-0.6356	-0.2647	0.2023	0.1304	0.6499	0.2200	0.3210
p	Same day	9.651286214662249e-09	0.0183	0.1618	0.3782	7.858877657040960e-05	0.0439	0.0485
	Previous day	2.762724702343184e-07	0.0504	0.2327	0.4281	0.0010	0.0898	0.1575
	Previous month	6.375818828452405e-08	0.0427	0.1244	0.3249	2.551537980899350e-08	0.0940	0.0132

3000 m from MISA RIVER								
River dischange		**Nitrate [µg/l]**	**Nitrite [µg/l]**	**Ammonia [µg/l]**	**Inorganic nitrogen [µg/l]**	**Total nitrogen [µg/l]**	**Silicate [µg/l]**	**Reactive silica [µg/l]**	**Trasparency (m)**
R	Same day	0.3405	0.3227	0.3383	0.5108	0.1149	NaN	-0.0234	-0.4057
	Previous day	0.3406	0.3012	0.4154	0.5107	0.1928	NaN	-0.0125	-0.3712
	Previous month	0.2785	0.3043	0.1686	0.4276	0.0924	NaN	-0.1816	-0.4302
p	Same day	0.0078	0.0119	0.0082	0.0002	0.7365	NaN	0.8732	0.0052
	Previous day	0.0083	0.0204	0.0011	0.0002	0.5700	NaN	0.9328	0.0111
	Previous month	0.0327	0.0191	0.2017	0.0024	0.7871	NaN	0.2167	0.0028

500 m from ESINO RIVER								
River discharge		**Temperature °C**	**Salinity**	**pH**	**Dissolved Oxygen (%)**	**Chl-a [µg/l]**	**Phosphate [µg/l]**	**Total Phosphorus [µg/l]**
r	Same day	-0.5914	-0.3189	0.1429	0.2458	0.1777	0.1643	0.2890
	Previous day	-0.5433	-0.3023	0.1474	0.2411	0.1408	0.1097	0.2343
	Previous month	-0.1019	-0.1382	-0.1442	0.1329	-0.0143	-0.0010	0.2849
p	Same day	9.228146905171138e-05	0.0510	0.3921	0.1368	0.2859	0.3244	0.0785
	Previous day	0.0004	0.0651	0.3770	0.1447	0.3990	0.5119	0.1567
	Previous month	0.5428	0.4079	0.3877	0.4262	0.9320	0.9954	0.0830

500 m from ESINO RIVER									
River dischange		**Nitrate [µg/l]**	**Nitrite [µg/l]**	**Ammonia [µg/l]**	**Inorganic nitrogen [µg/l]**	**Total nitrogen [µg/l]**	**Silicate [µg/l]**	**Reactive silica [µg/l]**	**Trasparency (m)**
R	Same day	0.3861	0.2623	0.3378	0.5542	0.3012	NaN	0.4550	-0.3717

	Previous day	0.4198	0.2896	0.4372	0.6166	0.3602	NaN	0.4084	-0.3941
	Previous month	0.1992	-0.0251	-0.0603	0.0756	0.1585	NaN	0.4228	-0.2137
p	Same day	0.0166	0.1117	0.0381	0.0061	0.2752	NaN	0.0291	0.0431
	Previous day	0.0087	0.0778	0.0061	0.0017	0.1872	NaN	0.0530	0.0312
	Previous month	0.2306	0.8810	0.7192	0.7317	0.5725	NaN	0.0444	0.2569

3000 m from ESINO RIVER								
River discharge		**Temperature °C**	**Salinity**	**pH**	**Dissolved Oxygen (%)**	**Chl-a [µg/l]**	**Phosphate [µg/l]**	**Total Phosphorus [µg/l]**
r	Same day	-0.5895	-0.2619	0.1589	0.3455	0.3018	-0.0241	0.0315
	Previous day	-0.5430	-0.2504	0.1614	0.3286	0.2320	-0.0346	-0.0451
	Previous month	-0.0995	-0.0908	-0.1149	0.2143	0.0582	-0.0353	0.1054
p	Same day	9.8574477252 6997e-05	0.1122	0.3408	0.0336	0.0656	0.8860	0.8511
	Previous day	0.0004	0.1294	0.3330	0.0440	0.1610	0.8364	0.7879
	Previous month	0.5524	0.5877	0.4920	0.1964	0.7284	0.8332	0.5287

3000 m from ESINO RIVER									
River dischange		**Nitrate [µg/l]**	**Nitrite [µg/l]**	**Ammonia [µg/l]**	**Inorganic nitrogen [µg/l]**	**Total nitrogen [µg/l]**	**Silicate [µg/l]**	**Reactive silica [µg/l]**	**Traspar ency (m)**
R	Same day	0.3595	0.2108	0.2892	0.4754	0.4202	NaN	0.1616	-0.2830
	Previous day	0.3754	0.1944	0.3121	05324	0.5324	NaN	0.1172	-0.3074
	Previous month	0.0401	-0.0922	-0.0398	0.0791	0.0791	NaN	0.4244	-0.1517
p	Same day	0.0266	0.2039	0.0783	0.0219	0.1189	NaN	0.4614	0.1296
	Previous day	0.0202	0.2422	0.0565	0.0089	0.1515	NaN	0.5943	0.0985
	Previous month	0.8109	0.5819	0.8123	0.7198	0.9972	NaN	0.0435	0.4236

500 m from MUSONE RIVER								
River discharge		**Temperature °C**	**Salinity**	**pH**	**Dissolved Oxygen (%)**	**Chl-a [µg/l]**	**Phosphate [µg/l]**	**Total Phosphor us [µg/l]**
r	Same day	-0.6823	-0.5200	0.041	0.1423	0.6545	-0.0143	0.1825
	Previous day	-0.6052	-0.5175	-0.0578	0.1111	0.6753	-0.0199	0.1576
	Previous month	-0.4987	-0.6215	0.2342	0.3523	0.5914	-0.0974	0.1068

p	Same day	2.3609953269 9985e-05	0.0027	0.9827	0.4450	3.594799 0146834 0e-05	0.9370	0.3095
	Previous day	0.0003	0.0029	0.7574	0.5517	1.622845 0898880 8e-05	0.9127	0.3811
	Previous month	0.0043	0.0002	0.2047	0.0520	0.0003	0.5895	0.5542

500 m from MUSONE RIVER									
River dischange		**Nitrate [µg/l]**	**Nitrite [µg/l]**	**Ammonia [µg/l]**	**Inorganic nitrogen [µg/l]**	**Total nitrogen [µg/l]**	**Silicate [µg/l]**	**Reactive silica [µg/l]**	**Traspa rency (m)**
R	Same day	0.4277	0.3882	0.3469	0.6252	0.1527	NaN	0.5394	-0.3328
	Previous day	0.4100	0.3782	0.3354	0.5876	0.2616	NaN	0.4775	-0.2888
	Previous month	0.4841	0.3490	0.3264	0.7409	0.1250	NaN	0.4743	-0.3819
p	Same day	0.0130	0.0256	0.0480	0.0014	0.6539	NaN	0.0096	0.0584
	Previous day	0.0178	0.0300	0.0564	0.0032	0.4372	NaN	0.0246	0.1031
	Previous month	0.0043	0.0465	0.0638	5.2637156 5557681e-05	0.7143	NaN	0.0257	0.0283

3000 m from MUSONE RIVER								
River discharge		**Temperature °C**	**Salinity**	**pH**	**Dissolved Oxygen (%)**	**Chl-a [µg/l]**	**Phosphate [µg/l]**	**Total Phospho rus [µg/l]**
r	Same day	-0.6373	-0.4242	-0.0037	0.0638	0.5463	-0.0832	0.1601
	Previous day	-0.5338	-0.4140	-0.0767	0.0558	0.5272	-0.0378	0.0963
	Previous month	-0.3583	-0.3293	0.2509	0.3181	0.2662	0.0417	-0.0173
p	Same day	0.0002	0.0218	0.9850	0.7424	0.0015	0.6562	0.3895
	Previous day	0.0029	0.0256	0.6926	0.7737	0.0023	0.8400	0.6062
	Previous month	0.0563	0.0811	0.1893	0.0927	0.1477	0.8238	0.9265

3000 m from MUSONE RIVER									
River dischange		**Nitrate [µg/l]**	**Nitrite [µg/l]**	**Ammonia [µg/l]**	**Inorganic nitrogen [µg/l]**	**Total nitrogen [µg/l]**	**Silicate [µg/l]**	**Reactive silica [µg/l]**	**Traspa rency (m)**
R	Same day	0.4211	0.4222	-0.1385	0.7717	-0.0397	NaN	0.6928	-0.1367
	Previous day	0.4090	0.4111	-0.0987	0.7393	0.0519	NaN	0.5975	-0.1521
	Previous month	0.3472	0.2341	-0.0341	0.7084	0.1768	NaN	0.3377	-0.1807
p	Same day	0.0183	0.0180	0.4574	6.7537230 7555426e-	0.9077	NaN	0.0007	0.4633

					05				
	Previous day	0.0223	0.0216	0.5973	0.0002	0.8795	NaN	0.0054	0.4141
	Previous month	0.0557	0.2049	0.8556	0.0005	0.6031	NaN	0.1453	0.3307

500 m from POTENZA RIVER								
River discharge		**Temperature °C**	**Salinity**	**pH**	**Dissolved Oxygen (%)**	**Chl-a [µg/l]**	**Phosphate [µg/l]**	**Total Phosphorus [µg/l]**
r	Same day	-0.4422	-0.4785	0.1338	0.2237	0.4546	0.2298	0.1663
	Previous day	-0.4411	-0.4839	0.1355	0.2068	0.4361	0.2133	0.1714
	Previous month	-0.4335	-0.5838	0.1755	0.2310	0.4221	0.1831	0.1218
p	Same day	2.91696475196446e-06	3.1925798238408e-07	0.1780	0.0231	1.1067707496037e-06	0.0201	0.0949
	Previous day	3.11033287303530e-06	2.2421892154067e-07	0.1725	0.0361	4.1272353290544e-06	0.0331	0.0883
	Previous month	4.77243277086092e-06	9.6495589296807e-11	0.0762	0.0189	8.9559403985140e-06	0.0683	0.2274

500 m from POTENZA RIVER									
River dischange		**Nitrate [µg/l]**	**Nitrite [µg/l]**	**Ammonia [µg/l]**	**Inorganic nitrogen [µg/l]**	**Total nitrogen [µg/l]**	**Silicate [µg/l]**	**Reactive silica [µg/l]**	**Traspa rency (m)**
R	Same day	0.2684	-0.0525	0.0873	0.6447	-0.2216	0.7622	0.3811	-0.5320
	Previous day	0.2828	-0.0446	0.0908	0.6415	-0.1719	0.7456	0.4071	-0.5115
	Previous month	0.2595	-0.0834	0.0491	0.5589	-0.1532	0.4887	0.3359	-0.4052
p	Same day	0.0064	0.6000	0.3829	2.71813902497087e-08	0.1585	0.0781	0.0005	1.0726089385 5710e-06
	Previous day	0.0044	0.6598	0.3692	4.37953942000746e-08	0.2826	0.0889	0.0002	4.3926840019 8589e-06
	Previous month	0.0091	0.4094	0.6278	4.21889597468361e-06	0.3390	0.3254	0.0025	0.0004

3000 m from POTENZA RIVER								
River discharge		**Temperature °C**	**Salinity**	**pH**	**Dissolved Oxygen (%)**	**Chl-a [µg/l]**	**Phosphate [µg/l]**	**Total Phosphorus [µg/l]**
r	Same day	-0.4076	-0.4541	0.1601	0.1876	0.3146	0.1133	0.2272
	Previous day	-0.4072	-0.4540	0.1594	0.1694	0.3023	0.1028	0.2294

	Previous month	-0.4045	-0.5150	0.2018	0.2197	0.3430	0.0681	0.1890
p	Same day	2.3269384554 1032e-05	2.084956 5590674 9e-06	0.1098	0.0604	0.0012	0.2615	0.0230
	Previous day	2.3767845736 6552e-05	2.096362 9294712 4e-06	0.1113	0.0904	0.0021	0.3137	0.0231
	Previous month	2.7297730487 5965e-05	4.189901 5701396 5e-08	0.0430	0.0273	0.0004	0.5050	0.0623

3000 m from POTENZA RIVER									
River dischange		**Nitrate [µg/l]**	**Nitrite [µg/l]**	**Ammonia [µg/l]**	**Inorganic nitrogen [µg/l]**	**Total nitrogen [µg/l]**	**Silicate [µg/l]**	**Reactive silica [µg/l]**	**Trasparency (m)**
R	Same day	0.1886	0.0439	0.1362	0.6120	-0.2663	0.2093	0.2920	-0.4563
	Previous day	0.2248	0.0520	0.1402	0.6394	-0.1986	0.1377	0.3086	-0.4349
	Previous month	0.1913	0.0619	0.1163	0.5539	-0.1754	0.1035	0.2940	-0.3866
p	Same day	0.0602	0.6649	0.1765	3.3182504 4996847e-07	0.0883	0.6906	0.0095	5.6188 9467370902e-05
	Previous day	0.0260	0.6109	0.1687	8.6417166 0897029e-08	0.2132	0.7947	0.0063	0.0002
	Previous month	0.0592	0.5452	0.2540	7.8427299 6479096e-06	0.2726	0.8452	0.0094	0.0009

500 m from TENNA RIVER								
River discharge		**Temperature °C**	**Salinity**	**pH**	**Dissolved Oxygen (%)**	**Chl-a [µg/l]**	**Phosphate [µg/l]**	**Total Phosphorus [µg/l]**
r	Same day	-0.0154	0.0934	0.1532	-0.2134	-0.1542	-0.2476	-0.2768
	Previous day	-0.0164	0.0783	0.1617	-0.1908	-0.1435	-0.1772	-0.1630
	Previous month	-0.0346	0.0437	0.2191	-0.2180	-0.1377	-0.1248	-0.1407
p	Same day	0.9025	0.4594	0.2231	0.0879	0.2164	0.0374	0.0195
	Previous day	0.8962	0.5353	0.1982	0.1278	0.2505	0.1833	0.2216
	Previous month	0.7830	0.7299	0.0796	0.0811	0.2701	0.3506	0.2921

500 m from TENNA RIVER									
River dischange		**Nitrate [µg/l]**	**Nitrite [µg/l]**	**Ammonia [µg/l]**	**Inorganic nitrogen [µg/l]**	**Total nitrogen [µg/l]**	**Silicate [µg/l]**	**Reactive silica [µg/l]**	**Trasparency (m)**
R	Same day	0.3309	0.2428	0.5130	0.4448	0.2385	0.7689	0.2212	-0.4843
	Previous	0.2888	0.1636	0.4721	0.4719	0.1494	0.8356	0.2577	-0.4292

	day								
	Previous month	0.3085	0.2711	0.5267	0.4668	0.1855	0.2812	0.2534	-0.5136
p	Same day	0.0048	0.0413	4.7678150 2112278e-06	0.0040	0.1190	0.0739	0.1046	0.0013
	Previous day	0.0279	0.2197	0.0002	0.0130	0.4223	0.0383	0.0575	0.0051
	Previous month	0.0185	0.0396	2.1684986 8701630e-05	0.0141	0.3177	0.5893	0.0619	0.0006

3000 m from TENNA RIVER								
River discharge		**Temperature °C**	**Salinity**	**pH**	**Dissolved Oxygen (%)**	**Chl-a [µg/l]**	**Phosphate [µg/l]**	**Total Phosphorus [µg/l]**
r	Same day	-0.0037	0.1827	0.1846	0.0156	-0.1820	-0.3263	-0.3374
	Previous day	-0.0094	0.1789	0.1902	0.0251	-0.1781	-0.2949	-0.3167
	Previous month	-0.0219	0.1360	0.2453	-0.0090	-0.1713	-0.2267	-0.2914
p	Same day	0.9768	0.1452	0.1442	0.9021	0.1468	0.0058	0.0043
	Previous day	0.9405	0.1538	0.1322	0.8424	0.1559	0.0260	0.0164
	Previous month	0.8622	0.2801	0.0507	0.9432	0.1725	0.0899	0.0279

3000 m from TENNA RIVER									
River dischange		**Nitrate [µg/l]**	**Nitrite [µg/l]**	**Ammonia [µg/l]**	**Inorganic nitrogen [µg/l]**	**Total nitrogen [µg/l]**	**Silicate [µg/l]**	**Reactive silica [µg/l]**	**Trasparency (m)**
R	Same day	-0.1490	-0.0445	-0.0085	-0.1673	-0.2331	0.3331	-0.2394	-0.5722
	Previous day	-0.1663	-0.1083	0.0033	0.2323	-0.3480	0.3699	-0.2124	-0.5398
	Previous month	-0.1290	-0.0195	0.0188	0.2222	-0.3094	0.0226	-0.1217	-0.5872
p	Same day	0.2182	0.7147	0.9440	0.3087	0.1278	0.5189	0.0812	0.0001
	Previous day	0.2162	0.4226	0.9807	0.2534	0.0551	0.4705	0.1232	0.0003
	Previous month	0.3387	0.8854	0.8898	0.2753	0.0903	0.9661	0.3806	6.7979729780787 2e-05

500 m from TRONTO RIVER								
River discharge		**Temperature °C**	**Salinity**	**pH**	**Dissolved Oxygen (%)**	**Chl-a [µg/l]**	**Phosphate [µg/l]**	**Total Phosphorus [µg/l]**
r	Same day	-0.5045	-0.2525	0.0892	0.0637	0.0203	0.0290	-0.0121
	Previous day	-0.4783	-0.3044	0.1369	0.0488	-0.0087	0.0588	0.1016
	Previous month	-0.5738	-0.5120	0.1645	0.1677	0.0480	0.1273	0.2032

p	Same day	3.3624118420 6720e-06	0.0289	0.4433	0.5874	0.8621	0.8061	0.9182
	Previous day	1.2404685343 6921e-05	0.0079	0.2385	0.6777	0.9406	0.6444	0.4245
	Previous month	6.0152319236 7282e-08	2.658865 9536308 5e-06	0.1557	0.1503	0.6802	0.3160	0.1073

500 m from TRONTO RIVER

River dischange		**Nitrate [µg/l]**	**Nitrite [µg/l]**	**Ammonia [µg/l]**	**Inorganic nitrogen [µg/l]**	**Total nitroge n [µg/l]**	**Silicate [µg/l]**	**Reactive silica [µg/l]**	**Traspa rency (m)**
R	Same day	0.4034	0.4705	0.0719	0.3962	0.3018	NaN	0.2097	-0.2268
	Previous day	0.4154	0.5315	0.0814	0.5449	0.2988	NaN	0.2201	-0.2143
	Previous month	0.6444	0.4835	0.0802	0.7863	0.4368	NaN	0.3933	-0.2311
p	Same day	0.0004	2.3323 579963 9298e-05	0.5429	0.0138	0.0415	NaN	0.1941	0.0763
	Previous day	0.0006	6.2121 665334 0362e-06	0.5225	0.0027	0.0767	NaN	0.1724	0.0944
	Previous month	9.1404 803725 9363e-09	5.1778 552141 3350e-05	0.5287	7.0593534 1641087e-07	0.0077	NaN	0.0121	0.0708

3000 m from TRONTO RIVER

River discharge		**Temperature °C**	**Salinity**	**pH**	**Dissolved Oxygen (%)**	**Chl-a [µg/l]**	**Phospha te [µg/l]**	**Total Phosphorus [µg/l]**
r	Same day	-0.5076	-0.4601	0.1143	0.0957	0.1792	-0.0477	-0.0243
	Previous day	-0.4820	-0.5220	0.1166	0.0624	0.2174	NaN	0.1859
	Previous month	-0.5550	-0.7144	0.2343	0.1733	0.2724	NaN	0.2554
p	Same day	5.3345563058 0271e-06	4.768478 6060209 2e-05	0.3392	0.4241	0.1349	0.7200	0.8548
	Previous day	1.8109607423 9884e-05	2.575228 9765090 8e-06	0.3294	0.6028	0.0686	NaN	0.2010
	Previous month	4.2045980486 1828e-07	1.840750 3432252 0e-12	0.0476	0.1454	0.0215	NaN	0.0765

3000 m from TRONTO RIVER									
River dischange		**Nitrate [µg/l]**	**Nitrite [µg/l]**	**Ammonia [µg/l]**	**Inorganic nitrogen [µg/l]**	**Total nitrogen [µg/l]**	**Silicate [µg/l]**	**Reactive silica [µg/l]**	**Traspar ency (m)**
R	Same day	0.3471	0.3465	-0.0472	0.5722	0.4737	NaN	0.3519	-0.1915
	Previous day	0.3791	0.4017	0.2601	0.7601	0.4597	NaN	0.3889	-0.2017
	Previous month	0.5304	0.3557	0.1386	0.8729	0.63020	NaN	0.5568	-0.1371
p	Same day	0.0071	0.0072	0.7224	0.0002	0.0012	NaN	0.0303	0.1426
	Previous day	0.0072	0.0042	0.0711	6.6218321 5959856e-06	0.0062	NaN	0.0191	0.1325
	Previous month	8.8583 728066 7490e-05	0.0121	0.3422	6.0410767 3146795e-09	6.492666 7134979 1e-05	NaN	0.0004	0.3092